Drug Resistance Mechanisms in a High Grade Glioma Cell Line

By

Ayat B. Al-Ghafari, M.Sc.

Thesis submitted to the University of Nottingham
for the degree of Doctor of Philosophy

March 2013

Table of Contents

Abstract

Glioblastoma multiforme (GBM) is the most common and aggressive primary brain tumour. Despite advances in GBM treatment, there is a high frequency of local relapse due to the acquisition of drug resistance. Investigation of glioma cell lines will help us to understand the molecular basis of this hard to treat tumour. In this study, the rat C6 glioma cell line was used as a model alongside two drug selected derivatives (C6-etoposide and C6-irinotecan) to investigate the mechanisms of chemo-resistance in glioma by identifying candidate proteins, genes, and key signalling pathways. Proteomic (2D gel electrophoresis) and genomic (gene array) analyses were performed to determine protein and gene expression changes. Integration of this data with cellular pathway analysis resulted in the prediction that cellular migration and the response to oxidative stress would be distinct in the drug selected C6 cell lines. Cell migration was subsequently assessed using wound scratch repair and transwell migration assays, whilst the response to oxidative stress produced by reactive oxygen species was determined fluorimetrically. The C6 cell line exposed to irinotecan (DNA topoisomerase I inhibitor) showed reduced migration, even under the influence of chemoattractant, compared to other cell lines, consistent with alterations in the expression of collagen genes. The C6 cell line exposed to etoposide (DNA topoisomerase II inhibitor) showed greater resistance to oxidative stress which was proposed to be due to alterations in the signalling pathways downstream of the PTEN/PI3Kinase. Future studies, investigating the effect of PI3Kinase pathway inhibitors are considered and it is proposed that further research into this signalling pathway will be able to uncover the molecular basis of distinct chemo-resistance in this important model cell system for aggressive glioma.

Acknowledgments

First of all, I would like to express my sincere gratitude to Allah the Almighty who gave me the strength and patience to complete my PhD. *Secondly*, I would like to thank my supervisor Dr. Ian Kerr for his continuous support during my PhD, for his patience, enthusiasm, time, effort, and motivation to carry on with this project. He taught me the alphabet of scientific research. Also, I would like to express my thanks to my co-supervisor Dr. Beth Coyle for her time, encouragement, and insightful comments. Thanks Beth for sharing your knowledge and experiences with me. I couldn't imagine that I would have better supervisors than both of you. *Besides my supervisors*, I would like to thank Dr. Wiyada Punjaruk for giving me the pellets for the C6 cell line and the drug derived cell lines. I would like to thank Dr. Rob Layfield and Dr. James Dorrian for their advice in performing and analysing 2D gels. My grateful thanks are also extended to Dr. Emma King and Ian Ward for their assistance in doing the scratch assay experiments on time-lapse microscope and analysing the data. I also wish to thank Dr. Peter Jones for giving me the transwell migration plates and Dr. Nick Holiday who helped me to run my transwell migration assay on the MDC fluorescent microscope. Finally, the advice given by Dr. Lisa Storer and Dr. Hazel Rogers has been a great help in performing the clonogenic assay and qRT-PCR experiments, respectively.

I would like to express my very great appreciation to King Abdul Aziz University in Saudi Arabia for giving me this valuable opportunity to do my PhD at the University of Nottingham and for their financial support.

A big THANK YOU to the lovely lady Deb Briggs (Mrs everybody) who made my time in the lab so relaxed and funny, who kept my secrets and mistakes. Thanks Deb for your time and support (you are really the best). Moreover, I would like to thank my colleagues in D72 and especially Dr. David Carrier, Dr. Ameena Haider, Dr. Christopher Kay, Kelvin Wong, and Maria

Isabel Haig as well as my colleagues in D18 Dr. Ramadhan Othman, Warisara Petchsri, and Durgagauri Sabnis for sharing their time with me and for being there for me all the time.

Finally, my deepest thanks are for my lovely family, the real motivation behind my strength and patience. My parents, you made me the person I am now and your prayers keep me going on and you have always supported me spiritually throughout my life. May Allah bless you and I hope that I made you both proud of me. My brother (Ehab) and my sisters (Elham, Enas, and Dina), thanks for every moment you shared with me and for your continuous support (Love you all). My dearest nephews (Badr and Omar) you don't know how much I love you both (you made my life better and happier).

Thank you all!

Declaration

Except where acknowledged in the text, I declare that this dissertation is my own work and is based on research that was undertaken by me in the School of Biomedical Sciences, Faculty of Medicine and Health Sciences, University of Nottingham during the period 31st October 2009 to 31st October 2013.

Ayat Al-Ghafari

4094204

13th March 2013

List of Figures

List of Tables

List of Abbreviations

.CEL	Cell intensity file
2-DIGE	Two-dimensional gel electrophoresis
AA	Anaplastic astrocytoma
ABC	ATP binding cassette transporter
ABCF2	ATP-binding cassette sub-family F member 2
ADM	Adriamycin
Akt	Serine-threonine protein kinase
ANOVA	Analysis of variance
APC	Aminopentanecarboxylic acid
APS	Ammonium persulfate
ATP	Adenosine triphosphate
ATP1B1	Sodium/potassium-transporting ATPase subunit beta-1
BBB	Blood-brain barrier
BCA	Bovine serum albumin
BCRP	Breast cancer resistance protein
BME	Basement membrane extract
BMP7	Bone morphogenetic protein 7
BVZ	Bevacizumab
CA9	Carbonic anhydrase 9
CBTRC	Children's brain tumour research centre
CD	Complementarity determining
CDDP	Cisplatin
ChIP	Chromatin immunoprecipitation
CI	Confidence interval
CNS	Central nervous system
CNV	Copy number variation
COL1A2	Collagen, type I, alpha 2
COL3A1	Collagen, type III, alpha 1

CSC	Cancer stem cell
CT	Computerised tomography
C_T	Cycle threshold
CYP3A4	Cytochrome P450
DAG	Diacylglycerol
DCF	Dichlorofluorescein
DCFH-DA	2'-7'-dichloroflurescin diacetate
DEPC	Diethylpyrocarbonate
DIPG	Diffuse intrinsic pontine glioma
DMEM	Dulbecco's Modified Eagle Medium
DMSO	Dimethyl sulphoxide
dsDNA	Double stranded DNA
DTT	Dithiothreitol
ECL	Enzymatic chemiluminescence
ECM	Extracellular matrix
EFS	Event-free survival
EGF	Epidermal growth factor
EGFR	Epidermal growth factor receptor
EGR1	Early growth response protein 1
EMT	Epithelial mesenchymal transition or transformation
FAK	Focal adhesion kinase
FBS	Foetal bovine serum
FC	Fold change
FDA	Food and drug administration
FDR	False discovery rate
GBM	Glioblastoma multiforme
GEMs	Glioma endothelial markers
GFAP	Glial fibrillary acidic protein
GST	Glutathione S-transferase

Gy	Gray unit
H3.3	Histone 3 variant 3
HBSS	Hank's Balanced Salt Solution
HGG	High grade glioma
HIF1α	Hypoxia-inducible factor 1α
HR	Hazard ratio
HRAS	Harvey-sarcoma virus
IDH	Isocitrate dehydrogenase
IEF	Isoelectric focusing
IGF	Insulin-like growth factor
IP	Intracranial pressure
IP3	Inositol-1, 4, 5-trisphosphate
IPA	Ingenuity pathway analysis
KRAS	Kirsten-sarcoma virus
LGG	Low grade glioma
LRP	Lung resistance-related protein
MALDI-MS	Matrix assisted laser desorption ionisation mass spectrometry analysis
MALDI-TOF	Matrix assisted laser desorption ionisation -time of flight
MDR	Multidrug resistance
MDR1	Multidrug resistance 1
MGMT	O^6 –methylguanine- DNA-methyl transferase
MM	Mismatch
MMP	Matrix metalloproteinase
MMR	Mismatch repair
MRI	Magnetic resonance imaging
MRP1	Multidrug resistance protein 1
MS	Mass spectrometry
MT	Metallothionein

MT1F	Metallothionein-1F
mTOR	Mammalian target of rapamycin
Mwt	Molecular weight
NaAc	Sodium acetate
NBD	Nucleotide binding domain
NCBI	National Centre for Biotechnology
NDBK	Nucleotide diphosphate B kinase
Nes-ΔTK-GFP	Nestin- ΔTK-IRES-GFP
NF	Neurofibromatosis
NRAS	Neuroblastoma virus
NSCLC	Non-small cell lung cancer
NTC	No template control
OR	Odds ratio
OS	Overall survival rate
OS	Oxidative stress
PBS	Phosphate buffer saline
PCA	Principal component analysis
PCD	Programmed cell death
PDGF	Platelet-derived growth factor
PDGFR	Platelet-derived growth factor receptor
PDK1	Phosphoinositide-dependent kinase 1
PFA	Paraformaldehyde
PFS	Progression-free survival
pI	Isoelectric point
PI3K	Phosphatidylinositol 3-kinase
PIP	Phosphatidylinositol 4-phosphate
PIP2	Phosphatidylinositol 4,5-bisphosphate
PIP3	Phosphatidylinositol 3,4,5-trisphosphate
PKC	Protein kinase C

PLC	Phospholipase C
PM	Perfect match
PMF	Peptide mass fingerprinting
PNS	Peripheral nervous system
PRP19	PRP19/PSO4 pre-mRNA processing factor 19 homolog (*S. cerevisiae*)
PTEN	Phosphatase and tensin homolog deleted on chromosome 10
PTMs	Post-translational modifications
qPCR	Quantitative PCR
Ras	Rat sarcoma
RAS/MAPK	Ras-guanosine triphosphate/mitogen-active protein kinase
RB	Retinoblastoma
RFU	Relative fluorescent unit
RIN	RNA integrity number
ROS	Reactive oxygen species
RR	Risk ratio
RT	Reverse transcriptase
RTK	Receptor tyrosine kinase
RT-PCR	Reverse transcriptase- polymerase chain reaction
SDS	Sodium dodecyl sulphate
SP	Side population or sub-population
SN-38G	SN-38 glucuronide
SNPs	Single nucleotide polymorphisms
ssDNA	Single stranded DNA
SVZ	Subventricular zone
Ta	Temperature (annealing)
TBHP	Tert-butyl hydroperoxide
TEMED	Tetramethylethylenediamine
TGFβ	Transforming growth factor beta

Tm	Temperature (melting)
TMA	Tissue microarray
TMD	Transmembrane domain
TMZ	Temozolomide
TNFα	Tumour necrosis factor alpha
TOP1	Topoisomerase I
TOP1MT	Mitochondrial topoisomerase I
TSC	Tuberous sclerosis
UGT1A1	Uridine diphosphate glucoronosyl-transferase isoform 1A1
UV	Ultraviolet
VEGF	Vascular endothelial growth factor
VEGFR	Vascular endothelial growth factor receptor
WB	Western blotting
WHO	World Health Organization

CHAPTER I

GENERAL INTRODUCTION

CHAPTER I: GENERAL INTRODUCTION

1. Overview

Cancer is a group of diseases characterised by the presence of abnormal cells which have lost their ability to control their growth (proliferation) and death (apoptosis). Although cancer research has improved in the last 25 years especially in the fields of diagnosis and treatment, the ability of tumours to resist the current advanced treatment and their tendency to recur is a major obstacle. Several studies have been made to understand the mechanisms by which tumours can be resistant to the chemo/radiotherapies. Understanding the biology, molecular and cellular mechanisms of tumour will help to overcome this resistance and will lead to a better response of the patients to the currently used therapies. The general introduction chapter is focusing on four major topics: cancer biology followed by an introduction about the human brain structure, functions, and tumours particularly high grade glioma (HGG) (Glioblastoma multiforme -GBM), the discovered drug resistance mechanisms in GBM, and finally the importance and need for cell line models which could help in understanding and discovering other drug resistance mechanisms in GBM. This chapter will be followed by three result chapters which investigate the different mechanisms of drug resistance in cell line models for GBM and finally a general discussion chapter which concludes all the findings from this study and the future directions.

1.1 Cancer biology

Cancer or malignant neoplasm disease is a group of diseases which is characterised by the uncontrolled growth of cells (proliferation), uncontrolled movement (migration and metastasis), ability to invade neighbouring tissues (invasion), and resistance to death (necrosis and apoptosis). These neoplasms result from the transformation of a normal cell to a malignant cell through a multistep process by the alteration of genes and pathways which normally

regulate cell growth, differentiation, and survival (oncogenes) as well as genes that control cell death (tumour suppressor genes). Tumours are heterogeneous because they often comprise cytogenetically different clones that arise from the initial genetically altered cell through secondary or tertiary genetic alterations. This heterogeneity results in differences in clinical tumour behaviour and responses to treatment. Moreover, tumours can also contain progenitor cancer cells (cells which may be able to repopulate tumour post-treatment; see section 1.1.2), which constitute a spectrum of cells with different genetic alterations and states of differentiation. These subpopulations are varied in their sensitivity to chemotherapy and radiotherapy making the management of the tumour more difficult (Croce, 2008).

1.1.1 Hallmarks of cancer

Tumorigenesis is a very complex process which requires the integration of many factors to transform the normal cell into a carcinogenic cell. Figure 1.1 summarises the different factors which define cancer development (the hallmarks of cancer). However, only three of these factors will be described in detail as they are relevant to this study (Hanahan and Weinberg, 2000).

The *first factor* is the acquisition of mitogenic growth signals which help in the transformation of a normal quiescent cell to a proliferative cell. These mitogenic signals are transmitted through binding to highly specific receptors (Hanahan and Weinberg, 2000). Additionally, the cancer cells can switch the type of the extracellular matrix (ECM) receptor depending on the needs of the cell for instance, when the cancer cells switch to an integrin receptor this results in changing the cell behaviour from a quiescent state into an apoptosis-resistant and highly migratory state (Giancotti and Ruoslahti, 1999). In addition, it is known that cancer cells have the ability to create their own growth signals (i.e., they do not depend only on the normal growth

signals from the surrounding environment) for example in glioblastoma, cancer cells have the ability to create platelet derived growth factor (PDGF) which serves as a major growth factor (angiogenic factor) in this tumour (Fedi et al., 1997).

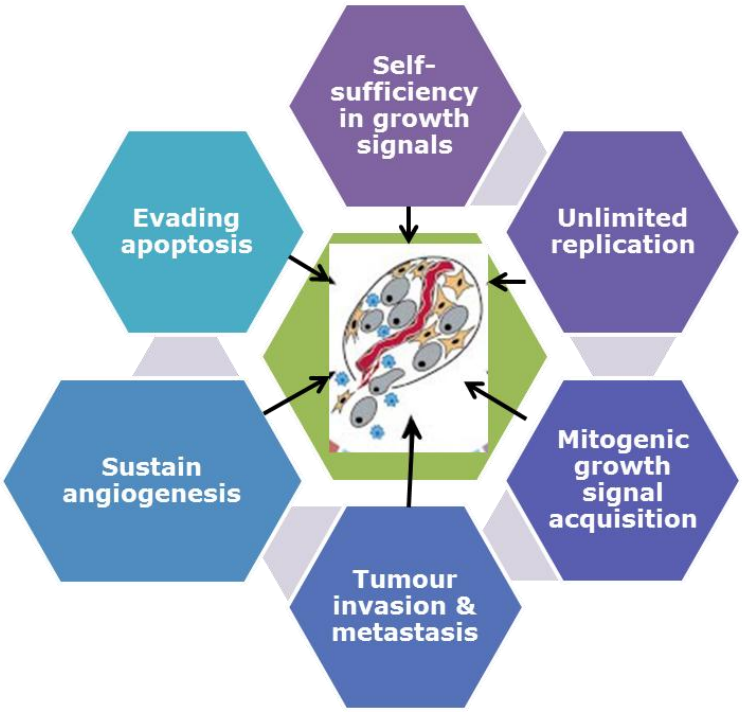

Figure 1.1 Hallmarks of cancer (the acquisition factors). Cancer is a multifactorial disease that occurs through a multistep process. Each of these steps reflects genetic alterations that drive the progressive transformation of normal human cells into highly malignant cells. Most cancers have acquired the same set of functional capabilities during their development, through various mechanistic strategies which make the cure of cancer difficult and complex. It is believed that for cancer to be established, all cancers must acquire the same six hallmark capabilities as pictured (Hanahan and Weinberg, 2000).

A *second factor* in tumorigenesis is the ability to invade or metastasise to the neighbouring or the distant tissues, respectively. The exact genetic and biological mechanisms of the invasion and metastasis are not fully understood. To be able to penetrate the surrounding tissues cells must change their structure and shape by remodeling their cell to cell and cell to matrix adhesion contacts which can be achieved by expressing integrins and releasing proteases. Moreover, cells must change their actin cytoskeleton as well as their signalling pathways (Hood and Cheresh, 2002). These changes occur through several steps for example, in gliomas during the mesenchymal migration, cells exhibit a highly polarised and fibroblastic morphology. First, cells are polarised and elongated which results in the formation of pseudopod (Actin filaments) from the extended part of the cell edge in the direction of movement. Secondly, the pseudopod of the cell is attached to the ECM substrate (substratum) in the direction which the cell is migrating. Thirdly, the pseudopod-ECM polymerisation initiates signal transduction pathways along the leading edge which helps the integrins to contact with ECM ligands and cluster to recruit intracellular signalling proteins that induce phosphorylation signalling via focal adhesion kinases (FAK). Then, surface proteases cleave ECM molecules via production of matrix metalloproteinases (MMPs). Finally, cell contraction occurs via myosin that leads to focal contact disassembly at the trailing edge and actin cleavage and filament turnover (Friedl and Wolf, 2003).

Cancer cells can mostly acquire the high ability to invade and metastasis by changing the expression of two major elements: (1) integrins and (2) proteases. It is evident that the invasive and metastatic cells shift their expression of integrins from those that favour the ECM present in normal epithelium to other integrins (e.g., α3β1 and αVβ3) that bind the degraded stromal component produced by extracellular proteases (Giancotti and Ruoslahti, 1999). In cancer cells, the protease genes are mostly up-regulated whereas, the protease inhibitor genes are down-regulated. The invasion

process starts when proteases bind to the cell surface receptors which leads to the invasion of cancer cells through epithelial layers or across the blood vessel walls into neighbouring tissue (Hanahan and Weinberg, 2000).

The *third factor* is the ability of the cell to escape from apoptosis. Apoptosis is a process of programmed cell death (PCD) that may occur as a result of changes in cellular morphology. Apoptosis and autophagy are both classified as PCD whereas, necrosis is not. Necrosis is a form of traumatic cell death that results from acute cellular injury or infection (Reed, 1999). Research on apoptosis has increased markedly since the early 1990s not only because apoptosis is an important biological process but also because defective apoptotic processes have been implicated in an extensive variety of diseases such as cancer. In a normal cell, there is a balance between the rate of cell proliferation and cell death (apoptosis). Cells can be terminated by apoptosis through several apoptotic factors such as cytochrome C, members of the Bcl-2 family (Bcl-2, Bax, Bak, Bid, Bim, Bcl-XL, and Bcl-W), the p53 tumour suppressor protein, and finally, the caspase family proteins which are activated by either a ligand such as FAS (also known as CD95 and APO-1) or cytochrome C (figure 1.2) (Green and Reed, 1998). In a cancer cell, there is an acquired resistance to apoptosis because there is no balance between the two major components of the apoptosis mechanism (sensors and effectors). The sensors are important in regulating the sensitivity of the cell to the changes in the intracellular and extracellular environments and conditions. These signals regulate the second class of components, which function as effectors of apoptotic death. The sensors include cell surface receptors that either bind to a survival or death factor such as insulin-like growth factor (IGF) or tumour necrosis factor alpha (TNFα), respectively (Giancotti and Ruoslahti, 1999). The effectors include intracellular proteases (caspases) (Hanahan and Weinberg, 2000). Resistance to apoptosis can be acquired through several mechanisms, for example in glioma mutations in a major tumour suppressor gene *TP53,* mutation in the PI3K/AKT/mTOR pathway, or

the mutation or loss of phosphatase and tensin homolog deleted on chromosome 10 (*PTEN)* gene, all contribute to evasion of apoptosis (Hanahan and Weinberg, 2000, Paugh et al., 2010, Lee et al., 2011a).

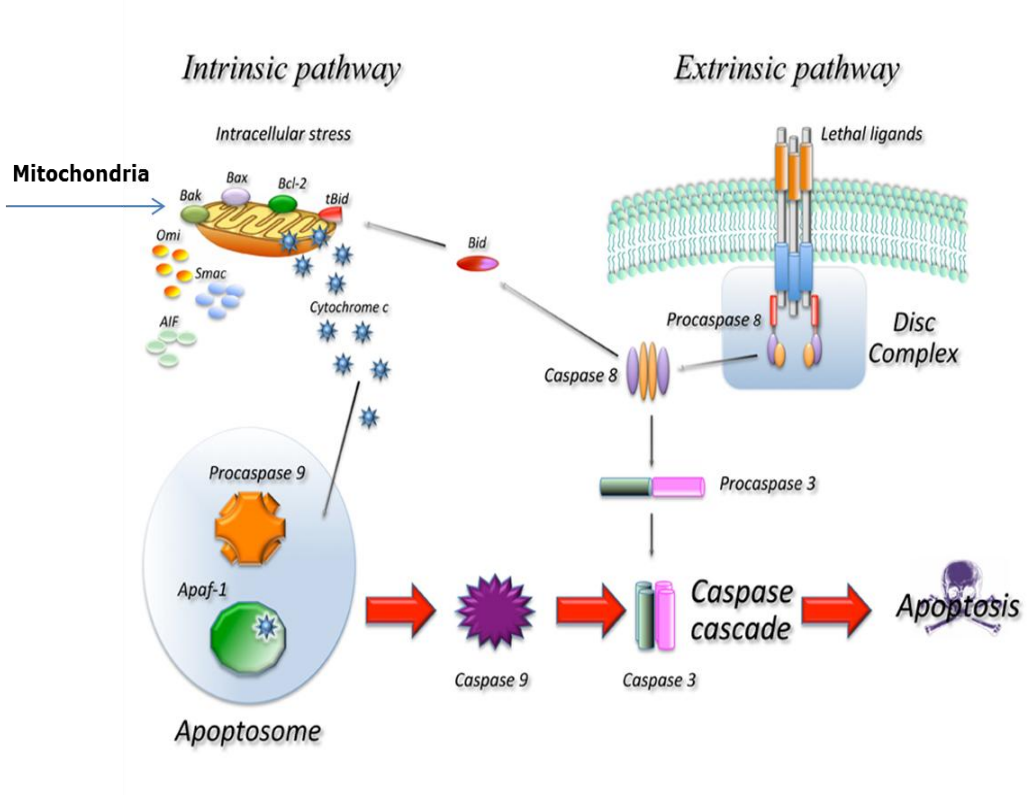

Figure 1.2 Schematic representation of the main molecular pathways leading to apoptosis. The apoptosis is a normal programmed cell death which can be activated either by extrinsic or intrinsic factors. The extrinsic pathway (CD95 pathway) indicates a form of death induced by extracellular signals that result in the binding of ligands to specific trans-membrane receptors, collectively known as death receptors (DR) belonging to the tumour necrosis factor (TNF) family which results in the activation of pro-caspase (caspase 8). In contrast, the intrinsic pathway is activated in response to a number of stressing conditions including DNA damage and oxidative stress which in turn release cytochrome c from the mitochondria and these results in the formation of the apoptosome and the activation of caspase 9. The Bcl-2 family proteins are essential regulators of intrinsic apoptosis. They can be classified as anti-apoptotic members (such as Bcl-2, Bcl-xl, Bcl-w, Mcl-1) and pro-apoptotic members (such as Bax, Bak, Bad, Bim). Pro-apoptotic members of the family mediate apoptosis by disrupting membrane integrity either directly forming pores or by binding to mitochondrial channel proteins, while anti-apoptotic members prevent apoptosis by interfering with pro-apoptotic member aggregation. Finally, the activated caspase 8 and 9 (initiator caspases) then activate downstream caspases such as caspase 3, 6, and 7 (effector or executioner caspases) resulting in cell death**.** Image adapted from (Favaloro et al., 2012)**.**

1.1.2 Cancer heterogeneity theory

Tumours are heterogeneous populations of cells with different biological characteristics. The first evidence of the heterogeneity of tumours was demonstrated in 1961 by Southam and Brunschwig. They harvested cancer cells at different cell densities from 35 recurrent tumours including (adenocarcinomas, epidermoids, and sarcomas) and auto-transplanted the cells at different sites. These experiments showed that among the total of 35 patients, only 7 developed nodules at an auto-transplant site, six of these were adenocarcinomas, none was epidermoid carcinoma, and 1 was a sarcoma. This suggested hypothesis that a subset of these cells, not all of them, had the ability to initiate the tumour and that there could be a hierarchy of tumour-initiating cells. Moreover, they showed that at least one million cells were needed to establish a new tumour as no growth appeared at sites of inoculation of less than 1 million cells (Southam and Brunschwig, 1961). By the early 1990s, it was clear from analysis of cell surface expressed proteins (complementarity determining (CD) proteins) that tumour cells were heterogeneous in terms of their protein expression. Lapidot *et al.,* demonstrated heterogeneity of function, when they found that $CD34^{+}CD38^{-}$ cells from patients with acute myeloid leukaemia were able to initiate tumour when they injected to non-obese diabetic severe combined immunodeficiency mice while injection of the $CD34^{+}CD38^{+}$ did not initiate the tumour (Lapidot et al., 1994). These findings confirmed that not all the cells in the tumour are responsible for the progression of the tumour and lead to the establishment of a new theory called the cancer stem cell (CSCs) hypothesis (section 1.1.3 for more details) which proposes that growth and progression of many cancers are driven by small subpopulations of CSCs rather than all the cells in the tumour (Reya et al., 2001). Since then, scientists have searched for the presence of CSCs in solid tumours and their unique CD markers for example, Al-Hajj *et al.,* found that $CD44^{+}CD24^{-}$ cells had significant tumour-initiating capacity in breast cancer (Al-Hajj et al., 2003). Following this discovery, CSCs

have been identified in other hematological and solid tumours such as brain tumours (Singh et al., 2004).

1.1.3 Cancer stem cells (CSCs) hypothesis

Stem cells are the cells that have the ability to control their growth and self-renewal as well as differentiate into the three germ layers: endoderm, mesoderm and ectoderm (pluripotency). The major function of stem cells is replacing dead and damaged cells in the tissue (Goldstein and Schneider, 2010). CSCs refer to a subset of tumour cells that has the ability to self-renew and generate a tumour which is drug-resistant through different mechanisms. These cells have been termed cancer stem cells to reflect their stem-like properties and their ability to continually sustain tumorigenesis. CSCs share common features with normal stem cells, including self-renewal and differentiation capacity (Reya et al., 2001).

Four methods are generally used to characterise CSCs: (1) the isolation of a "side population" or "sub-population" (SP) by flow cytometry, (2) identification of a small population of cells based on cell surface marker expression, (3) their ability to differentiate, and finally (4) by their ability to form spheres (colonies). The first observation of the SP was by Goodell and colleagues when they noticed that a small population of cells in bone marrow aspirates did not accumulate a cellular dye (Hoechst 33342) (Goodell et al., 1996). Subsequently, the SP has been shown to be the result of the dye being extruded by certain transporters of the ATP-binding cassette (ABC) family, such as ABCG2 (Zhou et al., 2001). However, the expression of ABCG2 might not be suitable to identify CSCs since purification of $ABCG2^{+}$ cells did not correlate with increased tumorigenesis when compared with $ABCG2^{-}$ cells. Therefore, the absence of Hoechst 33342 from cells may not depend completely on the efflux by drug transporters but it may also be because cells are in quiescence state, which is indeed another characteristic of stem cells (Hurt and Farrar, 2010).

Cell markers are proteins expressed on the surface of all cells and are used to identify and isolate cells. The first discovered cell markers used to identify CSCs were CD133 and CD44. Firstly, CD133, also known as Prominin-1 or AC133, is a single polypeptide chain of 865 amino acids with a molecular weight of 120 kD (due to glycosylation). Previously, CD133 was known as a haematopoietic stem cell marker and it remains an important marker for the determination and the isolation of primitive stem and progenitor cells in haematopoietic as well as non-haematopoietic tissues. Although CD133 function remains unknown, *in vitro* studies showed that CD133 expression is found on cells able to undergo differentiation to neural cells, endothelial cells and hepatocytes. For example, $CD133^+$ cells isolated from human fetal brain were able to form self-renewing neurospheres *in vitro* and subsequently differentiate to neurons and glial cells (Uchida et al., 2000). However, the role of $CD133^+$ in brain tumour initiation and progression is still controversial since research showed that $CD133^-$ brain tumour cells can also generate heterogeneous tumours *in vivo* (Cheng et al., 2009). On the other hand, CD44 is a glycoprotein that is a receptor of hyaluronic acid, a major component of the ECM. Unlike the unknown role of CD133, CD44 was found to play a role in the invasion of variety of tumour cells including breast and prostate tumours (Omara-Opyene et al., 2004, Sheridan et al., 2006). However, other cell surface stem cells markers have been shown to have prognostic significance role in CSCs identification such as $CD34^+CD38^-$ cells (Hurt and Farrar, 2010).

In addition to the previous, CSCs can also be identified functionally as they are able to form spheres in culture and differentiate into several brain cell types. In 1992 Reynolds and Weiss was the first to demonstrate that cells isolated from the striatum of adult mouse brain have the ability to form neurospheres and generate both astrocytes and neurons (Reynolds and Weiss, 1992). Similarly, Hussein *et al.,* characterised the ability of CSCs in 7 paediatric brain tumours (2 medulloblastomas, 2 ependymomas, 1

glioblastoma, 1 oligodendroglioma, and 1 CNS primitive neuroectodermal tumour) established within the Children's Brain Tumour Research Centre (CBTRC) to form neurospheres and to differentiate. They found that neurospheres derived from brain tumours can be serially passaged for up to 11 generations, and had retained the relative CSC component and characteristics. In contrast to cells grown in standard monolayer culture, CSCs grown in neurospheres can be differentiated into the three neural lineages indicating that neurospheres enriched with brain CSCs have a higher capacity to undergo multipotent differentiation (Hussein et al., 2011).

Understanding the biology of any tumour is an important step to designing the best system for diagnosis and treatment. Moreover, these discoveries (heterogeneity of cancer and the presence of CSCs) result in a more comprehensive understanding about the biology of several tumours including the brain tumours. Brain tumours are considered as one of the rare tumours but are associated with a high morbidity rate. In the next sections, more details about the structure of the human nervous system (brain and cells), functions, and tumours will be described.

1.2 Human nervous system

1.2.1 Structure and function

The human nervous system is a complex network of specialised cells which control all the vital functions in the human body such as detecting changes in external and internal environments, learning, memory, intellect and personality, transmitting signals to different parts of the body and therefore, organising the functions and bringing about appropriate responses to organs, glands, and muscles. The major structural and functional unit of the nervous system is the nerve cell or the neuron. Neurons in the brain can be classified broadly into three main types of cells: (1) sensory neurons (which transmit nerve impulses from sensory receptors to the central nervous system (CNS), (2) interneurons (which occur within the CNS), and (3) motor

neurons (which transmit nerve impulses from the CNS to either muscles or glands). The receiving and transmitting of information by neurons is highly controlled because this information is passing between adjacent neurons through specialised regions called synapses. Although there are different shapes and sizes of neurons in different parts of the nervous system, all neurons share the same characteristics [they all contain a single cell body from which a variable number of branching processes emerge (dendrites and axons) through which they receive signals from other nerves] (Crossman and Neary, 2005, Longstaff, 2009). Besides the neurons, the CNS is made of other types of cells. The most important cell types include neuroglia cells (also known as glial cells) and other non-specific CNS cells such as those forming the walls of blood vessels in the brain. Neuroglia cells are generally smaller but more numerous than nerve cells in the brain and unlike the neurons, they do not play any role in information processing but, nonetheless, provide support functions for neurons. There are three main neuroglia cell types: (1) microglia (digestion of parts of dead neurons), (2) astrocyte (providing physical and nutritional support for neurons), and (3) oligodendrocyte (manufacturing myelin for neurons) (Crossman and Neary, 2005, Longstaff, 2009).

The nervous system is divided into two main types, the central nervous system (CNS) and the peripheral nervous system (PNS). The CNS is made of the brain and the spinal cord; this is the most complex part of the nervous system, whereas the PNS is made of clusters of sensory neurons and peripheral nerves connecting it with the CNS. The CNS can also be divided into areas such as grey matter and white matter. Grey matter contains a high proportion of neurons and is found mainly in the cortical layers that line the surface of the brain and the spinal cord. On the other hand, white matter is composed mainly of myelinated axons and covers much of the interior areas of the brain and the spinal cord (Crossman and Neary, 2005). The human brain structure is divided into three main parts: forebrain, midbrain, and

hindbrain. The **forebrain** consists of cerebrum (cerebral cortex), thalamus, and hypothalamus, whereas the **midbrain** consists of the tectum and the tegmentum, and finally, the **hindbrain** consists of the cerebellum, pons, and medulla oblongata. The midbrain (minus the cerebellum), pons, and medulla oblongata are often referred to as the **brain stem** (figure 1.3).

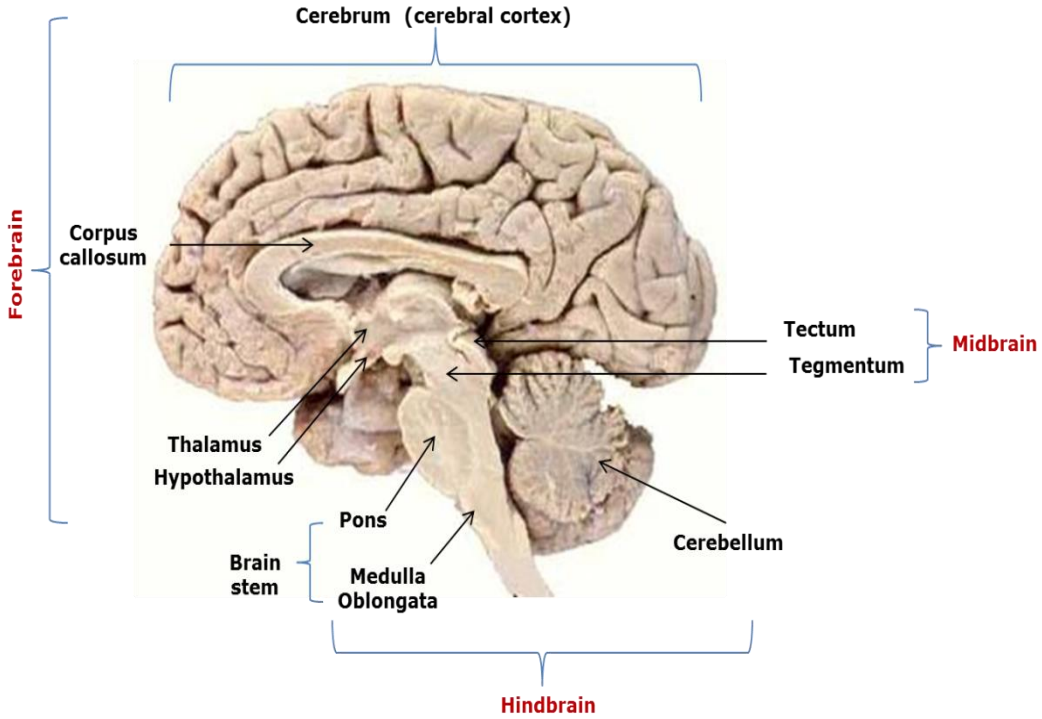

Figure 1.3 Human brain structure. The brain is divided into three main parts: forebrain, midbrain, and hindbrain. The forebrain contains cerebral cortex, corpus callosum, thalamus and hypothalamus. The midbrain contains tegmentum and tectum, and finally the hindbrain is composed from pons and medulla oblongata. Each part organises specific functions. For instance, the functions of the forebrain are wide-ranging and it is involved in the higher functions such as thinking, reasoning, processing of cognitive, auditory, sensual, and visual information, whereas, the midbrain is associated with vision, hearing, motor control, sleep/wake, and temperature regulation. Finally, the hindbrain organises important body functions such as breathing and controlling heart beats (Longstaff, 2009).

Regarding the **forebrain**, the *cerebrum* is the largest part of the human brain and it is also known as the cortex. It is involved in the higher brain functions such as learning, emotions, visual processing, reasoning, planning, and movement. It is composed of four major lobes: the frontal lobe, parietal lobe, occipital lobe, and temporal lobe (figure 1.4). Each lobe is responsible for a particular function for example (1) the frontal lobe is located at the front of the brain and is associated with reasoning, planning, parts of speech, movement, emotions, and problem solving , (2) the parietal lobe is located in the middle section of the brain and is responsible for movement organisation, orientation, recognition, and perception of stimuli, (3) the occipital lobe is located on the bottom section of the brain and is associated with visual processing , and (4) the temporal lobe is located at the back portion of the brain and is associated with the perception and recognition of auditory stimuli, memory, and speech (Longstaff, 2009). The *thalamus* is responsible for all sensory input except smell, it is connected with parts of the cerebrum which are concerned with movement, cognition, and emotion whereas, *hypothalamus* is smaller than the thalamus but it is involved in thermoregulation and in triggering sleep. In the **midbrain,** the *tegmentum* is responsible for motivation whereas, the *tectum* is responsible for the visual and auditory reflexes. The last part of the brain, the **hindbrain**, is composed of the *cerebellum* (literally "little brain") which comprises about a quarter of the mass of the brain and it is associated with control of the precise timing and execution of voluntary movement and has a role in cognition. The *medulla oblongata* and *pons* are involved in the control of the cardiovascular system, ventilation, and airway reflexes (Longstaff, 2009).

In addition, the human brain can be divided into either supratentorial or infratentorial regions. This classification is mostly used clinically to describe the location of a brain tumour. The tentorium cerebelli is an extension of the dura mater (the outermost of the three layers of the meninges surrounding the brain and spinal cord) that separates the cerebellum from the inferior

portion of the occipital lobe (see figure 1.4 for more clarification). The term "supratentorial" refers to the area located above the tentorium cerebelli i.e., the region of the brain which contains the cerebrum, whereas, "infratentorial" refers to the area located below the tentorium cerebelli i.e., the region of the brain which contains the cerebellum (Crossman and Neary, 2005).

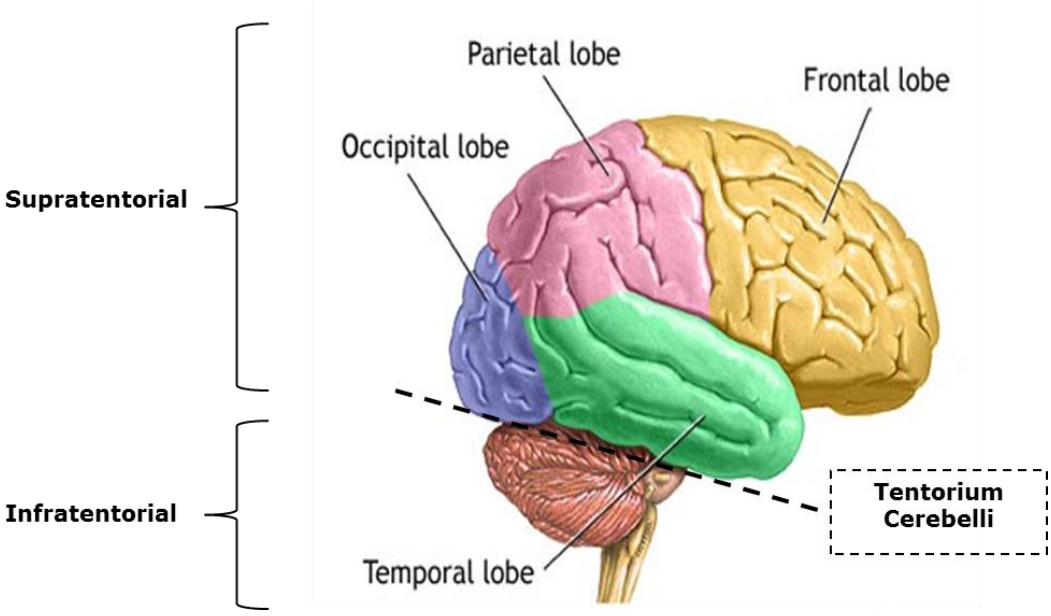

Figure 1.4 The major parts of the cerebrum. The cerebrum is the largest part of the brain and it is considered as a part of the forebrain part. It is divided into four major lobes. Each lobe has different set of functions for example: imaging, reasoning, and planning (frontal lobe), hearing and smelling (temporal lobe), senses organisation (parietal lobe) and processing images and linking them to memories (occipital lobe). Any damage to a particular lobe may determine the type of problems that could be expected. Moreover, the brain can be separated into two main parts by the tentorium cerebelli: the region of the brain which contains the cerebrum is known as supratentorial, in contrast, the region which contains the cerebellum is known as infratentorial. These two terms are important to classify the location of the tumours of the brain and the CNS (Longstaff, 2009).

1.2.2 Brain and central nervous system (CNS) tumours

CNS tumours are intracranial tumours which can develop at any site in the brain and spinal cord. They are rare tumours (accounting for 2% of all tumours) which affect both adults and children. CNS tumours are classified according to: (1) the site of the tumour within the brain, (2) the type of the tissue involved, and (3) whether the tumour is malignant or benign. In the UK, 4,785 new cases of malignant brain and CNS tumours were diagnosed in 2008. This equates to around 8 for every 100,000 people. According to the last incidence report from the Cancer Research UK, it has been estimated that the lifetime risk of developing a malignant brain and other CNS tumour in adults is 1 in 130 for men and 1 in 173 for women. These tumours can occur at any age, however, there are two peaks of incidence; one small peak in childhood, and a second larger peak in adults in their 70s (Office for National Statistics, 2010). Although cancer is rare in childhood, 1550 children are diagnosed annually with cancer in UK. Brain tumours are the second most common tumour in children (under the age of 15 years) after leukaemia and they considered as the most common cause of childhood cancer death, accounting for around a third of all cancer deaths in childhood (Cancer Research UK, 2010).

Although many risk factors have been examined to study the epidemiology of CNS tumours over the past several decades, there are few consistent findings possibly due to small sample sizes in individual studies, tumour types, and methods of classification. However, research suggested that there is an association between heritable diseases and the CNS tumours formation particularly gliomas, medulloblastomas and ependymomas. Although the genetic syndromes caused by rare inherited mutations and associated with higher risk of brain tumours account for few cases, they provide an important starting point for identifying candidate genes and pathways for pathogenesis of several brain tumours. The major genetic diseases contributing to brain tumours are phakomatosis which include

neurofibromatosis (NF), tuberous sclerosis (TSC), Li-Fraumeni syndrome and von Hippel-Lindau syndrome (Melean et al., 2004). Another cause for CNS tumours is the exposure to ionising radiation. The development of meningiomas in children and malignant glioma in adults are more common in patients who have had radiotherapy to the head in the past (Ron et al., 1988). Non-ionising radiation such as mobile phones did not correlate to the establishment of brain tumours even with longer duration of use (Cardis et al., 2007). However, a recent report from the International Agency for Research on Cancer (IARC) revealed that using mobile phones for ≥1640 hours in total increase the risks for glioma development (Odds Ratio (OR)=2.29, 95% confidence interval (CI)=1.56-3.37) (Hardell et al., 2012).

Approximately 60% of all primary brain tumours are gliomas. Glioma is a malignant brain or spine tumour. It is called a glioma because it arises from glial cells. The most common site of gliomas is the brain. There are 3 main types of glioma: astrocytoma, ependymoma, and oligodendroglioma. Regarding *astrocytomas*, they are the most common type of glioma in both adults (75%) and children (43%) and develop from astrocytes. Astrocytic tumours are diffusely infiltrative tumours i.e., having the ability to arise at any location in the CNS, but show a preference for the cerebral hemispheres (Kleihues et al., 2007a). More details about astrocytomas subclasses are in (table 1.1). *Ependymomas* represent about 5% of all brain tumours. These tumours are developed from the ependymal cells, which are cells that line the fluid filled areas of the brain (the ventricles) and the spinal cord. In contrast to astrocytomas, ependymomas are mostly diagnosed in children or young adults (Scheithauer et al., 2007). Finally, *oligodendroglioma* also accounts for 5% of all brain tumours and they originate from oligodendrocytes (Stiller, 2007). Despite advances in the diagnosis of primary brain tumours and the availability of successful therapies for some tumour types, brain tumours are one of the worse leading cause of cancer mortality in both children and adults (Office for National Statistics, 2010).

Table 1.1 The World Health Organization (WHO) classifications of astrocytomas

WHO grade	Astrocytomas	Description
I	Pilocytic astrocytoma, and Subependymal giant cell astrocytoma	• Slow growing • Benign and associated with long-term survival • Complete surgical remission is possible (Scheithauer et al., 2007)
II	Diffuse astrocytoma	• Relatively slow-growing tumours but they can evolve into higher grade tumours • Prevalent in younger people • They can penetrate into the neighbouring normal brain tissues, making a complete surgical cure more difficult • Recurrences are relatively common because this subtype is infiltrative • The 5-year survival rate for patients with WHO grade II tumours is about 34% without treatment and about 70% with radiation therapy (Von Deimling et al., 2007)
III	Anaplastic astrocytoma	• Fast growing, a diffusely infiltrating malignant astrocytoma • It is mostly affect adults • It is histologically characterised by nuclear atypia (abnormal appearance of cell nuclei), increase cellularity and significant proliferative activity • The standard initial treatment includes surgery, chemotherapy, and radiotherapy (Kleihues et al., 2007b)
IV	Glioblastoma Multiforme	• Fast growing • The most common and most malignant primary brain tumour with poor survival rate • Histologically it is characterised by nuclear atypia, cellular pleomorphism, mitotic activity, vascular thrombosis, microvascular proliferation and necrosis • They cannot be completely resected because of the infiltration (Kleihues et al., 2007a)

In this study, the high grade glioma (HGG) particularly WHO grade IV-glioblastoma multiforme (GBM) will be described in details as this tumour considered the major primary brain tumour.

1.3 Glioblastoma multiforme (GBM) (WHO grade IV)

1.3.1 GBM incidence, risk factors and symptoms

The term HGG includes glioblastoma multiforme (GBM), anaplastic astrocytoma (AA), and diffuse intrinsic pontine glioma (DIPG). These tumours are the most malignant primary brain tumours which typically affect adults more than children and are preferentially located in the cerebral hemispheres except for DIPG which occurs in the pons (middle brain stem) (Kleihues et al., 2007a, Kleihues et al., 2007b). GBM is one of the most frequent human brain tumours. Internationally, it accounts for 12-15% of the CNS tumours and 60-75% of astrocytic tumours (Kleihues et al., 2007a). In a series of 987 glioblastomas from University Hospital Zurich, the most frequently affected sites were the temporal (31%), parietal (24%), frontal (23%) and occipital (16%) lobes (see figure 1.3) (Ohgaki and Kleihues, 2005).

GBM can be clinically subdivided into either primary or secondary. Primary GBM accounts for the majority of patients (60%) in adults older than 50 years. This tumour manifests *de novo* (i.e., without clinical evidence of a pre-existing lesion), presenting after a short clinical history, usually less than 3 months. On the other hand, secondary GBM (40%) develop in younger patients (< 45 years old) through malignant progression from diffuse astrocytoma (WHO grade II) or anaplastic astrocytoma (WHO grade III). The time required for this progression varies considerably, ranging from less than 1 year to more than 10 years, with a mean interval of 4-5 years. Increasing evidence indicates that primary and secondary GBMs have distinct characteristics that evolve through alterations in different signalling pathways, affect patients at different ages, and differ in response to some of the current therapies (Kleihues et al., 2007a). For example, primary GBM is characterised

by overexpression or mutation of epidermal growth factor receptor (EGFR) (36%), genetic losses on chromosome 10 (70%), p16 or p19 alterations (31%), or loss of *PTEN* (25%) whereas, secondary GBM displays genetic alterations including *TP53* mutation (65%) or overexpression of platelet-derived growth factor receptor alpha (PDGFRα) (Biernat et al., 1997, Ohgaki et al., 2004). Interestingly, HGG exhibits different features in adults than in children regarding the incidence, molecular biology changes, and the treatment regimen used (Heideman et al., 1997). In the following sections, the major clinical features of GBM in adults will be discussed in details. However, in some sections a comparison between adults and paediatric will be mentioned when relevant. Mean survival is inversely correlated with age. Without therapy, patients with GBM die within 3 months. In contrast, patients treated with optimal therapy i.e., surgical resection, radiation therapy, and chemotherapy, have a median survival of approximately 12 months, with fewer than 25% of patients surviving up to 2 years and fewer than 10% of patients surviving up to 5 years (Ohgaki and Kleihues, 2005). Regarding the race and sex incidence, GBM is slightly more common in whites than blacks and males have a slight preponderance over females (male: female ratio of 3:2) (Ohgaki and Kleihues, 2005, Office for National Statistics, 2010).

Many *risk factors* were found to be contributing to the development of GBM. Ionising radiation is among the first studied risk factors and showed a positive relationship with several brain tumours including gliomas (Modan et al., 1974). Genetic abnormalities were also investigated for their association with GBM. However, only 5% of GBM cases are currently correlated with genetic disorders. Examples of genetic syndromes include neurofibromatosis 1 and 2 (*NF1* and *NF2* on chromosomes 17q11 and 22q12, respectively), tuberous sclerosis (*TSC1* and *TSC2* on chromosomes 9q34 and 16p13, respectively), retinoblastoma (*RB1* on chromosome 13q14), and Li-Fraumeni (*TP53* on chromosome 17p13) (Melean et al., 2004). Among all these syndromes, Li-Fraumeni syndrome and neurofibromatosis type I (NF-1) were

strongly correlated with GBM in both adults and children. Patients with the Li-Fraumeni syndrome have defects in the *TP53* gene that encodes for the *p53* suppressor protein. This gene is one of the major mutated genes in glioma. Therefore it is proposed that mutations in this gene increase the ability of the Li-Fraumeni patients to develop GBM (Melean et al., 2004). Patients with NF-1 have a deficient *NF-1* gene which encodes for the neurofibromin protein, which is expressed primarily in neurons and astrocytes. This protein acts as a regulator for cell growth and functions as a negative regulator of the *Ras* proto-oncogene. Indeed, the complete loss of *NF-1* gene leads to the development of a variety of benign and malignant tumours in both CNS and PNS (Ward and Gutmann, 2005). Additionally, several polyomaviruses such as John Cunningham and simian virus 40, have been found in human glioma tissue and can induce brain tumours establishment in animals (Rollison et al., 2003). Neurocarcinogens and metals have been studied to elucidate their role in the development of brain tumours. In one study to detect the effect of 6 occupational factors (agricultural, chemical, construction, metal, electrical/electronic and transport) on the transformation of low grade gliomas (LGGs), only the exposure to metal was correlated to an elevated risk for glioma (Schlehofer et al., 2005).

The major *clinical features* of patients with GBM include increased intracranial pressure (IP) which is characterised by headache, nausea, vomiting, and papilloedema (the swelling of the optic disk). Moreover, the clinical symptoms of this tumour are usually short (less than 3 months), unless the neoplasm developed from a lower-grade astrocytoma (secondary GBM) and up to one-third of patients experience an epileptic seizure. In a few cases, non-neurological symptoms can be observed such as personality changes. The Focal signs depend on the affected area of the brain and include hemiparesis (weakness in one side of the body), sensory loss, visual loss, and aphasia (the disturbance in the formulation and comprehension of language) (Kleihues et al., 2007a).

1.3.2 Glioblastoma multiforme (GBM) histopathology

As its name indicates (multiforme), the histopathology of this tumour is variable. The major histopathological features for GBM include nuclear atypia (pathological variation in the appearance of the nuclei), cellular pleomorphism (variations in the size and shape of cells or/and their nuclei), high mitotic activity, high vascular thrombosis, necrosis and hypoxia (figure 1.5a and b). Macroscopically, GBM is poorly delineated showing a variable colour with peripheral greyish tumour masses and central areas of yellowish necrosis resulted from myelin breakdown. The diagnosis of GBM depends on the tissue pattern (histological) more than the morphology of the cell types. The central necrosis typically accounts for 80% of the total tumour mass and it indicates the aggressive behaviour of GBM. The necrotic area is usually located in the centre of the tumour whereas the remaining viable cells are located in the periphery of the tumour (figure 1.5c). The vascular proliferation is seen often around the necrotic area (Kleihues et al., 2007a). Imaging studies of the brain are essential to understand the pathogenesis of GBM. On computerised tomography (CT) scans, GBM usually appears as irregularly shaped hypodense lesions with a peripheral ring like zone of contrast enhancement (figure 1.6).

1.3.3 Glioblastoma multiforme (GBM) prognostic markers

The current method of classification for GBM is based on the histopathology. Histopathology could be augmented by having prognostic markers that correlate with disease progression. Histologically marker such as glial fibrillary acidic protein (GFAP) remains the most valuable marker for neoplastic astrocytes (Jung et al., 2007). Although immunostaining is variable and tends to decrease with progressive dedifferentiation, many cells remain immunopositive for GFAP even in the most aggressive glioblastomas. Vimentin and fibronectin expression are common but less specific markers for GBM compared to GFAP (Ivaska et al., 2007).

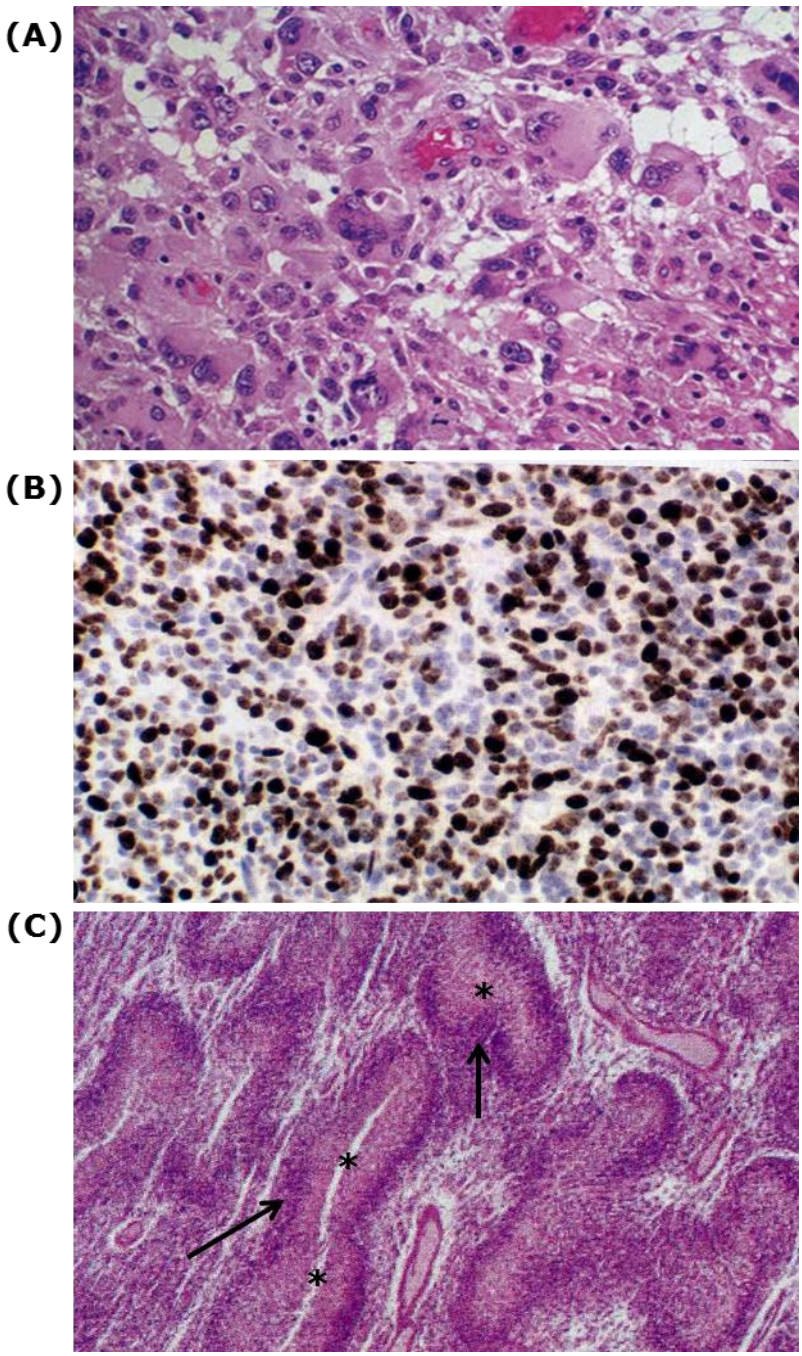

Figure 1.5 The histopathology of GBM. (A) Glioblastoma with a high degree of anaplasia. Anaplasia refers to the dedifferentiation of cells (loss of structural and functional differentiation of normal cells) and is a characteristic of malignant tumours. Lack of differentiation is considered a hallmark of aggressive GBM. (B) High proliferation capacity of GBM indicated by a high MIB-1 (Ki-67) labelling index (brown cells). Ki-67 is a cellular marker for proliferation and is present during all cell cycle phases (G_1, S, G_2, and mitosis) but not in the resting cell phase (G_0). (C) Large area of necrosis characterised by the formation of pseudopalisading necrosis (indicated with black arrow and asterisk). Pseudopalisades are characterised by an accumulation of tumour cells (↗) around central necrosis (*) and typically have internal, peripheral zones of fibrillarity. Images adapted from (Kleihues et al., 2007a).

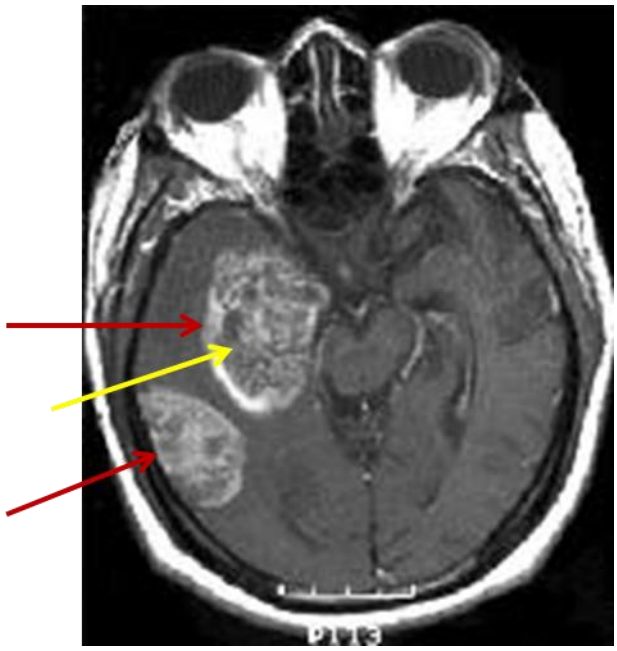

Figure 1.6 Computerised tomography (CT) scan for a GBM patient. A heterogeneous enhancement of the lesion is present within the right temporal lobe of the brain (red arrows). The hypo-intensity circumscribed within the enhancement is suggestive of necrosis (yellow arrow) (Kleihues et al., 2007a).

The reason behind the poor availability of prognostic markers of GBM is the heterogeneous nature of this tumour (section 1.1.2). The regional heterogeneity of glioblastomas is remarkable and makes histopathological diagnosis a serious challenge when it is based solely on biopsies. Tumour heterogeneity is also likely to play a significant role in explaining the insignificant success of all treatment regimens, including radiation therapy and chemotherapy (Bonavia et al., 2011).

Transcriptomic and proteomic approaches have been applied to identify specific markers which could help in the diagnosis of GBM as well as reflect the response of patients to therapy. For instance, in a microarray (transcriptome) study to identify markers for GBM and other astrocytomas, Reddy *et al.,* found that growth arrest and DNA-damage-inducible alpha and follistatin-like 1 were specific markers for GBM as they were up-regulated in most GBMs (both primary and secondary), whereas superoxide dismutase 2

and adipocyte enhancer binding protein 1 were considered as markers for primary GBM as they were up-regulated in the majority of primary GBM patients (Reddy et al., 2008). Another recent study used proteomic approaches to elucidate candidate proteins for the diagnosis of GBM, identifying 10 proteins which showed significant differences in expression between GBM samples and non-tumorous samples (Banerjee et al., 2012). However, the data from the last two examples have not been followed up either in GBM patient tissue microarrays (TMA) or in model systems and their putative role in GBM remains unclear.

1.3.4 Glioblastoma multiforme (GBM) treatment

Although this tumour is now being diagnosed earlier than before and localised more accurately due to the application of the magnetic resonance imaging (MRI), GBM remains difficult to treat. The classical treatment regimens for GBM involved surgery, radiotherapy, and chemotherapy which will be discussed below in more detail.

1.3.4.1 Neurosurgical approach

Surgery is an important and integral step in the treatment of GBM because it helps to establish a histopathologic diagnosis and to achieve safe maximal tumour resection, which may improve the patient survival. The basics of neurosurgery include the diagnosis of the tumour location with MRI and then the resection of tumour successfully by the neurosurgeon with minimised morbidity risks. The location of the tumour is a major factor for a complete or partial resection of the tumour. The role of the surgery in the survival rate of GBM patients is controversial. The data from 645 GBM patients in three prospective Radiation Therapy Oncology Group trials were analysed to determine the median survival rate for patients with total resection, partial resection, or biopsy only. Simpson *et al.,* found that the median survival was 11.3 months for total resection, 10.4 months for partial

resection, and 6.6 months for biopsy indicating that surgery is important but complete resection may not give added benefit to the survival rate of GBM patients (Simpson et al., 1993). In contrast, however, Stummer *et al.,* analysed the response of GBM patients with little or no residual tumour after surgery. Median survival was 16.9 months for patients with residual tumour diameters >0 to ≤1.5 cm (95% CI: 13.3–20.5, $P = 0.039$) and 8.5 months (6.2–10.9, overall $P \leq 0.001$) for patients with residual tumour diameters ≥1.5 cm. These findings suggested that the extent of resection was independently associated with survival (Stummer et al., 2012). In support of this, other trials showed that complete resection seems to improve to some degree the survival rate of the patients. However, these trials were usually combined with adjuvant chemotherapy and/or radiotherapy. For example, Abrudan *et* found that the mean survival for patients with complete resection was 11.5 months (95% CI from 10.7-12.4) compared to a survival rate for partial resection group of 7.1 months (95% CI from 5.5- 8.7, $p<0.005$) (Abrudan et al., 2011).

The combination of surgery, radiotherapy, and chemotherapy results in an improvement in the survival rate for GBM patients compared to the surgery alone. For instance, a cohort-based study on GBM cases in the Ontario Cancer Registry identified that the median survival rate for patients who received radiotherapy alongside surgery has increased their survival to 11 months compared to the median survival rate for patients with surgery alone of just 3 months (Paszat et al., 2001). In addition, in 2004 a phase III clinical trial conducted by the European Organisation for Research and Treatment of Cancer and the National Cancer Institute of Canada Clinical Trials Group revealed that patients with complete resections seemed to benefit more than those with partial resections and the worst outcome was in patients who had biopsy only (Stupp et al., 2009). The patients in this trial received either radio-and-chemotherapy or radiotherapy only alongside the surgical resection. The 5- year survival rate in patients who received

chemotherapy (temozolomide-TMZ) and radiotherapy was higher in GBM patients [9·8% (6·4–14·0) compared to patients who received radiotherapy alone 1·9% (0·6–4·4)] (Stupp et al., 2009).

1.3.4.2 Radiotherapy approach

The treatment of GBM in children is different from adult. The best treatment regimen in adult includes surgery and radiotherapy whereas, in children, radiotherapy is not recommended, especially for children less than 3 years because of its harmful effect on the developing nervous system since it can reduce the child intelligence quotient and moreover, it is considered as a possible cause for second malignancy (Heideman et al., 1997). The main goal of the radiotherapy is to introduce the best therapeutic ratio that kills all cancer cells which are able to go through clonogenic devisions without harming the neighbouring tissues and normal cells (Kun, 1997). Radiation therapy means using a high-energy x-ray to destroy the cancer cells or stop them from dividing. Ionising radiation include: (1) photons (which are produced from rapidly stopped accelerated electrons), (2) particulate radiations such as electrons, neutrons, and heavy charged particles (which are produced by high- energy electromagnetic devices), as well as (3) gamma rays (x-rays emitted from the decay of the radioactive materials). The amount of radiation used in photon radiation therapy is measured in gray units (Gy). One gray is the absorption of one joule of energy per Kg of tumour mass. The selection of the perfect radiation treatment type (curative, adjuvant, neoadjuvant, palliative, or therapeutic) and dose depends on (1) tumour type and size, (2) tumour location and (3) whether the tumour is susceptible to metastasis or not. Usually the local target volume is used for tumours that remain in a single anatomic area whereas, whole-brain radiation is preferred in tumours with high susceptibilty to metastasis (Kun, 1997, Kleihues et al., 2007a). The use of adjuvant external-beam radiotherapy is well established in the postoperative treatment of adult GBM. External-beam radiotherapy is

generally administered over 5–6 weeks, delivering a total dose of 50–60 Gy in 1.8 to 2 Gy fractions.

Although radiotherapy can result in undesirable side effects, it remains the first line of adjuvant treatment for GBM following the surgery (Heideman et al., 1997) and when combined with chemotherapy, a significant improvement in the survival has been shown. For instance, a pooled analysis of six randomized trials by Cancer Care Ontario reported a significant survival benefit with postoperative radiotherapy as compared to no radiotherapy (surgery alone). Overall, median survival was approximately 36–48 weeks with adjuvant radiotherapy as compared with 14–22 weeks with surgery alone (Kelly et al., 1984). Moreover, data from 340 patients with newly-diagnosed GBM were analysed to predict the factors which could affect the survival of the patients. Among several factors, radiotherapy with 45 Gy dose was found to be the predominant affecting factor that influenced the survival as shown from the univariate Log-rank test *P* value $<10^{e-10}$, followed by radical surgery, tumour location, age and finally chemotherapy (Mineo et al., 2007). In a recent phase II trial, 35 GBM patients underwent either surgical resection or biopsy followed by radiotherapy to a total dose of 60 Gy in 2-Gy daily fractions. The median survival for the entire cohort (n=35 patients) was 15.8 months compared with Radiation Therapy Oncology Group radiotherapy-alone historical control survivals of 11.1 months. In addition, 16 patients from the 35 patients received TMZ alongside radiotherapy. The median survival was 20.8 months, compared with European Organization for Research and Treatment of Cancer historical controls of 14.6 months (Einstein et al., 2012).

1.3.4.3 Chemotherapy approach

In a chemotherapy regimen, certain toxic drugs for the cancer are given to the patient usually orally or in injection. This may be given alone or in combination with other therapies (radiotherapy, immunotherapy, and surgery) and it is considered generally safer than radiotherapy. Chemotherapy

is given in cycles to the patients with a period of days between each cycle to assess the patient's response to the treatment dose. The first chemotherapeutic agents used in the treatment of GBM were nitrosureas. Several trials used high-dose nitrosoureas and showed an effective response on the glioma patients but unfortunately resulted in severe hepatic, pulmonary, as well as CNS toxicity. Usually the patients who are most likely to receive high dose chemotherapy are those with recurrent tumours who have previously either no chemotherapy at all or had minimal therapy before or those whose tumours showed sensitivity to conventional-dose therapy (Mason et al., 2007). For example, a phase II clinical trial evaluated the effect of carmustine or bis-chloroethylnitrosourea for 8 weeks (maximum 6 cycles) in 40 patients with recurrent GBM who had undergone surgery and radiotherapy. They found that the median time to progression was 13 weeks and the 6 month progression-free survival (PFS) was 17.5% compared to the previous reported studies. However, significant side effects included reversible hematologic toxicities and chronic hepatic and pulmonary toxicity were observed (Brandes et al., 2004). Therefore, other alkylating agents which reduce the toxicities were established. Temozolomide (TMZ) (an alkylating agent which transfers the methyl group to O-6 or N-7 of guanine bases in DNA) is considered to be a major chemotherapeutic drug for the treatment of GBM in adults particularly in patients with an epigenetically silenced O^6-methylguanine-DNA-methyltransferase (*MGMT*) gene. However, TMZ is not the preferred chemotherapeutic agent in children and the survival rate of children treated with TMZ does not appear to be improved when compared with historical controls due to low frequency of *MGMT* promoter hypermethylation (Bax et al., 2009). In contrast, Stupp *et al.,* found that the median survival rate for adult GBM patients who received radiotherapy and TMZ was 14.6 months in comparison to patients who received radiotherapy alone (12.1 months). Moreover, the two-year survival rate was 26.5% with radiotherapy and TMZ and 10.4% with radiotherapy alone (Stupp et al.,

2005). However, the epigenetic methylation status of the *MGMT* gene did affect the response of patients to the TMZ treatment (more explanation about this will be mentioned in section 1.3.5.3 in detail). The mechanisms behind the effectiveness of TMZ and radiotherapy have been investigated. For instance, the combination between TMZ with irradiation prevents the invasiveness of glioma. The irradiation activates the focal adhesion kinase (FAK) by phosphorylation, whereas TMZ promotes FAK cleavage (Wick et al., 2002). In another study, the cytotoxic effect of TMZ in combination with x-rays in human glioma-derived cell lines (D384 and U251) was investigated by the clonogenic assay. They found that the incubation of D384 cells with TMZ for 24 hours prior to or following irradiation resulted in a moderate enhancement of the cytotoxicity whereas, prolonged treatment (48-96 hours) with TMZ before x-rays, resulted in a stronger potentiation. In contrast, no enhancement was observed in irradiated U251 cells in combination with 24-96 hours TMZ treatment. Moreover, a further 96 hours exposure to TMZ with simultaneous doses of 2 Gy x-rays each 24 hours interval, results in a significant further reduction in cell survival as compared to fractionated irradiation only. Therefore, the treatment of glioma cell lines with TMZ and x-rays can have either an additional effect or potentiate cell killing depending on the cell line (van Rijn et al., 2000).

The penetration of the molecules into the brain is restricted due to the function of blood brain barrier (BBB). The BBB permits small molecular weight molecules (200 daltons), highly lipophilic, un-ionised (at physiologic pH) compounds only to penetrate into the CNS. Therefore, several attempts were made to improve the drug penetration into the brain. One of these methods is regional therapy which involves the usage of regional (carotid artery) infusions in order to use small drug doses without increasing the systemic exposure and toxicity. Although this method improved the response of the tumour to therapy, it unfortunately can cause retinal damage due to the penetration of the drug into the surrounding normal CNS tissue. Another

major method used in chemotherapy is the disruption of BBB by the application of mannitol, which reduce the increased intracranial pressure (ICP), in order to enhance the penetration of different compounds of various sizes, molecular weight, and liposolubility. This approach is important in increases the success of administering water-soluble and large molecular weight molecules (Heideman et al., 1997, Mason et al., 2007).

1.3.4.4 Advances in the treatment of GBM

In addition to the combination between chemotherapy and radiotherapy, current studies are combining more than one chemotherapeutic agent with other agents such as anti-angiogenics, growth factor receptor inhibitors and other biological therapies, including gene therapy. The major anti-angiogenic drug used currently for GBM is bevacizumab (BVZ) which is a major angiogenesis inhibitor for vascular endothelial growth factor (VEGF). In a study, the effect of etoposide (DNA topoisomerase II inhibitor) and BVZ, in the treatment of recurrent GBM was evaluated in phase II clinical trial. The expression of VEGF, VEGFR-2, carbonic anhydrase 9 (CA9) and hypoxia-inducible factor-2α were also assessed using immunohistochemistry and were correlated with outcome. Reardon *et al.*, found that the combination of both drugs was associated with encouraging anti-tumour benefit (the median overall survival (OS) was 46 weeks and the 6 months PFS was 44.4% compared to the data from the BVZ alone). The immunohistochemistry data revealed that high CA9 and low VEGF were associated with PFS (Reardon et al., 2009). Additionally, the combination between BVZ and irinotecan (DNA topoisomerase I inhibitor) was found to increase the response ratio and PFS in recurrent GBM patients. However, no improvement in median overall survival was observed compared with conventional chemotherapy. Nevertheless, the GBM patients who respond to treatment with BVZ and irinotecan survived significantly longer than non-responders, indicating that it could be beneficial for a selection of patients to receive this treatment (Jakobsen et al., 2011). In

fact the underlying mechanisms behind the improvement in the response of the patients in the last two clinical trials remain unknown but it reflects the importance to combine more than one anti-tumour agent in treatment especially in the recurrent tumour.

Although considerable advances have been made in the treatment of GBM, the survival rate remains poor. One of the major factors behind this is the differences in the molecular and cellular biology of the GBM. These genetic alterations showed a high degree of variability between individuals. Therefore, more studies are focusing now on the molecular side of the GBM in order to establish new therapies that are unaffected by such alterations and provide better responses. The following sections will describe the major differences between adults and paediatric GBM regarding the molecular biology field.

1.3.5 Glioblastoma multiforme (GBM) molecular biology

Understanding the major biological and molecular characteristics of any tumour is important as a first step to obtaining a comprehensive picture about it. It will help in addressing and designing new therapeutic regimens and therefore improving the survival outcome of patients. Several studies showed that in GBM molecular features are different in adult compared to paediatric. There are two main categories of molecular biology changes that occur in gliomas. Firstly, abnormalities of extracellular growth factors or growth factor receptors such as epidermal growth factor (EGF) or its receptor (EGFR) and PDGF or its receptor (PDGFR). Secondly, signal transduction cascades that connect the mitogenic signals to other cellular processes, such as gene transcription. An example for such mitogen and signalling pathway is the EGF effect on either the RAS and/or Akt pathways which are most commonly activated in gliomas. These two abnormalities occur together in most glioma cases (Lassman, 2004, Liu et al., 2009b).

1.3.5.1 Abnormalities in extracellular growth factors and their receptors

EGFR is also known as *ErbB1*, it was first discovered during studies of avian erythroblastosis virus (Downward et al., 1984). It is involved in normal cell growth, oncogenesis, and wound healing. Normally, binding of EGF to EGFR leads to receptor dimerization, activation of the intrinsic receptor tyrosine kinase (RTK) activity, tyrosine autophosphorylation, and recruitment of various signalling proteins to these autophosphorylation sites which are located primarily in the C-terminal tail of the receptor. The tyrosine phosphorylation of the EGFR leads to the recruitment of several diverse signalling proteins (Lassman, 2004). PDGFR is also classified as an RTK, and PDGF is the cellular homolog of the viral oncogene v-*sis*, which is present in Simian sarcoma virus. PDGF subunits (either α and β) are important factors regulating proliferation and differentiation. The regulation of the cellular processes by PDGF is activated by the dimerization of its receptor in a mechanism similar to the EGFR mechanism (Dalla-Favera et al., 1982).

EGFR is overexpressed in 50% to 60% of adult GBM tumours (The Cancer Genome Atlas Research Network, 2008). The most common EGFR mutant in glioblastoma is the deletion of exons 2-7 known as EGFRvIII, is expressed in 24% to 67% of cases (Davies et al., 2006). EGFR overexpression occurs almost exclusively in *de novo* (primary) rather than in secondary GBMs in adults (The Cancer Genome Atlas Research Network, 2008). However, the impact of EGFRvIII on survival of patients with GBM has not been definitively established. The expression of both EGFR and EGFRvIII was assessed to determine their effect on the overall survival of 196 GBM patients. Patients underwent a ≥95% tumour resection followed by conformal radiation. Their EGFR and EGFRvIII status was determined by immunohistochemistry. They found that 46% (n =91) of patients failed to express EGFR, 54% (n =105) had overexpression of the wild-type EGFR, and 31% (n =61) also expressed the EGFRvIII. The median overall survival times for patients with tumours

having EGFR expression absent, overexpressed only, or mutant EGFRvIII were 0.96, 0.98, and 1.07 years, respectively indicating that neither the overexpression of wild-type EGFR nor EGFRvIII was an independent predictor for median overall survival in patients who underwent extensive tumour resection (Heimberger et al., 2005a). In contrast to the previous study, Montano *et al.,* found that EGFRvIII is associated with prolonged survival of GBM patients treated with surgery and radio/chemotherapy (P=0.0023). Moreover, in recurrant GBMs, EGFRvIII expression was approximately two-fold lower than in primary tumours. Depletion of EGFRvIII in recurrent GBMs as well as differential sensitivity to TMZ in *in vitro* neurosphere cell cultures indicates that the EGFRvIII-negative cell fraction is involved in resistance to radio/chemotherapy and tumour repopulation (Montano et al., 2011).

Regarding PDGF and its receptor, GBM tumours were found to express more PDGF α and β than non-neoplastic glial cells. Moreover, PDGFα and β ligand genes are expressed in almost all glioma cell lines and in fresh surgical isolates of human glioblastoma tumours indicating that PDGF is an important mitogenic growth signal (section 1.1.1 for more explanation about mitogenic signals) for the development, proliferation and maintenance of the malignant astrocyte (Maxwell et al., 1990). There are multiple lines of experimental evidence that PDGF is an important pathway in the gliomagenesis. In a study by Heldin *et al.,* the growth of glioma cell lines was enhanced significantly by the addition of PDGF to the cell culture media (Heldin et al., 1980). In addition, the genetic modification of the T98G glioma cell line with PDGFβ results in the activation of the cells growth. The T98G cells do not form normally tumours when transplanted into mice. However, with the addition of PDGFβ these cells acquired tumorigenicity suggesting that increase PDGF activity enhances the malignant potential of the cells (Potapova et al., 1996). Interestingly, the amplification of PDGF and PDGFR in adults is not as common as the amplification of EGFR. Hermanson *et al.,* analysed 83 astrocytic tumours with *in situ* hybridisation. PDGF was found to be expressed

in 11-13% of all astrocytic tumours and to a greater extent in GBM implying that PDGF-α is actively involved in tumour cell proliferation in both early and late stages of glioma development. Moreover, the expression of PDGF-α was also significantly correlated with the loss of heterozygosity 17p (P<0.0002) (Hermanson et al., 1996, The Cancer Genome Atlas Research Network, 2008). In contrast to adult HGG, several studies showed that overexpression of EGFR and PDGFR are correlated with the transformation and progression of LGG into HGG in paediatric GBM. A study was performed on 85 patients (22 HGG and 63 LGG) to determine the effect of EGFR and PDGFR expression as well as the activation of two major pathways [Ras-guanosine triphosphate/ mitogen-activated protein kinase (RAS/MAPK) and phosphatidylinositol 3-kinase/serine-threonine protein kinase/mammalian target of rapamycin (PI3K)/AKT/mTOR] on the histology, progression, and worse survival of glioma patients. They found that overexpression of phosphorylated (p-PDGFRα), EGFR, PDGFRβ, and phosphorylated (pEGFR) was seen in 85.7%, 80.0%, 78.9%, and 47.4% of HGG and 40.0%, 87.1%, 41.7%, and 30.6% of LGG, respectively but only high expression of pPDGFRα and PDGFRβ was significantly associated with malignant histology (P=0.031 and 0.005, respectively). Moreover, the loss of PTEN expression was the only parameter associated with worse overall survival. However, none of these targets either alone or in combination was significantly associated with progression-free survival in either LGG or HGG (Thorarinsdottir et al., 2008).

1.3.5.2 Abnormalities in signal transduction

The most commonly activated cascades in gliomas are the AKT and RAS pathways (The Cancer Genome Atlas Research Network, 2008). Akt or protein kinase B is a serine-threonine specific protein kinase which plays an important role in cell processes such as proliferation induction and apoptosis inhibition, transcription and cell migration via the activation/inhibition of other important pathways components such as Bad, caspase 9, mTOR, and PTEN

(Hu et al., 2005). On the other hand, Ras (an abbreviation of Rat Sarcoma) is a small GTPase protein and it is an important cellular signal transduction protein which is involved in cellular growth and differentiation and it considered as an important oncogene. Three important members of the Ras family (KRAS, HRAS, and NRAS) are involved in cancer and they were discovered in independent studies of two-cancer causing viruses (Malumbres and Barbacid, 2003). KRAS and HRAS were discovered in the Kirsten-sarcoma virus and Harvey-sarcoma virus. These viruses were discovered initially in rats in the 1960s (Harvey, 1964, Kirsten and Mayer, 1967) whereas, the third Ras family member (NRAS) was identified in 1983 in human neuroblastoma cells (Shimizu et al., 1983).

Akt is activated indirectly in glioma by RTK which activates the enzyme PI3K, which phosphorylates phosphatidylinositol 4-phosphate (PIP) to phosphatidylinositol 4,5-bisphosphate (PIP2), and PIP2 to phosphatidylinositol 3,4,5-trisphosphate (PIP3), which are required for RTK activation of Akt. The activation of Akt leads to a subsequent activation of another effector (mTOR) which results in the activation of other important proteins in cell apoptosis and growth. The effect of Akt can be reversed by *PTEN* which dephosphorylates PIP3 to PIP2 (Vanhaesebroeck et al., 2012).

The major homozygous deletion in glioma is observed in the *PTEN* gene. *PTEN* was found to be homozygous deleted in 36% of adults GBM but this deletion is rare in paediatric GBM (The Cancer Genome Atlas Research Network, 2008, Bax et al., 2009). Another study on the *PTEN* gene mutations showed that these mutations are more common in GBM in adult than in children and this genetic abnormality is independent of the expression of *TP53* gene mutation (Rasheed et al., 1997). Moreover, in a study done on 33 patients with LGG to determine the malignant transformation in children, they showed that concomitant overexpression of phosphorylation of AKT pathway is consistent with inactivation of *PTEN* (P=0.015), although three tumours

(two LGG and one HGG) showed combined overexpression of pAKT without concomitant *PTEN* deletion (Broniscer et al., 2007).

In a recent study, the role of *PTEN* loss on the overall survival of GBM patients was investigated. These patients received TMZ with radiotherapy. The median overall survival (OS) was 20 months and 18.2 months in *PTEN* retained and *PTEN* loss patients, respectively (P = 0.71). Moreover, *PTEN* loss patients were also found to have amplifications of *EGFR* gene more frequently than patients with retained *PTEN* (70.8% *vs.* 47.8%, P =0.01). Therefore, loss of *PTEN* expression does not confer poor overall survival in GBM patients treated with TMZ and radiotherapy and reflect that TMZ may be equally as effective in eradicating GBM cancer cells with *PTEN* loss (as observed in the level the outcomes between the PTEN retained and loss groups) (Carico et al., 2012).

1.3.5.3 Abnormalities in genomic instability and epigenetic regulatory mechanisms

The major genomic instability in DNA that is related to cancer is change in DNA copy number. DNA copy number variation (CNV) is the alteration in the DNA that results in the cells having either more or less copies of one or more sections of the DNA. The major genomic variations are the insertion and the deletion on certain chromosomes (Hastings et al., 2009). Regarding DNA copy number, most DNA microarray data was shown that paediatric GBM displays less DNA copy number aberrations than adult GBM such as gain of chromosome 7 and 1q as well as loss of 1p, 4q, 9p, 10q, and 16q (Bax et al., 2009, Paugh et al., 2010) whereas, the major CNV in adults GBM include gains at chromosomes 1, 2, 7, 9, 12, 19, and 20 and losses at 6, 9, and 10 (Margareto et al., 2009).

One of the key mutations studied in GBM is isocitrate dehydrogenase enzyme (*IDH1*) mutations. IDH is one of the citric acid cycle enzymes. It catalyses the third step of the cycle: the conversion of isocitrate to α-

ketoglutarate and CO_2 while converting NAD^+ to NADH in two steps reaction. However, these mutations were found to be rare in paediatrics but occur in 98% of adult secondary GBM (Paugh et al., 2010). Moreover, the mutation in *IDH1* gene was found to be more useful as a prognostic factor for overall survival than standard histological criteria that differentiate high-grade astrocytomas. The mutation at codon 132 of IDH1 was found to be rare in glioblastoma patients (7.2%) and more in anaplastic astrocytoma (60%) and patients whose tumour had a mutation in this codon had a longer survival rate than patients with wild type *IDH1* mutations. This factor was the most prominent single prognostic factor (risk ratio (RR) 2.7; 95% CI 1.6–4.5) followed by age, diagnosis and MGMT status (Hartmann et al., 2010). The second set of key mutations is the histone H3.3. Histones are nuclear proteins which are responsible for the nucleosome structure of the chromosomes. The histone 3 variant 3 (H3.3) is encoded by the *H3F3A* gene and recently mutations in this gene were found to occur frequently in GBM especially in two nucleotides in K27 (Lys27Met) and G34 (Gly34Arg) and were associated with the patients survival based on the tumour location, age, DNA methylation status, and other cytogenetic mutations especially in paediatric GBM (Sturm et al., 2012). Another major studied histone is the histone H2A gene family member X (H2AFX), a major detector for the response to double-stranded DNA (dsDNA) breaks caused by ionizing radiation. It has been thought that genetic variants in the *H2AFX* promoter region may result in abnormal protein expression which could confer susceptibility to glioma. In a case-control study, three common single-nucleotide polymorphisms (SNPs) (rs643788, rs8551, and rs2509851) in the *H2AFX* promoter region in 669 adult glioma patients and 638 controls were examined. Among the three SNPs, the rs643788 genotype was significantly associated with reduced risk of glioma (GA vs. GG: OR = 0.72, 95% CI = 0.56-0.94; GA/AA vs. GG: OR = 0.75, 95% CI = 0.59-0.94), compared with the wild type GG. Furthermore, this decreased risk was more evident among patients aged ≥ 45 years (OR =

0.64, 95% CI = 0.45-0.90) and male subjects (OR = 0.70, 95% CI = 0.50-0.96). These results suggested that a common variant in the H2AFX promoter region may modulate risk of glioma, particularly in adult male glioma patients (Fan et al., 2011).

The methylation status of genes can often be used to predict response of tumour to therapy and therefore on the survival. Methylation occurs mostly in the CpG islands in the promoter region and therefore, affects the function of the gene by switching it on and off. The two methylated genes most studied in GBM are *MGMT* and *PTEN*. The methylation status of *MGMT* gene, which is involved in DNA repair, is often considered as an important prognostic factor in adult glioblastoma. However, the exact role is still controversial. When the *MGMT* promoter is methylated, this will result in silencing the gene which means that no MGMT repair enzyme will be produced, and therefore, there will be no correction of faults in the DNA, including those produced by the chemotherapy agent TMZ (Hegi et al., 2005). Lee *et al*., investigated the correlation between MGMT protein expression and *MGMT* methylation status and the prognostic relevance of TP53 and Ki-67 in 28 GBM patients with immunohistochemistry. They found that MGMT protein showed high expression (>30% positive cells) in 11 tumours, and low expression (<30% positive cells) in 17 tumours. Moreover, *MGMT* promoter methylation (P=0.8878) as well as MGMT protein expression (P=0.1803) was completely uncorrelated to survival prediction (Lee et al., 2011c). In contrast, a recent meta-analysis of published studies (2,986 GBM patients in total from 30 studies) investigated the effects of *MGMT* promoter methylation on both PFS and OS among GBM patients. To estimate the effect of the *MGMT* promoter methylation on PFS, five studies undertook univariate analyses and nine undertook multivariate analyses and the analyses of the data revealed that the hazard ratio (HR) for PFS was 0.72 (95 %CI 0.55–0.95) by univariate analysis and 0.51 (95 % CI 0.38–0.69) by multivariate analysis. Regarding the effect of *MGMT* promoter methylation on OS was evaluated in 15 studies

by univariate analysis and 14 studies by multivariate analysis. The HR was 0.67 (95 % CI 0.58–0.78) and 0.49 (95 % CI 0.38–0.64), respectively. These results showed that *MGMT* promoter methylation was associated with better PFS and OS in patients with GBM (Zhang et al., 2013). This gene and the protein expressed have been found to be relevant in childhood glioma as well. Although tumours can acquire deficits in mismatch repair (MMR) mechanisms following the exposure to TMZ alkylating agent which can then establish a resistance response to this alkylating agent (Pollack et al., 2006).

Regarding the PTEN methylation, the majority of studies have focused on adult glioma more than on paediatric glioma (The Cancer Genome Atlas Research Network, 2008, Paugh et al., 2010). For example, in a study by Wiencke *et al.,* they showed that there is a high degree of hypermethylation in grade II astrocytomas compared to the normal brain tissues and the degree of PTEN methylation corresponds to phosphorylation of Akt which reflects the activation of the PI3K pathway. Moreover, they showed that the methylation is rare in *de novo* GBM (primary glioma) where mutations in the gene predominant (Wiencke et al., 2007).

1.3.6 Glioblastoma multiforme (GBM) recurrence

Despite intensive treatment and better understanding of the molecular biology principles, this tumour has a high degree of recurrence. The reason behind the recurrence of GBM is believed to be due to multidrug resistance (MDR). The time to recurrence of GBM is usually short, with most recurrences diagnosed within two years from the time of initial diagnosis. Recurrences are generally local, meaning that they occur at the same site as the original tumour (Choucair et al., 1986). Survival after resection of recurrent GBM remains poor despite advances in imaging, operative technique, and adjuvant therapies. Barker *et al.,* identified tumour recurrence in 223 GBM patients and they found that the median interval from initial diagnosis to clinical or radiographic evidence of tumour recurrence was 4.9 months (Barker et al.,

1998). The recurrence of the tumour affects the PFS of the patients. Barker *et al.,* performed a retrospective review of 223 patients with recurrent GBM. They found that 46 patients who underwent secondary surgery and adjunctive therapy demonstrated a median survival time of 36 weeks following resection. In comparison, patients who received similar chemotherapy and/or radiation therapy without re-operation had a median survival time of 23 weeks (Barker et al., 1998). Moreover, in a study on recurrent HGG, Parekh *et al.,* found that children with recurrent HGG have a dismal outcome with a PFS of 12 weeks whereas, adults with recurrent HGG treated with irinotecan and BVZ reportedly have a 63% response rate and a PFS of 23 weeks (Parekh et al., 2011).

The role of microRNAs in recurrent GBM has also been investigated. MicroRNAa are small RNAs proposed to have important roles for cancer including proliferation, aggressiveness and metastases development (Stahlhut Espinosa and Slack, 2006). There are only few data on the involvement of microRNAs in glioblastoma recurrence. In a recent study by Ilhan-Mutlu *et al.,* seven microRNAs (microRNA-10b, microRNA-21, microRNA-181b, microRNA-181c, microRNA-195, microRNA-221 and microRNA-222) were selected and tested on 15 primary glioblastoma patients, for whom formalin fixed and paraffin embedded tissue from the primary and recurrent surgery were available as well as on 3 non-neoplastic brain tissue samples served as control. The expression pattern of the microRNAs was validated with qRT-PCR. They found that all microRNAs showed detectable levels of expressions in glioblastoma and controls, whereas microRNA-10b was not detectable in controls. Moreover, microRNAs except microRNA-21 showed significantly higher levels in controls when compared to the levels of first resection of glioblastoma. Comparison of microRNA levels between initial and recurrent resections revealed no significant change. Finally, Cox regression analyses showed no significant association of microRNA expression levels in the tumour tissue with progression free survival times (Ilhan-Mutlu et al., 2013).

In fact the recurrence % in GBM is different and the response of patients is less in recurrent GBM in children compared to adults. This may be because GBM has distinct molecular genetic patterns in adults than in children as mentioned in section 1.3.5 which could influence the individual response to therapy or the tumour is following different mechanisms to resist the therapy and repopulate the tumour.

Chemotherapeutics are essential for the control of the tumour mass but one of the major obstacles in treatment is the development of MDR. MDR is defined clinically as the development of simultaneous resistance of cancer cells towards a broad spectrum of drugs that have different modes of action. This resistance can be either intrinsic (treatment independent) or acquired (developed over the treatment time through genetic mutation). It is now known that MDR can have many different causes including: (1) failure of cancer cells to accumulate drugs, (2) failure of cancer cells to metabolise pro-drugs to toxic products, (3) increased drug-detoxification, and (4) failure to activate cell death (apoptosis) pathways (Gottesman, 2002b). MDR is not restricted to cancer cells and anticancer drugs; it also occurs in many other situations, such as the resistance of bacteria, fungi, and parasites, to antibiotics as well as antifungal and antiparasitic compounds (Boumendjel et al., 2009). In fact, the resistance and the recurrence of the tumour is still a primary cause behind the poor effectiveness of available treatment regimens. Drug resistance in glioma is complex and need more investigation. However, some of the cellular and molecular mechanisms in GBM have been studied comprehensively such as the presence of CSCs, the overexpression of drug efflux ABC transporters, and the evasion of apoptosis pathway whereas, other mechanisms such as increase the drug detoxification need more investigation (Lu and Shervington, 2008).

1.3.7 Drug resistance mechanisms in glioblastoma multiforme (GBM)

CSCs play an important role in the survival of tumour cells and subsequently in the recurrence of the tumour as mentioned earlier in section 1.1.3. In fact, CSCs result in the recurrence of glioma by two mechanisms: the *first* one is entrance of the CSCs into a quiescent state and the *second* one is the overexpression of ABC transporters by these cells (Dean et al., 2005, Moore and Lyle, 2010). Quiescence is a state of inactivity or resting in which the cells are not dividing. It usually represents the G0 phase in the cell cycle. Cells of the nervous system become quiescent when they reach maturity. Little research has been done to address how quiescence might play a role in CSC biology, but there are some indications that quiescent stem-like populations might contribute to at least some tumours (Moore and Lyle, 2010). Several studies have been performed on animal models to identify the occurrence rate of glioma and to determine if quiescent cells have a role in the recurrence. Chen *et al.,* used a genetically engineered mouse model of glioma to identify a subset of endogenous tumour cells that were the source of new tumour cells after the drug TMZ was administered. They found that the murine tumours reinitiated cell division and growth. Therefore, TMZ targeted proliferating cells but tumour recurrence was still inevitable. This was also shown by the nestin-ΔTK-IRES-GFP (Nes-ΔTK-GFP) transgene that was used to label quiescent subventricular zone (SVZ) adult neural stem cells and a subset of endogenous glioma tumour cells. On arrest of tumour cell proliferation with TMZ, pulse-chase experiments demonstrated a tumour re-growth cell hierarchy originating within the Nes-ΔTK-GFP transgene subpopulation indicating that a relatively quiescent subset of glioma cells, with properties similar to CSCs, is responsible for sustaining tumour growth via the production of transient populations of highly proliferative glioma cells (Chen et al., 2012).

$CD133^+$ was found to be a marker for several brain tumours including GBM as shown previously in section 1.1.3 and has been used as a marker for the CSC in these tumours. Moreover, $CD133^+$ GBM cells have been isolated and characterised as chemo-/radio-resistant tumour-initiating cells and were hypothesized to be responsible for post-treatment recurrence. In research done by Liu *et al*., isolated $CD133^+$ from recurrent GBM were purified and re-injected into mouse brain and they found that the $CD133^+$ GBM cells sorted from the $CD133^+$ GBM spheres also expressed SOX2 and CD44 (another cell surface markers for CSCs) and are capable of clonal self-renewal and dividing to produce fast-growing $CD133^-$ cells (the ability to differentiate) (Liu et al., 2009c).

The second mechanism by which CSCs may lead to MDR is the expression of drug efflux pumps. ABC transporters are one of the largest families of transmembrane proteins which exist in all prokaryotes and eukaryotes cell membranes. ABC transporters are active transporters; they utilize the energy from adenosine triphosphate (ATP) hydrolysis to transport various molecules through the cell membrane. They can function as importers, exporters or regulators. Importer ABC transporters are found mainly in prokaryotes and they function to transport nutrients such as amino acids, ions, peptide and sugars. Exporter ABC transporters are found in both prokaryotes and eukaryotes and play a role in the secretion of toxins and in bile and metabolites export. The third group of ABC proteins are not classified as transporters but they are involved in many vital cellular functions such as DNA repair, translation, and regulation of gene expression (Boumendjel et al., 2009). Several ABC genes such as *ABCB1/* multidrug resistance 1 *(MDR1), ABCC1/* multidrug resistance protein 1 *(MRP1), and ABCG2/*breast cancer resistance protein *(BCRP)* were found to be involved in MDR tumour cells (Dean et al., 2005, Higgins, 2007). The common feature of all ABC transporters is they contain two distinct domains, the transmembrane domain (TMD) and the nucleotide binding domain (NBD). The TMD consists of α-

helices, embedded in the membrane bilayer. Its function is to recognize the substrates and it undergoes conformational changes to transport the substrate across the membrane (Boumendjel et al., 2009, Jones and George, 2004). The NBD also known as ABC domain, is the site of ATP binding and hydrolysis. It is located in the cytoplasm and has a series of highly conserved sequence motifs. From amino to carboxy terminus, these are the Walker A (P-loop), a glycine-rich sequence found in most ATP binding proteins; a conserved glutamine (Q-loop), the family-specific ABC-signature (LSGGQ) motif, the Walker B motif, and a conserved histidine residue (His-switch). The ABC-signature motif is diagnostic for the family as it is present only in ABC proteins, while Walker A and B motifs are found in many other ATP-utilizing proteins (Walker et al., 1982, Kerr, 2002).

The expression of different members of ABC transporters in brain tumours either on surgical specimens or cell lines has been determined. The major studied members are MDR1 and MRP1. Although MDR1 has an important role at the BBB (Bredel, 2001), available data on its contribution to the intrinsic cellular drug resistance, especially in gliomas, is controversial. For example, Spiegl-Kreinecker *et al*., investigated the expression of two drug transporter proteins (MDR1 and MRP1) in cell lines (n = 24) and primary cell cultures (n = 36) from neuroectodermal tumours, as well as in brain tumour extracts (n = 18) and normal human astrocytes (n = 1). They found that expression of MDR1 was relatively rare in glioma cells, in contrast to MRP1, which was constitutively overexpressed in cells derived from astrocytomas as well as glioblastomas. Also, normal astrocytes cultured *in vitro* expressed high amounts of MRP1 but no detectable MDR1. Their data suggested that MDR1 contributes to cellular resistance in a small subgroup of gliomas, whereas MRP1 is demonstrated to play a constitutive role in the intrinsic chemoresistance of gliomas and their normal cell counterpart (Spiegl-Kreinecker et al., 2002).

MRP1 has also been suggested by others to be involved in drug resistance in human glioma cells (Abe et al., 1994). For instance, in a study performed by Mohri *et al.*, to investigate whether MRP1 is involved in the intrinsic drug resistance of human gliomas, 20 surgical specimens of gliomas (11 glioblastomas, 6 anaplastic astrocytomas, and 3 astrocytomas), 3 normal brain specimens, and 4 glioma cell lines (U87MG, U251MG, U373MG, and T98G) were analysed. The expression of MRP was determined by RT-PCR and immunohistochemistry in the surgical specimens and by quantitative RT-PCR and western blot analyses in cell lines. Moreover, the sensitivity to four drugs [Adriamycin (ADM), etoposide (VP-16), cisplatin (CDDP), and 1-(4-amino-2-methyl-5-pyrimidinyl) methyl-3-(2-chloroethyl)-3-nitrosourea], were determined by MTT assay. Analysis of the data from the surgical specimens revealed that MRP1 expression was present in 9 of 11 glioblastomas and 3 of 6 anaplastic astrocytomas whereas, MRP1 mRNA and protein levels were increased 4.5 fold in the T98G cells as compared to U87MG. The analysis showed that T98G cells had the highest resistance to all drugs therefore; this cell line was treated further with antisense nucleotide to turn the expression of MRP gene off. As expected, western blot analysis revealed that treatment with the antisense oligonucleotide reduced the level of MRP expression to 25% of the sense oligonucleotide treatment in T98G cells. The sensitivity to ADM, VP-16 and CDDP was significantly increased in the antisense-treated cells as compared with the sense-treated cells. These results suggested that the MRP expression may be related to the intrinsic MDR in human gliomas (Mohri et al., 2000).

The presence of CSCs and the ABC transporters results not only in enhancing the drug efflux but also in escaping the programmed cell death (apoptosis) which activates the general response mechanisms that detoxify drugs and repair damage to DNA in the tumour cells (Gottesman, 2002a). Apoptosis is a natural mechanism by which the cells are terminated (section 1.1.1 for more explanation about apoptosis). The important role of several

apoptotic genes in drug resistance of glioma has been examined. The major genes which increase the resistance of the cells to apoptosis and found to be mutated in GBM are *Bcl-2* and *TP53* (Lowe and Lin, 2000). Instead of disrupting proliferation, Bcl-2 promoted cell survival by blocking programme cell death (Hockenbery et al., 1990). Fels *et al.* investigated Bcl-2 expression in 86 HGG patients (29 anaplastic astrocytomas and 57 GBM). Although the expression of Bcl-2 was high in 48% of AA patients and in 51% GBM patients, Bcl-2 was not correlated with the survival of patients (P=0.0068). Moreover, Bcl-2 overexpressing human glioma cells were used for modelling the *in vivo* findings and for investigating the importance of Bcl-2 in tumour resistance against cytotoxic treatment (carmustine, paclitaxel, vincristine, and doxorubicin). They found that Bcl-2 overexpression results in a significant increase in the resistance to all these chemotherapeutic agents (Fels et al., 2000).

In addition to the Bcl-2 family, p53 is considered an important tumour suppressor protein that links to apoptosis. Mutations in *TP53* gene are found in many cancers including GBM and are related to the poor prognosis (Wallace-Brodeur and Lowe, 1999, The Cancer Genome Atlas Research Network, 2008). The role of *TP53* mutations in the drug resistance of glioma has been investigated on three TMZ chemo-resistant glioma cell lines T98G, U87, and U138. The mRNA expression of both *TP53* and *MGMT* was also determined. They found that T98G and U138 cells expressed mutant-type *TP53* and were positive for MGMT, while U87 cell expressed wild-type TP53 and were negative for MGMT. Moreover, knockdown of mutant *TP53* in T98G and U138 cells led to a fivefold increase in chemo-sensitivity to temozolomide via the reduction in *MGMT* expression whereas, the knockdown of wild *TP53* in U87 cell did not affect the chemo-resistance. This finding suggested that *TP53* mutation decreases the chemo-sensitivity of malignant gliomas to TMZ however; this drug resistance can be restored by increasing MGMT expression (Wang et al., 2012).

Less is known about drug detoxification as a mechanism of drug resistance in glioma compared to the other studied mechanisms (Tew, 1994). However, metallothionein (MT) was found to be correlated to drug resistance in GBM. MTs are a family of cysteine-rich, low molecular weight proteins. They are localized in the membrane of the Golgi apparatus. They are involved in the metabolism of metals and in the protection of oxidative stress (Takahashi, 2012). In 27 primary and 17 secondary glioblastomas and their astrocytic precursor tumours, the immunohistochemical expression of MDR1, MRP1, lung resistance-related protein (LRP), metallothionein, and topoisomerase II alpha was determined. Glial tumour cells in all glioblastomas showed constant up-regulation of LRP, MRP1, and topoisomerase II alpha whereas, MDR1 was found in 90% of the primary and 60% of the secondary glioblastomas. In contrast, in the precursor tumours, these drug resistance-related factors were expressed in varying proportions. Metallothionein was retained in all neoplastic phenotypes. Furthermore, metallothionein, MDR1, LRP, and topoisomerase II alpha were strongly expressed by normal and neoplastic vessels which may result in impaired penetration of therapeutic agents through the blood-brain and blood-tumour barrier (Tews et al., 2000). However, more studies need to be performed to explain further the involvement of MT and other parameters such as glutathione s-transferase (GST) and cytochrome p450 in drug detoxification in GBM.

We can conclude from these previous studies that GBM can recur as a result of several cellular and molecular mechanisms which are highly correlated to the drug resistance and result in the repopulation of the tumour and affect the survival of the patients and the success of the therapy. In fact, more studies need to be done to understand the biology of the recurrent glioma and to design a new complete therapy system which can improve the survival rate of GBM patients. To reach this level of understanding, several cell lines and animal models can be used as resources to understand the

biology of tumours and to design new therapies. The following section will illustrate the importance of cell line models in understanding GBM.

1.4 The importance of cell line models in understanding GBM biology

Reliable cell line models are required to pre-clinically assess the efficacy of experimental approaches for treatment and to help to achieve a comprehensive picture about brain tumours. In a meta-analysis study, the copy number alteration frequencies and the occurrence of cancer gene amplifications and homozygous deletions in seven *in vitro* cell lines were compared for 7 tumours (breast, ovary, sarcoma, melanoma, colon, pancreas and lung). On average, data obtained from array-based comparative genomic hybridization technology showed that cell lines preserve *in vitro* the genetic aberrations that are unique to the parent histology from which they were derived while acquiring additional locus-specific alterations. These data may enable a more predictive understanding of individual cell lines as *in vitro* models of cancer biology and therapy (Greshock et al., 2007). Therefore, these cell line models can serve as sources to better understand the biology of the tumours.

The rat and mouse have been two of the most widely used experimental animals, and rat and mouse brain tumour cell line models have been used extensively compared to other animal cell line models. However, if a study requires the usage of animal cell line models, then it is essential to recognise the limitations of the cell line models before using them and it is important to select the most appropriate model based on the nature of the study to be conducted (Barth and Kaur, 2009). There are 8 rat brain tumour cell lines which are widely used to study glioma. Among these, the C6 cell line is the most favoured model for glioma studies. The rat C6 glioma cell line was produced in 1968 by Benda *et al.,* by injecting new-born outbred Wistar rats with the carcinogen *N*-nitroso-*N*-methylurea in Sweet's laboratory at the

Massachusetts General Hospital (Benda et al., 1968, Benda et al., 1971). The rat glial tumour was plated and propagated in culture on plastic petri dishes and was incubated in 5% CO_2 in F10 medium supplemented with 15% horse serum and 2.5% fetal calf serum. Several clones were developed but among these clones only one clone was positive for S-100 proteins (10 times more than other clones). The S-100 proteins are highly acidic proteins which are unique to the vertebrate brain. They are involved in the regulation of protein phosphorylation, transcription factors, Ca^{++} homeostasis, the dynamics of cytoskeleton constituents, enzyme activities, cell growth and differentiation, and in the inflammatory responses. This protein was named S-100 based on its solubility in 100% saturated ammonium sulfate at neutral pH (pH=7) (Benda et al., 1968) and was used as an indicator of the power of cell lines to repopulate key tumour features. Initially, this tumour was histopathologically classified as an astrocytoma, but eventually it was designated as a glial tumour following accession by the American Type Culture Collection, Rockville, MD (ATCC# CCL-107). This cell line shares several similarities with GBM in human. These include: (1) changes in gene expression in the rat C6 glioma cell line were the most similar to those reported in human glioma (Barth and Kaur, 2009), (2) the high expression of PDGFβ in this cell line parallel their over-expression in human gliomas (Guo et al., 2003, Heimberger et al., 2005b), and (3) studies on tumour growth, invasion, migration which have been done on the rat C6 glioma cell line, are applicable and similar to those observed in human gliomas which make it a better cell line model to study migration *in vitro* (Gunnersen et al., 2000).

In this study, the rat C6 glioma cell line was used as a model to study different mechanisms of drug resistance in GBM. Alongside the parental C6 cell line, two drug derived cell lines with DNA topoisomerase I inhibitor (irinotecan) and DNA topoisomerase II inhibitor (etoposide) were established by Dr. Wiyada Punjaruk within the Children's Brain Tumour Research Centre (CBTRC), at the University of Nottingham by continuous culture at a

concentration of irinotecan/etoposide that resulted in 30% cell survival (IC_{70}) in clonogenic assays (Punjaruk, 2010). These two drugs were involved in this study as they are clinically being used in the treatment of glioma (especially the recurrent gliomas) as shown previously in section 1.3.4.4 and have shown promising response.

1.4.1 Etoposide

Etoposide (VP-16213) is an important anti-tumour agent used in several tumours such as lung cancer, lymphoma, leukaemia, and GBM. Etoposide is chemically derived from epipodophyllotoxin derived from the plant *Podophyllum peltatum* (figure 1.7). It was first chemically synthesised in 1966 and approved by the food and drug administration (FDA) in 1983 (Van Maanen et al., 1988).

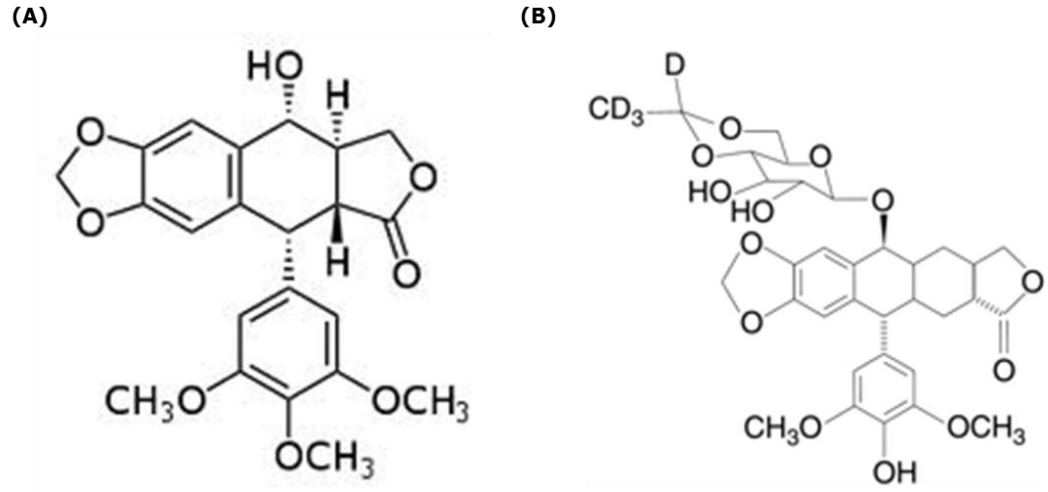

Figure 1.7 Chemical structure of etoposide. The figure shows the chemical structures of the original compound (podophyllotoxin) (A) and its derivative etoposide (B). Adapted from (Van Maanen et al., 1988).

DNA topoisomerase II enzyme is required for repairing "knots" and breaks in the DNA that are produced normally by physiological processes such as replication. In humans, topoisomerase II has two variants, topoisomerase IIα and topoisomerase IIβ. Topoisomerase IIα is a 170 kDa enzyme and it is more predominant than topoisomerase IIβ (180 kDa) and it can be detected in two stages in the cell cycle (G2 and S) whereas, topoisomerase IIβ can be detected in all cell cycle stages (Rojas et al., 2009). Although the mechanism of etoposide anti-tumour effects is still poorly understood, it is known that etoposide is acting as an inhibitor for the DNA topoisomerase II. Etoposide prevents cells from entering mitosis and blocks cell-cycle progression in the late S and G2 phases by binding irreversibly to the topoisomerase II enzyme causing breaks in DNA (both double and single strand breaks) (Rojas et al., 2009). In fact, etoposide can arrest cells in metaphase only at very high concentrations, which are probably irrelevant *in vivo*. Loike and Horwitz reported that the presence of a hydroxyl group in the C-4'position in the dimethoxyphenol ring was required for a podophyllotoxin derivative to induce strand breaks (Loke and Horwttz, 1976). Etoposide has molecular weight 588 and it is weakly soluble in water. Creaven and Allen found that 72 hours after intravenous administration of etoposide, 44% of it is excreted in the urine in the following percentages, 29% as unchanged drug and 15% as metabolites. Etoposide has many metabolites based on the physiological pH and the enzymatic and the nonenzymatic transformation of the lactone ring. Etoposide changes its chemical structure from the trans lactone form to the cis lactone form (picroetoposide) with alkaline hydrolysis at pH 9.3 which is subsequently open to form the cis hydroxy acid at pH 12. At lower pH (pH<4), the cis hydroxy acid recyclizes to picroetoposide (Van Maanen et al., 1988).

Moreover, studies showed that etoposide can utilise its antitumor effect by metabolic activation in oxidation-reduction reactions to produce derivatives that can bind directly to the cellular DNA (Van Maanen et al., 1988). Tumours can overcome the effect of etoposide in two different

mechanisms. The first one is the reduction of the drug concentration inside the tumour cells and the second mechanism is by target alteration. The first mechanism depends on the overexpression of *MDR1* and its product protein P-glycoprotein (P-gp, also known as ABCB1). In contrast, the other mechanism does not depend on the expression of the *MDR1* gene, but it depends mostly on the mutations that occur in the topoisomerase II enzyme regardless of the cellular concentration of P-gp which in turn lead to the formation of drug resistance to etoposide (Bugg et al., 1991, Punjaruk, 2010).

1.4.2 Irinotecan

Irinotecan (CPT-11) is an anti-tumour agent which was first synthesised in 1983 and used against colorectal cancer, but now has been shown to have potent anticancer activity against a wide range of tumours such as oesophageal, gastric, leukaemia, lymphomas, as well as malignant CNS gliomas (Xu and Villalona-Calero, 2002). It is a semisynthetic derivative of camptothecin (figure 1.8) which is extracted from a plant known as *Camptotheca acuminate* (Pommier, 2006).

The camptothecins are pharmacologically unique for several reasons: (1) topoisomerase I (TOP1) is their only target, (2) changes in camptothecin by inverting its chiral centre at position 20 completely inactivate it, (3) they can penetrate vertebrate cells readily and target TOP1 within minutes of exposure. Irinotecan-HCl is a water-soluble inhibitor for DNA topoisomerase I. Its carboxybispiperidine group (side chain attached to ring A) has to be hydrolysed by carboxyesterases to yield its active metabolite SN-38, which is 1000-fold more potent than irinotecan. The modification occurs in the chemical structure of irinotecan and is important because camptothecin is unstable under different pH due to the presence of hydroxylactone in ring E (Pommier, 2006).

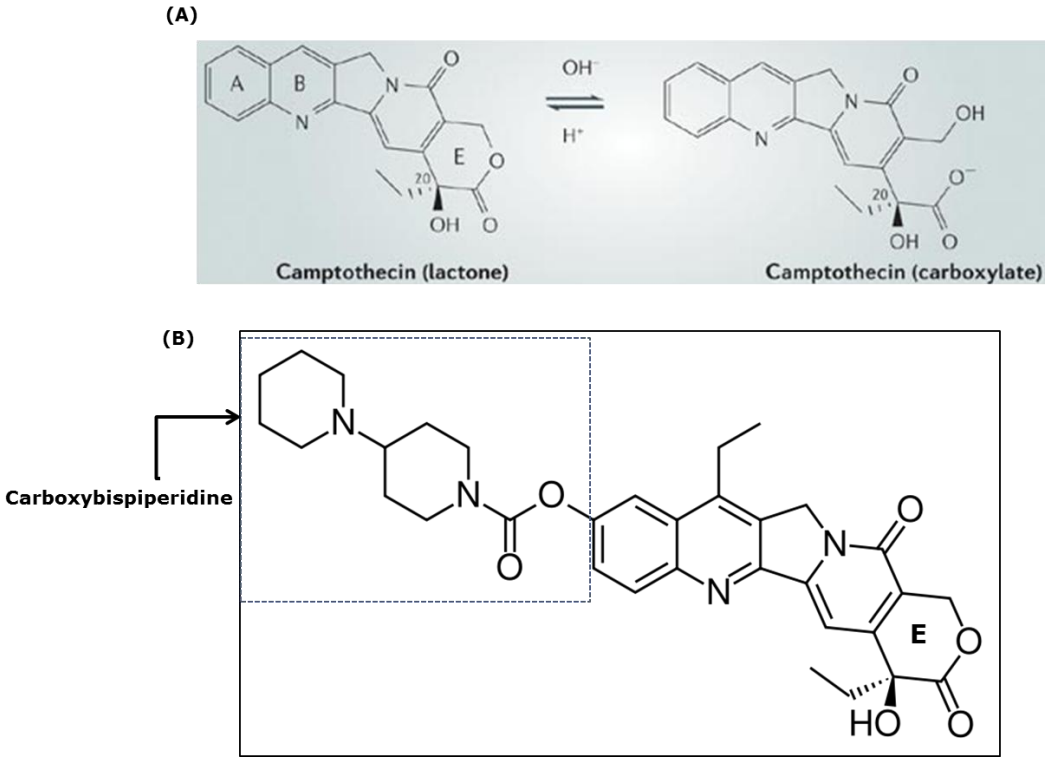

Figure 1.8 Chemical structures of camptothecin and its derivative irinotecan. (A) Represents the chemical structure for the active form of camptothecin (lactone) and the inactive form (carboxylate). (B) Represents the chemical structure of irinotecan (derivative of camptothecin) (adapted from (Pommier, 2006)).

The mammalian genome encodes seven topoisomerase genes; four of them encode type I topoisomerases. The 4 mammalian type I topoisomerase genes include one nuclear topoisomerase I (*TOP1*), the mitochondrial topoisomerase I (*TOP1MT*) gene, and two genes that encode TOP3α and TOP3β. DNA topoisomerases I enzymes are important as a regulators for DNA by reducing the DNA twisting and supercoiling. Irinotecan is a DNA topoisomerase I inhibitor which binds reversibly to DNA topoisomerase I complex and stops the replication of DNA in the G2 or S-phases. Therefore, it inhibits the resealing of single stranded DNA breaks and prevents accession of the replication fork leading to double stranded DNA breaks ultimately causing cell death. Irinotecan has the ability to bind to single stranded DNA (ssDNA) and double stranded DNA (dsDNA) (Xu and Villalona-Calero, 2002).

The metabolism of irinotecan includes the deactivation of SN-38 (irinotecan active form) through conjugation by uridine diphosphate glucuronosyltransferase isoform 1A1 (UGT1A1) in the liver to SN-38 glucuronide (SN-38G). The elimination of irinotecan and SN-38 is through biliary excretion. Moreover, irinotecan has another major metabolite known as aminopentanecarboxylic acid (APC) which is produced by the oxidation of the piperidine side chain by the cytochrome P-450 (CYP3A4) enzyme. However, APC does not hydrolyse to SN-38 and is a poor inhibitor of DNA topoisomerase I (Xu and Villalona-Calero, 2002).

Tumours can resist irinotecan through several mechanisms. Results from a study done on CNS tumours showed that irinotecan's complex metabolism makes this drug a target for potential interactions with other medications. Patients with CNS tumours which were taken enzyme-inducing antiepileptic drugs such as (phenytoin, carbamazepine and phenobarbital) led to the suspicion that induction of hepatic cytochrome P-450 enzymes, including CYP3A4, resulted in increased conversion of irinotecan to its APC inactive metabolite resulting in increased clearance rate of irinotecan in those patients (Friedman et al., 1999). The second mechanism by which cells can resist irinotecan effect is decreasing the intracellular level of irinotecan by active efflux due to overexpression of ABC transporters such as P-gp and MRP1 (Xu and Villalona-Calero, 2002, Punjaruk, 2010). The third mechanism includes the correlation between the cellular levels of DNA topoisomerase I with the irinotecan cytotoxic effect. In irinotecan-resistant cell lines the total activity of DNA topoisomerase I was shown to be reduced compared with the irinotecan-sensitive parental cell line such as in colon and prostate cancers (Husain et al., 1994).

1.5 Hypothesis and aims

Although the presence of CSCs and the expression of ABC transporters provide some explanations about the resistance to chemotherapy and to

radiotherapy, it is not the only determinant of resistance. Other mechanisms may include elevated DNA repair capacity of the resistant cells and their ability to "sidestep" apoptosis. Therefore, we aimed to determine other mechanisms of drug resistance in GBM. The application of proteomic and genomic approaches increases the chance to identify more protein and gene expression patterns or cell signalling pathways that could be associated with drug resistance and which can be used to improve diagnostic assays, in predicting the response to therapy as well as for developing new drugs.

In order to determine the different mechanisms of drug resistance, this project employed two drug selected derivatives of rat C6 glioma cell line which were derived by continuous rounds of treatment with two DNA topoisomerase inhibitors, etoposide and irinotecan. These two drug selected derivatives (C6-etoposide and C6-irinotecan) alongside the parental cell line were used:

- To identify several protein and gene candidates for chemo-resistance with the proteomic and genomic techniques (two dimensional gel electrophoresis (2-DIGE) followed by identification with mass spectrometry (MS) analysis, and gene expression microarray, respectively) (chapter3).
- To integrate these candidates by signalling pathway analysis to elucidate their role in several biological processes which might be correlated to drug resistance (chapter 3).
- To investigate the effect of topoisomerase inhibitors on the cellular migration (chapter 4).
- To determine the effect of topoisomerase inhibitors on cellular resistance to reactive oxygen species (ROS) (a common DNA damaging agent) (chapter 5).

CHAPTER II

MATERIALS AND METHODS

CHAPTER II: MATERIALS AND METHODS

2.1 Cell culture

2.1.1 Recovery of cells from liquid nitrogen

To recover cells from liquid nitrogen, cryovials were removed from the liquid nitrogen bank and rapidly thawed in a 37°C/5%CO_2 incubator. Then cells were immediately transferred into a 75 cm^2 flask containing pre-warmed Dulbecco's Modified Eagle Medium (DMEM) (Invitrogen, 31885-023) with 10% foetal bovine serum (FBS) and then incubated overnight. The media was replaced with fresh media after 24 hours, and cells were incubated until they became ready for subculture.

2.1.2 Subculturing rat C6 glioma cells as monolayers

When cells were approximately 70% - 80% confluent in the flask, they were subcultured. In order to detach cells from the flask surface, the media was removed, and then cells were washed with Hank's Balanced Salt Solution (HBSS) (Invitrogen, 14170-088). HBSS was removed and 2 ml of trypsin-EDTA solution (Fisher, VX15400-054) was added, then cells were incubated in a 37°C/5%CO_2 incubator for 5 minutes to promote detachment. Cells were resuspended in DMEM+10% FBS and $1/10^{th}$ – $1/40^{th}$ of the cells were re-plated into fresh medium. Any remaining cells were counted and harvested for further analysis.

2.1.3 Maintenance of drug selected C6 sub-lines

For C6-irinotecan cells, the culture medium was supplemented with irinotecan (Sigma, I1406) to a final concentration of 8 μM from a dimethyl sulphoxide (DMSO) stock solution (Sigma, D2650) such that the final concentration of DMSO was 0.05% (v/v). Cells were continually exposed to irinotecan during routine cell culture. For experiments with prolonged duration, irinotecan was removed after 96 hours based on previous study

(Pollack, 1994). On the other hand, for C6-etoposide cells, the culture medium was supplemented with etoposide (Sigma, E1383) to a final concentration of 10 μM from a DMSO stock solution, such that the final concentration of DMSO was 0.05% (v/v) and then the cells were incubated in a 37°C/5%CO_2 incubator for 2 hours then the medium was replaced based on previous study (Ermakova et al., 2006).

2.1.4 Liquid nitrogen preservation of cell lines

Periodically cells were harvested and resuspended in DMSO and FBS at ratio of 1:9 (v/v) respectively. Aliquots of this mixture (≈1x10^6 cells) were added to cryovials and allowed to freeze slowly to -80°C then after 24 hours removed to a liquid nitrogen bank for longer storage.

2.2 In *vitro* clonogenic assay

2.2.1 Principle

The clonogenic assay is a method used to determine the ability of single cell to grow and form a colony, and can be used to assess the response of cells to treatment with chemo- or radiotherapy. In this project, clonogenic assays were used to determine the inhibitory concentrations IC50 and IC70 for both etoposide and irinotecan for the three cell lines (Farnken et al., 2006).

2.2.2 Preparation of cells before the experiment

Cells were trypsinised and resuspended in complete media as in 2.1.2 and then passed through a 40 μM cell strainer to ensure the formation of a single cell suspension. The live cells were counted with trypan blue stain then a total of 100 cells were seeded into a 6-well plate in duplicate. After that, plates were incubated in a 37°C/5%CO_2 incubator for 24 hours to allow cells to attach. Then cells were treated with different concentrations of either

etoposide or irinotecan and plates were incubated for 7-10 days until colonies containing approximately 50 cells were visible (Figure 2.1 represents the design of the plate and the concentration of etoposide and irinotecan used in the clonogenic assay). In case of etoposide treatment, cells were incubated for 2 hours and then media was changed while for irinotecan treatment, cells were incubated for 96 hours then media was changed as described above in 2.1.2. Moreover, if PI3K pathway inhibitors were used, 20 μM of LY294002 (Source BioScience, ABE2892) or 1 μM of GDC-0941 (Selleckchem, S1065) were added with the drugs and after the media was replaced (after 2 hours for etoposide treatment), both inhibitors were added again and plates were incubated for 7-10 days until colonies containing 50 cells were formed.

Subsequently, media was removed and then 1 ml/well of 4% (w/v) paraformaldehyde (PFA) in PBS was applied for 20 minutes at room temperature. PFA was removed and colonies were stained with 0.5ml/well of 0.1% (w/v) crystal violet in dH_2O for 5 minutes at room temperature. Then colonies were washed gently with distilled water to get rid of crystal violet stain and then counted to investigate the survival of cells after drug treatment.

2.2.3 Statistical analysis for clonogenic assay

GraphPad Prism version 5.00 (San Diego California, USA) was used to fit the data to a sigmoidal dose response equation in the form (Y=Bottom + [(Top-Bottom)/1+$10^{(LogEC50\ -X).Hill\ \ Slope}$]) from which IC50 and IC70 values were determined for each etoposide and irinotecan.

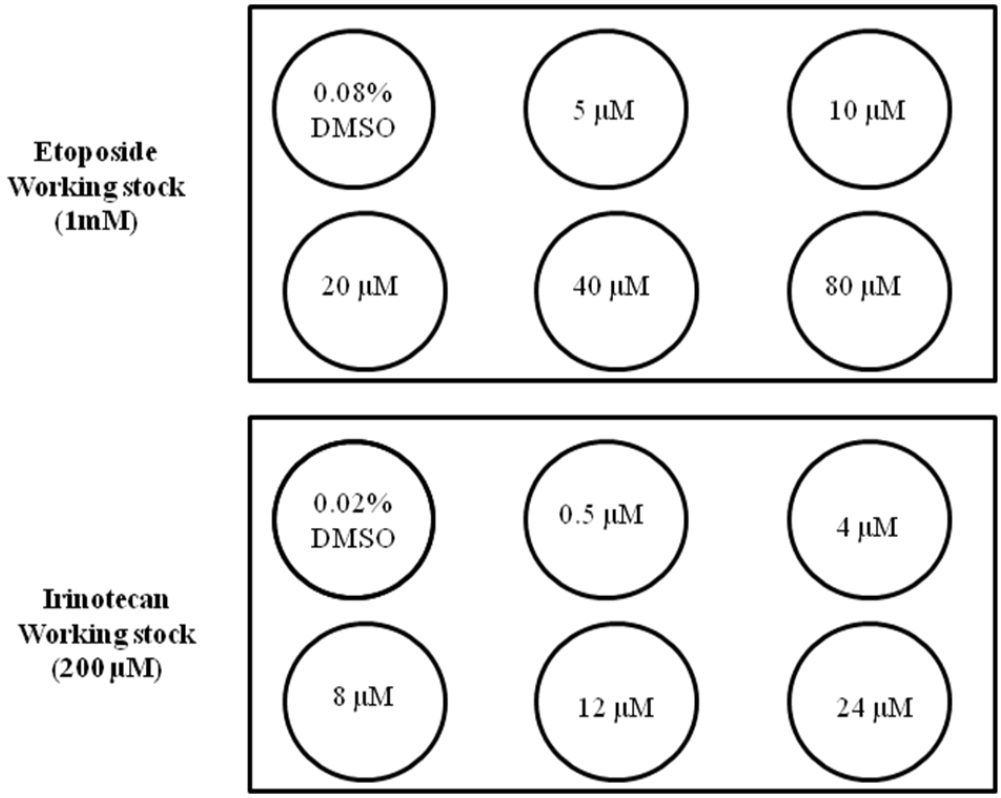

Figure 2.1 Clonogenic assay plate design. Each plate represents the concentrations of either etoposide or irinotecan which are used to determine the IC50 and IC70. The DMSO well was used as a control which represents (100%) cell survival and was used to compare the percentage of cell survival with different drugs concentration. The percentage of DMSO used was equivalent to the maximum amount of vehicle used in each plate (80 µM of etoposide is in 0.08% DMSO, 24 µM irinotecan is in 0.02%DMSO.

2.3 Proteomic approaches

To determine changes in protein expression across the cell lines and to identify candidate proteins, we performed two-dimensional gel electrophoresis and mass spectrometry. A detailed protocol for each technique is given in the following sections.

2.3.1 Two-dimensional gel electrophoresis (2-DIGE)

2.3.1.1 Principle

Two-dimensional gel electrophoresis (2-DIGE) is a technique used to separate proteins based on two properties. In the first dimension, proteins are separated according to their isoelectric point (pI) in a process known as

isoelectric focusing (IEF) along a strip that has an immobilized pH gradient range. Proteins will migrate within the strip until they reach their pI. In the second dimension, an electrical current is applied and proteins are separated in a perpendicular direction according to their denatured molecular weight through a gradient polyacrylamide gel.

2.3.1.2 Preparation of sample

Cell pellets (up to $8x10^6$ cells) were resuspended with 200-500 µl of ice-cold phosphate buffer saline (PBS) then centrifuged at 13,000 x g for 5 minutes at room temperature. After the PBS was removed, 60 µl of Destreak™ Rehydration Solution (GE Healthcare, 17-6003-19) was added to resuspend the pellet again. The cells were then incubated at room temperature on a rotary mixer for 1 hour to induce cell lysis, followed by centrifugation at 13,000 x g for 5 minutes at room temperature. The total cell lysate was loaded onto IEF strip as described below.

2.3.1.3 Protocol

Firstly, IEF strips (Immobiline™ DryStrip pH 3-11 NL, 18 cm (GE Healthcare, 17-6003-76) were rehydrated with 280 µl of Destreak™ Rehydration Solution and covered with 1 ml of mineral oil to prevent evaporation. The rehydration was performed passively overnight at 20ºC and 50 µA/strip in BIO-RAD PROTEAN IEF Cell. The focusing tray was then cleaned with 70% v/v ethanol and the electrodes in each well at the positive and negative poles were covered with electrode wicks (pre-wet with distilled water), and the rehydrated strips transferred to the focusing tray. Subsequently, 60 µl of the cell lysate was added to the positive electrode and then 1ml of mineral oil was added to each strip to prevent evaporation. The focusing conditions were as follows: step 1: 250V -15 minutes, step 2: 10,000V – 3hours, step 3: 10,000-50,000 volts/hour, and step 4: 500V-Hold

overnight. The strips were then washed firstly 3 times for 5 minutes with rocking in equilibration buffer I (0.375 M Tris pH8.8, 6 M Urea to unfold protein, 2% w/v SDS, 2% w/v dithiothreitol (DTT) to break disulfide bonds, 30% v/v glycerol) followed by 3 washes for 5 minutes in equilibration buffer II (as above with DTT replaced by 2.5% w/v iodoacetamide) to inhibit the ability of the protein to form-S-S- bond by binding covalently to thiol group of cysteine molecule. Subsequently, strips were rinsed in protein running buffer before mounting onto a gradient 5-20% w/v polyacrylamide gel (2.3.1.4). Finally, 2 ml of molten 1% w/v agarose was added to seal the strip in place. Then gels were electrophoresed for 6-7 hours at 40 mA/gel at 4°C. Subsequently, gels were transferred to a clean dish prepared with 100 ml fixative (40% v/v methanol and 10% v/v glacial acetic acid) and placed on rocker for 1 hour then washed twice for 10 minutes with distilled water on the rocker. Finally, gels were stained with Coomassie blue stain (50% v/v methanol, 20% v/v glacial acetic acid, and 0.12% w/v Coomassie brilliant blue R-250) by incubating overnight on a rocker then destained with coomassie blue destain (10% v/v methanol and 10% v/v glacial acetic acid) before being scanned. Gels were stored in sealed bags at 2-6°C until used in mass spectrometry.

2.3.1.4 Preparation of gradient gel

A gradient polyacrylamide gel was prepared by mixing a 5% w/v acrylamide gel solution and 20% w/v acrylamide gel solution. Each gel solution contained the indicated percentage of polyacrylamide in a buffer B (0.375 M Tris and 0.13% w/v sodium dodecyl sulfate (SDS); with buffer A also containing 10% v/v glycerol. Gels were polymerized by the addition of (0.1% w/v) ammonium persulfate (APS) and (0.01% w/v) tetramethylethylenediamine (TEMED). Then every gel was overlaid with 400 µl of water- saturated butanol immediately after pouring to ensure the production of an even gel surface and to remove air bubbles.

2.3.1.5 Statistical analysis of the protein expression

In order to determine the persistent and transient changes in protein expression, 20 gels were created with/ and without addition of etoposide or irinotecan and then grouped them as follow: group (1) parental C6, group (2) C6-etoposide (+ drug), group (3) C6-etoposide (- drug), group (4) C6-irinotecan (+ drug), and group (5) C6-irinotecan (- drug); in which each group contains 4 independent gels. After gels were destained several times, they were scanned on EPSON PERFECTION 2400 PHOTO scanner on TIFF format. The initial analysis of protein expression and the quality control of all scanned gels were investigated automatically by Progenesis SameSpots V4.1 (Non-Linear Dynamic, UK). The QC of all gels including the saturation and staining intensity was determined automatically by the software. Since several gels were performed under different conditions, it was important to align or "warp" the gels to a reference gel. For this reason, C6 (gel 3) was chosen as a reference gel. The alignment step was performed automatically and to increase the efficiency of the alignment a further manual alignment was performed by adding 130-300 vectors each of which matches the position of a protein spot in the reference gel to the equivalent spot on the subject gel. Following the previous step, another QC analysis was done by performing the principal component analysis (PCA). Finally, a one way ANOVA test was performed to determine the changes in the protein expression between the 5 groups and then proteins of interest were excised from C6 gel 3 (reference gel) and determined with mass spectrometry (MS).

2.3.2 Mass spectrometry analysis

2.3.2.1 Principle

Peptide mass fingerprinting (PMF) is an analytical technique that measures the mass to charge ratio of peptide fragmentation of proteins. It gives information about the composition of the molecule, and masses of the peptides.

2.3.2.2 Protocol

First, the protein of interest is enzymatically digested into smaller peptides with absolute masses which can be detected easily with a mass spectrometer. Usually matrix assisted laser desorption ionisation -time of flight (MALDI-TOF) is used in preference to other mass spectrometers because it can analyse several proteins at the same time in one experiment and only a small amount of the sample is required for the detection (1 µl). Then the Unique molecular ions (peak list) were identified either by interrogating genome databases which can translate the organism genome into proteins with advanced computer programmes or directly using the PMF application in several databases such as MASCOT software (Matrix Science) to compare the masses of the unknown peptide with known (theoretical) proteins. Finally, results were statistically analysed to find the best match.

2.3.2.3 Analysis of protein spots by Mass Spectrometry

The analysis of protein spots by PMF was done at the University of Nottingham by Dr. David Tooth. Protein spots were excised from C6 (gel 3) which was used as a reference gel.

2.4 Genomic approaches

RNA was extracted from cell lines and used to prepare cDNA which was used as template to detect changes in gene expression with gene expression microarray.

2.4.1 Extraction of RNA

2.4.1.1 Principle

The extraction of RNA from parental C6, C6-etoposide, and C6-irinotecan cell lines was performed with the *mir*Vana™ miRNA isolation kit (Ambion, AM1560) according to the manufacturer's instructions. This kit is

designed for the purification of RNA through two steps. The first step of the procedure is to disrupt cells in a denaturing lysis buffer. Then an organic extraction occurs by using acid phenol: chloroform providing a robust purification as well as removing most of the DNA and proteins from the sample.

2.4.1.2 Preparation of RNA sample

Cell pellets ($2x10^6$ cells) from parental C6, C6-etoposide, and C6-irinotecan cell lines were washed once with sterile PBS then processed as described in the *mir*Vana manufacture's manual for RNA isolation. Further DNase treatment of the resulting RNA was done by adding 12 µl of RQ1 RNase – free DNase (Promega, M610A), 14 µl RQ1 DNase 10x reaction buffer (Promega, M198A), and 14 µl ultrapure water to the RNA samples extracted (100 µl) and then incubating at 37°C for 30 minutes. EDTA was added to a final concentration of 25mM to inhibit DNase, and samples were incubated at 65°C for 10 minutes.

2.4.1.3 Precipitation of RNA sample

To precipitate RNA, a volume of $1/10^{th}$ of sodium acetate (NaAc) was added with 2 volumes of ethanol to the mixture prepared in 2.4.1.2. Then samples were kept at -80°C for at least 1 hour then were centrifuged at 4°C, 13000 x g for 15 minutes. Pellets were carefully washed with 1 ml 75% (v/v) ethanol and then were centrifuged again at 4°C, 6000 x g for 5 minutes. Finally, RNA was suspended in diethylpyrocarbonate (DEPC) treated RNase-free water to a final concentration of 1 µg/µl.

2.4.1.4 Determination of RNA concentration and quality

The concentration of total RNA in each sample was determined by two procedures. The first procedure is by using a Nanodrop spectrophotometer. The concentration was expressed in (ng/µl) unit and the absorbance was measured at two different wavelengths (260/280) and (260/230). The second procedure to detect RNA quality and concentration is by using an Agilent 2100 Bioanalyzer which gives measurements for the RNA integrity number (RIN), total RNA concentration (ng/µl), and quality of the sample by running the RNA sample on a gel and determining the degree of degradation by calculating the 28s/18s rRNA ratio.

2.4.2 Gene expression microarray

Around 100 ng/µl of RNA samples (3 replicates for each cell line) was aliquotted and sent to NASC's International Affymetrix service at Sutton Bonington campus at the University of Nottingham for further analysis with Affymetrix U133 plus 2.0 microarray. The experimental procedure of Affymetrix GeneChip microarray includes many steps from sample preparation to data analysis (figure 2.2). Finally, raw data reflecting the fluorescence intensities were statistically analysed to determine fold changes as compared to control sample with GeneSpring GX software (version GX11.5.1) (Agilent Technologies/Genomics).

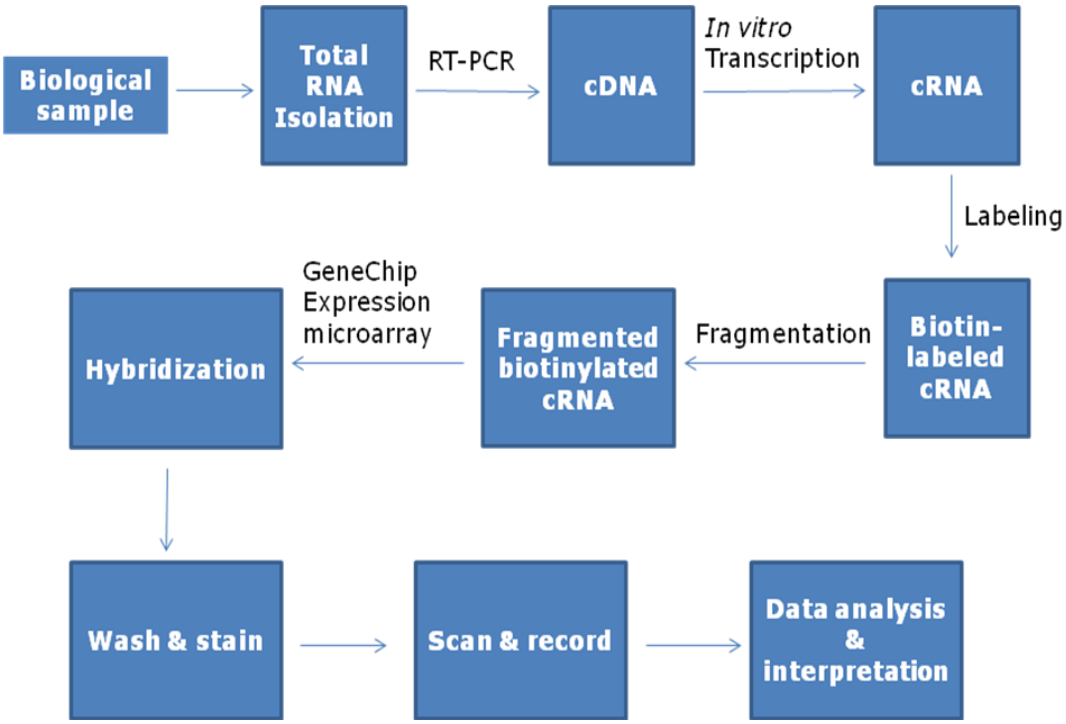

Figure 2.2 Workflow of Affymetrix GeneChip Microarray steps. Total RNA is isolated from cells and converted into cDNA by reverse transcription process because cDNA is more stable than RNA. Prior to the analysis, cDNA is used as a template to form cRNA again through *in vitro* transcription and labeled with Biotin. Then the Biotin-labelled cRNA is fragmented to give a products of 30-400 bp. Whenever the sequence of the fragmented biotin-labelled cRNA is complimentary to the probes in the chip they are hybridized (at this stage both the perfect match (PM) and the mismatch (MM) probes will bind to the fragmented biotin-labelled cRNA) then at the washing step, any Biotin-labelled cRNA fragment which is not matched with the probes (i.e, binding to MM probes) will be removed and then the chip is stained with a fluorescent molecule that has the ability to bind to Biotin (such as Cy5 conjugated to streptavidin). Finally, the entire array is scanned with a laser beam and the data is analysed through different software such as GeneSpring GX software (Agilent Technologies/Genomics).

2.4.3 Ingenuity pathway analysis (IPA)

Ingenuity pathway analysis (IPA) software (version 8.7, Ingenuity Systems, USA) was used to identify and understand the complex biochemical pathways and biological processes of the data obtained from the genomic analysis. All raw data files were exported as spreadsheet Excel files into IPA. In this analysis, a comparison was performed between two cell lines (1) C6-Irinotecan vs. C6, (2) C6-etoposide vs. C6, and (3) C6-irinotecan vs. C6-etoposide by applying an unpaired t-test. Then genes which were either up or

down regulated with a fold change (FC) of >1.5 and a *P* value <0.05 in each comparison made were identified and a general search in PubMed was made to identify their involvement in major biological processes and to design hypotheses.

2.5 Migration assays

2.5.1 Wound scratch assay

2.5.1.1 Principle

The wound scratch assay is a well-developed assay to study the migration ability of cells. This assay is based upon making an artificial scratch on a confluent well-attached monolayer. The migration of the cells towards the gap "scratch" is then determined as a function of time to cell migration rate (Liang et al., 2007). The procedure below is the optimised assay for C6 cell lines but discussion of the optimisation process is presented in chapter 4.

2.5.1.2 Determination of the migration rate for glioma cell lines

Approximately $0.5x10^6$ cells of C6, C6-etoposide, and C6-irinotecan were seeded into uncoated sterile 6-well plate (Costar, 3506) as well as to a rat tail collagen type I coated 6-well plate (GIBCO, A11428-01) and were incubated in 37°C/5% CO_2 incubator until cells were attached to the well and a confluent monolayer was formed. Then a scratch was made across the centre of the well with a sterile 200 µl pipette tip. The media was replaced with DMEM/F12 (with no serum added) to remove the cell debris then the plate was immediately incubated in a 37°C/free CO_2 incubator attached to a time lapse microscope (LEICA DMIRB Microscope, LEICA Microsystems) to assess the migration of the cells for 65 hours. Images were taken with Brightfield 10x Phase contrast objective lens, every 30 minutes at 3 positions along each scratch.

Moreover, in order to determine the effect of two PI3K pathway inhibitors on the migration response of the three cell lines, three independent scratch assay experiments were performed on the three cell lines. Approximately, $0.5X10^6$ cells of three cell lines were seeded into uncoated sterile 6-well plate (Costar, 3506) and treated following the same procedure in 2.5.1.2. Then subsequently after the scratch was made, the inhibitors [20 μM of LY294002 (Source BioScience, ABE2892) or 1μM of GDC-0941 (Selleckchem, S1065)] were added and immediately the migration response was assessed under the same conditions mentioned earlier on time lapse microscope (LEICA DMIRB Microscope, LEICA Microsystems).

2.5.1.3 Statistical analysis for scratch assay

ImageJ software was used to determine the % of wound closure over the time (scratch size). GraphPad Prism version 5.00 (San Diego California, USA) was used to fit the data with nonlinear regression fit curves analysis (plateau followed by one phase decay or one phase decay) and F-test was performed to choose the best fitting curve for the data points. The equations for the two fit curves are: Plateau followed by one phase decay [Y= If (X<X0, Y0, Plateau + (Y0-Plateau)*exp(-K*(X-X0))] and for one phase decay [Y=(Y0 - Plateau)*exp(-K*X) + Plateau]. Finally, the differences in migration rate of the C6 glioma cell lines were determined by applying the 1-way ANOVA test.

2.5.2 Transwell migration assay

2.5.2.1 Principle

This assay is used to study the migration response of endothelial cells to a chemo-attractant or chemo-inhibitor agent. The assay includes the addition of the cell suspension to a cell permeable membrane which is placed on a 96-well plate (lower plate). The lower plate includes a solution (either the chemo-attractant or inhibitor agent). This is followed by an incubation

period, after which cells that have migrated through the membrane are counted. The main advantages of the assay is its detection sensitivity and it studies the migration phenomenon only (not like the scratch assay which measures both migration and the proliferation).

2.5.2.2 Determination of migration of glioma cell lines by trans-well migration assay

ChemoTx®System (Neuro Probe, 101-3) transwell plate was used to assess the migration ability of the cells towards 10% foetal bovine serum (FBS) as the attractant. The kit is composed of a 96 well lower plate with 3μm pore size filter, and a lid to cover the filter. First, 29 μl of either HBSS (no phenol red) or 29 μl of 10% FBS was added to the lower plate. Then slowly the filter was replaced above the lower plate allowing the contact between the fluids in the lower plate with the filter. After that, 25μl of a $2x10^4$ cell suspension was added gently to the filter and the microplate was covered with the plastic lid and incubated in a $37^{\circ}C/5\%CO_2$ incubator for 24 hours. After 24 hours incubation, the plate was removed from incubator and media was aspirated. Cells were fixed with 4% (w/v) paraformaldehyde (PFA) in PBS for 20 minutes at room temperature. Then 30 μl of Hoechst 33342 stain was added to each well for 5 minutes at room temperature to stain the nuclei. Finally, 30 μl of PBS was added to remove excess Hoechst dye and the microplate was scanned on the ImageXpress^{MICRO} (Molecular Devices, USA).

2.5.3 Statistical analysis for the transwell migration assay

The total number of migrated cells was determined by the MDC microplate reader (ImageXpress^{MICRO}, Molecular Devices, USA). Then the fold change, which represents the total number of cells migrated into the 10% FBS wells (chemoattractant) relative to the total number of cells migrated into the HBSS wells (control), was calculated by applying the 1 way ANOVA test to

determine the difference in the migration response of the three cell lines under the influence of chemoattractant.

2.6 Response of cells to oxidative response

2.6.1 Principle

Cells were treated with 2',7'-dichlorofluorescin diacetate (DCFH-DA) (Invitrogen, D399), which is a fluorescent probe, to assess the response of cells towards oxidative stress (OS). The theory behind using DCFH-DA is that the nonionic, nonpolar DCFH-DA crosses cell membranes and is hydrolysed enzymatically by intracellular esterases to membrane impermeable DCFH. In the presence of reactive oxygen species (ROS), DCFH is oxidized to fluorescent dichlorofluorescein (DCF) and hence, the intracellular DCF fluorescence can be used as an index to quantify the overall OS in cells (Wang and Joseph, 1999). An optimisation for the assay on the C6 cell line is described in chapter 5. The protocol below describes the method used after experiment optimisation.

2.6.2 Determination of ROS amount produced with TBHP treatment

To determine the relative amount of ROS produced and the rate of ROS production, $1x10^4$ cells in 200 µl DMEM/well were seeded into a black clear bottom 96-well plate (Greiner Bio-one, 655097). The plate was incubated overnight to allow the cells to attach to the wells. After that, the media was replaced by 50 µM DCFH-DA in HBSS to each well and the plate was incubated in a 37°C/5% CO_2 incubator for 30 minutes. After the incubation period, excess DCFH-DA was removed and cells were washed with 200 µl HBSS then tert-butyl hydroperoxide (TBHP) was added. Increase in DCF, the fluorescence produced, was measured at λ_{530} nm after excitation at λ_{485} nm every 5 minutes for an hour followed by 30 minutes for 2 hours on a Flexstation 3 fluorescence microplate reader (Molecular Devices, USA).

2.6.3 Statistical analysis for ROS assay

The data obtained were analysed using linear regression in GraphPad Prism version 5.00 (San Diego California, USA) to calculate the rate of change of ROS production as function of TBHP.

2.6.4 Determination of cell death with cytotoxicity assay

To assess cell cytotoxicity (reported by changes in proliferation), MTT assay was performed on the three glioma cell lines. Approximately $1x10^4$ cells in 200 µl DMEM/well were seeded into a 96-well plate and incubated in a 37°C /5%CO_2 incubator for 24 hours. Subsequently the cells were treated with different concentrations of TBHP (0, 100, 250, 500 µM) for time intervals up to 3 hours. Following TBHP treatment, media was replaced and cells were incubated in a 37°C /5%CO_2 incubator for further 24 hours.

When cells in control, untreated wells were nearly confluent, MTT assay was performed by adding Thiazolyl Blue Tetrazolium Bromide (Sigma, M2128) to each well to a final concentration of 5 mg/ml in media and then incubated at 37°C /5%CO_2 for 3 hours. After the incubation period, DMSO was added to dissolve the insoluble purple formazan product, the intensity of which was measured at 550 nm using a microplate reader (Revelation-Dynex Technologies version 4.24). Absorbance of treated and untreated control cells was calculated and presented as relative cell viability following this formula: viability%= T/C x100%, where T and C refer to the absorbance of the treated wells and control wells, respectively.

2.7 Protein immunoblotting analysis

2.7.1 Preparation of sample

After harvesting cells, cell pellets were washed with 1X PBS buffer to get rid of any media present and then centrifuged at 2500 rpm for 5 minutes at room temperature. After that, cells were resuspended in PBS/glycerol (10%) and protease inhibitor cocktail set III, EDTA free (Calbiochem,

D00068078) was added. Then cells were lysed by sonicating for 3x at 40% power (JENCONS, Sonics and materials INC., USA).

2.7.2 Determination of protein concentration

Protein samples (5µl) were analysed in duplicate alongside a standard curve 0-10 µg of bovine serum albumin (BSA). Protein content was determined by addition of an alkaline copper tartrate solution, followed by the folin reagent, and room temperature incubation of 15 minutes. Protein concentration in C6 cell lysates was determined by interpolation to the standard curve.

2.7.3 Polyacrylamide gel electrophoresis

Ptrotein gel electrophoresis was carried out according to Laemmli 1970 (Laemmli, 1970) using a BioRad miniprotean III apparatus. 10% or 15% w/v resolving gels were poured with a 4% w/v stacking gel and used to separate proteins. Typically, 30 µg of protein was resolved in Laemmli running buffer (25 mM Tris base, 0.192 M Glycine, and 0.1%w/v SDS) until the dye font was eluted from the gel at 40 mA/gel or 160 volts/gel.

2.7.4 Protein transfer

Separated proteins were transferred onto nitrocellulose membrane (Hybond-C extra nitrocellulose, RPN203E, Amersham Biosciences) using a GeneFlow western blotting apparatus for 2 hours and 30 minutes at 200 mA in a tank filled with western transfer buffer (25 mM Tris.Cl, 0.19 M Glycine, and 20% methanol) with a frozen small bottle of water inside the tank, to prevent the elevation of the temperature which may affect the transfer of the proteins.

2.7.5 Primary and secondary antibodies treatment

Nitrocellulose membrane was stained with Ponceau stain (0.5% w/v Ponceau S in 5% v/v acetic acid) to verify transfer and residual Ponceau stain was removed by washing in PBST (PBS supplemented with 0.05% v/v Tween-20) for 3 minutes. Non-specific sites on the nitrocellulose membrane were blocked by incubation in blocking solution [5% w/v non- fat Marvel milk in PBST] at room temperature for an hour. Then the blot was incubated with the primary antibody in the blocking solution (table 2.1 shows primary and secondary antibodies used and their dilutions) overnight at 4°C on a rocker. Subsequently, blots were washed 3-5 times with PBST, and then they were incubated with secondary antibody diluted in 1% non-fat milk in PBST for an hour at room temperature on a rocker. After the 1 hour incubation, the wash step was repeated again and then a final wash with 1x PBS was performed.

2.7.6 Enzymatic chemiluminescence detection (ECL)

The peroxidase activity of secondary antibodies was detected by the enzymatic chemiluminescence (ECL) kit assay (SuperSignal® West Pico Chemilluminescent Substrate, Thermo Scientific, 34080) according to the manufacturer's instructions. For each blot multiple exposures were taken on Kodak medical x-ray film (SLS, 5256433) followed by scanning at 300-600 dpi.

Table 2.1 The primary and secondary antibodies used in western blotting

Primary antibody/Source/ Molecular weight (kDa)	Dilution*	Secondary antibody/Source/ Dilution*
Rabbit anti-Catalase (Abcam, ab16731) M.wt= 60 kDa	1:500	Swine Anti-rabbit HRP (Dako, P0217) 1:2000
Rabbit anti-PRP19 (Abcam, ab27692) M.wt= 55 kDa	1:500	
Rabbit anti-PTEN (Cell Signaling, 9559) M.wt= 54 kDa	1:500	
Rabbit anti- Lamin A/C (Cell Signaling, 2032) M.wt= 70 kDa	1:500	
Rabbit anti- Vimentin (Cell Signaling, 5741) M.wt= 57 kDa	1:5000	
Rabbit anti-caspase 3 (cell signalling, 9662) M.wt=35, 19, 17 kDa	1:1000	
Mouse anti- β-Actin (Sigma-Aldrich, A5316) M.wt= 42 kDa	1:5000	Anti- mouse HRP (Dako, P0260) 1:2000

*All primary antibodies dilutions were prepared in 5% non-fat milk in PBST, except for caspase-3 antibody which was diluted in Tris buffered saline supplemented with 0.1% v/v Tween-20. The secondary antibodies were diluted in 1% non-fat milk in PBST or TBST for caspase-3 blotting.

2.7.7 Densitometry analysis

The density of each band was determined with Scion Image software (NIH, USA) after scanning the blots on EPSON PERFECTION 2400 PHOTO scanner on the following conditions: grayscale, 24 bits, and 300 ppi on a reflective mode and saved as Windows Bitmap files. The mean of the relative expression for each protein from three independent blots was calculated and compared to the relative expression of the control used (β-Actin). Finally, one way ANOVA was performed on GraphPad Prism version 5.00 (San Diego California, USA) to determine the changes in the candidate proteins expression.

2.8 Reverse Transcriptase- Polymerase Chain Reaction (RT-PCR)

2.8.1 Preparation of cDNA

The RNA samples were diluted with DEPC water to a working concentration of 100 ng/µl. RNA (100 ng) was reversed transcribed in a reaction containing 500 ng oligo dT (12-18), 3 µg random primers and 0.5 mM dNTPs. Reactions were heated at 65°C to denature RNA for 5 minutes then a rapid annealing of oligo dT on ice for 1 minute. The next step was the reverse transcriptase (RT) reaction, 4 µl of 5x first strand buffer, 1 µl 0.1 M DTT, and 1 µl (200 u/µl) Superscript III reverse transcriptase (Invitrogen, 18080-093) were added to all tubes, mixed gently and incubated at 25°C for 5 minutes (to allow annealing of random primers) followed by another incubation at 50°C for 45 minutes (to allow reverse transcription) and finally at 70°C for 15 minutes (to inactivate the reaction). Finally, the 20 µl cDNA samples were diluted with 40 µl DEPC water (1:3), respectively. In parallel, reactions lacking RT were performed to detect the presence of amplification form of residual genomic DNA in downstream PCR.

2.8.2 Quantitative PCR (qPCR) Primers designing

When designing primers for quantitative PCR (qPCR) a number of considerations were uppermost; the size of the PCR product should be <150 bp, there should be no complementary sequence between forward and reverse primers and mismatches, the length of the primers should be between 18-30 nucleotides, the GC% content should be 40-60%, and most importantly they should span an intron (to distinguish genomic DNA). With these considerations, Primer BLAST (national centre for biotechnology (NCBI), www.ncbi.nlm.nih.gov) was used to design primer pairs for qRT-PCR. (Table 2.2 shows the primer pairs for each gene and the PCR products size).

2.8.3 Gradient annealing temperature (Ta) optimisation

Before using primers for the qPCR, a gradient PCR reaction was performed on all primer pairs to test the best annealing temperature for each. In each tube, a 25 µl mixture was made as follow: 1 µl of cDNA template was mixed with 11.1 µl of DEPC water, 0.2 µl of forward primer (0.4 µM), 0.2 µl of reverse primer (0.4 µM) and 12.5 µl of 2x BioMix red (Bioline, Bio-25005). A gradient PCR reaction was designed as follows: initial denaturation at 96°C for 5 minute, and then 40 cycles at 96°C for 35 seconds, annealing at 58°C for 35 seconds, and extension at 72°C for 45 seconds and final extension at 72°C for 4 minutes.

Table 2.2 Primer pairs for qRT-PCR

Gene Name	Ensembl rat transcript ID*	Forward primer	Reverse primer	PCR product size
BMP7	ENSRNOT00000009656	5′-CGCACCTGAAGGCTATGCTGCC-3′	5′-GCAGGGCTTGGGTACGGTGT-3′	139 bp
EGR1	ENSRNOT00000026303	5′-GGAGCCGAGCGAACAACCCT-3′	5′-TCCAGGGAGAAGCGGCCAGT-3′	150 bp
ATP1B1	ENSRNOT00000003932	5′-TTCGGCCCAGAAGGACGACA-3′	5′-ACCTGCACACCTTGCGCTCT-3′	110 bp
COL3A1	ENSRNOT00000004956	5′-TGGTGGACAGATGCTGGTGCTG-3′	5′-GGCCCGGCTGGAAAGAAGTCTG-3′	150 bp
COL1A2	ENSRNOT00000016423	5′-GCCCGCACATGCCGTGACTT-3′	5′-GGGCCTGGATGCAGGTTTCA-3′	142 bp
PTEN	ENSRNOT00000028143	5′-AGCCATTGCCTGTGTGTGGTGA-3′	5′-TCTGAGGTTTCCTCTGGTCCTGGT-3′	130 bp
ABCF2	ENSRNOT00000014718	5′-GCGCTACGGCCTCATTGGCT-3′	5′-TCGCTAGGGGGCATCTCCCG-3′	129 bp
B-Actin	ENSRNOT00000042459	5′-ACCGAGGCCCCTCTGAACCC-3′	5′-CCAGTGGTACGACCAGAGGCA-3′	134 bp
GAPDH	ENSRNOT00000050443	5′-CCCCCTGGCCAAGGTCATCCA-3′	5′-CGGCCATCACGCCACAGCTT-3′	126 bp

*****Transcript ID from Ensembl.org search and the search was made on *Rattus Norvegicus*.

2.8.4 Determination of primer efficiency

The efficiency of the primers is an important factor for successful qPCR. The efficiency values of each primer pair are also used to determine the relative gene expression by Pfaffl equation later. The cDNA and –RT samples prepared from C6 were used as a calibrator. The 2-fold series dilutions for cDNA sample were prepared and varied from one gene to another in order to get an efficiency value between 90-110% and a linear curve slope between -3.2 and -3.6. To determine the efficiency for each primer set, a mixture of 12.5 µl Sybr® green for IQ (Bio-Rad, 1708884), 2.5 µl of forward primer (1 µM), 2.5 µl of reverse primer (1 µM), and 6.5 µl DEPC water were added to each well then 1 µl of cDNA (1:3 dilution), -RT, and DEPC water were added to the assigned well (Figure 2.3 shows an example of a plate used to determine the efficiency of the primer).

The PCR reaction was run on CFX96 real time PCR (BIO-RAD) as follows: 96°C for 5 minutes, 96°C for 35 seconds, 60°C for 35 seconds, 72°C for 45 seconds for 40 cycles then a final extension at 72.0 C for 4 minutes followed by a melting curve from 65 to 95°C, increment 0.5°C to validate there is no contamination of the primer. Finally, the efficiency of each primer was calculated by this equation: Efficiency = $[10^{(-1/\text{slope})} - 1]*100$

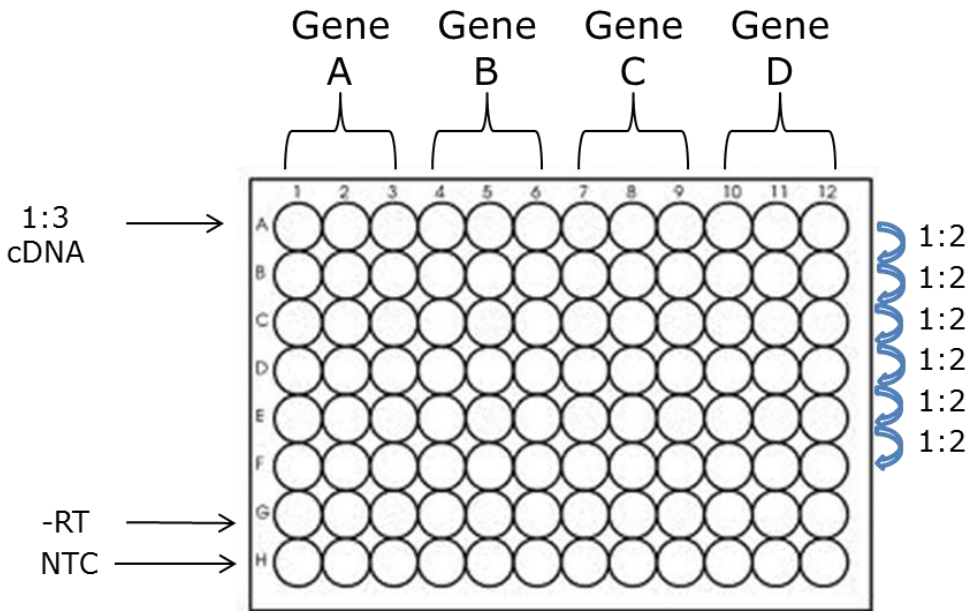

Figure 2.3 The design of primer efficiency plate. Serial 2-fold dilutions for cDNA from C6 were made to assess the efficiency of each primer pair. Each cDNA, -RT, and NTC (DEPC water) was analysed in triplicate for each gene. After 40 cycles, a standard curve was produced. The efficiency of the primers should range from 90-110%, the R^2 of the linear standard curve should be close to 1.00, and the slope of the curve should be between -3.2 and -3.6. NTC: No template control which is used as a negative control (it is only DEPC water). Dilution 1 which is used at the start of the experiment is the (1:3) cDNA dilution, produced by the RT step 2.8.1.

2.8.5 Determination of relative expression of candidate genes by qRT-PCR

In order to determine the relative expression of candidate genes with qPCR, a PCR reaction was performed following the protocol in 2.8.4. From this reaction, the relative cycle thresholds (C_T) were determined for each candidate and control genes. C_T represents the number of cycles required for the fluorescent signal to exceed the threshold of the background level. C_T levels are inversely proportional to the amount of cDNA in the sample. For each gene, 3 independent experiments were performed in order to have a better reproducibility results. The mean of the C_T values from 3 experiments was calculated and the relative expression for the test gene was determined by dividing it's relative expression by the geometric mean for the relative expression of GAPDH and β-Actin (which were used as controls)

(Vandesompele et al., 2002). The relative expression was calculated following the Pfaffl equation:

$$R = \frac{E\ \text{target}^{\Delta C_T\ (C_T\ \text{calibrator (C6)} - C_T\ \text{target gene sample})}}{E\ \text{control}^{\Delta C_T\ (C_T\ \text{calibrator (C6)} - C_T\ \text{control gene sample})}}$$

Where, *R* is the relative ratio of the difference in fluorescent signal between the target gene in the calibrator (C6) and other drug derived cell lines when compared to the control gene (Pfaffl, 2001), and E is the efficiency of the primer which has been explained in details in 2.8.4. Finally, 1-way ANOVA test was performed in GraphPad Prism 5.00 (San Diego California, USA) to compare the changes in candidate genes expression.

2.9 Determination of exons sequence of *PTEN* gene

To determine the genetic variance in *PTEN* gene exons in the three glioma cell lines, PCR was performed on the cDNAs using these primer pairs (forward 5'-GACAGCCATCATCAAAGAG-3' and reverse 5'-GATCAGCATTCACAAATTAC-3') to give a product with this size (1212 bp). In each tube, a 25 µl mixture was made as follow: 1 µl of cDNA template was mixed with 5 µl of Q5- 5X reaction buffer (1X) (NEB, B9027S), 0.5 µl of 10mM dNTPs (200 µM), 18 µl of DEPC water, 0.125 µl of forward primer (0.5 µM), 0.125 µl of reverse primer (0.5 µM) and 0.25 µl Q5 Hot Start High-Fidelity DNA polymerase (0.02 U/µl) (NEB, M0493S). A PCR reaction was designed as follows: initial denaturation at 98°C for 30 seconds, and then 35 cycles at 98°C for 10 seconds, annealing at 54°C for 30 seconds, and extension at 72°C for 30 seconds and final extension at 72°C for 2 minutes. The PCR products were run on 1% agarose gel to verify the correct product size before they were purified with QIAquick® PCR purification kit (QIAGEN, 28104). Finally, the PCR products were sequenced with Sanger sequencing at the DNA sequencing lab at the University of Nottingham.

CHAPTER III

INTEGRATED PROTEOMIC AND GENOMIC APPROACHES TO ELUCIDATE MECHANISMS OF DRUG RESISTANCE IN A HIGH GRADE GLIOMA CELL LINE MODEL

CHAPTER III: INTEGRATED PROTEOMIC AND GENOMIC APPROACHES TO ELUCIDATE MECHANISMS OF DRUG RESISTANCE IN A HIGH GRADE GLIOMA CELL LINE MODEL

3.1 Introduction

The abundance and activity of proteins in a cell determine its function. It is important to understand the relationship between protein expression and mRNA expression as this will help in the interpretation of gene expression and protein structure and function in the cellular system. Many post-translational modifications (PTMs) in proteins such as acetylation, amidation, glycosylation, and phosphorylation can alter the structure, chemical and physical characteristics of a protein which may in turn result in alterations in protein function (Dowsey et al., 2010). In order to identify protein and gene expression patterns that could be associated with drug resistance proteomic and genomic approaches can be applied. Indeed, there is an urgent need to integrate and collaborate efforts to elucidate the changes in the cancer proteome similar to the current efforts to explain the genomic alterations in cancer. For a complete picture, cancer research should firstly, integrate the result from proteomic and genomic analyses, and then secondly, study the biochemical pathways that are specifically related to therapy.

The analysis and identification of thousands of proteins in a cell or tissue mixture has become easier since the introduction of 2-DIGE in 1975 and protein MS in 1985 (O'Farrell, 1975, Whitehouse et al., 1985). 2-DIGE is a technique used to separate proteins based on two properties. In the first dimension, proteins are separated according to their isoelectric point (pI) and in the second dimension, proteins are separated according to their denatured molecular weight (O'Farrell, 1975). Alongside protein identification, gene expression analysis has an important role in cancer research. Microarrays represent a major technology in the field of molecular biology and medicine. Affymetrix GeneChip Microarrays have become a powerful technique in

measuring gene expression levels (at a transcriptional level) in order to improve disease diagnosis. Each array is composed of thousands of DNA oligonucleotide spots (probes) (>30,000 genes) that are factory designed and synthesized attached to a solid support (Li and Li, 2009).

In the current chapter the aim is to identify changes in protein modification and gene expression that occur in response to drug treatment (etoposide and irinotecan) and selection in a cell line model of high grade glioma (rat C6 glioma cell line). The chapter starts with a characterization of their drug resistance and then considers proteomic and transcriptome data. The preliminary experimental approach is described graphically in figure 3.1.

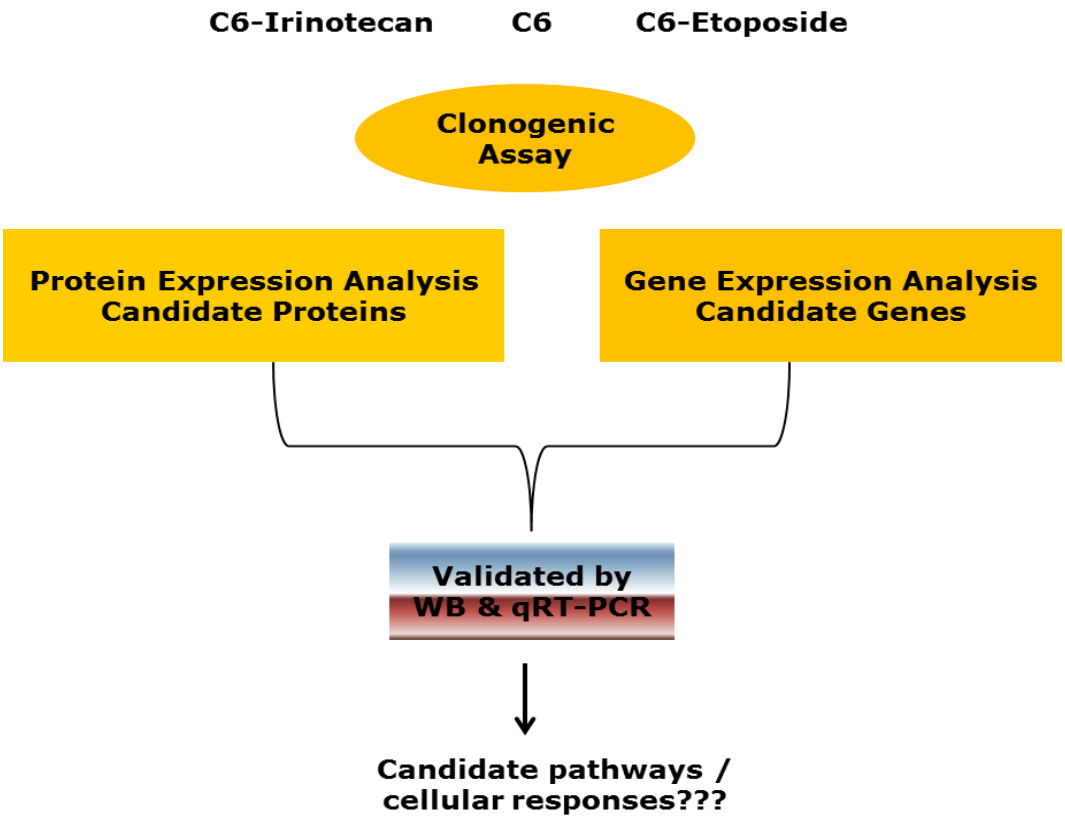

Figure 3.1 Preliminary experimental approaches for this study. Cell lines will be examined for changes in protein and gene expressions. The expression of candidates will be validated with western blotting (WB) and qRT-PCR, respectively. Integration of this data into pathway analysis will enable downstream analyses of biological responses and signaling pathways which will be studied in chapters 4 and 5.

3.2 Results

3.2.1 Clonogenic assay

Three cell lines were used in this study, the C6 glioma cell line and two drug selected sublines established by chronic exposure (continuous culture) to 10 μM and 8 μM of etoposide and irinotecan, respectively. At the beginning of this study, clonogenic assays were performed to determine the IC_{50} and IC_{70} of each cell line for both drugs. Six independent experiments were performed, with each experiment performed in duplicate following the protocol mentioned in (Farnken et al., 2006). Approximately 100 cells were seeded into a 6 well plate and were treated with different concentrations of either etoposide or irinotecan or a vehicle control (see section 2.2.2 for more details). After drug incubation media was replaced and after a total of 7-10 days, colonies were fixed with 4% paraformaldehyde (PFA), and stained with crystal violet and then counted (figure 3.2a and b). Analysis of the data showed that for etoposide treatment, the C6-etoposide cell line was clearly more resistant which was indicated by the rightward shift of C6-etoposide curve compared to the other two cell lines ($P \leq 0.001$) (figure 3.2c). On the other hand, for irinotecan treatment, no difference was observed in the response of the three cell lines to irinotecan ($P > 0.05$) (figure 3.2d).

The IC_{50} and IC_{70} of both etoposide and irinotecan for all three cell lines were also determined. With etoposide treatment, the C6-etoposide vs. C6 IC_{50} and IC_{70} concentrations were significantly increased confirming that C6-etoposide is more drug resistant [etoposide IC_{50} was 25 μM ± 8 vs. 10 μM ± 3, whereas, etoposide IC_{70} was 45 μM ± 18.6 vs. 16 μM ± 4, for C6-etoposide vs. C6, respectively] (figure 3.2e and f). The increase fold change difference in resistance in response was obtained with chronic exposure to etoposide. However, with irinotecan treatment, no significant differences in the IC_{50} & IC_{70} were observed (figure 3.2g and h).

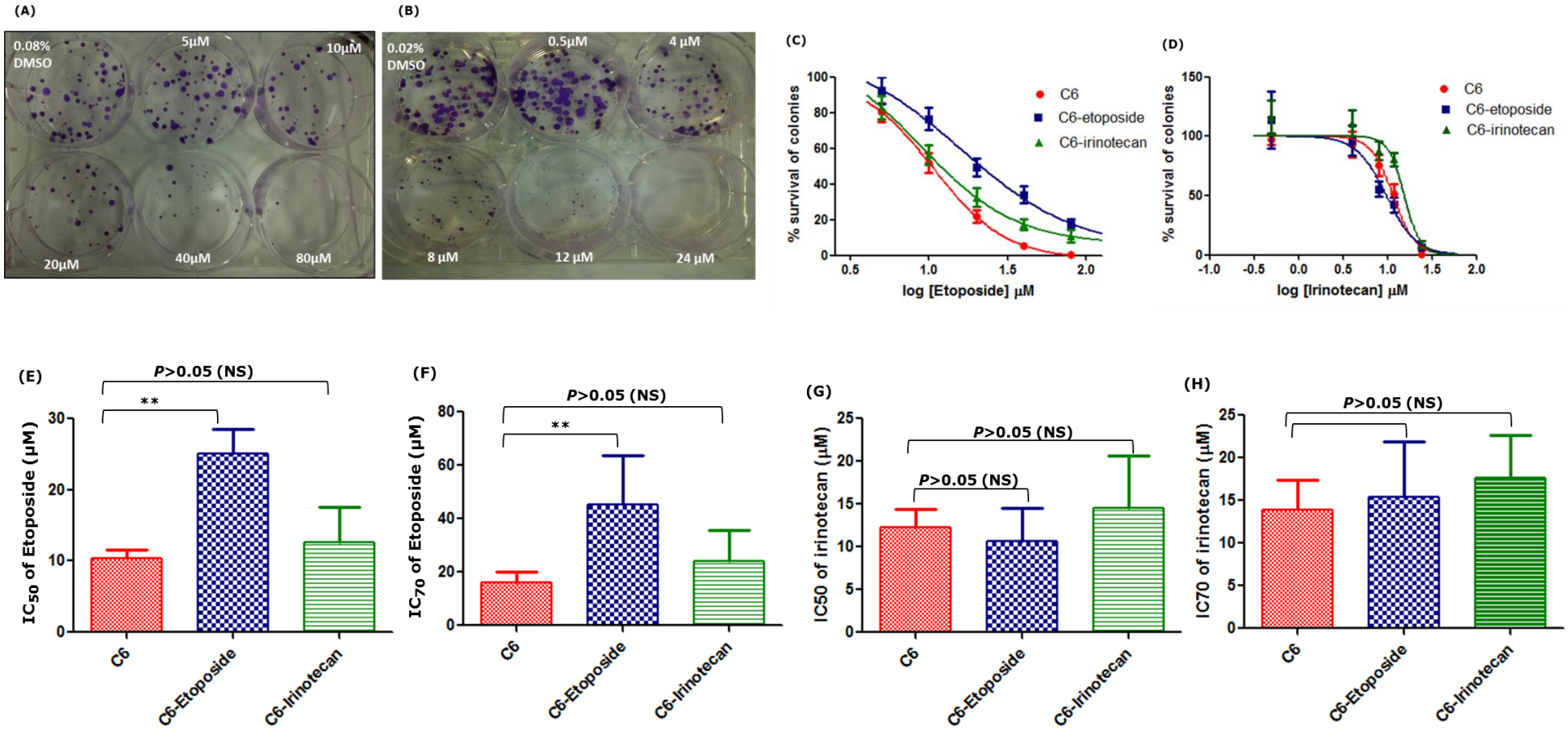

Figure 3.2 Drug resistance in drug selected derivatives and the parental C6 cell line. (A) & (B) Examples of clonogenic assay plates of C6-etoposide treated with increasing concentrations of etoposide (5-80 µM) or irinotecan (0.5-24 µM), respectively. (C) & (D) represent the clonogenic survival of the 3 cell lines (sigmoidal dose response curve) in the presence of etoposide (C) or irinotecan (D) relative to vehicle control. A rightward shift in the curve (C) compared to the parental line is indicative of etoposide resistance whereas all cell lines had a similar response to irinotecan ($P \geq 0.05$) in curve (D). (E) & (F) The IC_{50} and IC_{70} calculated for etoposide indicated that C6-etoposide cell line is more resistant to etoposide in comparison to the other cell lines, whereas (G) & (H) indicated that no differences in the IC_{50} and IC_{70} for irinotecan were observed. Unpaired t test $P>0.05$ (not significant) and $^{**}P \leq 0.001$, n=6.

3.2.2 Two-dimensional gel electrophoresis

3.2.2.1 Protein spot analysis

Following on from this analysis we examined the proteome of C6, C6-etoposide, and C6-irinotecan. For the two drug-selected sublines, acute and chronic changes in protein expression were determined after they were cultured in the presence or absence of IC_{70} levels drug, respectively. We reasoned that chronic changes in protein expression would still be evident when C6-etoposide and C6-irinotecan were cultured in the absence of drug; whereas acute changes should be evident upon addition of drug to the culture medium. Thus, cells were passaged alternatively in media either containing drug (8 μM of irinotecan or 10 μM etoposide) or in the absence of drug to detect these expression changes (figure 3.3).

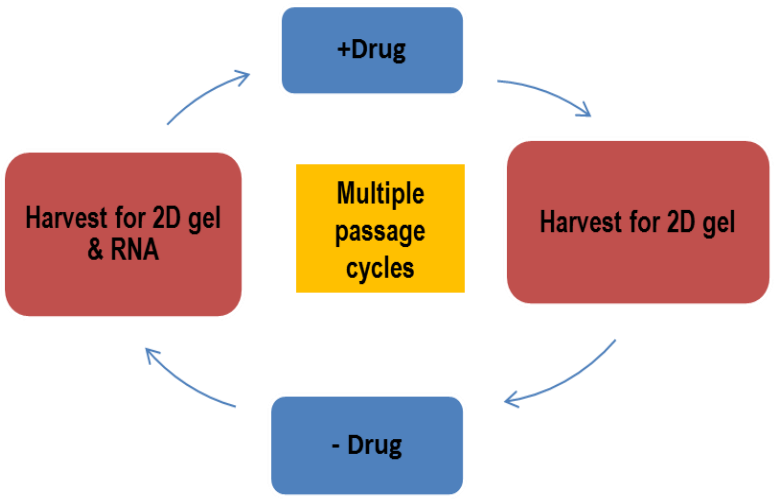

Figure 3.3 A schematic plan for deriving cell pellets for protein and gene expression. C6-Etoposide and C6-Irinotecan cell lines were treated alternatively in passages with either drug present (10 μM etoposide or 8 μM irinotecan) or with no drug. In cycles which did not have drug, cells were harvested to study the persistent changes in the level of protein and genes. Whereas, cycles which have drug were harvested to study the transient changes at the protein level.

At the beginning several optimisation experiments were performed to determine the best protein concentration to be loaded and also to adjust the conditions of 2-DIGE such as focusing steps, staining, and scanning. To resolve the proteome 2-dimensional gel electrophoresis was performed and 4 gels/condition were produced. Representative gel images from ≥4 independent 2-D gels with different cell passages are shown for C6 (figure 3.4), C6-irinotecan (figure 3.5a and b), and C6-etoposide (figure 3.6a and b).

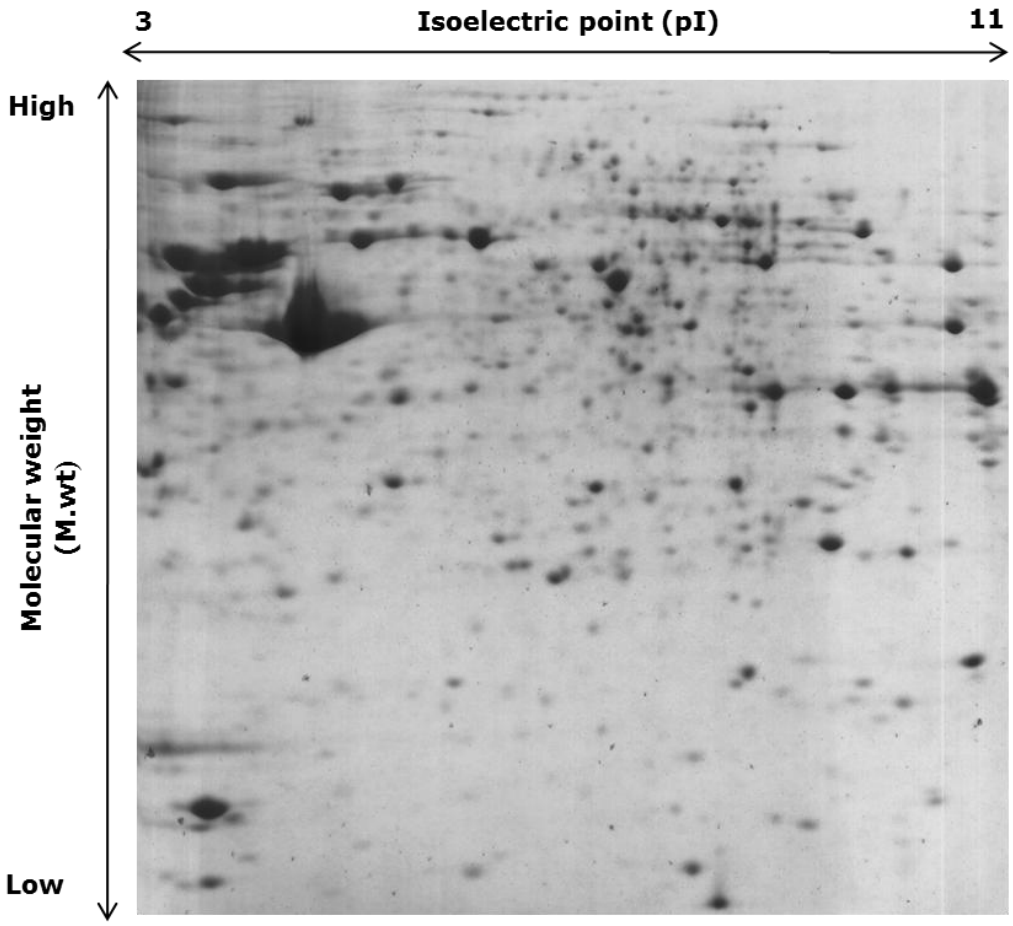

Figure 3.4 2D proteome of parental glioma (C6) cell line. Cells ($8x10^6$) were resuspended in DeStreak™ Rehydration solution and then loaded into the anode cup of a pre-hydrated IEF strip (16cm, pH 3-11). The strips were mounted onto 5-20% w/v gradient polyacrylamide gels. Gels were scanned as grayscale, 16 bits, 300 ppi TIFF images.

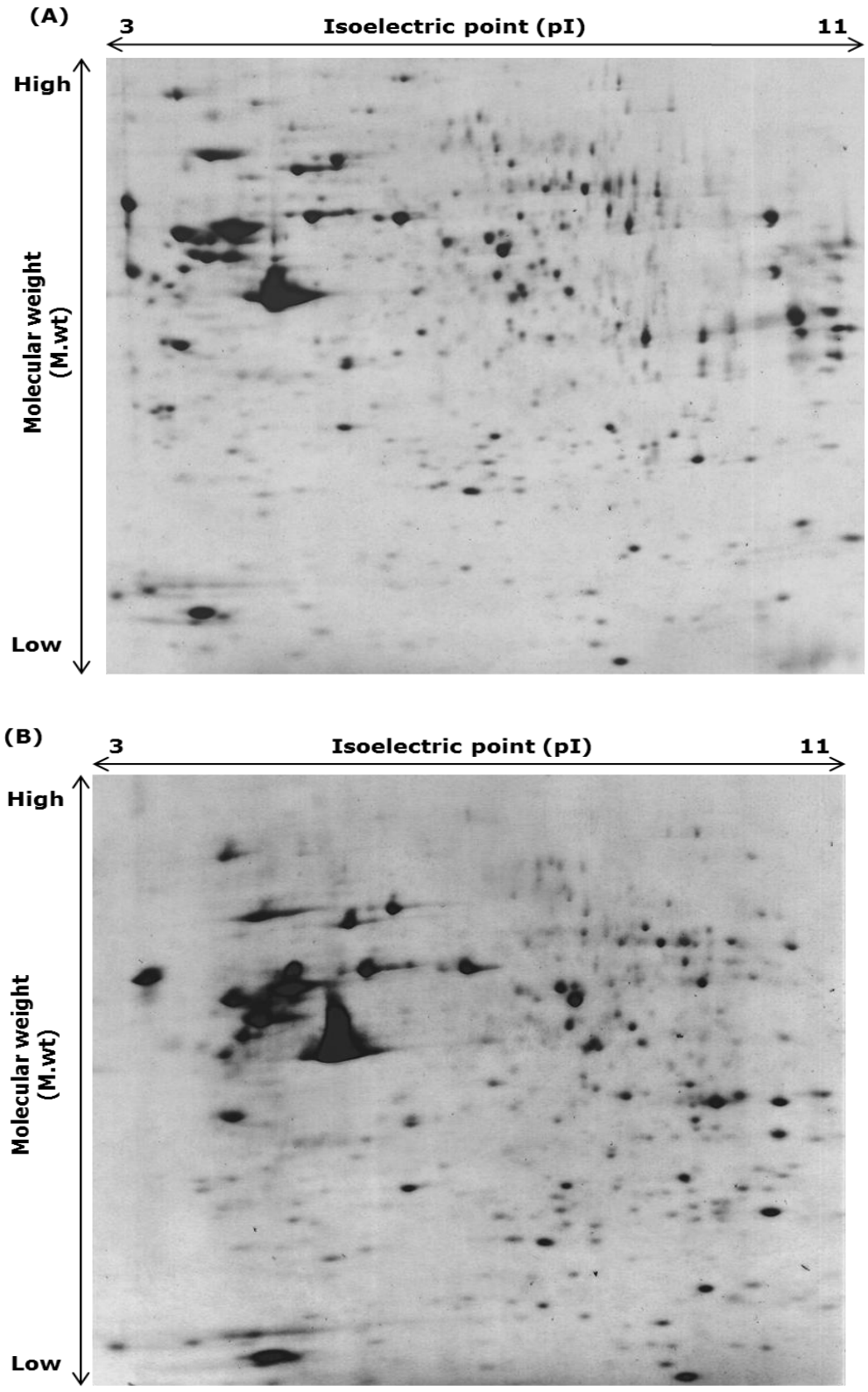

Figure 3.5 2D proteome of C6-irinotecan cell line. Cells ($8x10^6$) were processed identically as in figure 3.4. (A) The passage prior to harvesting did not contain drug. (B) The passage prior to harvesting has 8 μM irinotecan.

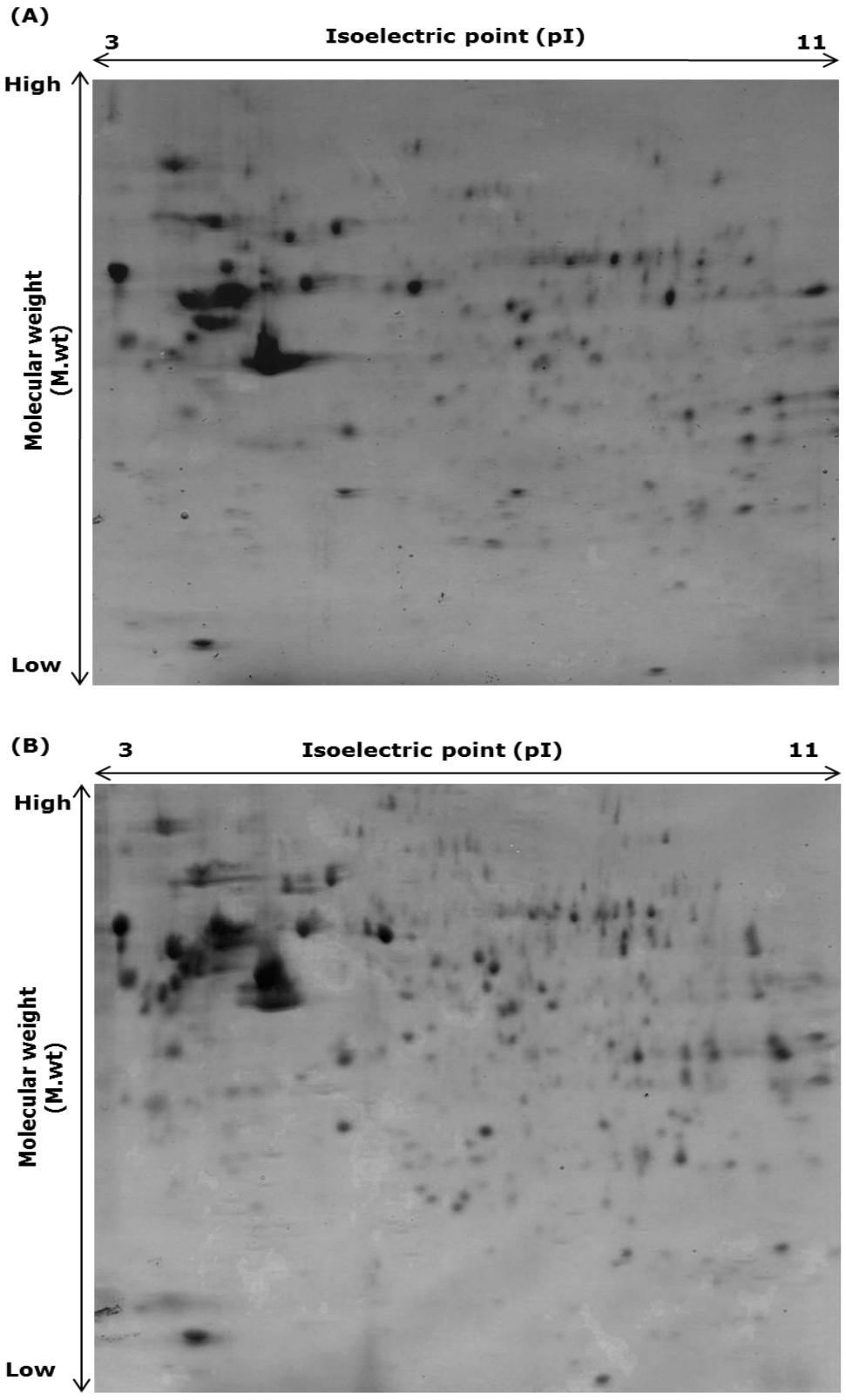

Figure 3.6 2D proteome of C6-etoposide cell line. Cells ($8x10^6$) were processed identically as in figure 3.4. (A) The passage prior to harvesting did not contain drug. (B) The passage prior to harvesting has 10 μM etoposide.

The initial analysis of protein expression was performed using Progenesis Samespots V4.1 (Non-Linear Dynamic, UK). The quality of all scanned gels was investigated automatically by the software before proceeding with the analysis. A parental C6 gel was selected as a reference gel to which all other gels were aligned. The alignment process is necessary because variations in electrophoresis mean that gels are not immediately superimposable. To enable the software to "warp" gels so that individual protein spots in all gels do superimpose, a series of vectors are defined (both automatically and manually). Each vector identifies a protein spot on a reference gel and its relative position on a target gel. All target gels were then warped using 300 vectors to enable overlay and comparison of spot intensities and volumes.

A one way analysis of variance (ANOVA) test was performed to identify protein spots showing different intensities between the 5 cell lines/conditions. At the end of this step, 26 spots were identified with (*P value < 0.05 and a fold change (FC) ≥ 1.5) and found to have pI values from 4-11 and molecular weight between 20,000 to 450,000 Daltons according to the initial analysis and molecular weight marker in the Progenesis software. These 26 spots were excised from the reference gel and sent for further identification by MS. The 26 protein spots sent for identification by MS are shown in figure 3.7.

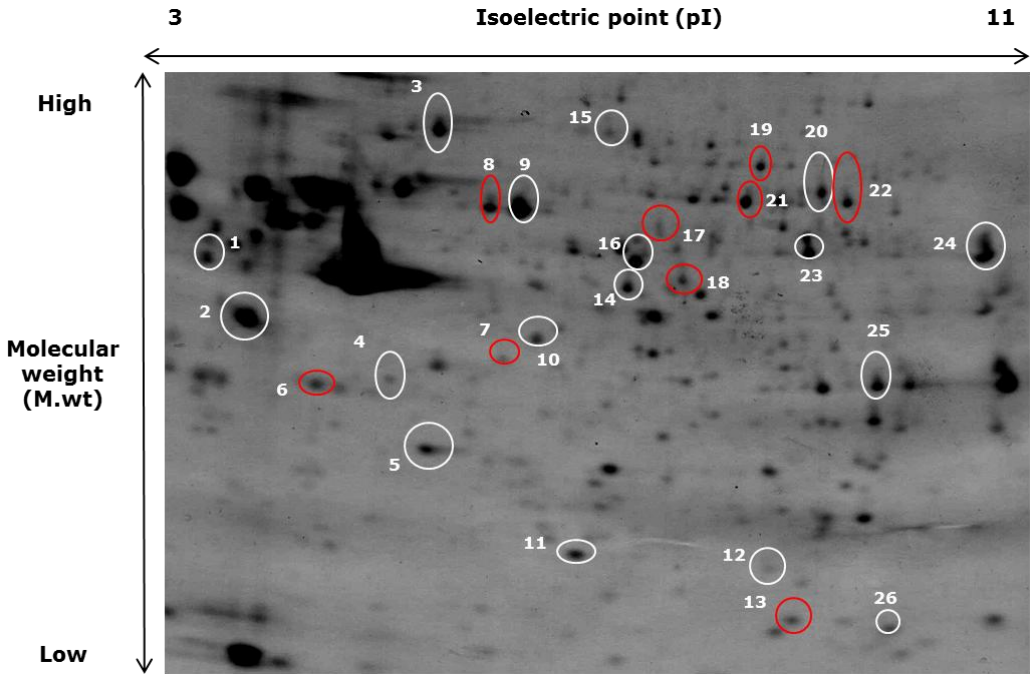

Figure 3.7 The 26 protein spots which were selected for analysis by mass spectrometry (MS). The gel represents the C6 (gel 3) which was chosen as a reference gel. The 26 protein spots showing different expression levels in glioma cell lines are indicated and were identified by peptide mass fingerprinting (PMF). The spots with red circles represent candidate proteins for involvement in drug resistance and will be further validated in the next two chapters.

3.2.2.2 Mass spectrometry (MS) results

The analysis of the 26 protein spots was done by Dr. David Tooth at the University of Nottingham. Briefly, this involved an in-gel tryptic digestion, peptide recovery and matrix assisted laser desorption ionisation mass spectrometry analysis (MALDI-MS). The PMF analysis for the 26 spots was as follows: (1) 9 spots produced confident peptide mass spectra to be used in the database search, (2) 7 spots produced mixed peptide spectra (non-confident match), and (3) 10 spots did not generate enough peptide spectra to be used in searching in the database. At the end of the analysis with MS, a further analysis with tandem repeat MS-MS was performed on the 9 spots to ensure the accuracy of the data obtained. Then a general search using PubMed was performed on the 9 proteins to determine their functions. These

9 proteins were included in the study because they met these two criteria: (1) significant *P* values≤0.05 and (2) fold change (FC) in protein expression ≥1.5 in pair-wise comparison of the cell lines using unpaired t test. These proteins are involved in drug resistance, migration, metastasis, DNA damage and apoptosis. Therefore, with the advanced proteomic approaches used, we were able to determine 9 candidate proteins from a total of 26 proteins and their involvement in several biological processes will be discussed later (table 3.1).

3.2.3 Gene expression microarray analysis

In parallel with the determination of acute and chronic changes in protein expression, the other aim of this project was to determine the persistent changes in gene expression in primary and drug treated glioma cell lines after treatment with etoposide or irinotecan.

3.2.3.1 RNA extraction

The RNA from different cell pellets was isolated with the *mir*Vana™ miRNA isolation kit as described earlier in 2.4.1.2. The concentration and the quality of total RNA in each sample were determined by Agilent 2100 Bioanalyzer (table 3.2 and figure 3.8).

3.2.3.2 GeneSpring GX11 analysis results

After determining the concentration and the quality control of RNA samples, each sample (3 independent preparations for each cell line) was sent to NASC's International Affymetrix service at Sutton Bonington campus, University of Nottingham for further analysis with Affymetrix GeneChip U133 plus 2 microarray.

Table 3.1 MASCOT database identification of protein spots analysed with PMF and tandem MS-MS

Spot number	Protein name	MASCOT Score*	MASCOT Mwt	MASCOT pI	*P*	Fold change	Cell Line comparison (highest expression first)
6	Serine-Arginine splicing factor	159	25688	10.81	$1.1e^{-10}$	2	C6-Irinotecan (+) vs. C6-Etoposide (+)
8	protein disulfide-isomerase A3	162	57010	5.88	$5.4e^{-11}$	1.5	C6 vs. C6-Irinotecan (+)
7	Ribosomal protein large P0	72	30736	5.90	0.052	1.5	C6-Irinotecan (+) vs. C6- Etoposide (+)
18	PRP19	72	52581	6.06	0.055	2	C6-Irinotecan (-) vs. C6-Etoposide (-)
17	Elongation factor 1-γ	73	50371	6.31	0.037	2	C6-Irinotecan (+) vs. C6
19	Lamin-A	250	65448	6.37	$8.6e^{-20}$	3	C6-Irinotecan (+) vs. C6
21	Progerin	198	69492	6.22	$1.4e^{-14}$	2	C6-Irinotecan (-) vs. C6
22	Catalase	237	60062	7.07	$1.7e^{-18}$	2	C6 vs. C6-Etoposide (-)
13	Nucleotide diphosphate kinase B	124	17386	6.92	$3.4e^{-7}$	2	C6-Irinotecan (-) vs. C6

*MASCOT score is used to calculate the *P* value for certain peptide sequences in the MASCOT search. If the *P* value is <0.05, this indicates a confident match and identification for the protein in the database. The PMF score to which peptide mass considered to give a *P* value<0.05 is 72 for all the peptide masses in the table. Spot number refers to the spots which are circled in red in figure 3.7.

Abbreviations: **PMF:** peptide mass fingerprint; **MS:** mass spectrometry**; Mwt:** molecular weight; **pI:** isoelectric point; and **PRP19:** PRP19/PSO4 pre-mRNA processing factor 19 homolog (S. cerevisiae).

Table 3.2 RNA concentrations determined by Agilent 2100 Bioanalyzer

Sample Name	Concentration (ng/µl)	RNA integrity number (RIN)
C6 (P22)	424	9.8
C6 (P23)	356	6.2
C6 (P24)	735	6.8
C6-irinotecan (P7)	615	9.2
C6-irinotecan (P9)	491	8.8
C6-irinotecan (P11)	474	9.3
C6-etoposide (P11)	475	2.7
C6-etoposide (P12)	1,652	9.1
C6-etoposide (P18)	296	7.9

*Where P in the brackets represents the passage number of the cell line. The RNA integrity number (RIN) is calculated automatically by Agilent 2100 Bioanalyzer software based upon the 18S/28S rRNA intensity signal of each sample.

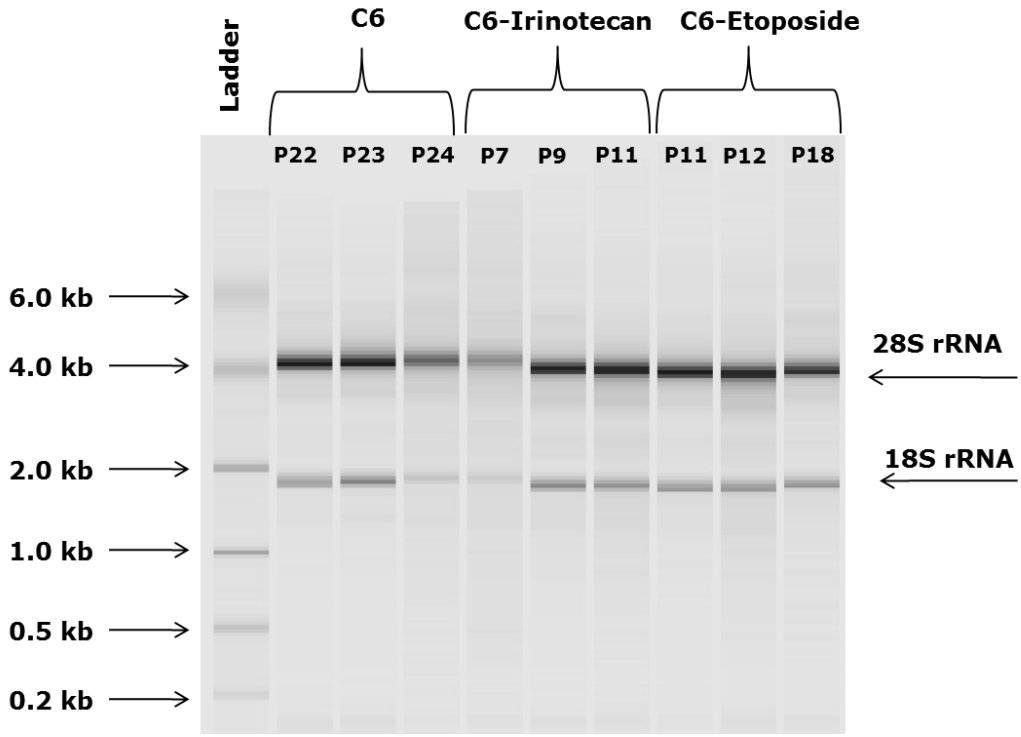

Figure 3.8 Electropherogram of RNA samples on Agilent 2100 Bioanalyzer. The determination of RNA concentration and quality is based on the separation of RNA samples by gel electrophoresis. An electrical current is applied into the NanoChip, which contains 12 wells of samples and ladder, each sample is separated into two distinct bands (18S and 28S subunits) and the data is detected through a laser-fluorescent beam and translated into a gel-like image (bands).

Regarding the reproducibility between replicates, the C6-etoposide (P11) sample had a low percentage "present call" (i.e., a low number of hybridization signals above a threshold). This may be linked to its RIN and therefore, was marked as an outlier and has been excluded from the analysis (figure 3.9). The determination of genes which showed expression changes among the three glioma cell lines and their role in different pathways and processes was done in two analytical steps. In the first step, all the raw data obtained from the Affymetrix GeneChip Microarray for all samples (except C6-etoposide P11) were imported into the GeneSpring GX11 software.

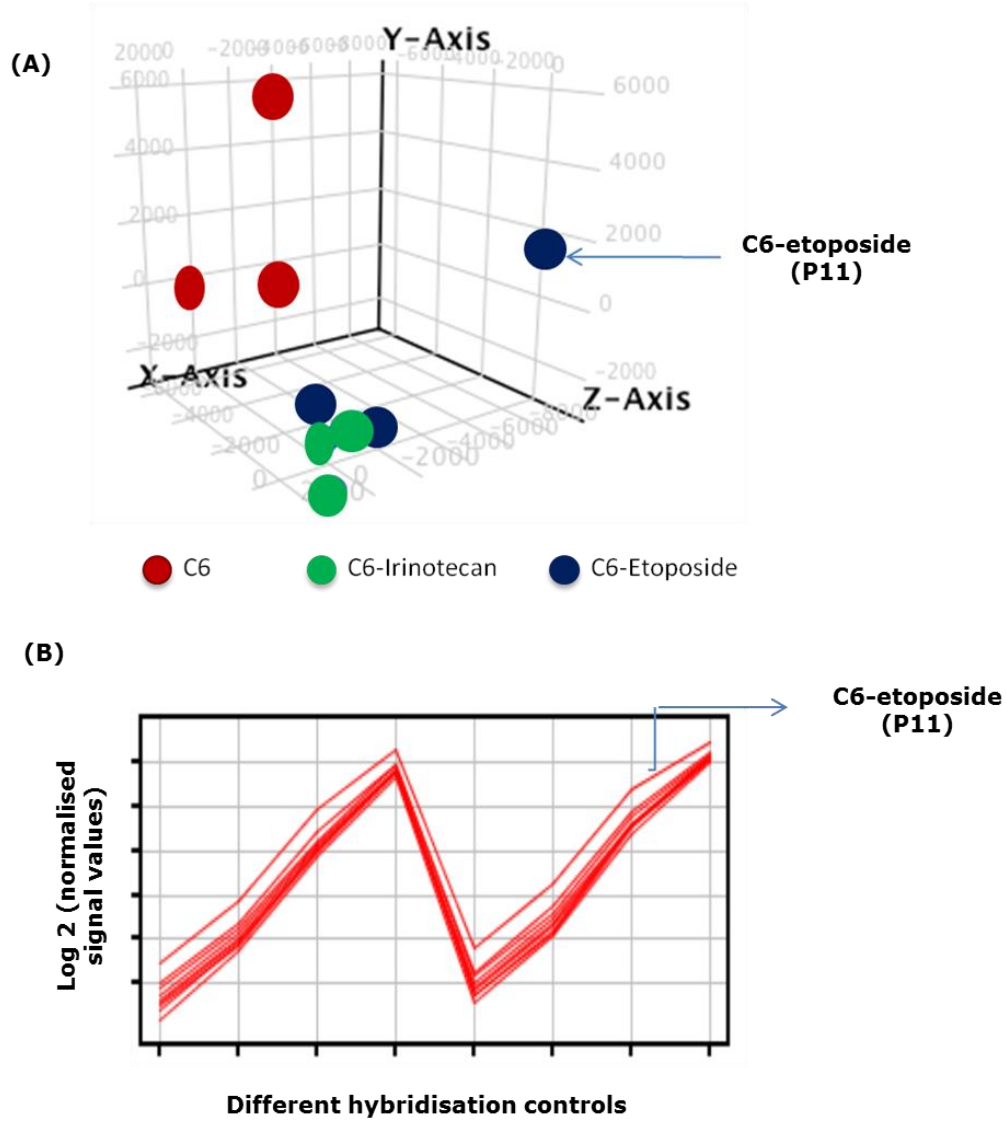

Figure 3.9 Hybridisation and data quality analysis of all microarray samples on GeneSpring GX 11. To ensure the quality of the array data before analysis, two important elements were calculated. The first one is the principal component analysis (PCA), which is shown in (A). It gives an indication about the similarity between the replicates of each group so that outlier samples can be excluded from the analysis. In this data, the PCA of all samples showed a deviation of C6-etoposide (P11) from the other C6-etoposide samples (outlier) and hence it has not been included in the analysis. The second element is the calculation of the overall normalization values for each sample regarding to different hybridisation controls used (B). As it appears from curve B, all samples hybridisation and labelling were good except for C6-etoposide (P11) and therefore, based on these two properties it is confirmed as an outlier.

To start analysis on GeneSpring GX11, the .CEL files were loaded into the software. The cell intensity (.CEL) file is one of the different files generated from the microarray and it contains the information for viewing the images that result from scanning the hybridized arrays. The normalisation step was aimed to detect and correct any abnormalities in the chips intensities by organising all the information in the .CEL files generated by the microarray software. The .CEL file contains a captured image of the GeneChip scan and calculations of hundreds of intensities for all probes set which represent the x probes and y mismatch probes for z genes (Gautier et al., 2004). In this step, the background noise is calculated and adjusted to give a single signal for each chip. Finally, the signals were scaled using a trimmed mean (Affymetrix, 2002). The trimmed mean is defined as taking the average of the readings after excluding the highest and the lowest 20-25% values and therefore, it decreases the outlier bias.

After the normalisation step was completed, the data were statistically calculated using one way ANOVA test to compare three cell lines or unpaired T test to compare two groups each time. Table 3.3 showed the total number of entities which have been identified from several statistical analyses. These results were obtained only when no false discovery rate (FDR) was applied and when the analysis was restricted on identifying the genes which showed significant differences in their expression with 1.5 or 2 fold changes (up or down). The low number of identified genes might be due to the usage of a human microarray chip on rat RNA samples. In addition, the "filter by volcano plot" analysis was performed to look at the number of differentially expressed genes. It looks like that the similarity between samples means that there are very few differentially expressed genes. If FDR test was applied then there are no genes (fold change >1.5, $P<0.05$), but without FDR there are 83 genes (fold change >1.5, $P<0.05$) between C6-irinotecan and parental C6 and 70 genes between C6-etoposide and parental C6. Using a Venn diagram there are 14 genes common between these two lists (figure 3.10).

Table 3.3 Total entities (probes) identified as having different expression level between cell lines

Statistical test used	C6-irinotecan vs. C6	C6-etoposide vs. C6	C6-irinotecan vs. C6-etoposide	All cell lines
Test 1	153	165	117	N/A
Test 2	17	25	19	N/A
Test 3	N/A	N/A	N/A	264
Test 4	N/A	N/A	N/A	37

*Four possible statistical analyses were used. Test 1 is unpaired t test no FDR with *P*<0.05 and FC>1.5, test 2 is unpaired t test no FDR with *P*<0.05 and FC>2, test 3 is one way ANOVA with no FDR *P*<0.05 and FC>1.5, and test 4 one way ANOVA with no FDR *P*<0.05 and FC>2. Where FC is the fold change in expression between compared cell lines, and N/A is not applicable. To compare the expression changes between two groups, unpaired T test was used whereas; one way ANOVA was used to compare the three cell lines.

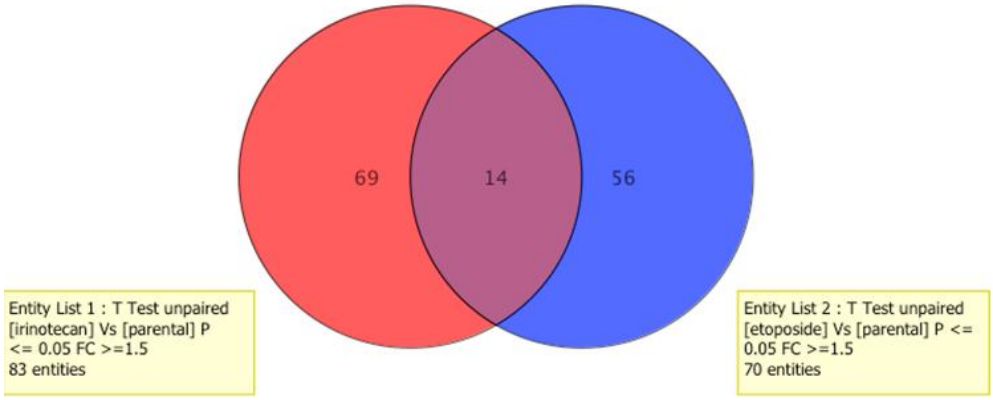

Figure 3.10 The number of differentially expressed genes determined with volcano plot analysis. A volcano plot is a type of scatter plot that is used to quickly identify changes in large datasets composed of replicate data. By applying unpaired t test, P<0.05, and FC≥1.5, two possible lists were determined with 83 genes and 70 genes showed significant differences between C6-irinotecan vs. C6 and C6-etoposide vs. C6, respectively. Among these two lists, only 14 genes were commonly expressed between the three cell lines.

3.2.3.3 Signalling pathway profiling results

In the second step of analysis, after identifying entities showing altered expression, further analysis of genes was performed to identify their functions, and their context within different signalling pathways and biological processes. The analysis was performed using Ingenuity Pathway Analysis (IPA) software version 8.7. Three possible comparisons were performed on genes (resulted from test 2 in table 3.3); (1) C6-irinotecan vs. C6, (2) C6-etoposide vs. C6, and (3) C6-irinotecan vs. C6-etoposide. To start the analysis on IPA, data from GeneSpring GX11 was exported as an Excel file format containing the gene ID and the fold change for all comparisons made. At the end of each analysis a report was produced describing the major signalling pathway or major biological processes and a list of the candidate genes which showed either up or down expression differences in each comparison made. For example in the comparison between C6-irinotecan and C6 cell lines, the pathways controlling cellular growth and proliferation are predicted to be different, as a number of genes involved in these pathways (such as *BMP7*, *COL3A1*, and *EGR1*) show differential expression between the two cell lines. However, from the comparison made between the three cell lines there was only one gene continually altered in each data set that is bone morphogenetic protein 7 (*BMP7*). The comparisons made between paired cell lines revealed that 72 genes, 55 genes, and 65 genes were differentially expressed in C6-irinotecan vs. C6, C6-etoposide vs. C6, and C6-irinotecan vs. C6-etoposide, respectively. The symbol of genes and their possible functions are listed in (tables 3.4, 3.5, and 3.6).

Table 3.4 Pathway analysis of differential gene expression between C6-irinotecan vs. C6 cell lines

Gene symbol *	Major biological functions
BMP7, *CAMK2N1, CDH10, CDH11,* ***COL3A1***, *DOK1, EED,* ***EGR1***, *EIF5, FGG, MAF, MED21, MEF2C, MS4A1,* ***MT1F***, *MT2A, NIPBL, NKRF, NR2F1, RUVBL2, SOX5, STARD10, TCF4, ZFP36L1*	Gene expression, cellular development, cellular growth and proliferation
BACH2, CAMK1, CPEB2, DNAH1, ETV1, FOXP1, GNAT2, HIPK3, PPAP2A, RASSF8, SETD5, SRGAP3, TNRC6B, USP19	Cell death, nervous system development and functions
CXXC5, FAR1, KIAA1468, RBM39, RRP8, SH3KBP1, SLC44A1, SYNCRIP, TMEM48, UBFD1, UHMK1, USP15, ZNF32	Lipid metabolism, small molecules biochemistry, cellular assembly and organization
CCDC80, CEP76, CNPY2, COL16A1, FAM120A, HNRNPD, MAD1L1, OLFML2B, RPL32, TP53INP2, WNK1, ZFHX4	Organism injury and abnormalities, organ development, respiratory system development and function
ARIH1, C13ORF27, CRYAB, MT1H, MT1X, PAK3, PPAP2A, TLN1, ZFR	Genetic disorders, skeletal and muscular disorders, cardiovascular disease

*Only genes which showed changes with ±1.5 fold in their expression and *P* value <0.05 are listed in the table. The major biological functions were determined in Ingenuity Pathway Analysis (IPA). Genes in red bold font indicate the up-regulated genes and the ones in green bold font represent the down-expressed genes in C6-irinotecan vs. C6 which are selected for further determination (table 3.7).

Table 3.5 Pathway analysis of differential gene expression between C6-etoposide vs. C6 cell lines

Gene symbol*	Major biological functions
BMP7, CDH2, CDH10, ***COL1A2****, CRYAB, DAB2, DOK1, EGFR,* ***EGR1****, HMGB1, LOX, MYH1, NEDD4L, NEO1, PARVA,* ***PTEN****, SRGAP3*	Cellular movement, cell to cell signalling and interaction, cellular function and maintenance
ABCF2*,* ***ATP1B1****, AZIN1, C90RF25, CEP76, MYH1, OLFML2B, PSMC2, PTPN12, SCHIP1, SMC3, WNT6, ZIC3, ZNF367*	Cell cycle, cellular development, connective tissue development and function
CDK5, EIF5, GPHN, IVNS1ABP, MAF, MEF2A, MLL3, PMP22, RHEB, RUNX1T1, SRPK2, TPM2	Cellular development, nervous system development and function, cell morphology
FBXO11, LRRFIP2, NIPBL, ORC5L, PRR7, SSBP2, TLE4, ZFHX4, ZNF32	Lipid metabolism, molecular transport, small molecule biochemistry
C11ORF67	Cellular development, gene expression, infection mechanism
TSC22D2	Carbohydrate metabolism, gene expression, genetic disorder
RNASET2	Cell cycle, reproductive system development and function, RNA damage and repair

*Only genes which showed changes with ±1.5 fold in their expression and *P* value <0.05 are listed in the table. The major biological functions were determined in Ingenuity Pathway Analysis (IPA). Genes in red bold font indicate the up-regulated genes and the ones in green bold font represent the down-expressed genes in C6-etoposide vs. C6 which are selected for further determination (table 3.7).

Table 3.6 Pathway analysis of differential gene expression between C6-Irinotecan vs. C6-Etoposide cell lines

Gene symbol*	Major biological functions
ARNTL, CDK5, GRIP1, HES1, IGFBP7, KIF5B, LIPE, MEF2A, MLL3, MT1X, NEO1, NR2F1, RBM39, RHEB, SGK1, SRPK2, TAF10, TCF4	Cell cycle, nervous system development and function, developmental disorder
BMP7, *CAMK2N1, COL1A1,* ***COL1A2***, ***COL3A1***, *EGFR, HMGA2, KLF12, LOX,* ***MT1F***, *PAK3, PARVA,* ***PTEN***, *TIMP2*	Cellular assembly and organization, cellular function and maintenance, connective tissue disorders
CELF2, COL11A1, COPB1, ERGIC2, FAR1, FASTK, FEZ1, KIAA1468, ORC5L, PSMC2, RNF141, SRP72	Cell morphology, cellular assembly and organization, nervous system development and function
CCDC80, DGAT2, FAM160A2, FNDC3B, SERPINB1, SSBP2, TLE4, TNPO3, UBQLN2, WNT6, ZFP36L2	Gene expression, cellular development, lipid metabolism
ABCF2, ATP1B1, BACH2, FOXP1, GPHN, PRR7, SMC3, TNPO1, TSHZ1	Cell cycle, developmental disorder, genetic disorder
MLL5	Cell cycle, embryonic developmental, cellular development

*Only genes which showed changes with ±1.5 fold in their expression and *P* value <0.05 are listed in the table. The major biological functions were determined in Ingenuity Pathway Analysis (IPA). Genes in red bold font indicate the up-regulated genes and the ones in green bold font represent the down-expressed genes in C6-irinotecan vs. C6-etoposide which are selected for further determination (table 3.7).

3.2.3.4 Integration of proteomic and genomic data to generate hypotheses for future work

Having performed genomic and proteomic analysis of C6 and drug selected cell lines we wished to determine whether these data sets correlate with alterations to the cell biology of the 3 cell lines. To do this required further stratification and simplification for the expression array data. To better understand this data, we focused on genes which had these two criteria (1) expression fold change (FC) between two or more cell lines is ≥ 2 identified with unpaired t test or 1-way ANOVA comparisons, respectively, and (2) *P* values for expression level difference of ≤0.05. Furthermore, these genes are contributed to a particular biological function such as drug resistance, cancer cells survival/apoptosis, migration, response to oxidative stress as well as tumour progression. Using the IPA analysis, detailed searches of candidate genes on PubMed were performed to see if there was any previous identified role in cancer cell biology which enabled a number of more concise conclusions to be drawn. Table 3.7 shows possible functional involvement of these genes in C6 cell lines.

The profiling of gene expression in tissues is a key strategy to discover biomarkers for cancer which may help in the early diagnosis, prediction of treatment response efficiency and developing new therapeutic agents. In our study, the data obtained from protein and gene expression data analysis was used to propose different hypotheses for C6 and its drug selected sublines. Several of these hypotheses were selected for further examination, and these will be elaborated upon below.

Table 3.7 The candidate genes which showed expression differences and their biological functions in glioma cell lines

Biological function/ Gene symbol	Fold change*	Cell lines showing significantly different gene expression
(1)Migration/tumour invasiveness		
BMP7	+3	C6-irinotecan vs. C6
	+2	C6-irinotecan vs. C6-etoposide
(2)DNA damage		
MT1F	+2	C6-irinotecan vs. C6
	+3	C6-irinotecan vs. C6-etoposide
(3)Tumour metastasis		
ATP1B1	+2	C6-etoposide vs. C6
COL3A1	-4	C6-irinotecan vs. C6
	-3	C6-irinotecan vs. C6-etoposide
COL1A2	+4	C6-etoposide vs. C6
	-4	C6-irinotecan vs. C6-etoposide
(4)Apoptosis/angiogenesis		
PTEN	-2	C6-etoposide vs. C6
	+3	C6-irinotecan vs. C6-etoposide
EGR1	-3.5	C6-etoposide vs. C6
	-2	C6-irinotecan vs. C6
(5)Translational control		
ABCF2	+2.5	C6-etoposide vs. C6

*The (-) indicates that (fold change is down-regulated) and (+) indicates the (up-regulation of fold change). The major biological functions were identified with the IPA analysis. Abbreviations: ***BMP7*****:** Bone morphogenetic protein 7; ***MT1F*****:** Metallothionein-1F; ***ATP1B1*****:** Sodium/potassium-transporting ATPase subunit beta-1; ***COL3A1*****:** Collagen, type III, alpha 1; ***COL1A2*****:** Collagen, type I, alpha 2; ***PTEN*****:** Phosphatase and tensin homolog deleted on chromosome 10; ***EGR1*****:** Early growth response protein 1; and ***ABCF2*****:** ATP-binding cassette sub-family F member 2.

Notably the gene expression data indicates alterations in collagen genes in the drug treated cell lines. Interestingly, a paper on brain tumours (Liu et al., 2010) identified a conserved over-expression for 13 glioma endothelial marker genes (GEMs) which play a role in the metastasis and angiogenesis of the tumour cells in glioma brain tumours. These genes are mostly found on the cell surface or in the ECM such as *COL3A1* and *COL1A2*. The gene expression analysis showed down-regulation of both collagens *COL3A1* and *COL1A2* in C6-irinotecan compared to C6 and C6-etoposide. Since collagen proteins play a role in the metastasis of tumours, this presents the possibility of *COL3A1* and *COL1A2* to play a protective role in the C6-irinotecan cell line against the angiogenesis and metastasis of the tumour i.e., irinotecan treatment leads to a decrease in the migration rate of the cells. Moreover, the expression of *ATP1B1* in C6-etoposide is 2 fold higher than the parental C6 cell line. Research on ATP1B1 has revealed that ATP1B1 expression is high in well- differentiated tumour cell lines and plays a role in tumour metastasis (Yancy et al., 2007). Therefore, the possible role of collagens and ATP1B1 in the migration of cells will be examined with several migration assays in chapter 4 and their expression will be validated by western blotting and/or qPCR.

The regulation of cell survival and death (apoptosis) is a critical step in controlling tumour growth and tissue homeostasis. Several signalling pathways, proteins and enzymes are required to maintain this and any defects or mutations in such proteins can cause harmful effects on the survival of tumour cells. *PTEN* is a well-known tumour suppressor gene (Chu and Tarnawski, 2004) that can function via several pathways but the main one is the PTEN/PI3K/Akt pathway. In glioma, *PTEN* is severely mutated (homozygous deleted) in glioma patients and it's expression is highly related to the survival of the patients (The Cancer Genome Atlas Research Network, 2008). In addition to *PTEN*, *EGR1* also known as Zif268 (zinc finger protein 225) which is a nuclear transcription factor act as a direct regulator for PTEN

(Baron et al., 2006). In the C6-etoposide cell line, the expression of both (*PTEN* and *EGR1*) was found to be down-regulated (2 and 3.5 fold), respectively compared to parental C6. This data lead to the hypothesis that the C6-etoposide cell line will be more resistant to apoptosis compared to the other two cell lines. Therefore, alterations in *PTEN* and *EGR1* expression prompt validation and functional assessment of response to cellular stress which leads to apoptosis. The comprehensive research on the candidate proteins also showed that Lamin A, catalase, and PRP19 are involved in oxidative stress by following other mechanisms such as genomic instability (lamin A), failing to regulate the breaking down of peroxides (Catalase), and defect in apoptosis response (PRP19) (Gonzalez-Suarez et al., 2009, Lu and Legerski, 2007, Papacocea et al., 2011). All genes and proteins which are related to apoptosis will be examined in chapter 5 by determining the percentage of dead cells from the oxidative damage produced by the treatment with exogenous reactive oxygen species (ROS) inducer. Their expression will be validated with qPCR and western blotting, respectively.

3.3 Summary

To understand better why glioma presents as difficult to treat with chemotherapy, the rat C6 glioma cell line was involved and used to establish two drugs derived cell lines with two major chemotherapeutic agents namely etoposide and irinotecan. Our aim is to determine mechanisms for drug resistance in HGG with proteomic and genomic approaches. The summary of this chapter is as follow:

- With the proteomic approaches, we were able to identify 9 proteins with confident matches in the MASCOT database search (table 3.1).
- With the gene expression approach, 72 genes, 55 genes, and 65 genes showed expression changes in C6-irinotecan vs. C6, C6-etoposide vs. C6, and C6-irinotecan vs. C6-etoposide, respectively (tables 3.4, 3.5, and 3.6).

- Integration of our data with the published literature identified 8 genes with significant FC>2 and *P*<0.05 (table 3.7).
- These genes involved in several biological processes that are related to drug resistance and mainly in migration and resistance to oxidative stress.
- These two biological responses are the features of the next two results chapters (figure 3.11).

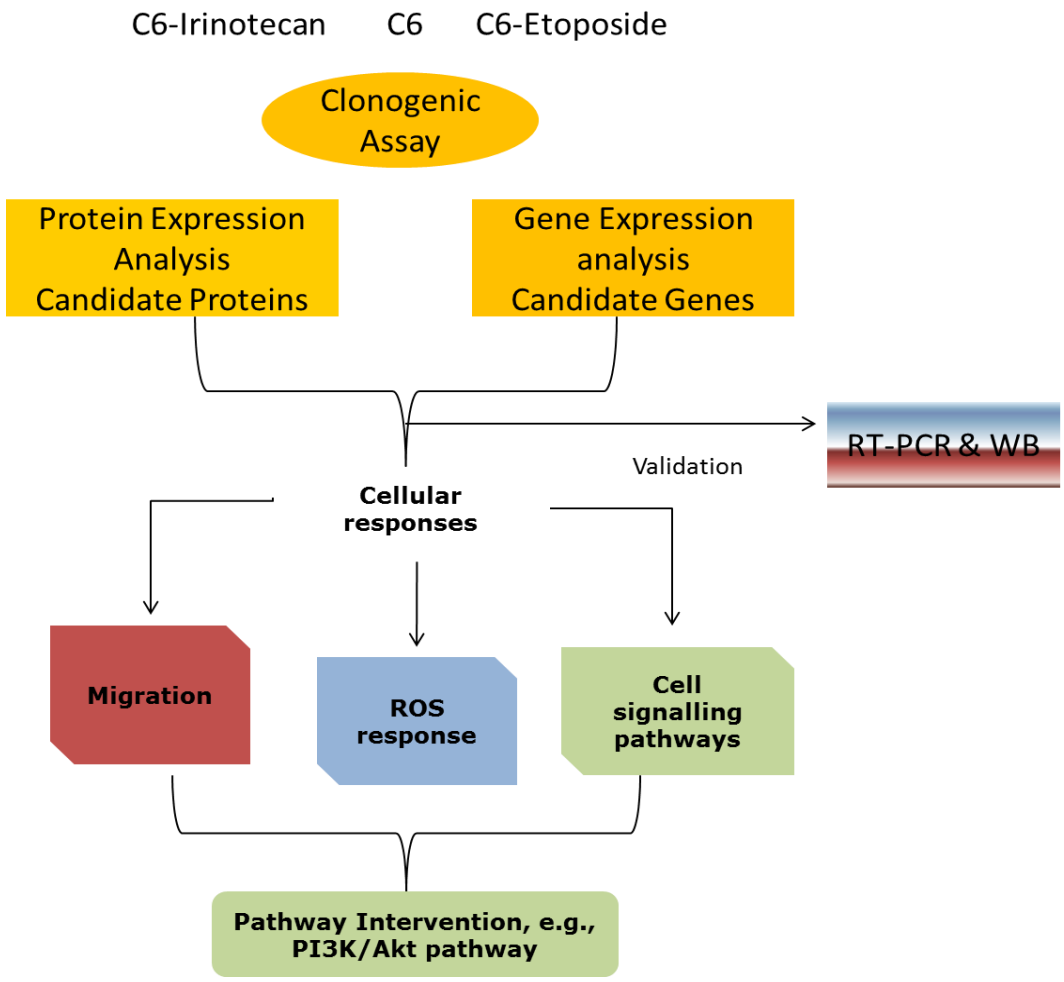

Figure 3.11 Overall strategies to determine drug resistance mechanisms in HGG cell line. The identified proteins and genes with proteomic and genomic approaches were integrated into pathway analysis software (IPA) to hypothesize downstream analyses of biological responses related to drug resistance. These responses will be examined in the following results chapters: chapter IV (migration) and chapter V (oxidative stress and apoptosis). The expression of candidate proteins and genes will be validated with western blotting and qRT-PCR, respectively in each corresponding chapter. ROS: reactive oxygen species.

CHAPTER IV

A TOPOISOMERASE (I) INHIBITOR (IRINOTECAN) DECREASES THE MIGRATION IN A DRUG-SELECTED HIGH GRADE GLIOMA CELL LINE

CHAPTER IV: A TOPOISOMERASE (I) INHIBITOR (IRINOTECAN) DECREASES THE MIGRATION IN A DRUG-SELECTED HIGH GRADE GLIOMA CELL LINE

4.1 Introduction

Cell migration and invasion are critical parameters in metastasis, the process of tumour spread and migration, and is considered as one of the major reasons behind the failure of the chemo- or radiotherapy and the poor outcomes of cancer patients. Cell migration and invasion share similarities. Both are defined as the ability of the cells to move from one tissue to another one in response to a chemical signal such as the presence of growth factors. However, invasion process differs in that cell penetrate the ECM or the basement membrane extract (BME) barrier (Hanahan and Weinberg, 2000). Although metastasis is rare in GBM, this tumour is highly invasive and this invasive behaviour limits the effectiveness of local therapies and contributes to the high mortality rate seen in this tumour. GBM typically invades the brain by migrating long distances through white matter tracts and by infiltrating cortex and subcortical grey matter structures (Beadle et al., 2008).

The epithelial-mesenchymal transition or transformation (EMT) is one of the major programmes which define the migration of cancer cells. EMT is a developmental programme characterised by the loss of cell adhesion and increased mobility of epithelial cells as they trans-differentiate into mesenchymal cells. EMT is an important process in embryogenesis, but inappropriate regulation is the major reason for the progression of cancer arising from epithelial tissues (Radisky, 2005). In this case, cancer cells become more motile because they lose the characteristics of epithelial cells including the loss of E-cadherin and at the same time they acquire the characteristics of mesenchymal cells such as the expression of N-cadherin and vimentin. As a result, cells are more invasive and metastatic, creating their

own cell-ECM which is characterised by the production of MMPs and the induction of epithelial cell transformation with growth factors such as EGF and transforming growth factor beta (TGFβ). EMT transition has also been linked to type I collagen expression and reactive oxygen species (ROS) production in response to MMP activation especially MMP-3 (Radisky et al., 2005, Kalluri and Weinberg, 2009).

EMT can be classified into three major classes. Firstly, class I EMT includes the cells that are associated with implantation, embryo formation, and organ development; however, these cells neither cause fibrosis nor induce an invasive phenotype. Secondly, class II EMT is associated with wound healing, tissue regeneration and fibrosis. The repair mechanism in this class begins with the generation of fibroblasts and other related cells in order to reconstruct tissues following inflammatory injury. In contrast to cells of class I EMT, cells of class II EMTs are associated with inflammation. Thirdly, class III EMTs occur in cancer cells that have previously undergone genetic and epigenetic changes. These changes affect oncogenes and tumour suppressor genes and create invasive and metastatic cells (Kalluri and Weinberg, 2009). Indeed, class III EMT is the most relevant to our research. Many cell culture experiments have demonstrated that cancer cells can acquire a mesenchymal phenotype and express mesenchymal markers such as vimentin and these cells are present usually at the invasive part of the primary tumours and are considered to be the cells which initiate the subsequent steps of the invasion-metastasis cascade (Yang and Weinberg, 2008).

Many studies have sought to understand the cell migration phenomenon in cancer. These studies have found that the response of the cells is quite different between the *in vivo* and the *in vitro* studies. In particular, *in vivo* experiments show longer, stable protrusions pointing in the direction of migration compared to *in vitro* studies (Colucci-Guyon et al., 1999, Gunnersen et al., 2000, Beadle et al., 2008). However, *in vitro* studies

can still explain several aspects of the cancer cell migration and can be used as a guide to elucidate the role of mechanisms which affect migration (Horwitz and Webb, 2003).

In this study proteomic and genomic approaches identified several candidates which have previously been associated with migration and metastasis of cancer. In this chapter, we will focus on some of these candidates and investigate their role in migration by use of scratch wound closure and transwell migration assays. Expression of candidate proteins and genes is then validated by western blotting and qRT-PCR.

4.2 Results

Through proteomic and genomic approaches, we were able to identify one candidate protein, nucleotide diphosphate B kinase (NDBK), and three candidate genes, *ATP1B1, COL1A2,* and *COL3A1*, for involvement in cell migration. NDBK was excluded from the study as no suitable antibody was available to validate protein expression and instead we focused on the candidates from gene expression analysis. These candidates and their possible role in cancer cell migration, invasion and metastasis are listed in table 4.1. In addition to these candidate genes, we also validated the expression of vimentin by western blotting as it showed a significant difference in its expression by the IPA analysis and because it is an important marker for high grade glioma progression and for EMT (Bax et al., 2009).

Table 4.1 Candidate genes related to cell migration and metastasis showing different expression in C6 cell lines

Candidate Genes		
Gene Name	**Function**	**Reference**
ATP1B1	It plays a role in cell growth and differentiation. It is postulated that a decrease in ATP1B1 expression is related to the progress of cancer.	(Liu et al., 2009a)
COL1A2	As a structural protein, COL1A2 can anchor cells into the matrix by interacting with fibronectin. Moreover, it can regulate cell growth, motility, and differentiation by binding to the proper integrin receptors on the cell surface.	(Liang et al., 2005, Huijbers et al., 2010)
COL3A1	It is one of the major genes which are overexpressed in EMT.	(Liu et al., 2010)
Vimentin	It has a role in cell-adhesion and migration by controlling integrin functions.	(Ivaska et al., 2007)

4.2.1 Optimisation of an *in vitro* scratch assay

Before studying the migration ability of the three glioma cell lines, optimisation experiments were performed to identify the appropriate cell density and to choose the best needle or tip to make the scratch with. Parental C6 cells were seeded at varying densities ($0.25x10^6$, $0.5x10^6$, and $1x10^6$ cells) into 6-well plates in duplicate. Following attachment, a scratch was made with different tips and needles of different sizes including 23G 1¼" needle, 19G 2" needle, 16G 1½" needle, 200 µl pipette tip, and glass Pasteur pipette by drawing them across the centre of each well (figure 4.1b). After making the scratch, the media was changed to remove cell debris and then the plate was incubated for 72 hours during which closure of the wound was assessed every 4 hours by photomicroscopy (Denker and Barber, 2002).

The analysis of the data obtained from the optimisation experiments regarding the cell count revealed that there was too much cell detachment when seeding $1x10^6$ cells. In optimisation assays, $0.5x10^6$ cells was found to be suitable for all 3 cell lines (figure 4.1a). Regarding the best tip or needle to choose for making the scratch, figure 4.1b shows that optimal wounding was obtained with a 200 µl pipette tip since all the other items used resulted in damage to cell layer and to the well itself, which would affect the assessment of cell migration.

4.2.2 Determination of migration rate for glioma cell lines with an *in vitro* scratch assay

According to the optimised protocol, three independent experiments were set up with each of the 3 cell lines. In order to determine the migration rate for the three glioma cell lines, the wound scratch assay was performed on $0.5x10^6$ cells in DMEM-10% FBS seeded in duplicate in either sterile uncoated 6-well plates (Costar, 3506) or collagen type I coated 6-well plates (GIBCO, A11428-01). Scratch was then made with sterile 200 µl pipette tip. The migration of the cells was then assessed with time lapse microscope (LEICA DMIRB Microscope, LEICA Microsystem) at 37°C for 65 hours. Images were taken with Brightfield 10x Phase contrast objective lens, every 30 minutes at 3 different positions along each scratch to ensure that the initial size of the wound gap was constant at the beginning of the experiment. ImageJ was used to measure the scratch size (Abràmoff et al., 2004).

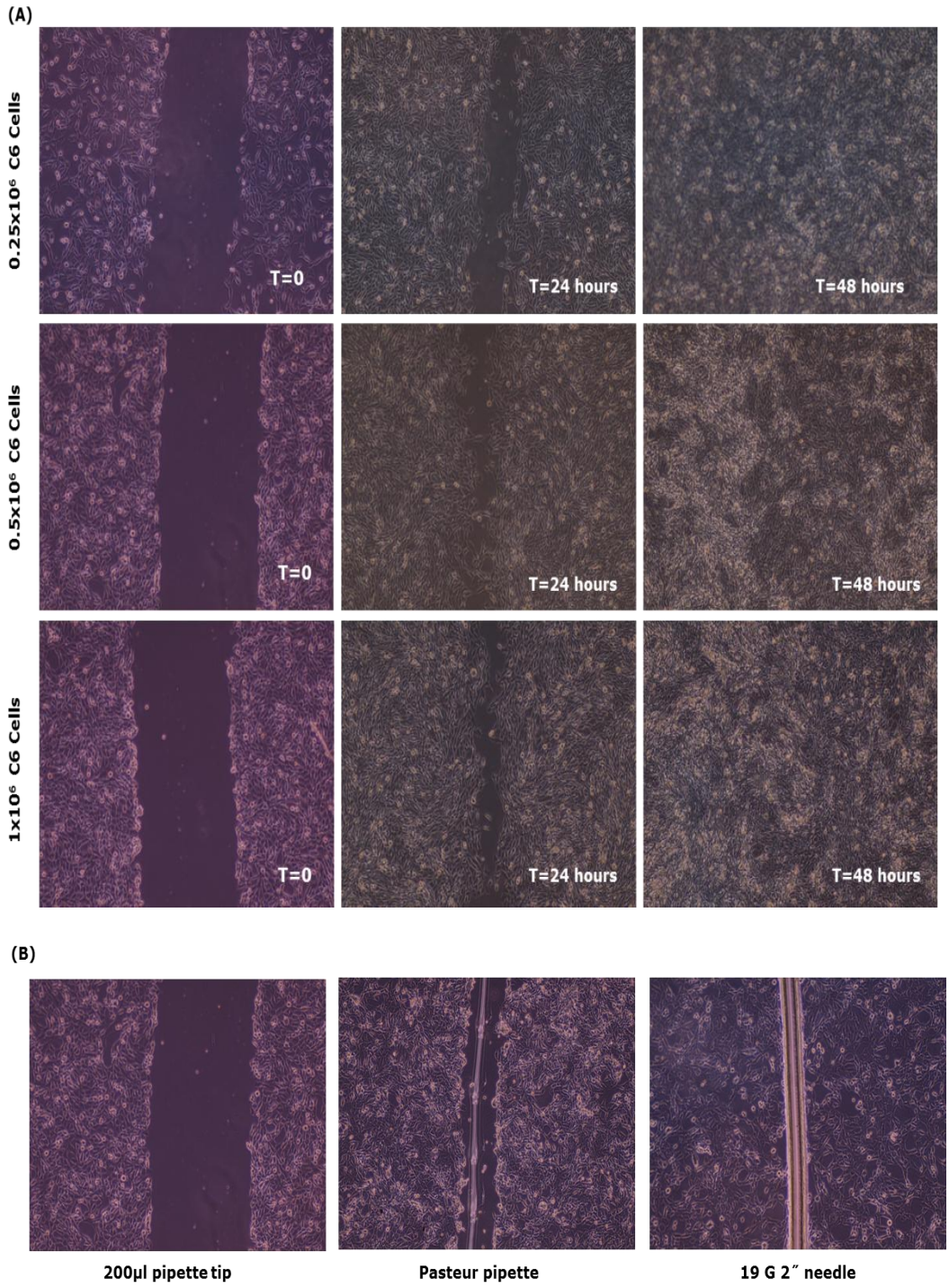

Figure 4.1 Optimisation of scratch assay. (A) C6 cells were seeded at different densities into 6-well plates, a scratch was made, and then wound healing was assessed for 72 hours. The best cell count was found to be $0.5x10^6$ cells where cells are not overlaid and close the wound. Although these series of images look similar, the $1x10^6$ cell seeding shows considerable detachment. (B) Represents the different items used to make the scratch. Unlike the other items tested, the 200 µl pipette tip did not result in damage to the cells or the well surface.

For the scratch assay, two ways are used to assess the migration ability of the cells. Either the number of cells migrating into the scratch area can be counted, or the scratch size can be measured. This second approach was selected. To analyse the time lapse data, all images were saved first on TIFF file format and then compiled into stacks to make the analysis easier. For each cell line a stack was performed containing 131 images (x3) (which represent the whole experiment from T=0 to T=65). To measure the scratch size with ImageJ software, there are two methods: (A) edge-detection/thresholding method and (B) background subtraction/thresholding. We chose the edge-detection/thresholding method to analyse the size of the scratch for two reasons. Firstly, it is considered to be more accurate (based on ImageJ reference manual online source). Secondly, since there was no change in the media colour during the whole experiment, we did not need to subtract the background to achieve a better resolution for the images. In the edge-detection method, the size of the scratch is detected by measuring the size of the image particles and the threshold. The threshold is defined as the cut-off for the brightness of a pixel that is used to detect the cell wound, whereas, particle size is detected to prevent small gaps in the cell monolayer from being considered as "gap". Combination of threshold and particle size enables the software to discriminate cells from plastic-ware, and between a small gap in the cell monolayer and the closing wound, providing an accurate start point for measurements and to produce accurate measurements (i.e., initial wound is set at 100%).

Representative data is shown by non-linear fit analysis in GraphPad Prism version 5.00 for Windows, GraphPad Software, San Diego California USA. For all data sets two fits were compared; namely a single exponential and a lag followed by a single exponential. An F-test was employed to determine which analysis produced the better fit. For the experiments performed on the uncoated 6-well plate, analysis of the data showed that for the C6 cell line, the lag-exponential fitted the data better than a simple

exponential plot indicating that these cells are delayed in their recovery from the initial wounding. Analysis of the exponential phase of the recovery showed that C6 cells remained in a lag period for 8 hours then they started to move quickly toward the gap. By 24 hours, the wound was healed completely. On the other hand, the drug derived cell lines both fitted better on a single exponential plot (which means that they start the migration immediately at the beginning of the experiment). Analysis of the data showed that C6-etoposide cell line migrated at a faster rate than the C6-irinotecan cell line and they have different behaviour in the response to environment conditions i.e., phenotypically, the C6-irinotecan cell line proliferated rather than migrated at areas surrounding the wound and then when they became too confluent, they started to migrate toward the wound (i.e., they took around 48 hours to close the gap) whereas, C6-etoposide rapidly migrated and filled the gap (figure 4.2 and figure 4.3). A CD enclosed with this thesis illustrates this in a movie, showing an example for one scratch assay experiment performed on each of the three cell lines.

In contrast, analysis of the data for experiments performed on the collagen type I coated 6-well plates revealed pronouncedly different behaviour of the three glioma cell lines especially the drug treated ones. For the C6 cell line, analysis revealed that a simple exponential plot fitted the data better than the lag-exponential fit (i.e., the cells did not enter a lag period, they started immediately to move toward the gap and by 24 hours, the wound was healed completely). For the drug treated cell lines, both cell lines have different migration response. For C6-etoposide, they were fitted better on lag exponential fit curve (they entered a lag period for 13 hours then by 48 hours the gap was healed). In contrast, for C6-irinotecan, the cells continue to proliferate rather than migrating to the gap. However, this cell line fitted better on the simple exponential curve and the wound was never healed even after 48 hours (figures 4.4 and 4.5).

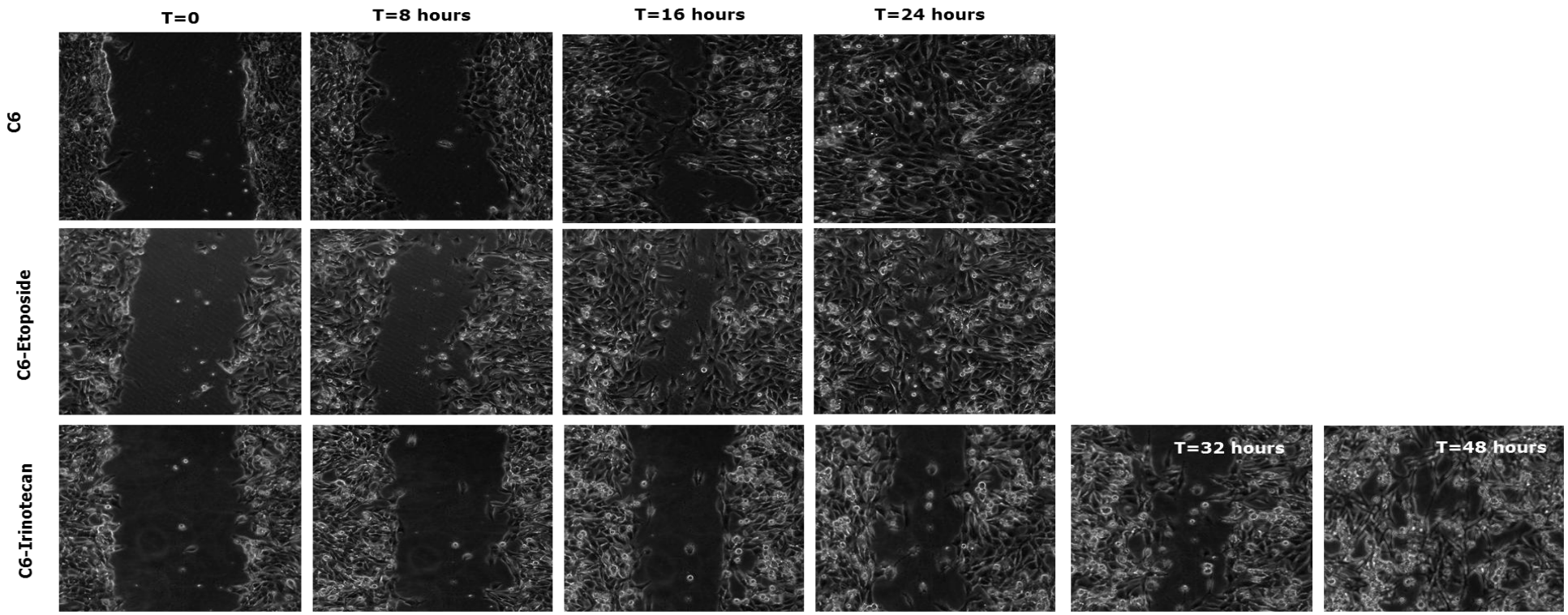

Figure 4.2 Wound closure in C6 cell lines. $0.5x10^6$ cells of each cell line were seeded in uncoated 6-well plates in duplicate. Then a scratch was made across the centre of the monolayer with a 200µl pipette tip after 24 hours. Cells were washed and media replaced by DMEM/F-12 and immediately the migration of the cells was observed with time lapse microscope every 30 minutes at 3 different positions across the well. Although C6 and C6-etoposide look very closely matched for wound healing, they have different t½ and follow different fit curves (see figure 4.3). As images show, C6 cell line has the fastest migration rate among the three cell lines. However, treating cells with irinotecan decreases the migration rate (indicated by taking more than 48 hours to heal the wound), n=3.

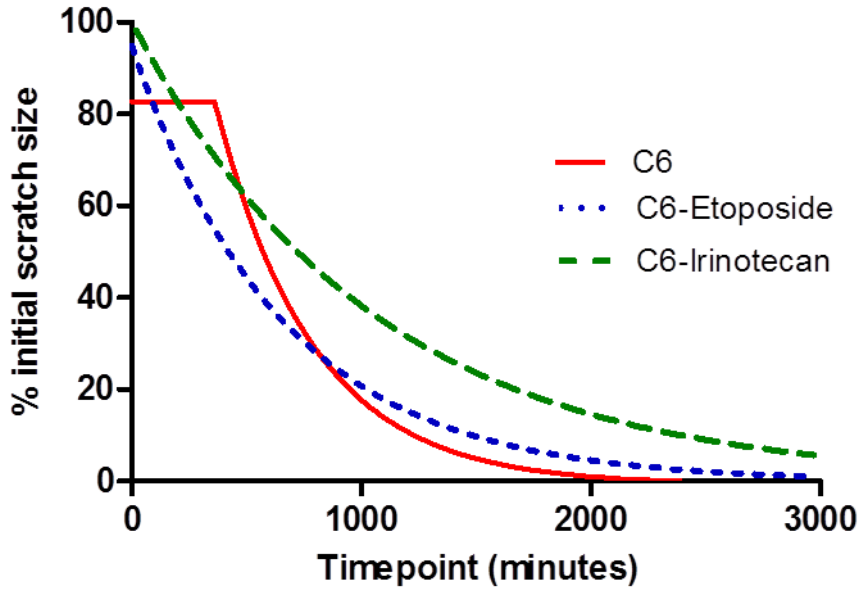

Figure 4.3 Treatment of glioma cell lines with irinotecan decreases the migration rate. The three cell lines were prepared for the scratch assay followed the protocol in section 4.2.2. Images obtained from time lapse were analysed on ImageJ by stacking them into TIFF files and the data obtained used to plot the % scratch size as a function of time. Non-linear fit analysis showed that parental C6 cell line migrated faster than other cell lines (t½ = 294 minutes ± 24). However, this cell line entered a lag period for 8-10 hours before rapidly closing the wound (plateau curve followed by one phase decay curve) whereas, the drug derived cell lines had slower migration rate than parental C6 cell line (t½ = 720 minutes ± 35 for C6-irinotecan and t½ = 457 minutes ± 24 for C6-etoposide) and they followed a one phase decay fit curve, n=3. In this figure, each fit curve represented the mean of 9 closures over 3 independent experiments. Individual time points were not shown as there were 131 timepoints/ line.

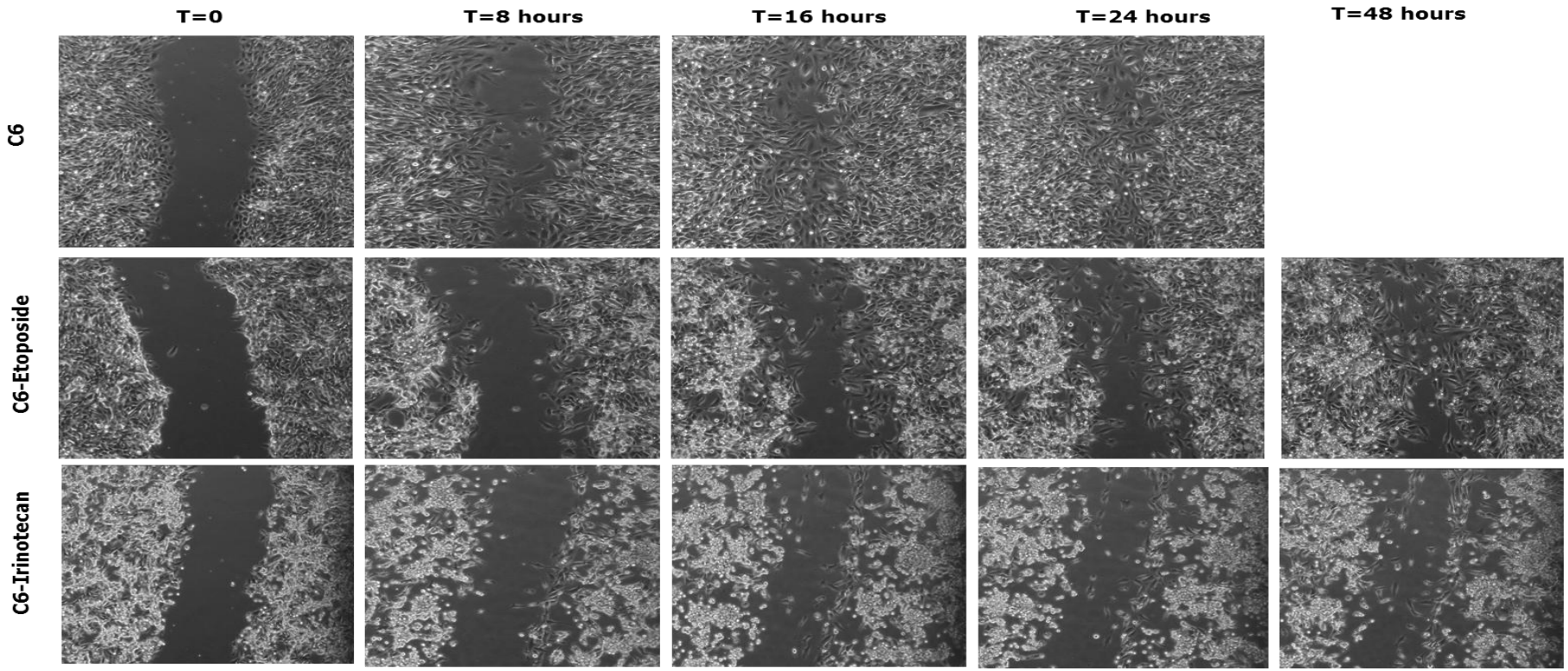

Figure 4.4 Wound scratch assay on collagen coated plates. The experiment was performed exactly the same as in figure 4.2 except for the type of plate used. As the images show, the 3 glioma cell lines have totally different behaviour than the ones obtained in the uncoated plates. However, the C6 cell line still has the fastest migration rate among the three cell lines. Moreover, treating cells with irinotecan again strongly affected the migration of the cells [i.e., decreases the migration rate (even after 48 hours the wound never healed)]. For C6-etoposide, the migration ability of the cells were reduced by the collagen in the plate, and they took a longer time to close the gap, n=3.

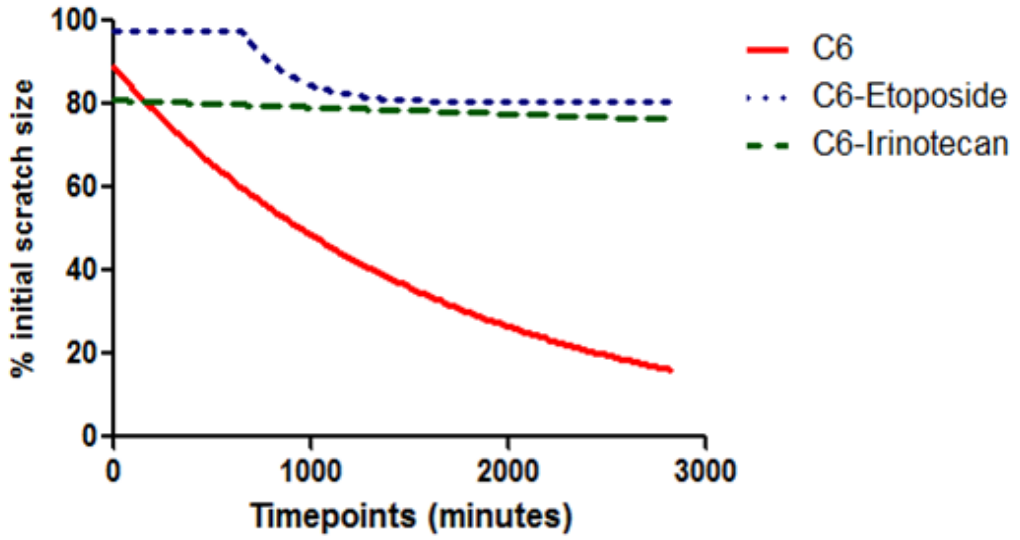

Figure 4.5 Collagen type I affects the migration in glioma cell lines. The three cell lines were prepared for the scratch assay followed the protocol in section 4.2.2. Images obtained from time lapse were analysed on ImageJ by stacking them into TIFF files and the data obtained used to plot the % scratch size as a function of time. Non-linear fit analysis showed that parental C6 cell line still has the fastest migration rate compared to other cell lines even on collagen coated plate (t½ = 1147 minutes ± 54). However, this cell line did not enter a lag period as before and they now fitted better with one phase decay curve) whereas, the drug derived cell lines had a different migration response. On one hand, C6-etoposide fitted better on lag exponential curve (lag period=13 hours) and they took longer (up to 48 hours) to close the gap. Whereas, C6-irinotecan proliferated rather than migrating to the gap and even after 48 hours, they failed to healed the wound, n=3. As in figure 4.3, each fit curve represented the mean of 9 closures over 3 independent experiments and individual time points are not shown (131 timepoints/ line).

4.2.3 Determination of migration rate for glioma cell lines with trans-well migration assay

The scratch assay was used to determine the migration response of the cells without the influence of any chemoattractant. To complement this, a transwell migration assay was applied to determine the response under the influence of a chemoattractant (10% serum). For the transwell migration assay, four independent experiments were performed using the ChemoTx®System kit (Neuro Probe, 101-3). This kit comprises a lower 96 well plate and 3 µm pore size upper filter. In the lower plate, either HBSS or 10% FBS is used as an attractant then the filter was placed gently on the lower plate. Subsequently, $2x10^4$ cells were added to the filter and the microplate was incubated in a 37°C/5% CO_2 incubator for 24 hours. Then the cells were fixed with 4% w/v PFA and nuclear DNA was stained with Hoechst 33342. Finally, the number of the migrated cells to the wells in the lower plate was detected by scanning the plate on ImageXpress^{MICRO} fluorescent microscope (Molecular Devices, USA).

For each well, the camera was programmed to take an image for 9 different areas. An in built algorithm enabled the detection of cells automatically based upon the size of fluorescent particles (nuclei) (figure 4.6). For each cell line, the increase in migration in the presence of chemoattractant (10% serum) was represented as a fold change. Under the influence of chemoattractant, the data showed that C6-irinotecan had the lowest percentage of migrated cells even under the influence of 10% serum as chemoattractant whereas C6-etoposide had the highest fold change (i.e., the ability of cells to migrate increased under the effect of chemoattractant) (figure 4.7). Indeed, analysis data of the transwell migration assay appears to agree with the data obtained from scratch assay.

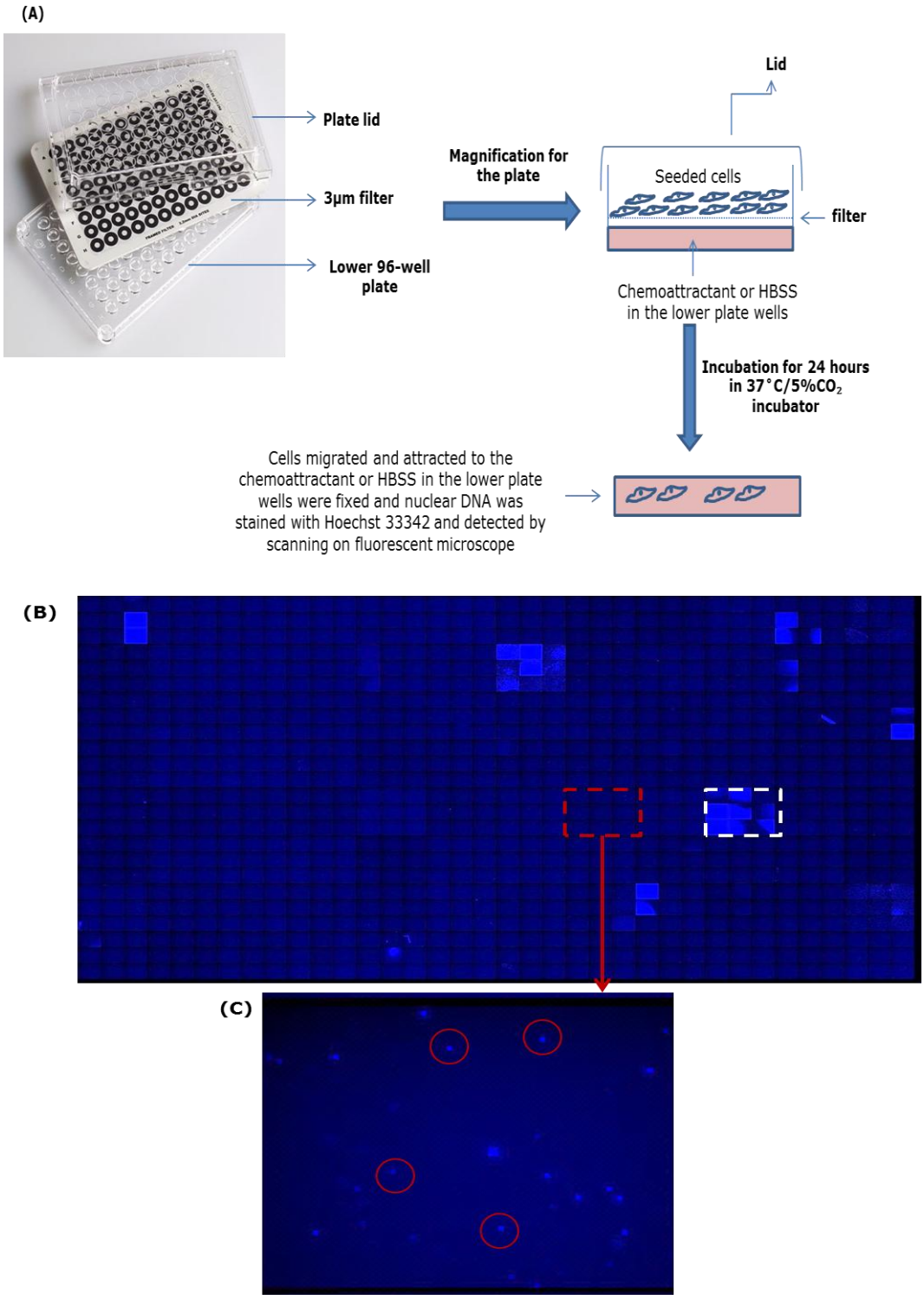

Figure 4.6 Transwell migration of C6 cell lines. (A) Schematic illustration for the experimental approach. (B) Representative image for the whole 96 well plate as obtained from ImageXpress. Area with red rectangle is an example for one well which shows 9 images/well taken by the camera. The area surrounded with white rectangle represents an example for the wells which have been excluded from the analysis as all cells were migrated to the lower wells presumably, because the filter was damaged. (C) Magnification from the selected area of the plate showing the nuclei which were detected by ImageXpress, by detecting the Hoechst 33342 fluorescence signal. The red circles represent example nuclei (4 of the 28) which have been counted.

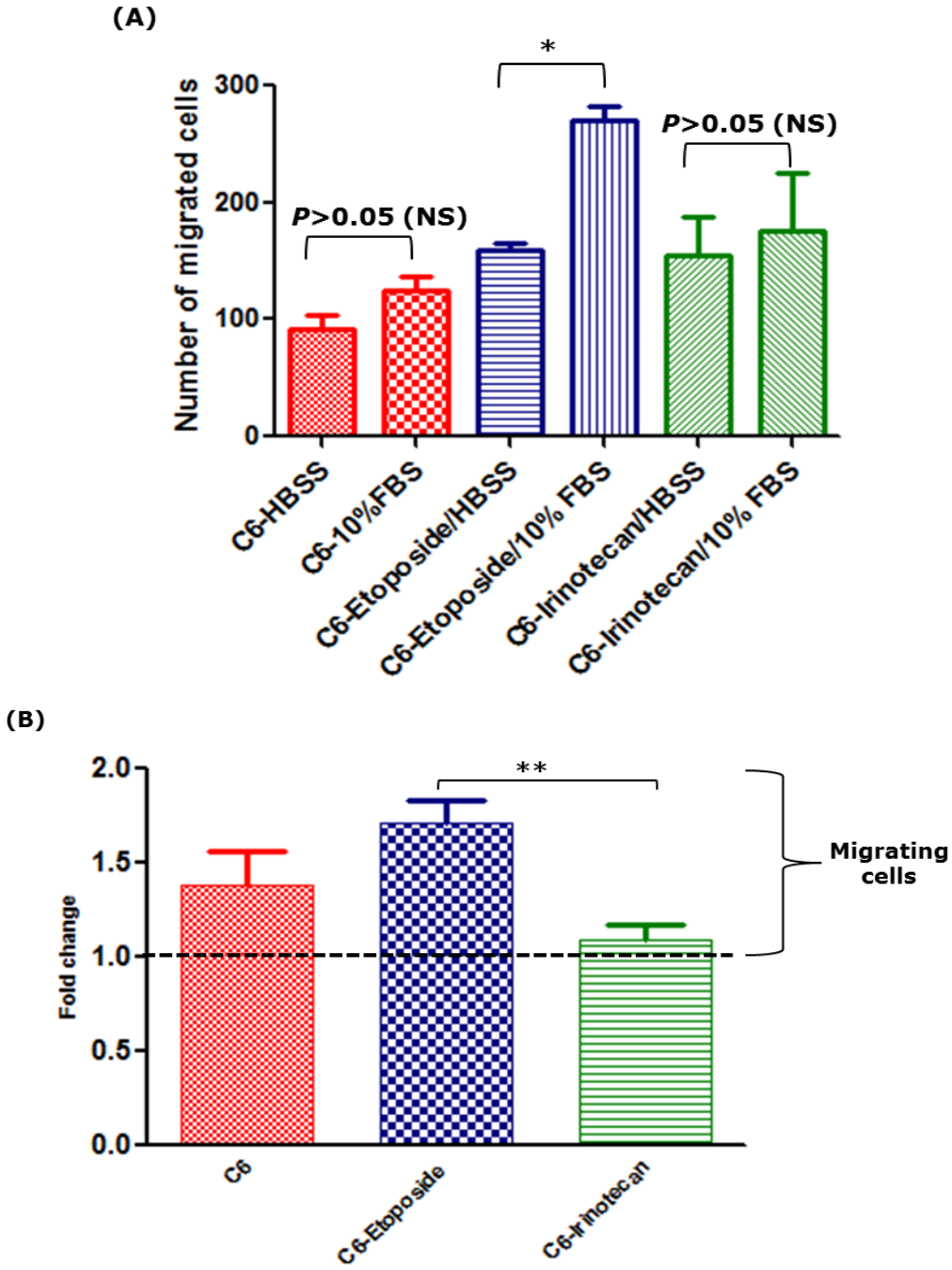

Figure 4.7 C6-etoposide migration rate increases under the influence of chemoattractant. The ability of the cells to migrate in response to chemoattractant was assessed by transwell migration assay. (A) Represents the total number of migrated cells (raw data) to either HBSS (control) or 10% FBS (chemoattractant). There was a significant difference in the migration rate for C6-etoposide only (1-way ANOVA with Bonferroni's multiple comparison test *P<0.05). (B) The fold change is defined as the change in number of migrating cells in the presence of 10% serum compared to the absence. One-way ANOVA analysis showed that the response to chemoattractant is different in the three cell lines (P<0.05), with post-test analysis (Bonferroni's multiple comparison test) indicating that the C6-irinotecan is a slower migrating cell line, ** P<0.001, n=4. The black horizontal line represents the % of migrating cells in each cell line.

4.2.4 Correlation of gene and protein expression differences with changes in cell migration response

As one of the aims of this project is to identify several candidates with proteomic and genomic approaches in order to correlate biological processes such as migration of cancer cells to drug resistance, candidates from mass spectrometry and IPA analysis (table 4.1) were validated with western blotting and qRT-PCR.

4.2.4.1 Analysis of vimentin expression levels

Before examining the expression of vimentin with western blotting, several experiments were performed to optimise the antibody diluent, and protein quantity to be loaded. The same procedures were performed to optimise the conditions of western blotting for all candidate proteins. From the optimisation experiments it was determined that all primary antibodies could be diluted in 5% non-fat milk in 0.1% PBST or TBST, whereas, the secondary antibodies were diluted in 1% non-fat milk in PBST or TBST. Figure 4.8 is an example of the blots produced to optimise the primary antibody dilution for vimentin and β-Actin and to determine the consistency of the densitometry signals produced from loading different protein quantities.

Vimentin is an intermediate filamentous protein and it is a major marker for mesenchymal cells. It is important as a regulator for cell to cell adhesion by binding to integrins and especially for endothelial cells and immune cells (Ivaska et al., 2007). To examine the expression of vimentin with western blotting, approximately 30 μg of protein from 3 independent passages were separated on 12% SDS-PAGE and then were incubated with 1:5000 of Rabbit anti-vimentin (see section 2.7 for more details) and the expression of the proteins was detected with the ECL assay. Three independent blots were performed on samples with and without drug treatment to assess the transient and persistent changes in the expression of the vimentin, and the expression of vimentin to the relative expression of β-

Actin was analysed by densitometry analysis. This analysis was determined by two independent assessors each time to be confident of the expression result. The densitometry results (using 1-way ANOVA analysis) showed no significant difference in the expression of vimentin between the C6 cell lines (figure 4.9).

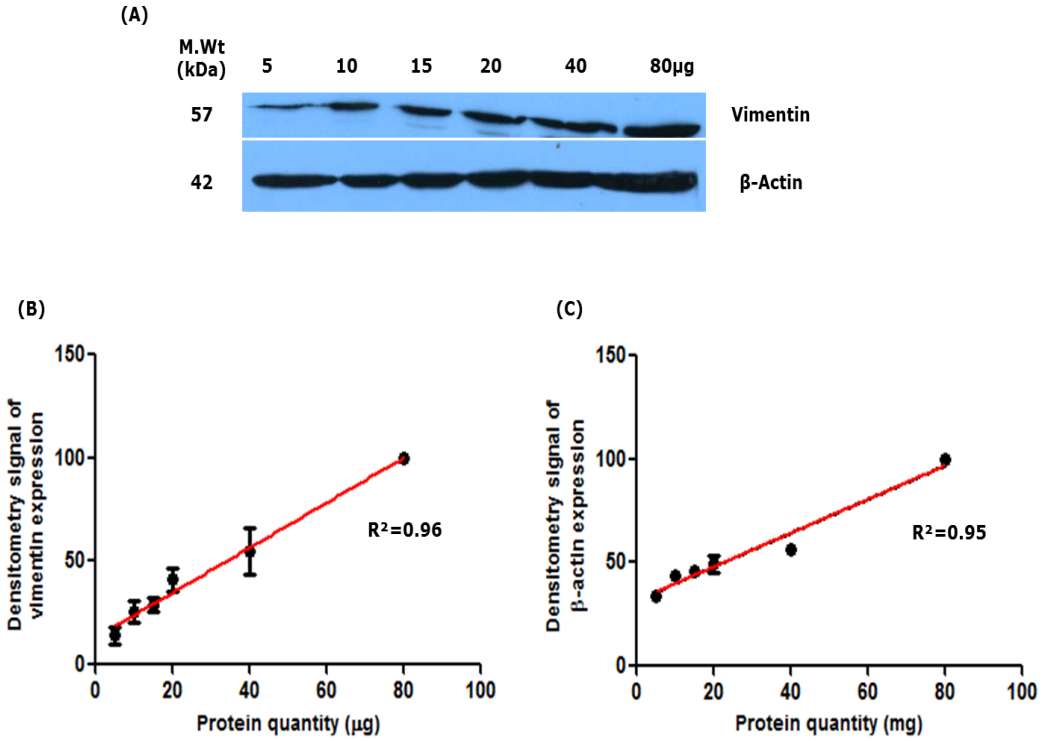

Figure 4.8 The optimisation of vimentin and β-Actin by western blotting. (A) In the two blots 5-80 µg of protein lysates from C6 cell line were loaded and separated on 12% SDS-PAGE and incubated with (1:5000) of anti-vimentin and anti- β-Actin antibodies in 5% non-fat milk/PBST followed by (1:2000) dilution of the secondary antibody in 1% non-fat milk/PBST. The detection of the vimentin and β-Actin expression was performed with ECL assay. (B) & (C) Represent the linear regression curves obtained by plotting the densitometry signals of two exposures for the protein expression vs. the protein quantity used. These optimisation experiments showed that the densitometry signal produced is consistent as linear curve is produced with gradual increase in protein quantities [the goodness of fit of the slope (R^2) is near 1].

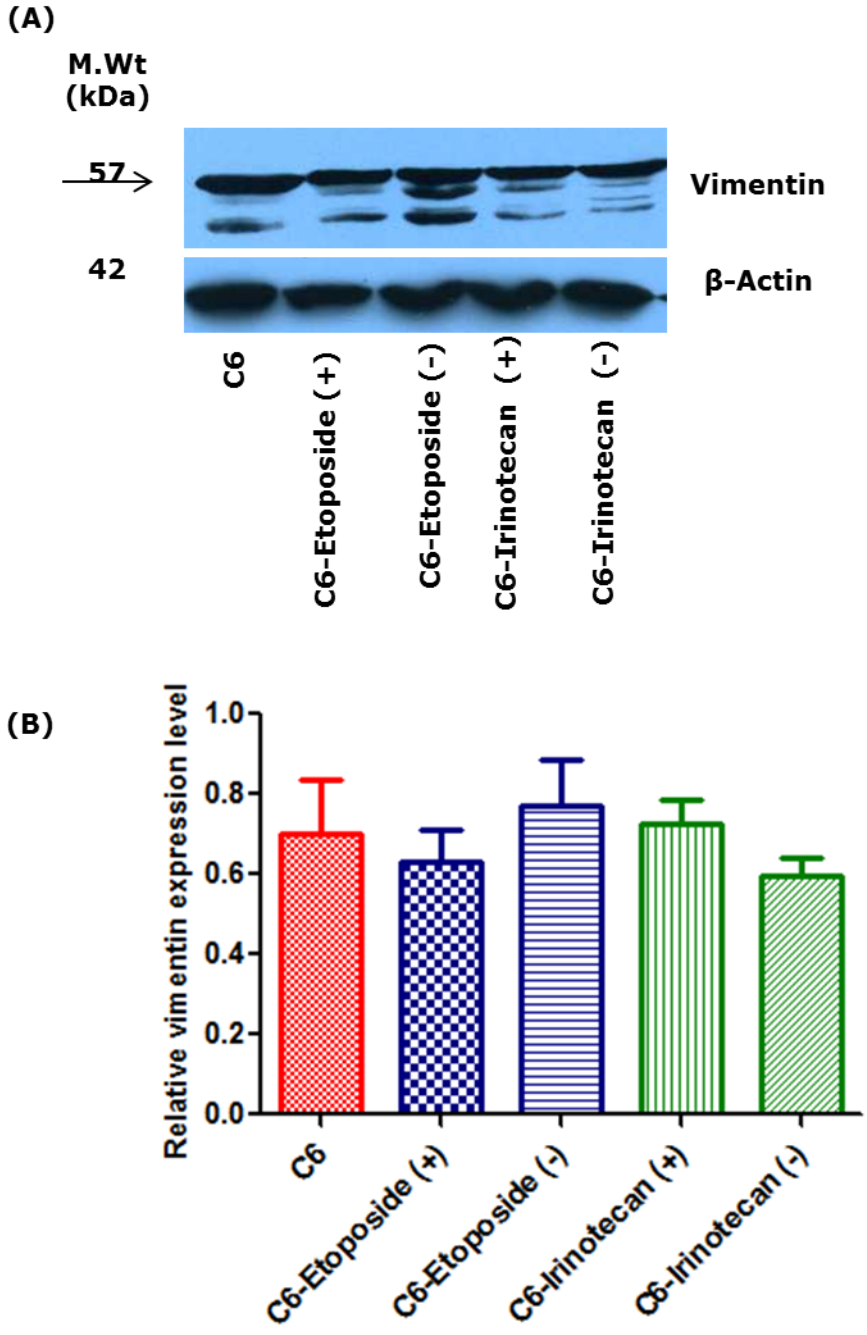

Figure 4.9 Vimentin expression showed no differences in C6 glioma cell lines. (A) 30 µg total protein cell lysates were separated by 12% (w/v) SDS-PAGE and incubated with rabbit anti-vimentin (1:5000) in 5% non-fat milk in PBST with the corresponding β-Actin blot as control (1:5000) in 5% non-fat milk in PBST. (B) The densitometry analysis for vimentin expression which was calculated by comparing the mean of vimentin expression to the relative expression of β-Actin which is used as control. The Bonferroni's multiple comparison test showed no significant difference in the expression of vimentin in the C6 cell lines ($P>0.05$, n=3). (+) indicates with drug treatment and (-) indicates without treatment.

4.2.4.2 Optimisation and validation of real time PCR (qRT-PCR) for candidate genes

The validation of all migration and metastasis candidate genes (*ATP1B1, COL1A2, and COL3A1*) was performed with qRT-PCR. This verification required optimisation at many steps including primer pair design, annealing temperature (Ta) optimisation, and determination of the primer efficiency. The best primer pairs to use for qRT-PCR should span an exon-intron junction to prevent amplification of contaminating genomic DNA (figure 4.10). Primer blast was used to design the qRT-PCR primer pairs. After designing the primers, a gradient annealing PCR reaction was performed to determine the best Ta for qPCR (Figure 4.11).

The most important step in the optimisation is the determination of the primer efficiency. Primer efficiency is determined by 2 key parameters; the first is that the reaction should produce double the yield every cycle and the second is that a primer pair should amplify a single specific amplicon. The former is analysed/ determined with a template DNA standard curve (62.5 ng doubling step-wise to 1000 ng) and determining the C_T (threshold cycle for product detection) in a qRT-PCR reaction (figure 4.12a and b show an example for the C_T amplification curves produced for β-Actin and ATP1B1). Re-plotting the C_T versus log DNA quantity should give a straight line with a slope of (-3.32) which is the [-1/log (2)], although common acceptable limits to the slope are -3.2 to -3.6 (figure 4.12c and d show an example for the standard curves produced for β-Actin and ATP1B1). The slope gradient is converted to a value describing primer efficiency that is used in the Pfaffl equation by the mathematical transformation $Ef= 10^{(-1/slope)}$ (table 4.2).

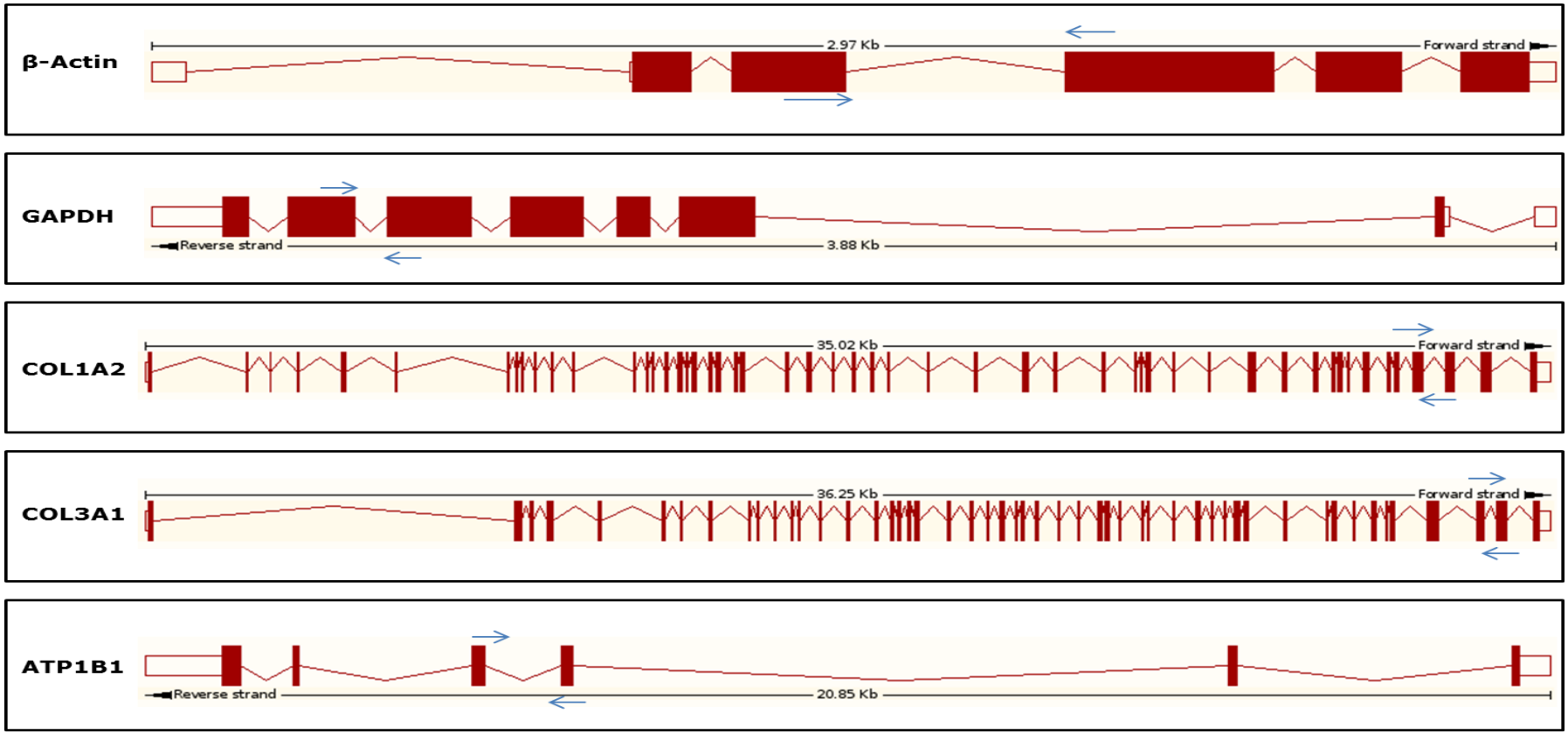

Figure 4.10 Designing of primers for control and migration candidate genes. These figures represent the full length transcript, in which, the bold red boxes represent the exons and the red line between them represents the introns. All transcripts information was obtained from Ensembl website (http://www.ensembl.org). The blue arrows represent the exons used to design the primers for qRT-PCR on primer blast (http://www.ncbi.nlm.nih.gov/tools/primer-blast/).

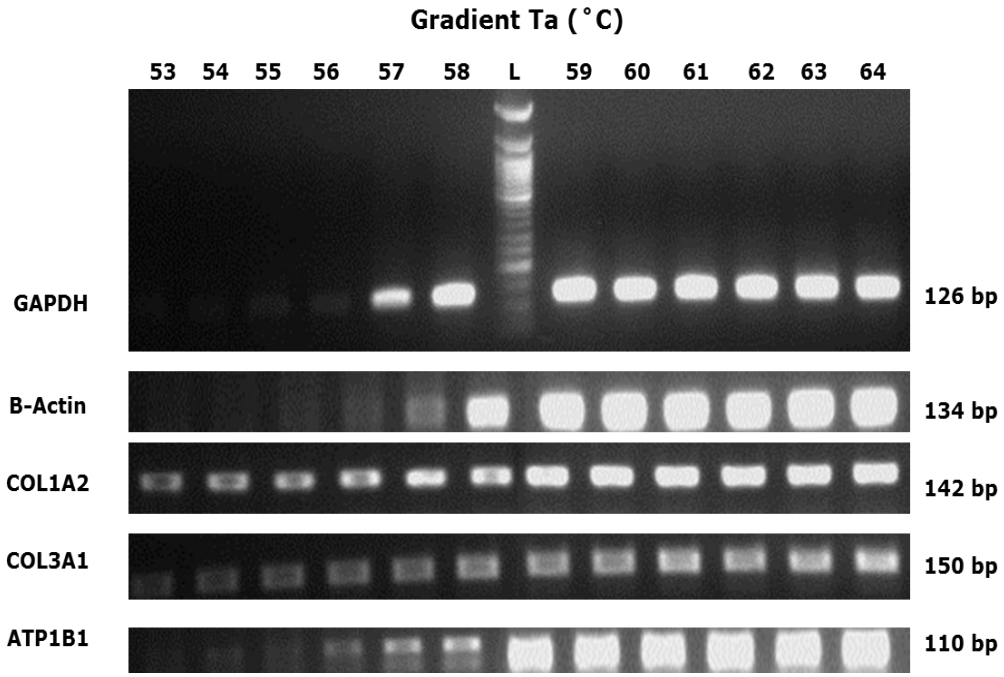

Figure 4.11 Determination of optimal primer annealing temperatures (Ta) for candidate genes. In order to determine the best annealing temperature for each primer pair to be used in the qRT-PCR reaction, a gradient PCR reaction was performed following the protocol in section 2.8.3. Strong PCR product bands within the appropriate sizes were produced. The absence of non-specific product in temperatures above 60˚C supported the use of Ta=60˚C as the annealing temperature in qPCR. L: DNA Ladder (50 bp, NEB).

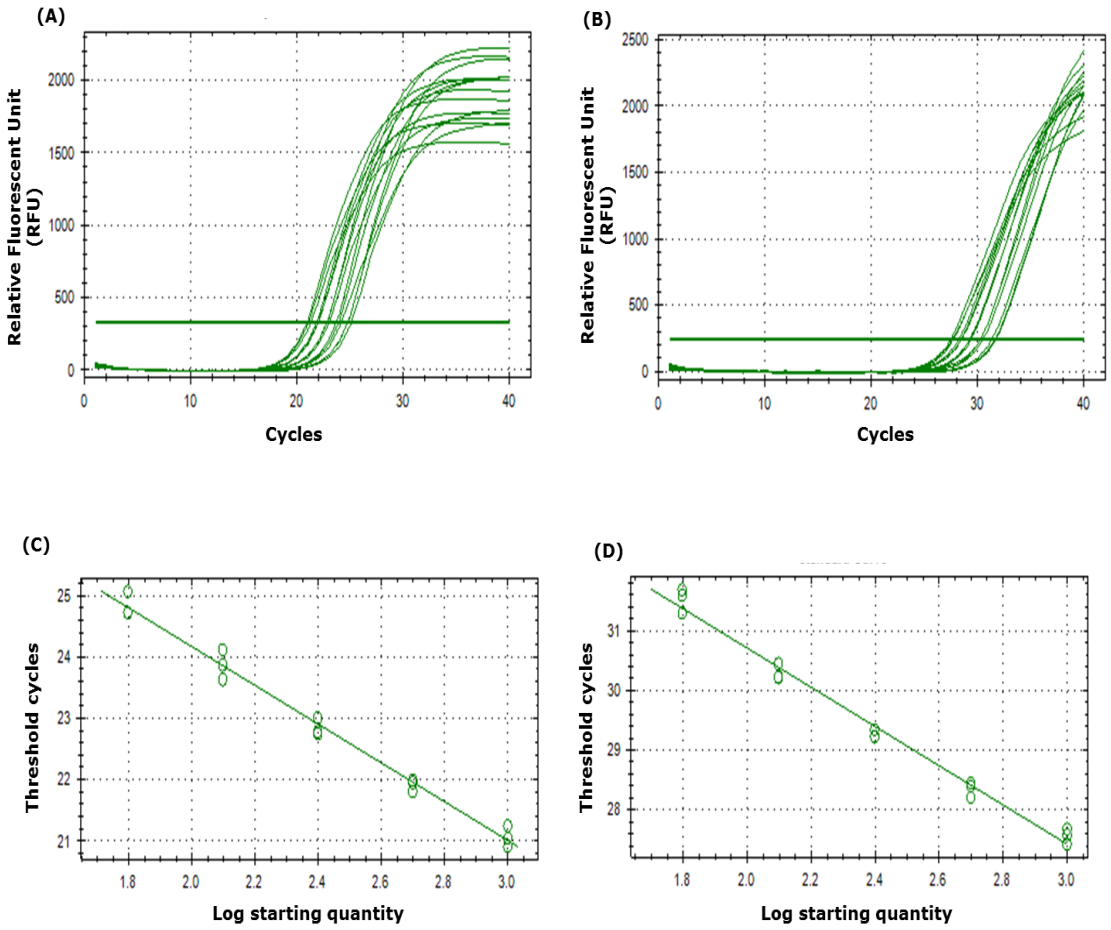

Figure 4.12 Optimisation of primer efficiency for β-Actin and ATP1B1 primers. Optimisation was performed by using two fold serial dilutions of cDNA from parental C6 cell line as template following protocol in section 2.8.4. (A) & (B) represent the amplification curves for β-Actin and ATP1B1, respectively. Each curve results from a different template DNA quantity and the threshold (C_T) at which specific amplification is demonstrated is shown by the horizontal line. (C) and (D) represent the standard curves for β-Actin and ATP1B1, respectively. This curve was plotted by using the C_T values obtained from the amplification curve vs. serial dilution of cDNA to determine the slope. For β-Actin (C) the slope is -3.16 and for ATP1B1 the slope is -3.28 (D) indicating that primers resulted in efficient quantitative doubling of product per cycle. Moreover, the (-RT) and the (NTC) samples are not shown but they resulted in no fluorescent signals. The slope and primer efficiency values were calculated from the amplification curves. The ideal slope for the standard curve should range from -3.2 to -3.6 and primer efficiency should be between 1.9 and 2.1.

Table 4.2 Primer efficiency for candidate genes involved in migration

Gene Name	Slope of standard curve	Primer efficiency %
ATP1B1	-3.284	101.6 %
COL1A2	-3.162	107.2 %
COL3A1	-3.200	109.7 %
GAPDH	-3.146	107.9 %
β-Actin	-3.155	107.5 %

The primer efficiency values and the slope values were obtained from the standard curve.

It is important to verify that the PCR amplification is specific under the used qRT-PCR conditions. This can be achieved by the melting temperature (Tm) analysis at the end of the PCR run. Detection of fluorescence production takes place in the extension step of real-time PCR. Signal intensity increases with increasing cycle number because the PCR product is accumulated. At low temperature, the amplicons are all double stranded (dsDNA) and bind to the SYBR Green I dye strongly resulting in a strong fluorescence signal. However, nonspecific PCR products and primer-dimers will also contribute to the fluorescent signal. Therefore, high PCR specificity is required when using SYBR Green I. Fluorescence measurements were made while slowly increasing the temperature of the reaction products from 60°C to 95°C. As the reaction temperature increases, the PCR products are denatured, resulting in a decrease in fluorescence signal because each product has its own dissociation temperature. Figure 4.13 shows a symmetrical style peak which is used as an indication of specific amplification.

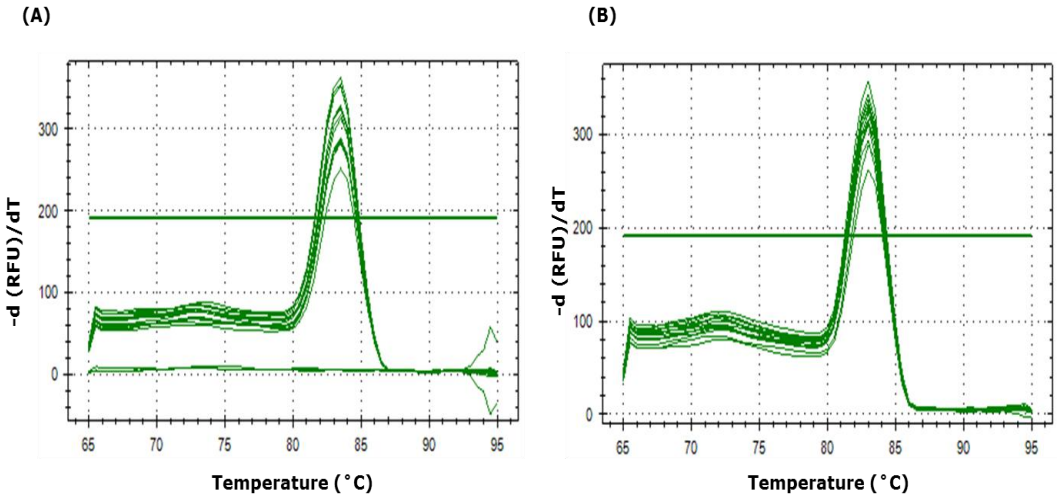

Figure 4.13 Melting curves of β-Actin and ATP1B1. This curve is produced as a result of a reduction in the fluorescent signal of SYBR Green I as the temperature is gradually increased. The ideal melting temperature curve is indicated by a symmetrical curve of that peaks within a short temperature range. (A) & (B) represent the melting curves produced from the optimisation of primer efficiency for β-Actin and ATP1B1 primers, respectively. In both cases, a major symmetrical melting peak is seen at Tm>80°C indicating a single specific amplicon.

4.2.5 Expression of candidate migration genes in C6 cell lines

After optimising the primer efficiency on the parental C6 cell line for candidate genes and control genes, qRT-PCR was performed on the three glioma cell lines to determine and validate the expression of these candidate genes in the three glioma cell lines. The qRT-PCR reaction was performed following the procedure in section 2.8.5. To detect the relative expression of each gene, three independent experiments were performed on cDNA samples which were prepared from RNA extracted from different cell passages in the absence of drug treatment. Then in each individual experiment, the 3 threshold cycle values (C_T) were averaged and divided by the geometric mean for the C_T values for GAPDH and β-Actin to determine the relative expression of ATP1B1, COL1A2 and COL3A1 using the Pfaffl equation (section 2.8.5 for explanation about Pfaffl equation).

We applied the geometric mean for more than one housekeeping gene rather than the arithmetic mean because the former is better in determining if there are outlying values. For brain tumours, a previous study showed that two to three housekeeping genes are enough to normalise the expression of a particular gene by qRT-PCR (Vandesompele et al., 2002). Moreover, the application of more than one control gene is important since housekeeping gene expression can vary under different treatment conditions.

Finally, the data calculated with the Pfaffl equation were compared and analysed on GraphPad Prism version 5.00 for Windows, GraphPad Software, San Diego California USA to examine the difference in the relative expression of each gene between the three cell lines. One way ANOVA analysis revealed that the expression of the three candidate genes is significantly decreased in C6-irinotecan cell line compared to C6 and C6-etoposide ($P<0.0001$, n=3) (figure 4.14). Encouragingly, this low expression of the three candidate genes in C6-irinotecan (especially *COL3A1* expression compared to C6 and C6-etoposide) can explain why this cell line has the slowest migration rate which is indicated by its low ability to heal the wound and to migrate under the influence of a chemoattractant. Therefore, treatment of cells with a topoisomerase I inhibitor can decrease the migration of the cancer cells by inhibiting the expression of three major genes involved widely in the migration and metastasis. Interestingly, the validation of gene expression by qRT-PCR corroborates the observations within the microarray data.

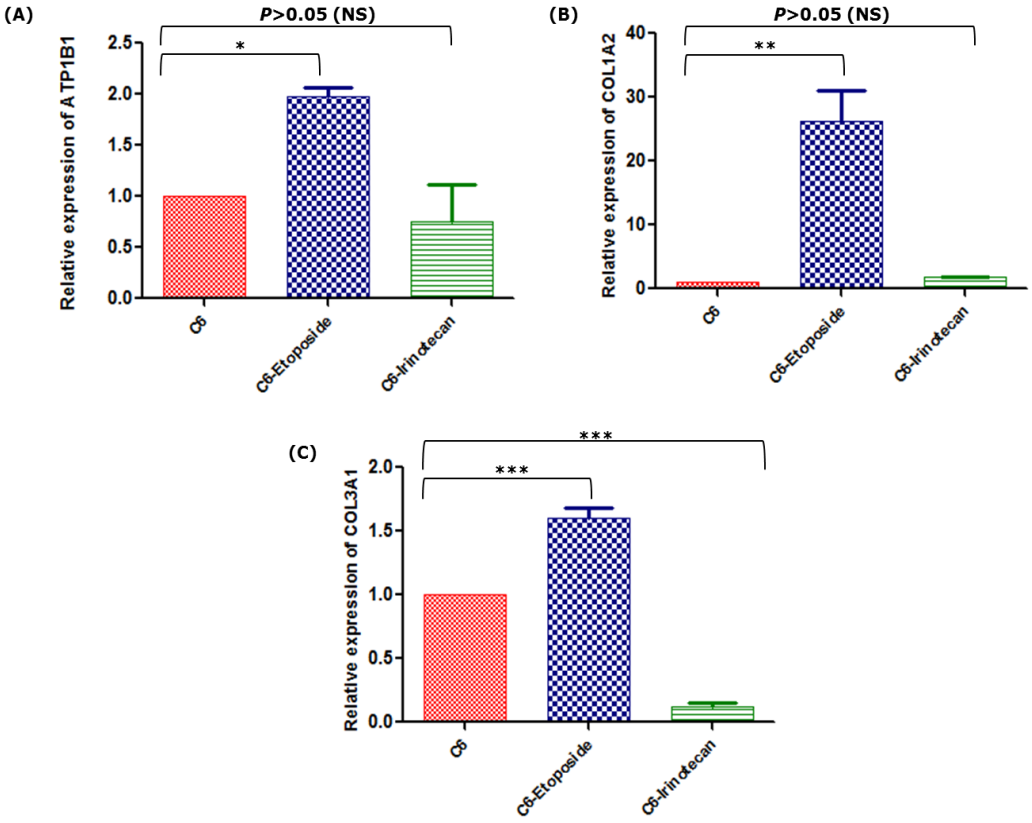

Figure 4.14 qRT-PCR representations for the relative expression of ATP1B1, COL1A2 and COL3A1 in the glioma cell lines. qRT-PCR reaction was performed according to the protocol in section 2.8.5. For each candidate gene, the relative expression was measured by applying the Pfaffl equation to calculate expression of each gene relative to the geometric mean of β-Actin and GAPDH in comparison to C6. From the analysis with 1-way ANOVA, there is a significant reduction in the expression of the three candidate genes in C6-irinotecan compared to the other cell lines (particularly for *COL3A1*) which can contribute to the lowest migration rate for this cell line. *$P \leq 0.05$, **$P \leq 0.001$, *** $P \leq 0.0001$, and n=3. (A) For *ATP1B1*, the ANOVA analysis determined that the expression of this gene is different between the 3 cell lines ($P<0.001$) and the post-test (Bonferroni's multiple comparison test) confirmed that C6-etoposide had higher expression compared to C6 ($P<0.05$) and C6-irinotecan ($P<0.001$). (B) For *COL1A2*, the ANOVA test and the Bonferroni's multiple comparison test revealed that this gene is highly expressed in C6-etoposide compared to C6 and C6-irinotecan ($P<0.0001$). (C) For *COL3A1*, analysis with ANOVA followed by the Bonferroni's multiple comparison test showed that there is a highly significant reduction in the expression in C6-irinotecan compared to C6 and C6-etoposide ($P<0.0001$). The expression of the candidates with qPCR showed the same pattern of expression as the gene expression microarray.

4.3 Summary

In this chapter, two different migration assays were performed to determine the migratory response of the three glioma cell lines and these results were further investigated through western blotting and qRT-PCR. These results were analysed to validate the expression of our proposed protein and gene candidates and to correlate the expression of these candidates with the biological process of cell migration. The conclusions of our results in this chapter are as follows:

- Wound scratch assays were performed to assess the migration response of the cell lines. Cell lines showed changes in migration. Analysis of data showed that C6 cell line has the fastest migration rate compared to other cell lines. However, this cell line has a lag period for 8 hours. For drug derived cell lines, C6-etoposide has a faster migration rate than C6-irinotecan with no lag period for both (figure 4.3). Interestingly, analysis of wound scratch assay performed on collagen coated plates showed that the expression of collagen can alter the migration response of the 3 cell lines (figure 4.5).
- Transwell migration assays confirm the data obtained from wound scratch assays. The results revealed that C6-irinotecan has the lowest fold change (which represents the total number of cells migrated under the influence of 10% FBS) compared to C6-etoposide ($P<0.001$), n=4 (figure 4.7).
- The validation of vimentin with western blotting showed no significant difference in its expression in the C6 glioma cell lines, $P>0.05$, n=3 (figure 4.9).
- Gene expression data by qPCR showed that expression of *COL1A2*, *COL3A1*, and *ATP1B1* is significantly lower in C6-irinotecan cell line compared to the other cell lines (figure 4.14). These findings agreed with the GeneSpring GX11 software analysis performed on raw microarray data.

CHAPTER V

A TOPOISOMERASE (II) INHIBITOR (ETOPOSIDE) INCREASES THE RESISTANCE TO OXIDATIVE STRESS IN A DRUG-SELECTED HIGH GRADE GLIOMA CELL LINE

CHAPTER V: A TOPOISOMERASE (II) INHIBITOR (ETOPOSIDE) INCREASES THE RESISTANCE TO OXIDATIVE STRESS IN A DRUG-SELECTED HIGH GRADE GLIOMA CELL LINE

5.1 Introduction

The redox state is a consequence of the balance between the levels of oxidising reactive oxygen species (ROS) and reducing agents. ROS are highly reactive molecules due to the presence of unpaired valence electrons. They are produced by the partial reduction of oxygen as electrons leak out of the electron transport chain during respiration in mitochondria in response to exogenous factors such as chemotherapeutic agents, ultraviolet (UV) light, and γ-irradiation. The most common forms of ROS include superoxide anion ($O_2^{\cdot -}$), hydrogen peroxide (H_2O_2), and the highly reactive hydroxyl radical ($OH^{\cdot}$) (Davis et al., 2001, Marnett et al., 2003). Normal cells are able to protect themselves from ROS with antioxidants. An antioxidant is a molecule which has the capacity to inhibit the oxidation process by transferring an electron or hydrogen from a substrate to an oxidising agent. Major antioxidants include enzymes such as catalase, glutathione peroxidase and superoxide dismutase as well as small antioxidant molecules such as vitamins C and E, uric acid and glutathione (Lee et al., 2011b).

The production of ROS in cancer cells is both complex and paradoxical. It is still unknown whether cancer cells are producing ROS at the same level as normal cells but with a suppressed antioxidant system, or whether they are normally producing ROS at higher level without the need for exogenous stimulation (Schumacker, 2006). In fact, ROS can affect many cellular processes in different ways based on many factors such as (1) the amount of ROS produced, (2) the duration of exposure to oxidative molecules, (3) the type of antioxidant defence mechanisms which are affected and (4) how effectively the cellular repair systems are working. In all cases, elevated

levels of ROS result in potentially cytotoxic "oxidative stress" to macromolecules in the cell such as DNA, RNA, proteins, and lipids and therefore lead to cell death (Conklin, 2004). Several chemotherapeutic agents such as the anthracyclines (e.g., doxorubicin) (Gille and Nohl, 1997) and epipodophyllotoxins (e.g., etoposide) (Oh et al., 2007) depend exclusively or partially on the production of ROS for their cytotoxicity. These drugs can induce their cytotoxic effects by several mechanisms such as the elevation of lipid peroxidation products, the reduction in plasma levels of antioxidants such as vitamin E, vitamin C, and β-carotene, and the decrease in tissue glutathione levels (Conklin, 2004, Oh et al., 2007). Therefore, the sensitivity of tumour cells to oxidative stress resulted from chemotherapy may affect the treatment success (chemo-resistance) (Schumacker, 2006).

Apoptosis is well known to be mediated by oxidative stress. Since 1991, it has been shown that ROS and mitochondria have an important role on the regulation of apoptosis under both normal physiological and pathological conditions. For example, under normal conditions in neutrophils H_2O_2 is able to induce apoptosis, which is prevented by the action of catalase (Kasahara et al., 1997). In contrast, TNF-induced ROS can also activate anti-apoptotic pathways through the activation of the transcription factor NF-*k*B. The major activated anti-apoptotic enzymes are catalase and superoxide dismutase (Wong and Goeddel, 1988). However, there is considerable evidence that apoptosis does not require ROS and that their generation occur as a late event after cells are already committed to apoptosis (Jacobson, 1996, Clutton, 1997). This effect has been suggested to be related to the expression of Bcl-2 (major proto-oncogene) in the inner membrane of mitochondria which is the centre of redox reactions in the cell. Bcl-2 was found to suppress the programmed cell death (PCD) by inhibiting the formation of ROS (i.e., act as an antioxidant) (Kane et al., 1993, Korsmeyer et al., 1995).

It is postulated that cancer cells may have other anti-oxidation mechanisms in addition to those mentioned above (Schumacker, 2006). Candidate proteins and genes which were identified in chapter III prompted the hypothesis that an altered response in drug derived cell lines vs. parental C6 cell line to oxidative stress would be observed in the three glioma cell lines. In the current chapter, the expression of these candidates will be further validated with western blotting and qRT-PCR. Moreover, their potential role in chemo-resistance and the possible mechanisms for resisting apoptosis, resulting from an altered response to oxidative stress in high grade glioma will be revealed.

5.2 Results

Three candidate proteins were identified with mass spectrometry and were found to be involved in the response to DNA damage. Additionally, two candidate genes identified with IPA analysis were also found to be correlated to apoptosis and resistance to oxidative stress. These candidates and their putative role in DNA damage and apoptosis are listed in table 5.1. The basis of the experiments carried out in this chapter is to produce ROS in cells using tert-butyl hydroperoxide (TBHP), determine the cellular response to ROS, and correlate this response with candidate proteins and genes expression level which will be validated with western blotting and qRT-PCR, respectively.

Table 5.1 Candidate proteins and genes related to oxidative stress resistance showing different expression in C6 cell lines

Candidate Proteins		
Protein Name	**Function**	**Reference**
Lamin A	Mutations in lamin A lead to defective DNA replication and repair which disrupts mitosis and induces DNA damage leading to genomic instability	(Gonzalez-Suarez et al., 2009, Ragnauth et al., 2010)
Catalase	Prevents the formation of ROS by breaking down the H_2O_2 into H_2O and O_2, and it also uses the H_2O_2 to oxidise toxins such as phenols, formaldehyde, and alcohols in the peroxisome	(Toyokuni et al., 1995)
PRP19	Reduces the apoptosis response after exposure of cells to DNA damage	(Lu and Legerski, 2007)
Candidate Genes		
Gene Name	**Function**	**Reference**
PTEN	Common mediator for ROS production (inhibits) and neuronal death and it is a known tumour suppressor gene for PI3K/Akt pathway	(Zhu et al., 2007, Song et al., 2012)
EGR1	Transcription factor that regulates growth and differentiation. Overexpression of EGR1 is mediated by the high level of ROS through ERK and JNK signalling pathways.	(Nair et al., 1997, Aggeli et al., 2010)

5.2.1 Optimisation of TBHP concentration and cell count

Initially, three independent optimisation experiments were performed to optimise the concentration of TBHP to be used and to investigate whether this response was cell number dependent. To optimise the total number of cells, parental C6 glioma cells were seeded either at $1x10^4$ or at $0.25x10^6$/well of a 12-well plate. Plates were incubated in a 37°C /5% CO_2 incubator for 24 hours to ensure cell attachment. Subsequently, cells were treated with increasing concentrations of TBHP and examined 2 hours and 24 hours post treatment. These observations were important to assess the cells' response to the ROS-inducing chemical, and to identify the optimal final concentrations of TBHP for ROS production without killing the cells (i.e., not cytotoxic dosage). From the optimisation experiments, we found that C6 cells tolerate and survive exposure to TBHP concentrations up to 250 μM as cells continued to proliferate, whereas, with 500 μM 50-100% of cells start to die (depending on the cell count used) and with 1mM TBHP concentration cell death occurs (presumably due to oxidative stress) immediately after 2 hours (figure 5.1).

5.2.2 Assessment of oxidative resistant response

After optimising the TBHP concentration, which showed relatively little dependence on cell number, the response to oxidative stress (OS) for the three glioma cell lines was determined. To examine this, firstly, 10^4 cells were seeded in a black clear-bottom 96-well plate and incubated for 24 hours to allow the cells to attach. Cells were then treated with 50μM of 2', 7'-dichlorofluorescin diacetate (DCFH-DA) and incubated for 30 minutes in 37°C/5% CO_2. This fluorescent probe is oxidised to DCF in the presence of ROS which is used as an index to quantify the overall ROS in cells. Cells were then washed with HBSS to remove any remaining DCFH-DA. Subsequently, cells were treated with different concentrations of TBHP (0, 100μM, 250μM, and 500μM) to induce ROS production, and the fluorescent signal [relative fluorescent unit (RFU)] was measured at λ_{530} for 3 hours in total at 37°C.

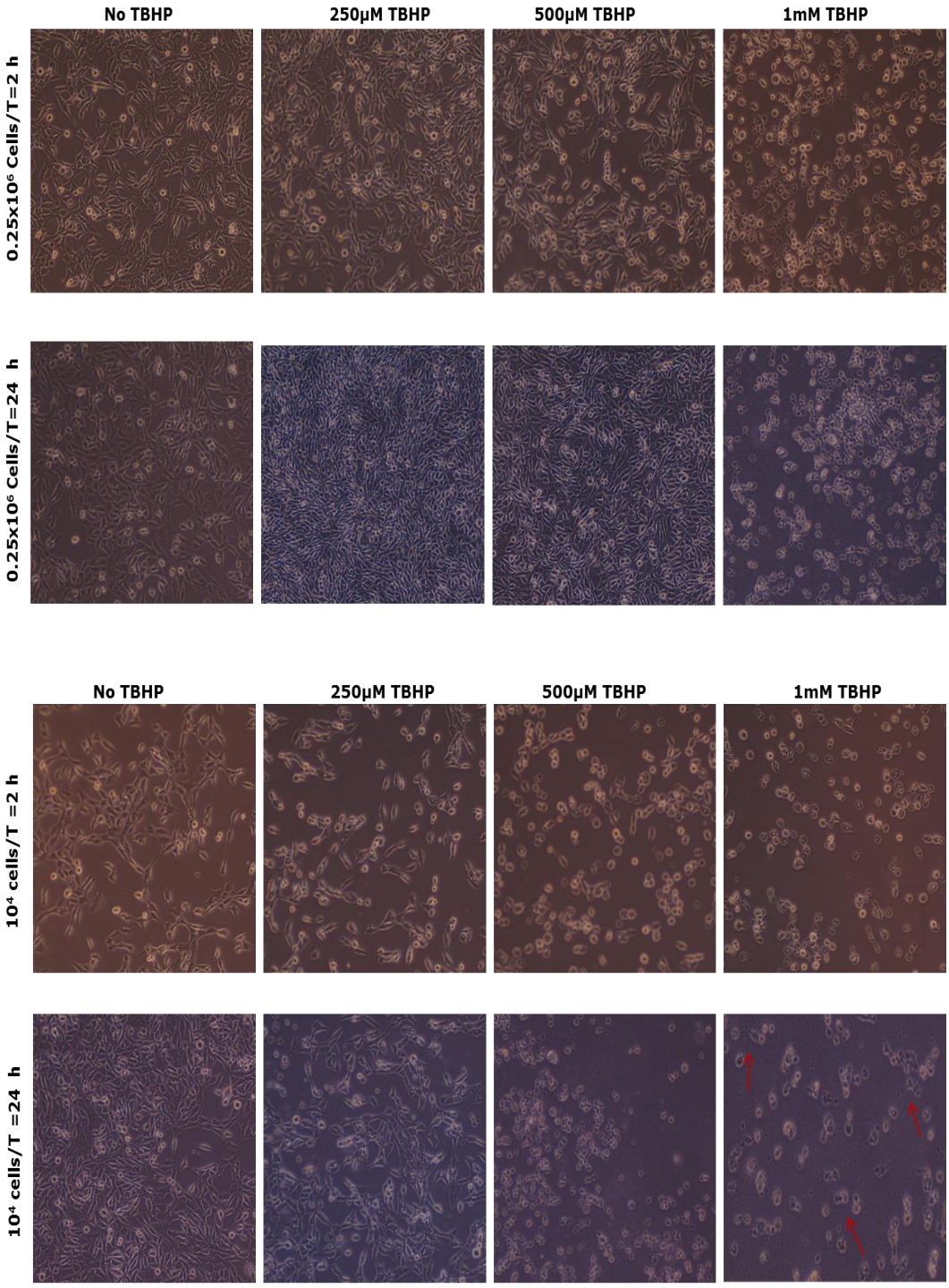

Figure 5.1 Optimisation of cell count and TBHP concentrations. Approximately $1x10^4$ or $0.25x10^6$ C6 cells were treated with different concentrations of TBHP. The response of the cells towards TBHP was monitored for 2 and 24 hours. Cells were able to resist the effect of oxidative damage produced by TBHP up to 250 µM and continued to proliferate. At 500 µM TBHP 50%-80% of cells showed changes in morphology (more visible in the lower panels at t= 24 hours and it depends on cell count) and with 1mM TBHP, the cells were no longer able to tolerate oxidative stress damage which as indicated by the 100% cell death (as shown by rounded up cells-red arrow) (regardless of initial cell density).

Initial analysis revealed that the three cell lines showed a time dependent ROS production after exogenous treatment with TBHP (figure 5.2a). However, the three cell lines in general tolerated the oxidative stress induced by ROS production for 30-50 minutes (i.e., respond linearly to the oxidative stress). After 1 hour, there was a drop in the linearity of the curves slopes presumably due to cell death by oxidative damage (figure 5.2b). The gradient in figure (5.2a) is the rate of ROS production. This gradient was used to compare treatments and cell lines. Drug treated cell lines have a lower gradient i.e., a lower rate of ROS production. We infer this as a greater resistance to ROS inducing agents; i.e., a ROS tolerance. However, the data in figure 5.2 are from a single TBHP concentration (100 μM). When we repeated the experiments with different concentrations of TBHP we were able to established dose: response data for the 3 cell lines (figure 5.3). For the C6 cell line, there was a significant reduction in the ROS generation response of the cells at higher TBHP concentrations (1-way ANOVA *P* value≤0.0001) (figure 5.3a). For C6-irinotecan, the rate of ROS produced by 250 μM TBHP was higher compared to 100 μM TBHP but at 500 μM, there was a significant drop in the response (1-way ANOVA *P* value ≤0.0001) (figure 5.3b). In contrast, C6-etoposide showed increasing ROS production in a TBHP dose dependent manner with no reduction in the ROS response until 1 mM TBHP was applied (figure 5.3c). These results are interpreted as follows. The C6 parental cell line is most sensitive to ROS production and use of elevated (>100 μM) TBHP causes cell death hence a drop in the apparent ROS level. For C6-etoposide, the other extreme is apparent. The cells produce ROS in a TBHP dose dependent manner and survive with >500 μM TBHP being required to see a cell death associated decrease in ROS. C6-irinotecan response is intermediate between the two other cell lines.

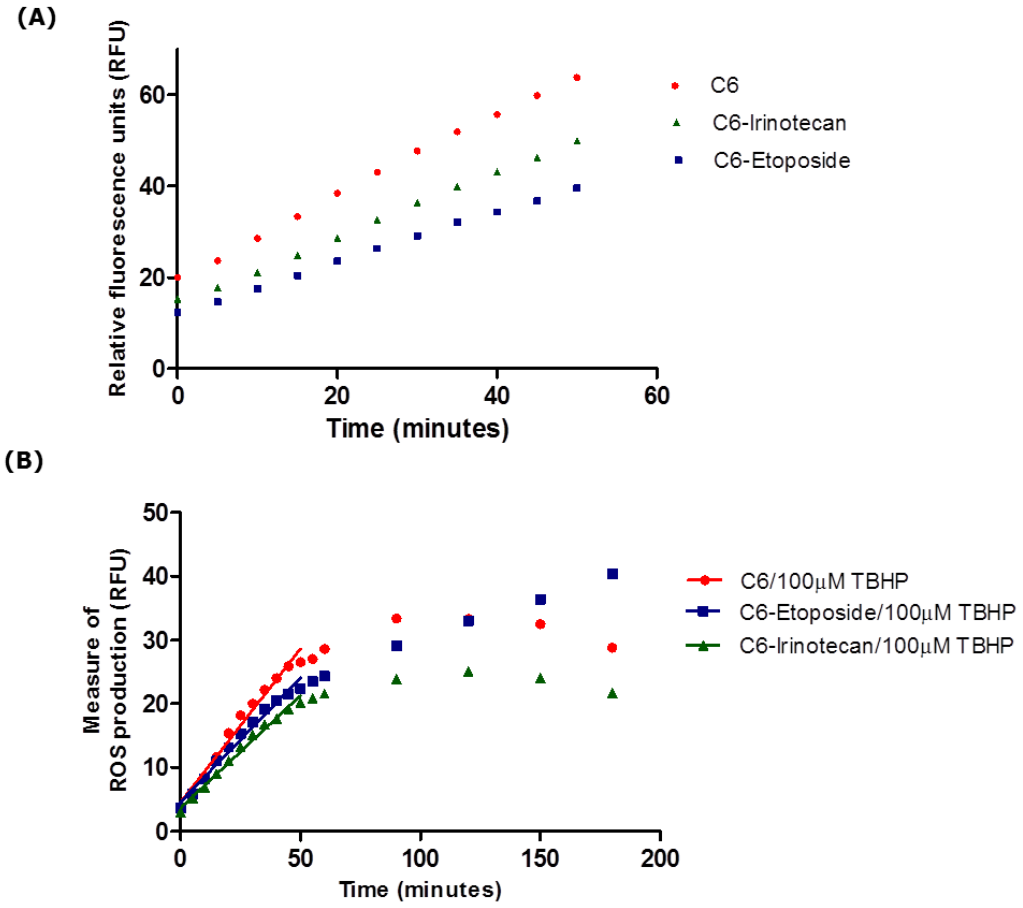

Figure 5.2 Kinetics of ROS production in glioma cell lines. 10^4 cells were seeded in a black clear bottom 96 well plate and treated with 50µM DCFH-DA (fluorescent probe) followed by the addition of 100 µM TBHP, then RFU was measured at λ_{530} nm on fluorescent micro-plate reader for 3 hours. (A) Represents the linear section of the experiment which was used to compare rates of ROS production under different conditions. The response to TBHP treatment shows biphasic kinetics. An initial phase of linear increase in ROS production (1 hour) is followed by a gradual plateauing of ROS production (B).

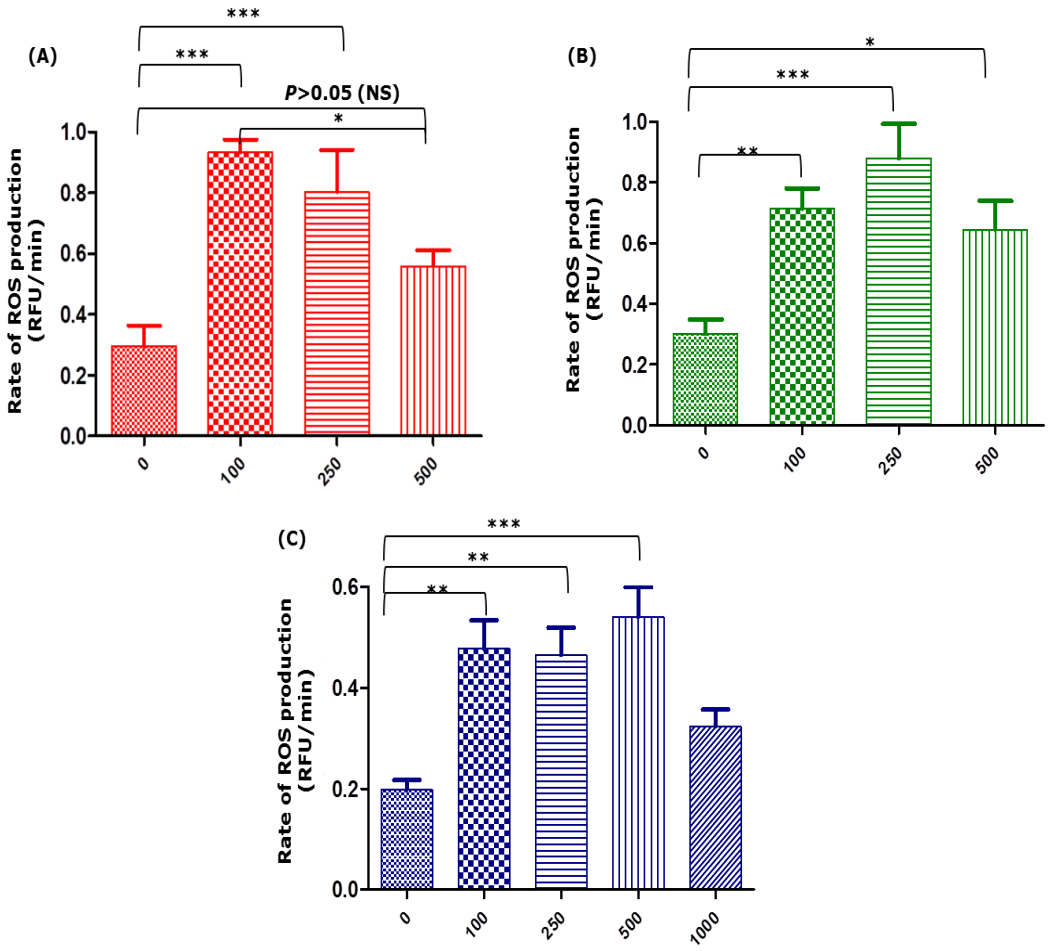

Figure 5.3 C6-Etoposide is more resistant to oxidative stress. Approximately, 10^4 cells of the three cell lines were incubated with DCF as in figure 5.2 followed by treatment with different TBHP concentrations (0, 100μM, 250μM, and 500μM) then RFU was measured at λ_{530} nm on a Flexstation3. (A) Parental C6 was more sensitive to oxidative stress as the rate of ROS production was decreased with higher concentrations of TBHP (250μM and 500μM) (inverse relationship) (1-way ANOVA $P \leq 0.0001$). (B) In contrast to C6, C6-irinotecan was more resistant to ROS at lower TBHP concentrations (100μM and 250μM) but at 500μM, the cells became sensitive to oxidative stress (1-way ANOVA $P \leq 0.0001$). (C) Interestingly, C6-etoposide showed higher resistance to oxidative stress as there was no difference in the rate of ROS production with the (100, 250, and 500μM) TBHP concentrations, whereas, with 1mM TBHP, 50-80% of cells start to respond which indicates that C6-etoposide can tolerate oxidative stress better than the other two cell lines (1-way ANOVA $P \leq 0.0001$). *P* values and (*) in the graphs were determined by 1-way ANOVA followed by the post test (Bonferroni's multiple comparison) where; *$P \leq 0.05$, **$P \leq 0.001$, *** $P \leq 0.0001$, and n=6.

5.2.3 Determination of cell cytotoxicity

Our interpretation of the data in figure 5.3 is that the drug treated C6 cell lines are more resistant to ROS production than C6 and thus as TBHP concentrations increase so does the rate of ROS production, until a point is reached when the rate of ROS production falls indicating that this concentration of TBHP is cytotoxic. To support this, the MTT cytotoxic assay was performed. Approximately, 10^4 cells were seeded into a 96-well plate and incubated in a 37°C /5%CO_2 incubator for 24 hours. Then the cells were treated with different concentrations of TBHP (0, 100, 250, 500 μM) for different time periods (30, 90, and 180 minutes) and subsequently incubated in a 37°C /5%CO_2 incubator for approximately 24 hours. When the cells were confluent in the control wells, the MTT assay was performed as in 2.6.4 and the intensity of formazan product was measured at 550 nm using a micro-plate reader.

Results from MTT assay (figure 5.4) agreed with the data from ROS generation assay and confirmed that the reduction in the rate of ROS generation was due to the death of the cells. In general, for the three cell lines the number of viable cells was reduced at concentration of TBHP higher than 100 μM and it was a time-dependent response. For example, with 250 μM TBHP, in the C6 and C6-irinotecan cell lines, there was no cells death when exposed to TBHP for 30-40 minutes but there was reduction in viability after 90 minutes exposure (figure 5.4a and b). In contrast, for C6-etoposide the cells were resisting the effect produced by the treatment with 250 μM even after 180 minutes exposure. Interestingly, C6-etoposide cells start to die only at 500 μM TBHP after 180 minutes (figure 5.4c). Thus, MTT assay successfully explained the response of the cells to ROS and confirmed that the observed reduction in ROS production rate was due to cell death.

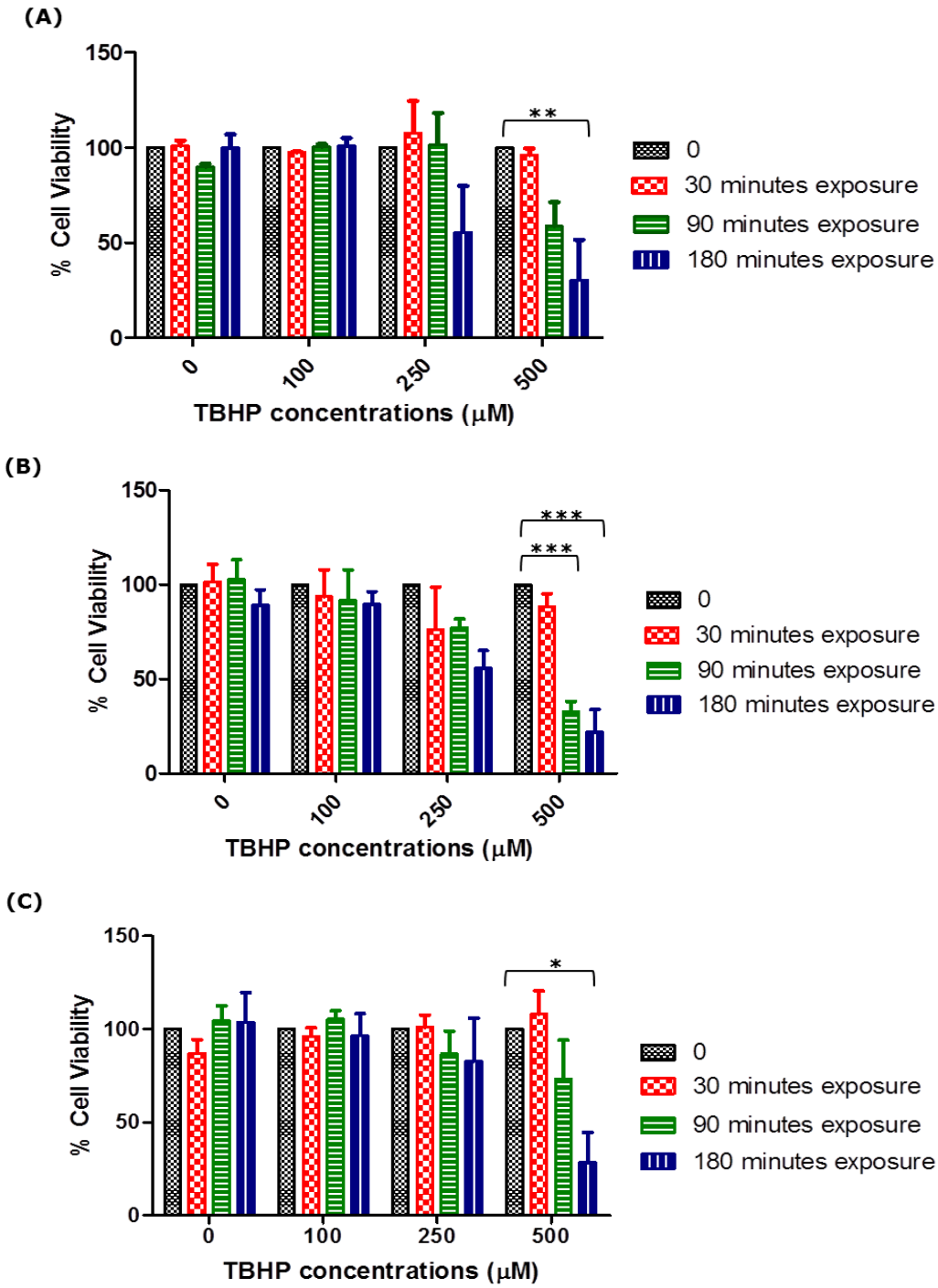

Figure 5.4 The MTT assay confirms C6-etoposide tolerates ROS. The % cell viability of glioma cell lines was determined with MTT assay. (A) For C6, the % of viable cells decreased dramatically after 90 minutes exposure with both 250 µM and 500 µM TBHP. However, with 250 µM the *P* value reached significance level. (B) C6-irinotecan has the same response as C6 with 250 µM TBHP whereas, with 500 µM the % viable cells was affected severely after 90 minutes. (C) C6-etoposide tolerates ROS better than other cell lines as this cell line can survive the oxidative damage produced with 250µM and there was a significant reduction in the % of viable cells only with 500 µM TBHP and after 180 minutes exposure. The (*) was calculated by applying 1-way ANOVA followed by Dunnett's multiple comparison test in which *P<0.05, **P<0.001, and ***P<0.0001, n=3.

5.2.4 Validation of candidate proteins with western blotting

In order to shed light on the mechanisms underlying the different response to ROS, candidate proteins (lamin A, catalase, and PRP19) were validated with western blotting. Approximately 30 µg of protein from different passages were separated on 12% SDS-PAGE followed by incubation with the appropriate dilutions of primary antibodies (see section 2.7). Finally, proteins expression was determined by densitometry analysis. In each case, the expression of the candidate protein was performed relative to that of β-Actin which served as a control for equal protein loading. This analysis was performed by two people for many of the candidate proteins to rule out any subjectivity in the data analysis. However, statistical analysis (1-way ANOVA) results failed to correlate any of the candidate proteins to the oxidative resistance as the expression was the same between the three cell lines ($P>0.05$, n=3) (figure 5.5).

Although PTEN was identified as being differentially expressed by transcript level analysis, the availability of robust PTEN antibodies prompted investigation of protein level between the cell lines. The expression of PTEN was measured by densitometry analysis and significantly lower levels were identified in C6-etoposide cell line compared to other cell lines (1-way ANOVA followed by Dunnett's multiple comparison test $P<0.05$, n=3) (figure 5.6).

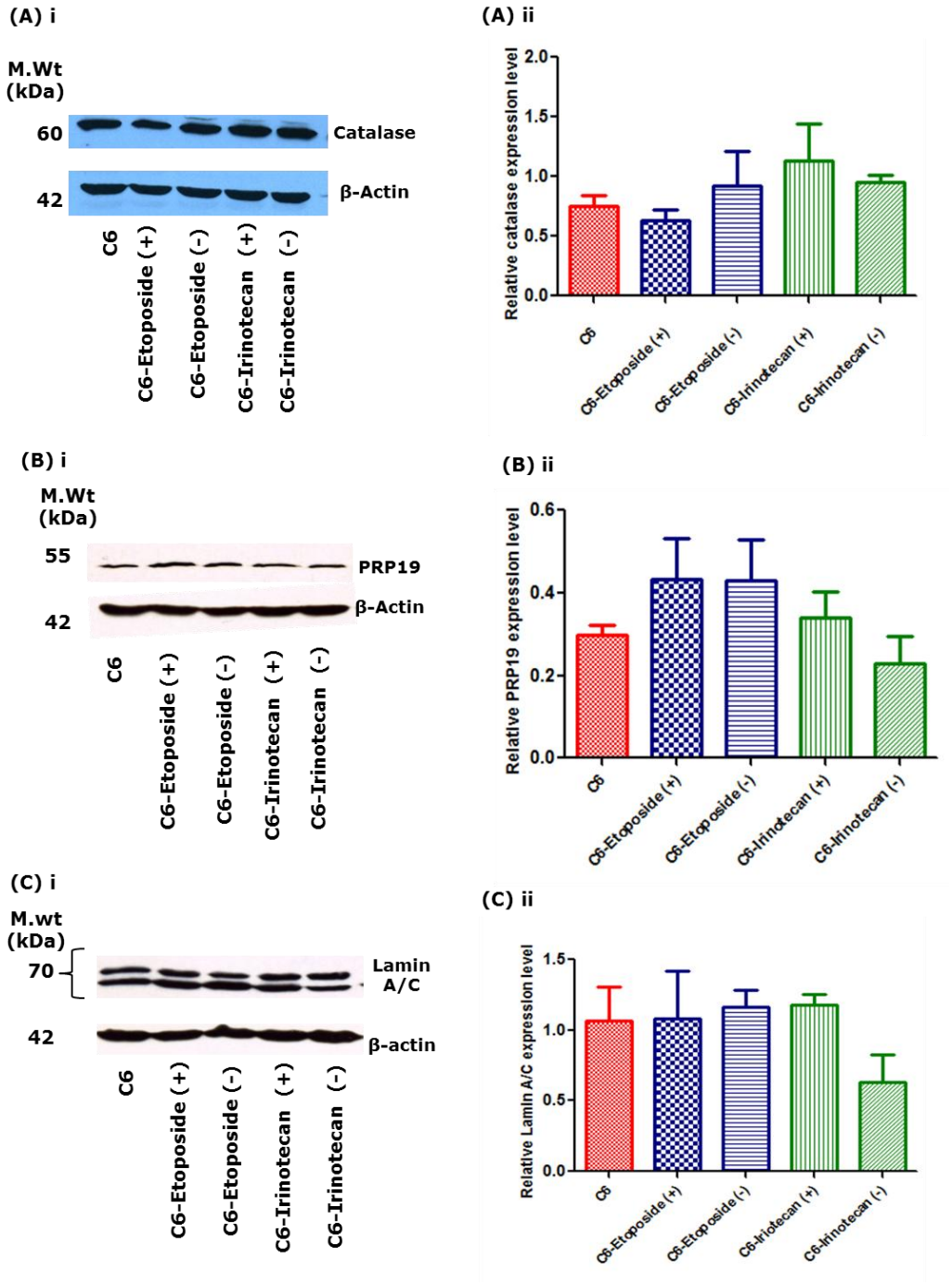

Figure 5.5 Candidate proteins failed to explain the mechanisms underlying ROS response. 30 µg total cell lysates from different passages were separated by 12% (w/v) SDS-PAGE and incubated with primary antibodies. Representative gels for each are shown: (Ai) anti-catalase (1:500), (Bi) anti-PRP19 (1:500), and (Ci) anti-lamin A (1:500) diluted in 5% non-fat milk in PBST. The relative expression of the candidate protein to the β-Actin expression signal was then calculated. One-way ANOVA analysis with Bonferroni's multiple comparison post test showed that there was no difference in the expression of each of the candidate protein between the three cell lines (P>0.05, n=3). The two bands in figure (Ci) represent the full length of lamin A (upper band) and lamin C (lower band) and the combined signal was analysed in densitometry. (+) indicates with drug treatment and (-) indicates without treatment.

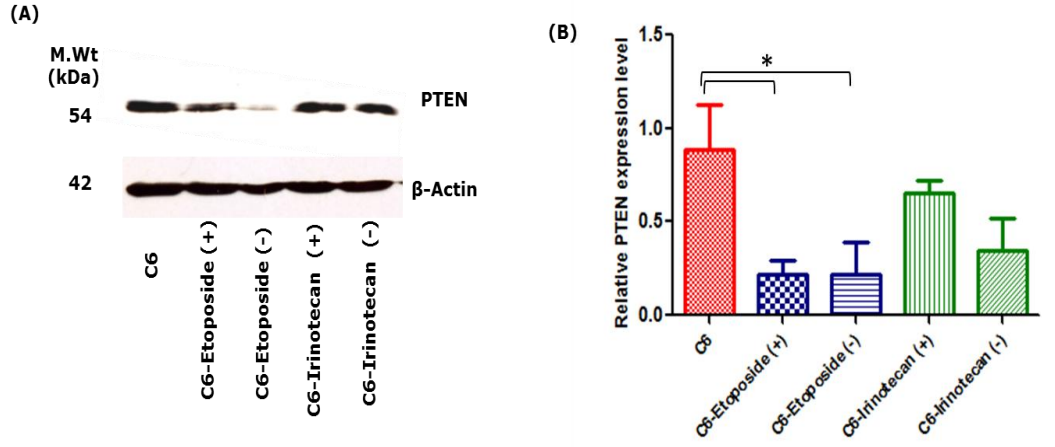

Figure 5.6 PTEN expression showed chronic expression changes in C6-etoposide. (A) A representative gel showing 30 µg total protein cell lysates separated by 12% (w/v) SDS-PAGE and incubated with anti-PTEN (1:500) in 5% non-fat milk in PBST using the correspondent β-Actin gel as control (1:5000) in 5% non-fat milk in PBST. (B) The 1-way ANOVA followed by Dunnett's comparison test for PTEN expression which showed a significant reduction (chronic effect) in the expression of PTEN in the C6-etoposide cell line (*P<0.05, n=3), in the presence (+) and the absence (-) of etoposide compared to the other cell lines.

5.2.5 Validation of candidate genes by qPCR

Gene transcript analysis in chapter III had identified two genes which showed different expression in drug selected cell lines. The validation of these candidate genes (*PTEN* and *EGR1*) was performed with qRT-PCR. This validation went through the same steps as described fully in chapter IV. First, the full transcript of the *EGR1* and *PTEN* which were used as a reference to design the primers on primer BLAST for qRT-PCR is illustrated in (appendix 1). The second step was the optimisation of the annealing temperatures (Ta) for each primer pair (appendix 2). For both primer pairs the ideal annealing temperatures which produce good PCR products were 60°C and above, as these annealing temperatures produced a high yield of product with little or no non-specific amplification. In the third step (the determination of the primer efficiency), the standard curve and the amplification curve were produced and the generation of all products was visualized on a melt curve

following the amplification reaction (appendices 3 and 4). Table 5.2 represents the slope for the standard curves and the efficiency factor (Ef) for each primer pairs for the oxidative stress candidate genes.

Table 5.2 Primer efficiency for candidate genes involved in oxidative stress and apoptosis

Gene Name	Slope of standard curve	Primer efficiency %
PTEN	-3.491	93.2 %
EGR1	-3.213	104.8 %

The primer efficiency values and the slope values were obtained from the standard curve.

5.2.6 Role of candidate genes in oxidative stress resistance

After optimising the primer efficiency on parental C6 cell line for PTEN and EGR1, qRT-PCR was performed on the three cell lines to confirm any altered expressions of these two candidate genes in the three glioma cell lines. The qRT-PCR reaction was performed according to the procedure described in section 2.8.5 and also described in details in chapter IV. Figure 5.7 revealed that the expression of both *PTEN* and *EGR1* is significantly decreased in C6-etoposide cell line compared to parental C6 and C6-irinotecan (1-way ANOVA P value<0.001 and P<0.0001 for *PTEN* and *EGR1*, respectively). The relative expression data on qPCR for *PTEN* agreed with the results from the gene expression and IPA analyses indicating that *PTEN* expression is 2 fold lower in C6-etoposide compared to C6. However, the IPA analysis suggested that *PTEN* expression is 3 fold higher in C6-irinotecan compared to C6-etoposide, which did not match with the qPCR validation whilst *PTEN* expression remains the same. Similarly, for *EGR1*, IPA analysis suggested that this gene is down-regulated (3.5 and 2 fold) in C6-etoposide and C6-irinotecan compared to C6, respectively. This was the case for C6-

etoposide (0.33 relative to C6) but not C6-irinotecan (1.2 times overexpressed).

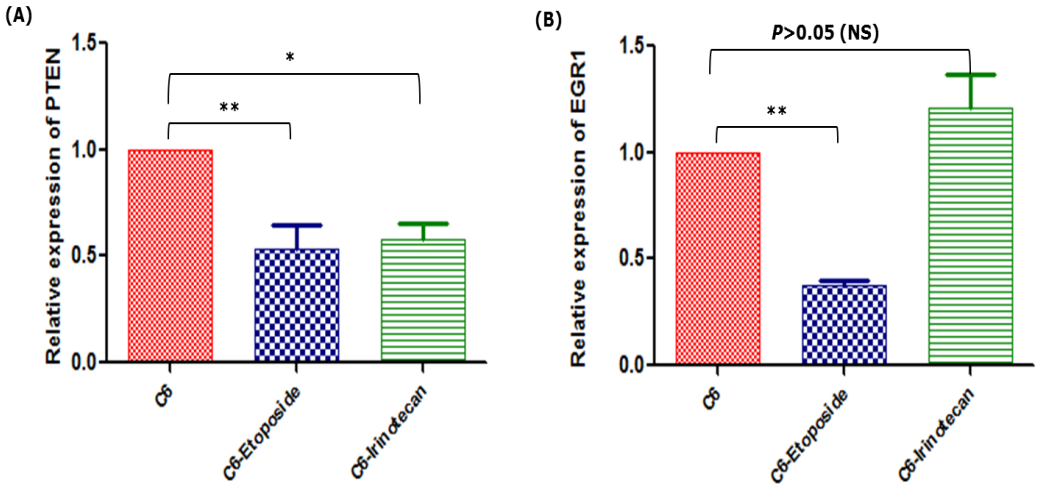

Figure 5.7 *PTEN* and *EGR1* expression is down-regulated in C6-etoposide cell line. qPCR reaction was performed on the three glioma cell lines according to the protocol described in section 2.8.5. For each gene, the relative expression was determined with the Pfaffl equation. The 1-way ANOVA followed by Bonferroni's multiple comparison test showed that there was a significant reduction in the expression of *PTEN* in both drug derived cell lines compared to C6 (A) and there was also a significant reduction in the expression of *EGR1* in C6-etoposide cell line compared to other cell lines (B), where *$P \leq 0.05$, **$P \leq 0.001$, and n=3.

5.2.7 Determination of drug-induced apoptosis

Western blotting and qRT-PCR validations identified a reduction in the expression of PTEN and EGR1 in C6-etoposide cell line which may be related to the increased resistance to ROS production. Another way that this resistance maybe manifest is through a reduction in apoptosis. Therefore, validation of caspase-3 activation (the most predominant executioner caspase in apoptosis) was performed with western blotting. Caspases or *c*ysteine-aspartic proteases or cysteine-dependent aspartate-directed proteases are cysteine proteases family which play an important role in apoptosis, necrosis, and inflammation. So far, there are 12 caspase proteins discovered. Caspase-3, also known as CPP32, SCA-1, and CPP32B, is activated by other caspases such as caspase 8, 9, and 10. When it is activated, it well then activates other

caspases such as caspase 6 and 7. Caspase-3 exists as inactive proenzyme (35kDa) and when it is undergo proteolytic hydrolysis it is divided into two active subunits with 19 and 17 kDa. These active forms are responsible for the apoptotic activity of caspase 3 (Wyllie, 1997). In this study, the expression of caspase 3 (both the non-active and active forms) in the three cell lines was determined with western blotting. The initial analysis of the data suggested that there is a consistent expression of the active forms of caspase-3 in C6-irinotecan (+), which is apoptosis sensitive, but not in C6-etoposide (+), which is apoptosis resistant (data not shown). However, more experiments are required to validate the data and compare it with parental C6 (treated with both drugs).

5.3 Summary

In this chapter, the response of the three glioma cell lines to oxidative stress was studied and candidate proteins and genes were validated using western blotting and qRT-PCR. The conclusions of this chapter are as follows:

- We found that parental C6 cell line is more sensitive to oxidative damage whereas, C6-etoposide cell line is more resistant to oxidative stress since it can tolerate higher concentrations of ROS inducer TBHP compared to other cell lines (figures 5.3 and 5.4).
- Although the proteomics approach identified 3 candidate proteins which showed expression changes between the three cell lines (table 3.1), western blotting failed to correlate any of these candidates to oxidative stress resistance since altered levels of candidate proteins were not detected indicating that they are not associated with drug treatment (figure 5.5). However, the validation of PTEN with western blotting found that this protein expression is low in C6-etoposide (chronic effect) (figure 5.6).

- qRT-PCR validation for candidate genes found that expression of *PTEN* and *EGR1* is decreased in C6-etoposide cell line, which could explain the ability of this cell line to resist the oxidative stress (figure 5.7).
- Nuclear PTEN is important to protect the cells from oxidative stress independently of its phosphatase activity. However, oxidative stress prevents PTEN from this protective role by inhibiting the localisation of PTEN from the cytoplasm to the nucleus (Chang et al., 2008). As PTEN is a major gene in the high grade glioma and it is found to be deleted in 5-40% of HGG cases, and since it plays a role in apoptosis, in the next chapter, the major signalling pathways in which PTEN can introduce its function will be analysed. Three major signalling pathways were identified with IPA analysis (Akt/PI3K, NFkB, and TGFβ). However, the major classical pathway of PTEN is the Akt/PI3K pathway (which is also altered in the majority of HGGs (The Cancer Genome Atlas Research Network, 2008)), therefore, preliminary experiments with PI3K inhibitors were performed to determine if these inhibitors will alter the resistance response of C6-etoposide and make it more sensitive.

CHAPTER VI

GENERAL DISCUSSION

CHAPTER VI: GENERAL DISCUSSION

6.1 Overview

Brain and CNS tumours are among the 20 most common tumours in adults in the UK (Office for National Statistics, 2010). Brain tumours are typically comprised of morphologically diverse cells that express a variety of neural lineage markers. Glioblastoma (WHO grade IV) is the most frequent primary brain tumour (accounting for 12-15% of intracranial tumours and 60-75% of astrocytic tumours) (Kleihues et al., 2007a). Although major advances have been made to understand the molecular and genetic alterations of malignant gliomas, the median survival rate for patients with glioma is only 12-14.6 months (Cancer statistics registrations, 2008). The presence of a subpopulation of transformed CSCs which are resistant to chemotherapy and radiotherapy is believed to be one of the reasons behind the initial tumour formation, the recurrence of the tumour following surgical resection, and the development of multidrug resistance (MDR) (Mohri et al., 2000, Tews et al., 2000, Bredel, 2001, Beier et al., 2011). These difficulties in treatment of glioma (i.e., it is resistant to chemotherapy and radiotherapy) reinforce the need to better understand glioma at a cellular and molecular level. In glioma and other tumours, cell line models can offer some advantages to complement analysis of patient's clinical samples. These advantages include: (1) the avoidance of the presence of non-tumour cells in the cell line model compared to surgical samples (no further purification is required), (2) cell line models can be genetically modified, (3) they resemble and share the same characteristics as the original tumour, and (4) experiments can be repeated for several times (more reproducible results) (Barth and Kaur, 2009, Yamada et al., 2009).

In the current study, the rat C6 glioma cell line was used as a cell line model to investigate drug resistance mechanisms. Alongside the parental C6 cell line, two drug-derived C6 cell lines that had been established through

chronic exposure to two major drugs used clinically to treat glioma [etoposide (DNA topoisomerase II inhibitor) and irinotecan (DNA topoisomerase I inhibitor)] were also studied. In order to decipher drug-resistance mechanisms, proteomic approaches (2D gels followed by identification with MS) and genomic approaches (gene expression microarray followed by signalling pathway analysis identification with IPA) were applied to the three glioma cell lines. A comprehensive search on candidate proteins and genes was performed to determine their putative roles in different aspects of cancer biology and based on this to design downstream experiments which would help in identifying drug resistance mechanisms in glioma.

6.2 Identification of candidate proteins and genes

In this study, 9 candidate proteins were successfully identified with proteomic analysis. These proteins met 2 major criteria in pair-wise comparison of the cell lines using unpaired t test: (1) $P \leq 0.05$ and (2) expression fold change (FC) ≥1.5. They were found to be involved in migration and metastasis of cancer (nucleotide diphosphate kinase B) (Malmquist et al., 2001), in tumour aggressiveness and progression (ribosomal protein large P0, elongation factor 1-γ, and protein disulphide-isomerase A3 precursor) (Mao-De and Jing, 2007, Mimori et al., 1996, Odreman et al., 2005), DNA damage, oxidative stress and apoptosis (PRP19, catalase, and Lamin A) (Lu and Legerski, 2007, Toyokuni et al., 1995, Gonzalez-Suarez et al., 2009), stem cell differentiation (Progerin) (Scaffidi and Misteli, 2008), and mRNA splicing (Serine-Arginine splicing factor) (Hertel and Maniatis, 1999). Commercial antibodies were only available for 3 of the 9 candidates allowing validation by western blotting.

Several other studies have also used proteomics as a technique to draw a comprehensive picture about the protein expression pattern in glioma and to determine the relevance of using GBM cell lines as a model to study HGG instead of surgical tumour specimens. These studies reflect that

proteomic techniques permit a broader research on proteins, in which many diverse cell types, under different environmental conditions and stresses, can be compared (Vogel et al., 2005, Puchades et al., 2007, Banerjee et al., 2012). Vogel *et al.,* compared the protein expression pattern in the absence of any drug treatment in four glioma cell lines U87, U118, U251, and A172 with eight primary GBMs micro-dissections. The comparison was made in two steps: (1) investigate the proteins that were uniquely identified in the 2D gels in the GBM tumour samples or in the GBM cell lines as a whole, and (2) compare the two groups with each other and identify the differences in the proteins expression. The analysis of the primary GBM tumour samples and the GBM cell lines revealed a reproducible similar proteomic patterns for each group. However, the analysis of the 2D gels of the cell lines revealed that, from ~500 protein spots, 160 proteins are gained and 60 proteins are lost during cell culture. Moreover, the differential protein expression between cell lines and GBM tumours showed that seven proteins found in the cell lines were significantly increased when compared with the GBM tumours ($P<0.05$), whereas 10 proteins were significantly decreased in cell lines compared with the GBM tumours. Proteins identified included transcription factors, tumour suppressor genes, cytoskeletal proteins, and cellular metabolic proteins (Vogel et al., 2005), although no proteins were identified common to the current study. In conclusion, findings from this study showed significant differences between the GBM cell lines and the surgical tumour specimens which reflect that *in vitro* culture can exert selection pressures that drive the GBM cell lines toward cellular homogeneity, with a consistent pattern of either over-expression or down-expression of proteins. This significant difference was probably due to several factors such as the availability of growth factors and metabolites in the culture, the cells are normally grown under a constant source of oxygen and optimised pH range whereas, the tumour cells *in vivo* have to fight for the nutrition and to establish a new blood vessels (angiogenesis) as a source for oxygen to grow.

Transfecting glioma cell lines with wild-type tumour protein p53 triggers the apoptosis if a cell line harbours mutant p53, whereas if the cell line harbours wild-type p53 this will reduce invasion and mobility (Lang et al., 2002). In a study by Puchades *et al*., proteomic analysis was used to identify proteins that could trigger apoptosis and have potential future therapeutic value. The U87 MG cell line which carries the wild-type p53 genotype was treated with adenovirus Ad-p53 (adenoviral vector construct, which carries the tumour suppressor gene *TP53*) or with 0.1 μM cytotoxic chemotherapy SN-38 (irinotecan active metabolite) either alone, or in combination. Proteins identified to be altered by treatment were galectin-1, caspase 14, galactokinase 1, and GRP-78. Among these proteins, galectin-1 (a cell-cell interaction and cell-matrix interaction protein) was found to be dramatically modulated when the cells were treated with wild type p53 and SN-38. The expression of this protein increased when cells were treated with SN-38 alone whereas, the combination treatment of wild type-p53 transfection prior to SN-38 resulted in a notable down-regulation of galectin-1. These results demonstrated the utility of using proteomic approaches to interrogate and identify potential useful targets for response to GBM therapy under different conditions (Puchades et al., 2007).

To complement the proteomic analysis we undertook a genomic approach and identified 8 genes in this study with the following criteria: (1) *P* value for expression level difference of ≤0.05, and (2) expression FC between two or more cell lines is ≥ 2 with unpaired t test or 1-way ANOVA, respectively. These genes are involved in migration/metastasis (*BMP7*, *ATP1B1*, *COL1A2*, and *COL3A1*) (Bujis et al., 2007, Alarmo et al., 2009, Yancy et al., 2007, Qi et al., 2009, Liu et al., 2010), DNA damage /apoptosis (*MT1F*, *PTEN*, and *EGR1*) (Korshunov et al., 1999, Hu et al., 2005, Chang et al., 2008, Baron et al., 2006), and translational control (*ABCF2*) (Ogawa et al., 2006). Unlike the proteins identified by proteomic approach, most of the gene candidates were included in this study (*PTEN*, *EGR1*, *ATP1B1*, *COL1A2*, and

COL3A1). *MT1F* was excluded due to difficulties with optimising qRT-PCR primer design. Similarly, *BMP7* and *ABCF2* primers were not conducive to reliable qPCR and were excluded from the study.

In contrast to the proteomic studies in glioma, many studies have also been conducted to reveal the signature gene expression patterns in GBM (Markert et al., 2001, The Cancer Genome Atlas Research Network, 2008, Hodgson et al., 2009, Liu et al., 2010, Paugh et al., 2010). These studies demonstrate that the gene expression approach is a useful tool for identifying key molecular characteristics of patient tumours, and highlighting putative therapeutic opportunities for GBM treatment. For example, Hodgson *et al.,* compared the DNA copy number and mRNA expression between 21 independent GBM tumour cell lines not exposed to any drug treatment and GBM clinical specimens derived from the Cancer Genome Atlas (TCGA) (The Cancer Genome Atlas Research Network, 2008). They found that the DNA copy number was the same in both groups characterised mainly by the gain of chromosome 7 and loss of chromosome 10. Regarding the mRNA expression level, the genomic expression pattern was also the same in the two groups. The major genes which are over-expressed include *EGFR* (which is a major over-expressed gene in GBM), *MDM2*, *CDK6*, and *MYCN*, and novel genes include *NUP107*, *SLC35E3*, *DDX1, MMP1*, and *MMP13* (MMPs are important modulators for the migration and invasion as described in chapter 1) (Hodgson et al., 2009).

Although tumour cell lines are an indispensable tool for cancer research, heterogeneity may be present between several cell lines of the same pathological origin. The major heterogeneity can present in gene expression, gene mutation, and cellular response to various treatments. For instance, the expression of 588 cellular genes in three GBM cell lines (U251, D54, and LN-Z308) was investigated using cDNA array technology. Comparison of the expression profiles revealed that among the 588 genes, 197 genes were expressed in the three cell lines and 56 genes were not

expressed in any of them; total of 222 genes were expressed in only two of the three cell lines, and 113 genes were expressed in only one of the three cell lines. These results provide molecular evidence that cell lines of the same pathological origin can be highly heterogeneous (Rhee et al., 1999). Another study determined the genomic status in five glioma cell lines (U87, U251, T98G, U373, and SNB-19) and 83 primary human gliomas. They found that although genomic alterations known to occur in primary tumours were identified in the cell lines, several novel recurrent aberrations were also observed in the glioma cell lines that are not frequently represented in the primary tumours (Li et al., 2008). Therefore, results from these studies reinforce the notion that caution must be exercised when correlative studies using cell lines are conducted and that further validation need to be done when performing gene expression studies.

Therefore, both proteomic and genomic approaches have the power to identify expression changes that could be correlated with aspects of tumour cell phenotype. To my knowledge, this is the first study which has attempted to provide expression change information from BOTH genomics and proteomics, and to integrate that data in pathway analysis. In so doing, this project was able to consider two aspects of tumour cell biology (namely the ability to migrate, and the ability to resist oxidative damage) in the context of altered expression profiles.

6.3 Cell migration in glioma cell lines

Cell migration is implicated in the pathophysiology of cancer as it is considered as the first step in the metastasis. Metastatic tumours are consisting of cells much more resistant, aggressive and efficient than those present in the primary tumour. For the cell to be able to migrate several molecular and cellular characteristics have to be modulated, therefore, the study of this characteristic in cancer is difficult and complex (Bozzuto et al., 2010).

Although the metastasis in GBM is rare, this tumour shows a high degree of migration and invasion (Beadle et al., 2008). Analysis of the data from scratch and transwell migration assays in chapter IV revealed that the three glioma cell lines showed a considerable degree of variation in migration in response to either the absence or the presence of chemoattractant (figures 4.3, 4.5, and 4.7). The major finding from chapter IV is that chronic exposure of the C6 cell line to irinotecan (DNA topoisomerase I inhibitor) results in a significant reduction in the migration rate of the cells compared to parental C6 and C6-etoposide cell lines. Further validation of the migration gene candidates by qRT-PCR revealed that these genes (*ATP1B1, COL1A2*, and *COL3A1*) are significantly down regulated in C6-irinotecan cell line compared to C6 and C6-etoposide (figure 4.14). These variations in genes expression may explain the altered migratory response of C6-irinotecan cell line.

Collagen is the most abundant protein in mammals (about 25-35% of the whole protein content in the body) (Revest, 2009). It is one of the major components of the ECM alongside other important protein families such as the glycosaminoglycans, proteoglycans, laminin, fibronectin, and elastin (Rangaraj et al., 2011). Up to now, 28 types of collagen have been identified but the five most common types are: collagen I which is the most abundant collagen in the human body (over 90%- it found mainly in skin, tendon, vascular ligature, organs, and bone) (Di Lullo et al., 2002), collagen II (present in the cartilage), collagen III (found in the reticular fibers in soft tissues such as liver and bone marrow and it is found commonly alongside type I), collagen IV (major component of the cell basement membrane), and collagen V (in hair and placenta) (Enoch and Leaper, 2008, Rangaraj et al., 2011).

The collagens are produced mainly by fibroblasts and they play an important role in endothelial cell migration. This type of migration is important in many physiological and pathological conditions, including wound healing, angiogenesis and tumour growth (Dale et al., 1997, Lamalice et al., 2007).

There are two main types of collagens involved in the wound healing, I and III (Dale et al., 1997). In response to injury, fibroblasts migrate into the wound domain from the surrounding unwounded areas and from the underlying subcutaneous tissue. Subsequently, the motile fibroblasts synthesise chains of amino acids called pro-collagens, these pro-collagens are activated by several growth factors, including in particular transforming growth factor beta (TGFβ) into the active collagen forms (Appling et al., 1989).

Several studies have examined whether there is a correlation between the expression of collagens and cancer migration, invasion, and metastasis (Ahmed et al., 2005, Bartling et al., 2009). Indeed, collagens are often express in areas where tissue invasion is observed, commonly in the form of linearized fibre-like structures, along which cancer cells have been observed to rapidly migrate (Provenzano et al., 2006). Additionally, live imaging studies have shown that cancer cells migrate rapidly on collagen fibers in areas enriched in collagen (Condeelis and Segall, 2003, Provenzano et al., 2006). In normal brain tissue the level of collagens is relatively low (Paulus et al., 1991). In contrast, in glioma and other brain tumours, the level of collagen expression is higher presumably because the cancer cells can establish their own collagens (Huijbers et al., 2010). These collagens are important for the migration and translocation of the tumour cells between different brain tissues. For instance, Huijbers *et al.,* found that fibrillar collagens are extensively deposited in GBM and that the collagen internalization receptor Endo180 is highly expressed in GBM compared to anaplastic astrocytoma and this receptor serves to mediate the invasion of tumour cells through collagen-containing matrices (Huijbers et al., 2010).

The current study, to the best of my knowledge, is the first study to examine changes in collagen expressions and migration in the same glioma cell lines exposed to chronic drug treatment. However, studies of collagens and migration do exist for example; a comparison study between the less migratory MCF-7 cells (invasive breast carcinoma cell line) and the highly migratory U251 cells (glioma cell line) was performed using Chromatin Immunoprecipitation (ChIP)-on-Chip microarray. This analysis was focusing on the identification of genes which are important in migration, proteolysis, and tumorigenesis. The gene expression analysis indicated that U251 express high levels of several collagens (*COL11A1*, *COL7A1*, *COL8A1*, *COL5A1v* and *COL1A1*) and these collagens were epigenetically silenced and down-regulated in MCF-7 cell line. Moreover, the transcriptional activity of the collagen genes in U251 cells also correlated with the significant expression levels of *TGFβ1*, which encodes an RGD-containing adhesion protein which binds to type I, II, and IV collagens and that plays an important role in cell-collagen interactions (Chernov et al., 2010). The finding from this study is similar to our observations i.e., the lowest expression of collagens was observed in less migratory cell line (C6-irinotecan). However, more studies are required to explore the mechanism by which irinotecan alters the expression of collagens in our cell lines.

The effects of irinotecan on apoptosis and proliferation are well described. For instance, Al-Dasooqi *et al.,* found that irinotecan inhibits proliferation and increases apoptosis through the reduction of several components of ECM such as collagen IV, fibronectin, and laminin 1 and 2. This reduction affects the kinetics of the epithelial cells in both the colon and the jejunum and results in the loss of mucosal layer integrity (Al-Dasooqi et al., 2011). In contrast, the effect of irinotecan effect on migration, via the ECM, is less well studied. It is believed that irinotecan can inhibit migration through different mechanisms such as the reduction of growth factors and angiogenic gene expression rather than through the ECM components (Hurwitz et al.,

2003). In a recent microarray study to characterise the *in vivo* tumour response of colorectal carcinoma xenografts to irinotecan, data revealed that irinotecan inhibits the migration of cancer cells and angiogenesis by inhibiting the expression of 18 genes, none of them belongs to the collagen family (Guérin et al., 2012). These genes belong to the HIF1α- or hypoxia induced target genes (*VEGFA*, *SLC2A1*, *SLC2A3*, *SLC6A8*, *PFKFB3*, *PFKP*, *ALDOC*, *PGK1*, *ENO2*, *ADM*, *ANKRD37*, *BHLHB2*, *BNIP3L*, *DDIT4*, *ERO1L*, *NDRG1*, *P4HA1* and *PLOD2*). However, the underlying mechanisms by which irinotecan can inhibit the expression of HIF1α and other genes are not well-defined. A role for HIF1α in migration has previously been described, Higgins *et al.,* found that HIF1α enhanced EMT *in vitro* and induced epithelial cell migration in mouse kidney through several mechanisms including up-regulation of lysyl oxidase genes, reduction in collagen deposition, and a reduction in the number of fibroblast-specific protein-1-expressing interstitial cells (Higgins et al., 2007). There was no overlap between genes but they showed evidence of migration effects.

6.4 Response to oxidative stress in glioma cell lines

Brain tumorigenesis is highly associated with oxidative stress (Papacocea et al., 2011). Among several targets for ROS, DNA is the most important target in the cell. It has been shown that ROS can contribute to brain tumour development at two levels. At one level, ROS result in DNA strand breakage, appearance of point mutations and aberrant DNA cross-linkage. At level two whilst additionally, ROS may initiate signal transduction pathways and activate several transcription factors such as NF-kB, Nrf2 or HIF-1 which known to be involved in brain tumour development (Rajaraman et al., 2008).

In the current study, the response of the three glioma cell lines to oxidative stress was assessed. Analysis of the three glioma cell lines revealed that chronic exposure of cells to etoposide (DNA topoisomerase II inhibitor)

increases the resistance of the cells to oxidative stress (figure 5.3). Five candidates (lamin A, PRP19, catalase, *PTEN*, and *EGR1*) were validated with western blotting and qRT-PCR to mediate this effect. Unfortunately, the validation of 3 of the candidate proteins showed no significant difference in their expression between the three cell lines (either in the absence or the presence of drug treatment) (figure 5.5). On the other hand, the validation of the tumour suppressor protein PTEN with western blotting showed a significant reduction in its expression in the chronically exposed C6-etoposide cell line (figure 5.6). Furthermore, qRT-PCR analysis showed that *PTEN* is down regulated in both drug derived cell lines compared to the control cell line whereas *EGR1* showed low expression in the C6-etoposide compared to C6 and higher expression in C6-irinotecan. The expression of PTEN at both protein and gene levels lead to a major question which is "can the reduction in PTEN expression explain the resistant to oxidative stress in C6-etoposide cell line".

Among all the candidates, only PTEN expression showed a significant reduction in the C6-etoposide cell line compared to the other two cell lines. This tumour suppressor gene *PTEN* is among the most commonly inactivated or mutated genes in human cancer such as endometrial carcinoma, melanomas, and prostate cancer (Thorarinsdottir et al., 2008, Chalhoub and Baker, 2009, Liu et al., 2009b). In addition to our data it is worth noting that (1) this gene was found to be mutated in GBM (predominantly in adults) (Rasheed et al., 1997, The Cancer Genome Atlas Research Network, 2008), and (2) loss of PTEN would result in the activation of the PI3K pathway which is related to the cellular proliferation, differentiation, survival and cell motility (Kallergi et al., 2007, Conte et al., 2011) and all these processes contribute to the progression of cancer. As the focus of this discussion is now centred on PTEN, and the need to explore the role of PTEN expression level changes in our glioma cell lines through PI3K pathway, this requires an understanding of this pathway.

6.5 PI3K pathway

Phosphoinositide 3-kinases (PI3Ks) are important lipid and protein kinases which act as modulators for the growth, proliferation, apoptosis, and metabolism of cells. They can be activated by genetic mutations as seen in several cancer types such as colon, breast, brain, liver, stomach, and lung or inactivated as observed in some neuropathies and myopathies (Vanhaesebroeck et al., 2012). The PI3K family contains 14 members, which are classified as types I to IV. Types I, II, and III are lipid kinases whereas type IV is a protein kinase. The most studied classes of the PI3K family are class I and class IV, the latter of which is often referred to as the mammalian target of rapamycin (mTOR) pathway (Liu et al., 2009b).

PI3K pathway can be seen as one element in a balance between two major signalling cascades (figure 6.1). The first signalling cascade involves the generation of second messengers known as diacylglycerol (DAG) and inositol-1, 4, 5-trisphosphate (IP_3) through the hydrolysis of phosphatidylinositol- 4, 5-bisphosphate (PIP_2) with phospholipase C (PLC). These second messengers produce signals inside the cells through the activation of protein kinase C (PKC) and the mobilisation of calcium (figure 6.1) (Vanhaesebroeck et al., 2012). On the other hand, the second signalling cascade involves the phosphorylation of phosphatidylinositol-4, 5-biphosphate (PIP2) to phosphatidylinositol-3, 4, 5- trisphosphate (PIP3) under the effect of the catalytic subunit (p110) of the PI3K. The resulting PIP3 assists the recruitment of phospholipid binding domain-containing proteins to the plasma membrane. The serine-threonine specific protein kinase (Akt) is then activated by phosphoinositide-dependent kinase 1 (PDK1) before moving to the cytoplasm and to the nucleus where it phosphorylates a multitude of downstream targets which affect important cellular processes such as proliferation and growth (Gharbi et al., 2007). The activity of PI3K and Akt is opposed by the action of PTEN, which removes the 3-phosphate of PIP3,

regenerating PIP2 and attenuating signalling downstream of activated PI3K (apoptosis activation) (figure 6.1) (Angelo et al., 2007).

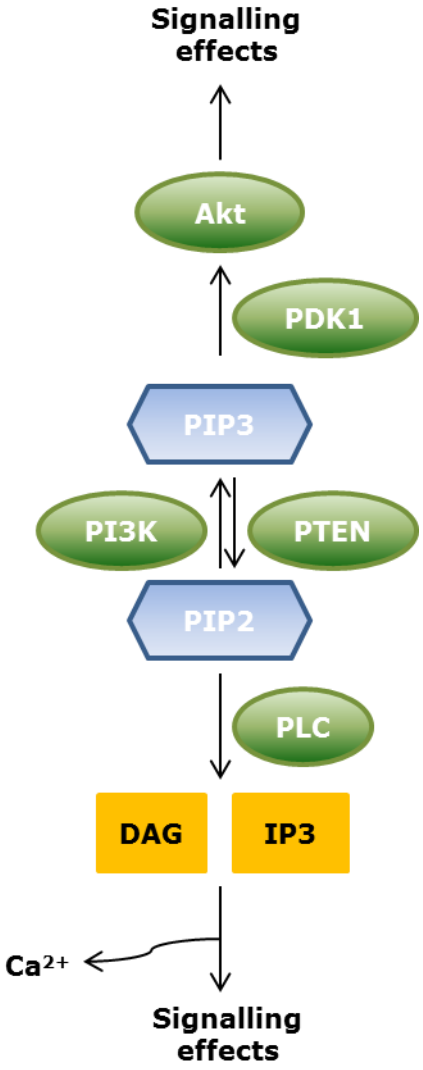

Figure 6.1 PTEN and PI3K one master regulators of the PI3K pathway. PI3Ks are heterodimeric lipid kinases composed of a p110 catalytic subunit and a p85 regulatory subunit. When PI3K is recruited to the cell membrane, the p110 catalytic subunit phosphorylates phosphatidylinositol-4, 5-bisphosphate (PIP2) to produce phosphatidylinositol-3, 4, 5- trisphosphate (PIP3). PIP3 then recruits phosphoinositide-dependent kinase 1 (PDK1) to the plasma membrane which in turn activates the serine/threonine kinase (Akt) resulting in the activation of several cellular and signalling pathways. A concomitant decrease in Akt activity then occurs through the lipid phosphatase activity of cytoplasmic PTEN which dephosphorylates PIP3 thereby decreases PIP3 levels and increases levels of PIP2. In another cascade, PIP2 cellular concentration can be decreased by the effect of phospholipase C (PLC) which results in the production of two important secondary messengers [diacylglycerol (DAG) and inositol-1, 4, 5-trisphosphate (IP_3)] which are involved in several signalling processes. Where =enzymes, =signalling molecules, and =lipids.

This pathway is mutated in several human cancers. However, I will focus on the role of the PI3K pathway in the tumorigenesis of sporadic breast cancer as an example to shed light on the importance of this pathway. Several studies have found that PI3K plays a central role in sporadic breast cancer biology and that this pathway is aberrantly activated in around one quarter of the cases of sporadic breast cancer patients (8-40%) (Bachman et al., 2004, Li et al., 2006). The majority of mutations related to PI3K pathway involve the *PTEN* gene and the *PIK3CA* gene, which is the gene responsible for the formation of the catalytic subunit p110α (Brugge et al., 2007). Regarding the *PTEN* mutations, several studies investigated the role of *PTEN* mutations in sporadic breast carcinogenesis. In a study performed on 50 early-stage, sporadic breast cancer patients, the *PTEN* mutation spectrum and the protein expression in sporadic breast cancers, adjacent hyperplastic lesions, benign breast lesions and normal breast tissues was determined by sequencing the 9 exons of the *PTEN* gene. They found that *PTEN* mutations were detected in 11 of 50 (22%) breast cancers and 4 of 50 (8%) adjacent region of ductal hyperplasia, whereas no *PTEN* mutation was detected in all adjacent normal breast tissue or in the 50 cases of breast benign lesions. These mutations were found mostly in exons 3, 4, 5 and 7 with the hot-spots missense mutation present in exon 5. This indicates that the incidence of *PTEN* mutations is high in patients with sporadic breast cancer and plays a role in the progression of the tumour as they exist at an early stage (Yang et al., 2010). In another study, *PTEN* mutation was compared between the primary and the metastatic breast tumours. *PTEN* was lost in 14 (30%) primary tumours and 13 (25%) metastatic tumours. Additionally, there were five cases of *PTEN* loss and eight cases of *PTEN* gain from primary tumours to metastases (26% discordance) which may have been influenced by the patient selection and response to the PI3K-targeted therapies (Gonzalez-Angulo et al., 2011). However, results from this study indicated that PI3K

pathway disruption is not uniform, i.e. PTEN expression can be up or down in this study and be associated with metastasis.

Regarding the *PIK3CA* gene, the most common single nucleotide mutations are E542K, E545K in (exon 9) and H1047R in (exon 20) (Li et al., 2006). These mutations were found to enhance the enzymatic function, therefore, activate the downstream signalling (Akt) which results in the promotion of oncogenic transformation (Li et al., 2006, Gymnopoulos et al., 2007). However, unlike *PTEN* mutations role, the prognostic significance of *PIK3CA* mutations remains unclear in breast cancer as different studies showed inconsistent results, from no survival effect at all (Saal et al., 2005), to decreased overall survival rate (OS) (Li et al., 2006), to improved progression- free survival rate (PFS) (Kalinsky et al., 2009).

PTEN/PIK3CA mutations in breast cancer appear to affect the response of the patients to treatment. In a study done by Berns *et al.*, the effect of *PTEN/PIK3CA* mutations in patients who had been treated with trastuzumab, a widely used monoclonal antibody in breast cancer treatment that interferes with the HER2 receptor, was investigated. They found that tumours with the *PTEN* deletion and *PIK3CA* mutations responded less efficiently to trastuzumab, which suggests that trastuzumab act as a marker for drug resistance in HER2-breast cancer (Berns et al., 2007). In another study on advanced HER2-positive breast cancer patients, the primary or the acquired resistance to lapatinib, a small tyrosine kinase receptor for HER2, was investigated with a genome short hairpin RNA screen. They found that deletion of *PTEN* or *PIK3CA* resulted in lapatinib resistance whereas in the control wells, cells were sensitive to the effect of lapatinib. Interestingly, the observed resistance to lapatinib can be effectively reversed by the effect of NVP-BEZ235, a dual inhibitor for PI3K/mTOR pathways (Eichhorn et al., 2008).

From studies such as those highlighted here, it has been concluded that mutation in either *PTEN* or *PIK3CA* genes are not only correlated to the tumorigenesis but also affect the response of the tumour to currently used therapies. Hence many pharmacological and clinical studies are focusing on the development of inhibitors that target different components of this pathway in order to overcome this resistance. In fact, inhibitors specific to either PI3K, Akt, mTOR, or to growth factors such as vascular endothelial growth factor receptor (VEGFR) and EGFR have already been developed (table 6.1) (Liu et al., 2009b).

Table 6.1 Select list of Phase III and II PI3K pathway inhibitors*

Name	Company	Cancer under investigation	Phase
	PI3K pathway		
BKM120	Novartis	Uterine , NSCLC	II
GS-1101	Gilead Sciences	CLL, NHL	II
PX-866	Oncothyreon	Brain tumour	II
SAR245408	Sanofi	Uterine, breast	II
GDC-0941	Genetech	Metastatic breast	II
	Akt		
Perifosine	Keryx Biopharmaceuticals	MM, CRC	III
MK-2206	Merck & Co	NSCLC, haematological	II
VQD-002	VioQuest Pharmaceuticals	Solid tumours	II
	Dual PI3K–mTOR inhibitors		
BEZ235	Novartis	Uterine	II
SAR245409	Sanovi	Breast	II

*For more details about these clinical trials, please visit the clinical trials website http://www.clinicaltrials.gov/. **Abbreviations**: **NHL**: non-Hodgkin's lymphoma, **NSCLC**: Non-small cell lung cancer, **CLL**: Chronic lymphocytic leukaemia, **MM**: Multiple myeloma, **CRC**: Colorectal cancer.

As PTEN expression was altered in our C6 cell lines and it is an important regulator for PI3K pathway, it would be of interest to further map the role of this gene and this pathway onto the differences between the three cell lines. Some preliminary experiments have been undertaken to initiate this. Firstly, the *PTEN* cDNA was sequenced to determine if any of the previously reported mutations (see above; (Yang et al., 2010, Gonzalez-Angulo et al., 2011)) were present, and secondly, the pharmacological modulation of the PI3K pathway was investigated by determining the effect of two specific PI3K inhibitors (LY294002 and GDC-0941) on the survival and the migration of the cells with clonogenic and scratch assays, respectively. Regarding the PI3K pathway inhibitors, these two inhibitors were selected for this study because they have been previously shown to produce a positive inhibitory effect on the proliferation and migration in several cancers including glioma (Gharbi et al., 2007, Burrows et al., 2011, Conte et al., 2011, Kwei et al., 2012, Wallin et al., 2012). LY294002, also known as (2-(4-morpholinyl)-8-phenyl-4H-1-benzopyran-4-one), is one of the first generation of PI3K inhibitors and it was the first synthetic PI3K inhibitor to be derived from the flavonoid quercetin at Lilly research laboratory. It is capable of reversibly targeting PI3K family members such as mTOR, and other protein kinases such as casein kinase 2 and Pim-1 at concentrations in the micromolar range (Gharbi et al., 2007). LY294002 has the ability to dephosphorylate Akt at both phosphorylation sites (T308 and S473) which subsequently induces the arrest of the cell cycle at G1 and finally leads to cell apoptosis (Bondar et al., 2002). LY294002 unfortunately demonstrated a considerable toxicity in animals consequently this inhibitor is not involved widely in the clinical trials and more inhibitors have since been discovered and tested. Regardless of the *in vivo* limitations of this inhibitor, several studies performed in *in vitro* indicate that this inhibitor has a significant effect on several biological functions of the cells mainly cell growth and differentiation, migration, and apoptosis (Marone et al., 2008, Liu et al., 2009b, Tian et al., 2012).

GDC-0941 on the other hand, was developed by Genentech / Piramed / Roche and entered Phase I trial in April 2008 on non-small cell lung cancer (NSCLC) patients. It is designed to bind the ATP-binding pocket of PI3K and prevent formation of the second messenger PIP_3, thereby inactivating the downstream PI3K pathway (Folkes et al., 2008, Kwei et al., 2012). GDC-0941 inhibits the proliferation of the MCF7-neo/HER2 (breast cancer cell line) and the PC3-NCI (prostate cancer cell line) with IC_{50} of 0.72 μM and 0.28 μM, respectively by inhibiting the phosphorylation of Akt (Folkes et al., 2008) and was shown to be effective against the U87MG glioblastoma and IGROV-1 (human ovarian cancer xenograft models in athymic mice) (Raynaud et al., 2009). Currently, GDC-0941 is in phase II clinical trial in NSCLC and metastatic breast cancer (Genentech, 2011, Levy, 2011, Salphati et al., 2011).

6.5.1 Determination of the exons sequence of *PTEN* gene

PTEN gene mutation and expression was found to play an important role in the occurrence and development of gastric cancer (Guo et al., 2008) and GBM (Rasheed et al., 1997, Bax et al., 2009, Paugh et al., 2010), and in the invasion of lung cancer (Hong et al., 2000). In the current study, *PTEN* validation with western blotting and qRT-PCR showed a reduction in its expression in C6-etoposide cell line. The differences in the expression between the three cell lines might be explained by the presence of mutations which destabilize the protein and/or silencing of the gene. Therefore to explore the former, the exons of the *PTEN* gene were sequenced in this study. A PCR reaction was performed on the cDNA samples of the three cell lines using these primer pairs (forward 5'-GACAGCCATCATCAAAGAG-3' and reverse 5'-GATCAGCATTCACAAATTAC-3'). The size of the PCR product (1200 bp) was run on 1% agarose gel to verify the correct size product then subsequently confirmed by electrophoresis before it was sequenced.

The sequence of each PCR product was compared to the rat cDNA for *PTEN* gene in the database (Ensembl [ENSRNOT00000028143]) to identify if there is any difference in exon sequences between our cell lines which could explain the different function and behaviour of C6-etoposide. The comparison was made on the Multialign software (Corpet, 1988) and revealed that there was no genetic variances in the 9 exons sequence between the three cell lines (figure 6.2). Based on this result, the methylation status of the *PTEN* gene was investigated to determine if the epigenetic modification of this gene affects the protein expression. Unfortunately, we were unable to investigate methylation of the PTEN promoter region despite following protocols established in the literature (Bian et al., 2012) and this remains an avenue for future research.

6.5.2 The effect of PI3K inhibitors on cell survival

The clonogenic assay performed on the three cell lines (section 3.1.1) revealed that C6-etoposide is more resistant to etoposide in comparison to C6 (figure 3.2). We decided to investigate whether PI3K inhibitors altered this resistance to etoposide. Four independent clonogenic assay experiments were performed on C6 and C6-etoposide with either 20 μM LY294002 (Kawanabe et al., 2003, Li et al., 2011, Tian et al., 2012) or 1 μM GDC-0941 (Junttila et al., 2009) alongside the different concentrations of etoposide (5-80 μM). For the C6 cell line, both inhibitors produced the same significant inhibitory effect on the colony survival as shown by the reduction in survival at etoposide IC_{70} concentration from 29.5 μM ± 4 (no inhibitors) to 11.7 μM ± 1.5 and 10 μM with LY294002 and GDC-0941, respectively (figure 6.3a). In contrast, in C6-etoposide the analysis revealed that although both inhibitors have an effect on the survival of colonies, only LY294002 reached significance level. The IC_{70} values for etoposide reduced from 48 μM ± 15 (no inhibitors) to 15 μM ± 4.3 and 23.4 μM±3 with LY294002 and GDC-0941, respectively (figure 6.3b).

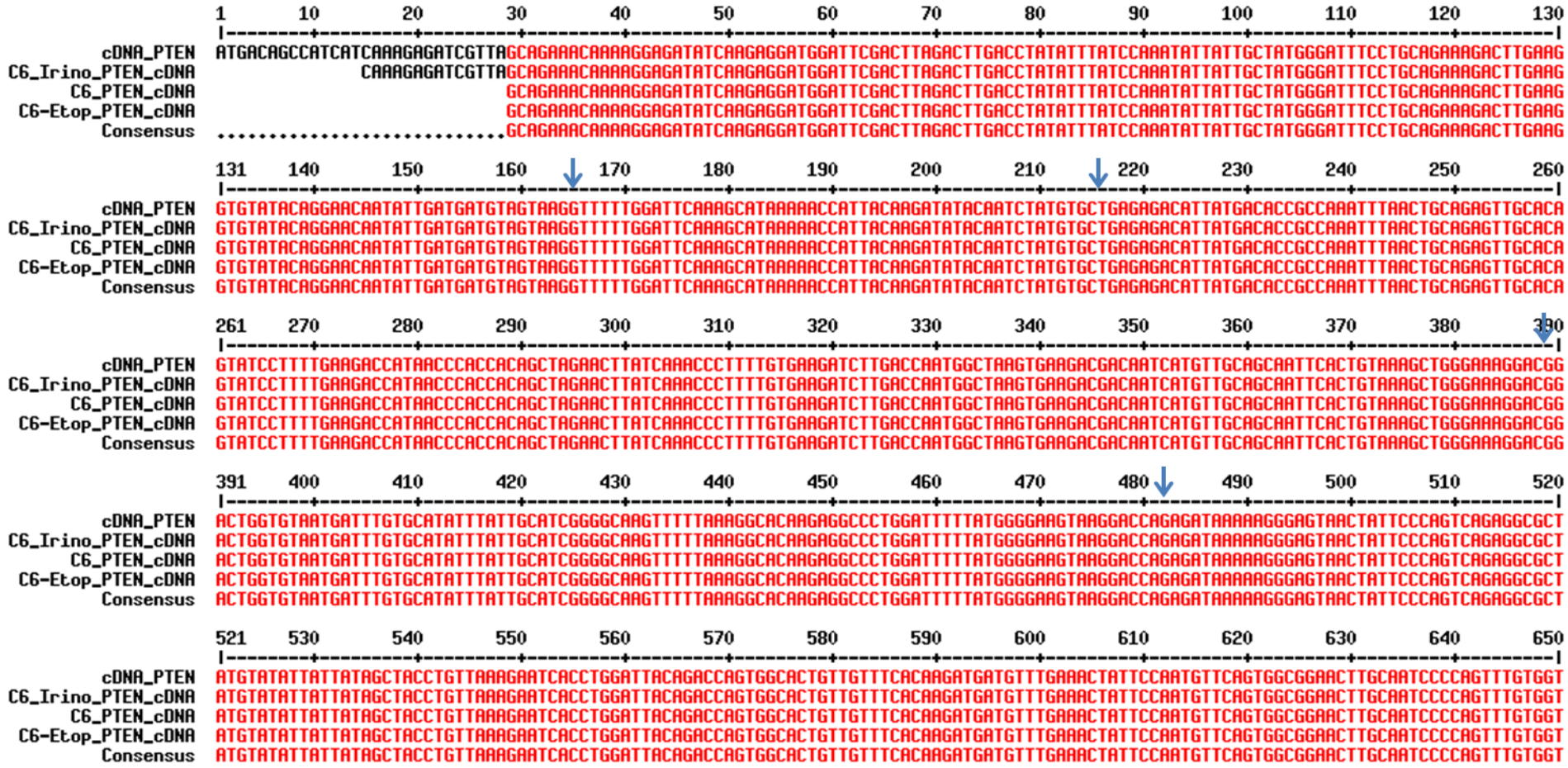

Figure 6.2 The alignment of cDNA for *PTEN* gene. The whole sequence of the cDNA from the three glioma cell lines was sequenced in an online Multi-alignment website (http://multalin.toulouse.inra.fr/multalin/cgi-bin/multalin.pl) to determine if there are any differences in the sequence of *PTEN* exons. No differences in the cDNA were observed when compared to the published *PTEN* mutations data (165 G>T, 216 T>C, 389 G>A, 482G>T, and 766 G>A) as shown by the blue arrows.

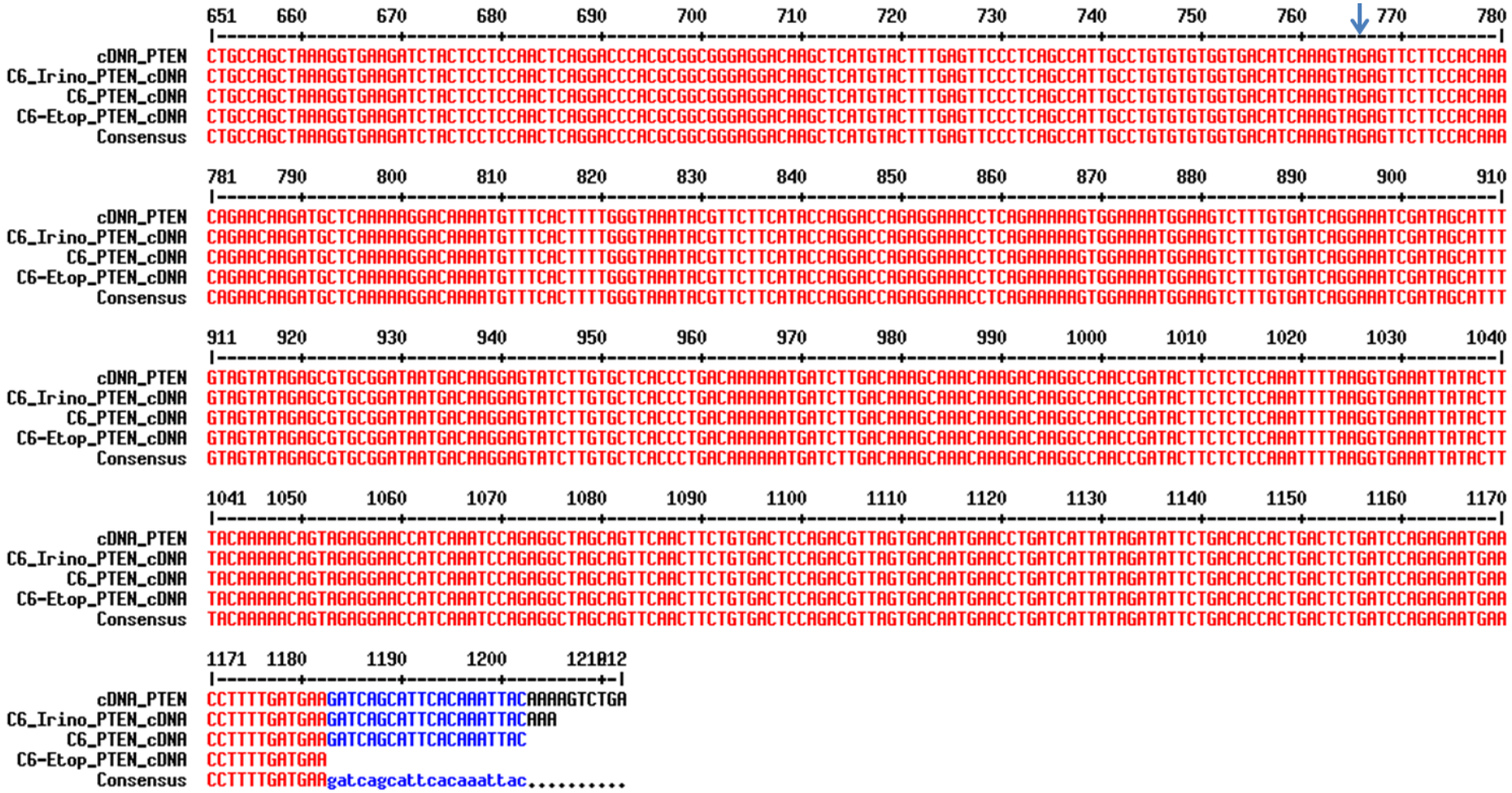

Figure 6.2 The alignment of cDNA for *PTEN* gene (continued).

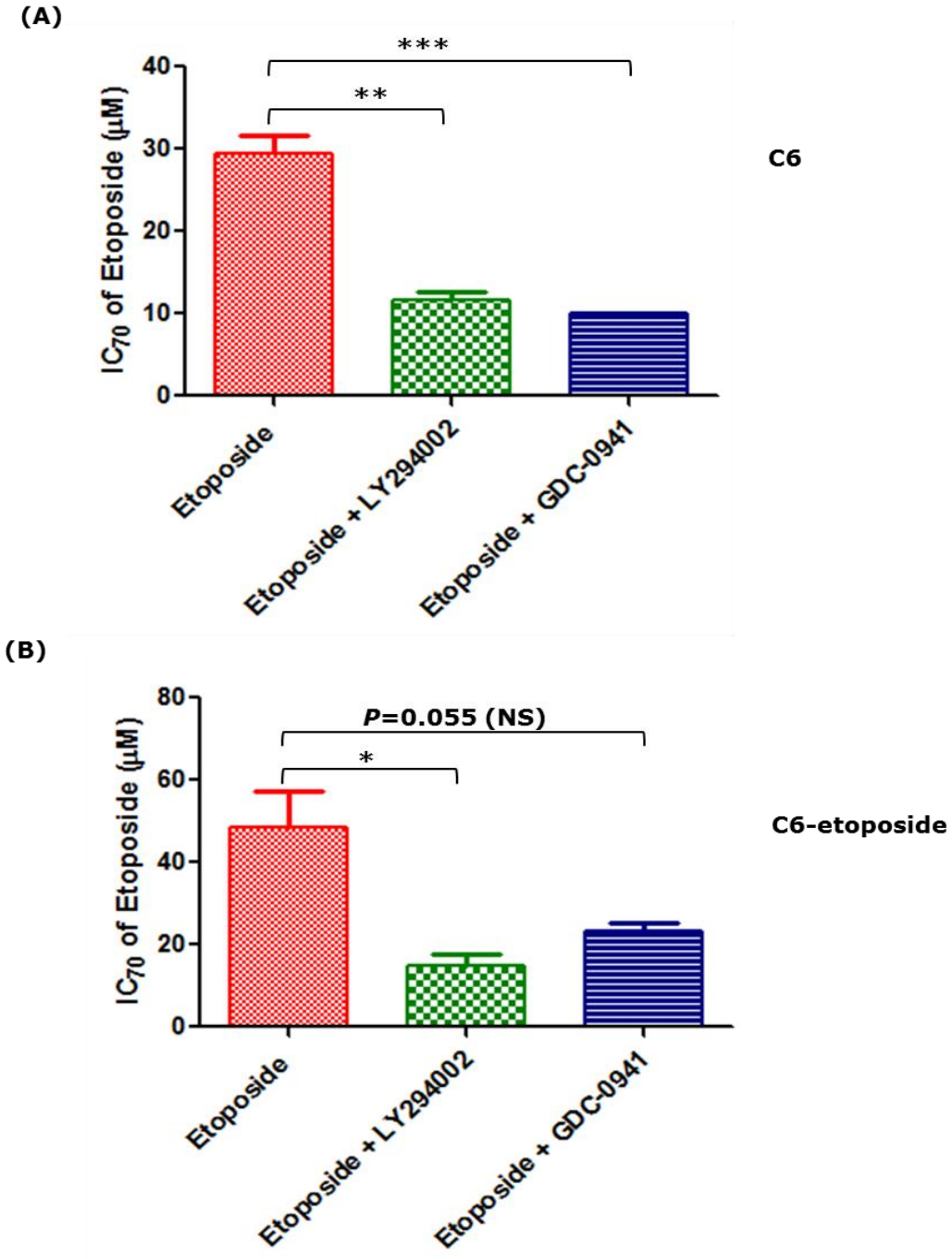

Figure 6.3 PI3K pathway inhibitors affects clonogenic survival in C6 glioma cell lines. Clonogenic assays were performed on C6 and C6-etoposide with either 20 μM LY294002 or 1 μM GDC-0941. (A) For C6, both inhibitors reduce C6 survival significantly by 2.5 and 3 fold with LY294002 and GDC-0941, respectively. (B) For C6-etoposide, both inhibitors also resulted in a reduction in the colony survival% as the IC70 of etoposide reduced significantly by 3.2 and 2 fold with LY294002 and GDC-0941, respectively. However, only *P* value with LY294002 reached significance while with GDC-0941 the *P* value was close to the significance. The *P* values are calculated by unpaired t test, *$P \leq 0.05$, **$P \leq 0.001$, ***$P \leq 0.0001$, NS: not significant, and n=4.

LY294002 and GDC-0941 have not been used in conjunction with etoposide in previous cell lines studies, but they have been combined with other chemotherapeutic agents to increase the effectiveness of the chemotherapy in both *in vitro* and *in vivo* model systems. For example, in a study by Shingu *et al.,* LY294002 was tested in combination with anti-microtubule agents (vincristine and paclitaxel), drugs that block the cell growth through the interfering with microtubules and hence inhibit chromosomes movement during mitosis, with other drugs such as an alkylating agent 1, 3-bis (2-chloroethyl)-1-nitrosourea, and a DNA cross-linking agent cisplatin on several human glioma cell lines U87, A172, LN18, and LN229. They found that LY294002 combined with anti-microtubule agents can augment synergistic apoptosis to a greater extent than other chemotherapeutic agents through an increase in caspase 3-dependent apoptosis (Shingu et al., 2003). GDC-0941 was found to increase the rate of apoptosis in several breast carcinoma models arrested in mitosis upon the co-treatment with docetaxel, anti-microtubule agent used widely in breast cancer treatment, in both *in vivo* and *in vitro* models. The effect of this inhibitor with the docetaxel was stronger and observed within 1 hour in the xenograft models compared to the cell lines (Wallin et al., 2012). However, more experiments need to be performed to elucidate the mechanisms by which PI3K inhibitors affect the survival in C6 glioma cell lines.

6.5.3 Determination of the effect of PI3K inhibitors on cell migration

The migratory response to the PI3K inhibitors was investigated for two reasons: (1) migration is one of the hallmarks of cancer and it is considered as a first step in the invasion and angiogenesis of the tumour, and (2) in chapter IV the migration of the C6 cell line treated with irinotecan was decreased compared to other cell lines. In addition, *PTEN* gene expression showed a significant reduction in C6-irinotecan cell line compared to C6.

Three independent scratch assays were performed on the three glioma cell lines. After the scratch was made, 20 μM LY294002 or 1 μM GDC-0941 were added to the corresponding well and the migration of the cells was then assessed as in section 4.2.2. Analysis of the data revealed that treating the glioma cell lines with PI3K inhibitors changed the migration behaviour significantly. Specifically, the cells in the three glioma cell lines failed to heal the wound completely even after T=65 hours (figure 6.4). Our data agreed with other studies which used these two inhibitors to inhibit the migration of several tumours. However, to the best of my knowledge, this is the first study regarding the effect of LY294002 and GDC-0941 on the migration of glioma cell lines treated with DNA topoisomerase inhibitors. For instance, in a study on leukaemia cell line Liu *et al.,* showed that LY294002 could suppress leukaemia cell invasion and migration through up-regulation of *EGR1*, independently of its PI3K-Akt inhibitory activity (Liu et al., 2008). In another study, the migration of HeLa cells can be totally blocked in epitheloid by PI3K pathway inhibitor LY294002 through SDF-1α–induced migration and Akt activation (Peng et al., 2005). Less is known about the role of GDC-0941 on the migration of tumour cells. Although GDC-0941 is a specific PI3K pathway inhibitor, it was found to inhibit the migration of thyroid cells by inhibiting the hypoxia/anoxia-induced factors (HIF-1α) and (HIF-2α) expression and HIF activity in the thyroid carcinoma cells (Burrows et al., 2011). However, these hypotheses need further validation in our cell lines.

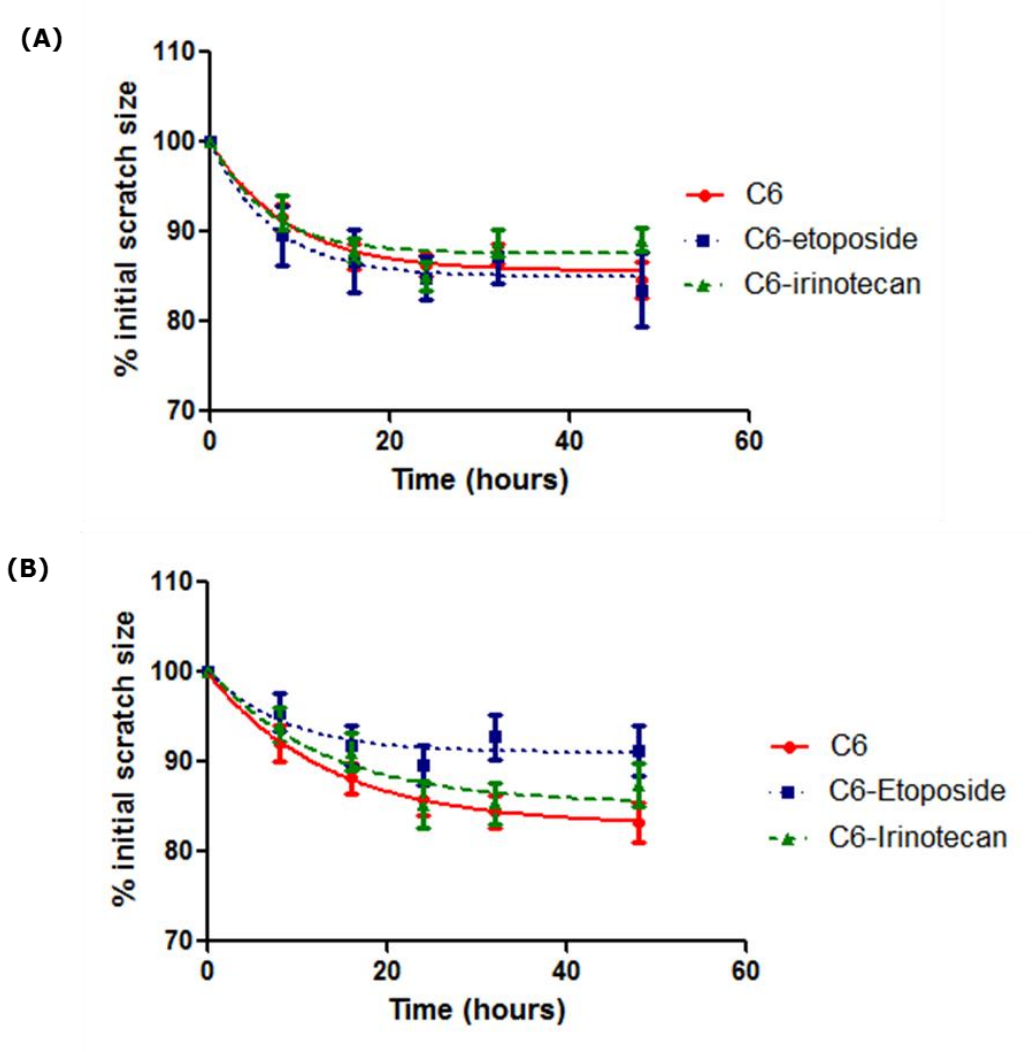

Figure 6.4 PI3K inhibitors severely inhibit the migration of C6 glioma cell lines. The three cell lines were prepared for the scratch assay following the protocol in section 4.2.2 and the data obtained from ImageJ was used to plot the % scratch size as a function of time. (A) and (B) Represent the non-linear fit analysis of the LY294002 and GDC-0941 experiments, respectively. Both figures indicated that the three cell lines fitted better with the single exponential fit curve with no complete wound healing (even for T>65 hours) which indicate that both inhibitors resulted in a severe reduction in the migratory behaviour of the C6 glioma cell lines, n=3.

6.6 Future work

The main aim for this study was the determination of drug resistance mechanisms in glioma. We were able to successfully identify several candidate proteins and genes which are important in different aspects of the tumour biology. Some of these candidates were validated in the current study and showed to play a role in either the migration or oxidative stress resistance. Regarding the migration response, analysis of the data from migration assays revealed that irinotecan can inhibit the migration of glioma cells through the suppression of several genes expression particularly the collagens. However, the exact mechanisms by which irinotecan can affect the expression of collagens are under investigation as it's unclear if irinotecan affects directly the expression of collagens or indirectly via other mechanisms. As discussed earlier in section 6.3, irinotecan was found to inhibit the migration and angiogenesis in colorectal cancer xenografts by inhibiting *HIF1a* and other genes expression (most importantly among these genes is *VEGFR* which is one of the major growth factors in glioma and plays an important role in the angiogenesis of this tumour) (Kleihues et al., 2007a). At the current time, the exact role of irinotecan in the inhibition of hypoxia inducible genes remains unclear and need further validation. Moreover, as our cell lines showed differences in the migration response and as collagens are important components of ECM, *in vitro* invasion assays can be performed to elucidate the role of the collagens in the invasion and *in vivo* experiments can be done to determine the role of collagens and VEGFR in angiogenesis.

Response to oxidative stress, analysis of the data showed that etoposide increased the resistance through the suppression of PTEN. This creates the question about the role of PTEN in the resistance observed in C6-etoposide compared to the other cell lines. However, the sequencing of the cDNA of *PTEN* failed to explain the detected reduction in PTEN expression level and lead to predictions that epigenetic modification (promoter methylation) which could silence this gene may have occurred.

Promoter hyper-methylation has recently been identified as an alternative mechanism of tumour suppressor gene inactivation in cancer such as *PTEN* (see section 1.3.5.3 for more details). In this study, we tried to identify the methylation status of *PTEN* following the protocol published in (Bian et al., 2012). Unfortunately, we were unable to get any result which leaves this as a goal for further investigation. Moreover, PTEN can be knockdown in animal model to assess its effect on the response to oxidative stress *in vivo*. Finally, as there are many other glioma cell line models available it would be beneficial to investigate how consistent altered PTEN status is.

The application of PI3K inhibitors showed a positive effect on the inhibition of both survival and migration of C6 glioma cell lines. However, the underlying mechanisms need to be explained as the current study is the first established study on glioma cell line treated with two major DNA topoisomerase inhibitors and inhibited with LY294002 and GDC-0941. The IPA analysis also identified signalling pathways other than PI3K pathway. These pathways could have a role in the chemo-resistance in high grade glioma such as NF-kB and TGFβ. TGFβ was found to play a role in the activation of pro-collagen to active collagen type and therefore, can act as a central signalling pathway in the migration of glioma cells whereas NF-kB is an important transcription factor that are involved in proliferation and differentiation and hence can be correlated to the oxidative stress and to the consequence DNA damage and probably apoptosis. The activity of these signalling pathways can be determined by reporter assays and by electrophoretic mobility shift assays.

Since temozolomide (TMZ) is the standard chemotherapeutic agent currently used in the treatment of adult HGG, another goal is to establish a C6 glioma cell line treated with TMZ and employ this as a model system to identify protein and genes expression changes that underlie TMZ resistance.

Finally, a longer term goal is to employ this information to determine potential markers of glioma that could be investigated in patient tissue microarray (TMA) to better identify patients likely to respond to particular chemotherapy and radiotherapy regimes.

REFERENCES

ABE, T., HASEGAWA, S., TANIGUCHI, K., YOKOMIZO, A., KUWANO, T., ONO, M., MORI, T., HORI, S., KOHNO, K. & KUWANO, M. 1994. Possible involvement of multidrug-resistance-associated protein (MRP) gene expression in spontaneous drug resistance to vincristine, etoposide and adriamycin in human glioma cells. *International Journal of Cancer,* 58**,** 860-864.

ABRÀMOFF, M., MAGALHÃES, P. J. & RAM, S. J. 2004. Image processing with ImageJ. *Biophotonics International,* 11**,** 36-42.

ABRUDAN, C., COCIS, A., CERNEA, D., SUCIU, B., CHEPTEA, M. & FLORIAN, I. 2011. Surgery of high grade gliomas - pros in favor of maximal cytoreductive surgery. *Romanian Neurosurgery,* XVIII**,** 38-53.

AFFYMETRIX 2002. Statistical algorithms description document.

AGGELI, I., BEIS, I. & GAITANAKI, C. 2010. ERKs and JNKs mediate hydrogen peroxide-induced Egr-1 expression and nuclear accumulation in H9c2 cells. *Physiological Research,* 59**,** 443-454.

AHMED, N., RILEY, C., RICE, G. & QUINN, M. 2005. Role of integrin receptors for fibronectin, collagen and laminin in the regulation of ovarian carcinoma functions in response to a matrix microenvironment. *Clinical and Experimental Metastasis,* 22**,** 391-402.

AL-DASOOQI, N., BOWEN, J. M., GIBSON, R. J., LOGAN, R. M., STRINGER, A. M. & KEEFE, D. M. 2011. Irinotecan-induced alterations in intestinal cell kinetics and extracellular matrix component expression in the dark agouti rat. *International Journal of Clinical and Experimental Pathology,* 92**,** 357-365.

AL-HAJJ, M., WICHA, M., ITO-HERNANDEZ, A., MORRISON, S. & CLARKE, M. 2003. Prospective identification of tumorgenic breast cancer cells. *Proceedings of the National Academy of Sciences U.S.A.,* 100**,** 3983-3988.

ALARMO, E., PARSSINEN, J., KETOLAINEN, J., SAVINAINEN, K., KARHU, R. & KALLIONIEMI, A. 2009. BMP7 influences proliferation, migration, and invasion of breast cancer cells. *Cancer Letters,* 275**,** 35-43.

ANGELO, P., ANITA, M., AMALIA, A. & STEFANIA, T. 2007. Phosphatidylinositol 3-kinase in breast cancer: where from here? *Clinical Cancer Research,* 13**,** 5988-5990.

APPLING, W. D., O'BRIEN, W. R., JOHNSTON, D. A. & DUVIC, M. 1989. Synergistic enhancement of type I and III collagen production in cultured fibroblasts by transforming growth factor-fl and ascorbate. *FEBS Letters,* 250**,** 541-544.

BACHMAN, K. E., ARGANI, P., SAMUELS, Y., SILLIMAN, N., PTAK, J., SZABO, S., KONISHI, H., KARAKAS, B., BLAIR, B. G., LIN, C., PETERS, B. A., VELCULESCU, V. E. & PARK, B. H. 2004. The PIK3CA gene is mutated with high frequency in human breast cancers. *Cancer Biology and Therapy,* 3**,** 772-775.

BANERJEE, H. N., MAHAFFEY, K., RIDDICK, E., BANERJEE, A., BHOWMIK, N. & PATRA, M. 2012. Search for a diagnostic/prognostic biomarker for the brain cancer glioblastoma multiforme by 2D-DIGE-MS technique. *Molecular and Cellular Biochemistry,* 367**,** 59–63.

BARKER, F. G., CHANG, S. M., GUTIN, P. H., MALEC, M. K., MCDERMOTT, M. W., PRADOS, M. D. & WILSON, C. B. 1998. Survival and functional status after resection of recurrent glioblastoma multiforme. *Neurosurgery,* 42**,** 709-723.

BARON, V., ADAMSON, E., CALOGERO, A., RAGONA, G. & MERCOLA, D. 2006. The transcription factor Egr1 is a direct regulator of multiple tumor suppressors including TGFβ1, PTEN, p53 and fibronectin, Egr1 is a potential target of gene therapy for prostate cancer. *Cancer Gene Therapy,* 13**,** 115-124.

BARTH, R. F. & KAUR, B. 2009. Rat brain tumor models in experimental neuro-oncology: the C6, 9L, T9, RG2, F98, BT4C, RT-2 and CNS-1 gliomas. *Journal of Neuro-oncology,* 94**,** 299-312.

BARTLING, B., DESOLE, M., ROHRBACH, S., SILBER, R. E. & SIMM, A. 2009. Age-associated changes of extracellular matrix collagen impair lung cancer cell migration. *The FASEB Journal,* 23**,** 1510-1520.

BAX, D., LITTLE, S., GASPAR, N., PERRYMAN, L., MARSHALL, L., VIANA-PEREIRA, M., JONES, T., WILLIAMS, R., GRIGORIADIS, A., VASSAL, G., WORKMAN, P., SHEER, D., REIS, R., PEARSON, A., HARGRAVE, D. & JONES, C. 2009. Molecular and phenotypic characterisation of paediatric glioma cell lines as models for preclinical drug development. *PLOS one,* 4**,** e5209-e5218.

BEADLE, C., ASSANAH, M., MONZO, P., VALLEE, R., ROSENFELD, S. & CANOLL, P. 2008. The role of myosin II in glioma invasion of the brain. *Molecular Biology of the Cell,* 19**,** 3357-3368.

BEIER, D., SCHULZ, J. & BEIER, C. 2011. Chemoresistance of glioblastoma cancer stem cells-much more complex than expected. *Molecular Cancer,* 10**,** 128-138.

BENDA, P., LIGHTBODY, J., SATO, G., LEVINE, L. & SWEET, W. 1968. Differential rat glial cell strain in tissue culture. *Science,* 161**,** 370-371.

BENDA, P., SOMEDA, K., MESSER, J. & SWEET, W. 1971. Morphological and immunochemical studies of rat glial tumors and clonal strains propagated in culture. *Journal of Neurosurgery,* 34**,** 310-323.

BERNS, K., HORLINGS, H. M., HENNESSY, B. T., MADIREDJO, M., HIJMANS, E. M., BEELEN, K., LINN, S. C., GONZALEZ-ANGULO, A. M., STEMKE-HALE, K., HAUPTMANN, M., BEIJERSBERGEN, R. L., MILLS, G. B., VAN DE VIJVER, M. J. & BERNARDS, R. 2007. A functional genetic approach identifies the PI3K pathway as a major determinant of trastuzumab resistance in breast cancer. *Cancer Cell,* 12**,** 395-402.

BIAN, E. B., HUANG, C., MA, T. T., TAO, H., ZHANG, H., CHENG, C., LV, X. W. & LI, J. 2012. DNMT1-mediated PTEN hypermethylation confers hepatic stellate cell activation and liver fibrogenesis in rats. *Toxicology and Applied Pharmacology,* 264**,** 13-22.

BIERNAT, W., TOHMA, Y., YONEKAWA, Y., KLEIHUES, P. & OHGAKI, H. 1997. Alterations of cell cycle regulatory genes in primary (de novo) and secondary glioblastomas. *Acta Neuropathologica,* 94**,** 303-309.

BONAVIA, R., INDA, M., CAVENEE, W. & FURNARI, F. 2011. Heterogeneity maintenance in glioblastoma: A social network. *Cancer Research,* 71**,** 4055-4060.

BONDAR, V. M., SWEENEY-GOTSCH, B., ANDREEFF, M., MILLS, G. B. & MCCONKEY, D. J. 2002. Inhibition of the phosphatidylinositol 3'-kinase-AKT pathway induces apoptosis in pancreatic carcinoma cells in vitro and in vivo. *Molecular Cancer Therapeutics,* 1**,** 989-997.

BOUMENDJEL, A., BOUTONNAT, J. & ROBERT, J. 2009. *ABC Transporters and Multidrug Resistance. ,* New Jeresy, A John Wiley & sons, INC., publication.

BOZZUTO, G., RUGGIERI, P. & MOLINARI, A. 2010. Molecular aspects of tumor cell migration and invasion. *Ann Ist Super Sanità,* 46**,** 66-80.

BRANDES, A. A., TOSONI, A., AMISTÀ, P., NICOLARDI, L., GROSSO, D., BERTI, F. & ERMANI, M. 2004. How effective is BCNU in recurrent glioblastoma in the modern era? A phase II trial. *Neurology,* 63**,** 1281-1284.

BREDEL, M. 2001. Anticancer drug resistance in primary human brain tumors. *Brain Research Reveiws,* 35**,** 161-204.

BRONISCER, A., BAKER, S., WEST, A., FRASER, M., PROKO, E., KOCAK, M., DALTON, J., ZAMBETTI, G., ELLISON, D., KUN, L., GAJJAR, A., GILBERTSON, R. & FULLER, C. 2007. Clinical and molecular characteristics of malignant transformation of low-grade glioma in children. *Journal of Clinical Oncology,* 25**,** 682-689.

BRUGGE, J., HUNG, M. C. & MILLS, G. 2007. A new mutational *akt*ivation in the PI3K Pathway. *Cancer Cell,* 12**,** 104-107.

BUGG, B. Y., DANKS, M. K., BECK, W. T. & SUTTLE, P. 1991. Expression of a mutant DNA topoisomerase II in CCRF-CEM human leukemic cells selected for resistance to teniposide. *Proceedings of the National Academy of Sciences U.S.A.,* 88**,** 7654-7658.

BUJIS, J., RENTSCH, C., VAN DER HORST, G., VAN OVERVELD, P., WETTERWALD, A., SCHWANINGER, R., HENRIQUEZ, N., DIJKE, P., BOROVECKI, F., MARKWALDER, R., THALMANN, G., PAPAPOULOS, S., PELGER, R., VUKICEVIC, S., CECCHINI, M., LOWICK, C. & PLUIJM, G. 2007. BMP7, a putative regulator of epithelial homeostasis in the human prostate, is a potent inhibitor of prostate cancer bone metastasis in vivo. *The American Journal of Pathology,* 171**,** 1047-1057.

BURROWS, N., BABUR, M., RESCH, J., RIDSDALE, S., MEJIN, M., ROWLING, E. J., BRABANT, G. & WILLIAMS, K. J. 2011. GDC-0941 inhibits metastatic characteristics of thyroid carcinomas by targeting both the phosphoinositide-3 kinase (PI3K) and hypoxia-inducible factor-1α (HIF-1α) pathways *The Journal of Clinical Endocrinology and Metabolism,* 96**,** E1934-E1943.

CANCER RESEARCH UK 2010. Childhood cancer- Great Britain & UK.

CANCER STATISTICS REGISTRATIONS 2008. Registrations of cancer diagnosed in 2008, England. Office for National Statistics.

CARDIS, E., RICHARDSON, L., DELTOUR, I., ARMSTRONG, B., FEYCHTING, M., JOHANSEN, C., KILKENNY, M., MCKINNEY, P., MODAN, B. & ET AL. 2007. The INTERPHONE study: design, epidemiological methods, and description of the study population. *European Journal of Epidemiology,* 22**,** 647-664.

CARICO, C., NUNO, M., MUKHERJEE, D., ELRAMSISY, A., DANTIS, J., HU, J., RUDNICK, J., YU, J. S., BLACK, K. L., BANNYKH, S. & PATI, C. G. 2012. Loss of PTEN is not associated with poor survival in newly diagnosed glioblastoma patients of the temozolomide era. *PLOS one,* 7**,** e33684-e33691.

CHALHOUB, N. & BAKER, S. J. 2009. PTEN and the PI3-kinase pathway in cancer. *The Annual Reveiw of Pathology,* 4**,** 127-150.

CHANG, C., MULHOLLAND, D. J., VALAMEHR, B., MOSESSIAN, S., SELLERS, W. R. & WU, H. 2008. PTEN nuclear localization is regulated by

oxidative stress and mediates p53-dependent tumor suppression. *Molecular and Cellular Biology,* 28**,** 3281-3289.

CHEN, J., LI, Y., YU, T., MCKAY, R., BURNS, D., KERNIE, S. & PARADA, L. 2012. A restricted cell population propagates glioblastoma growth after chemotherapy. *Nature Letter*.

CHENG, J., LIU, B. & ZHANG, X. 2009. How powerful is CD133 as a cancer stem cell marker in brain tumors? *Cancer Treatment Reveiws,* 35**,** 403–408.

CHERNOV, A., BARANOVSKAYA, S., GOLUBKOV, V., WAKEMAN, D., SNYDER, E., WILLIAMS, R. & STRONGIN, A. 2010. Microarray-based transcriptional and epigenetic profiling of matrix metalloproteinases, collagens, and related genes in cancer. *The Journal of Biological Chemistry,* 285**,** 19647-19659.

CHOUCAIR, A. K., LEVIN, V. A., GUTIN, P. H., DAVIS, R. L., SILVER, P., EDWARDS, M. S. & WILSON, C. B. 1986. Development of multiple lesions during radiation therapy and chemotherapy in patients with gliomas. *Journal of Neurosurgery,* 65**,** 654-658.

CHU, E. C. & TARNAWSKI, A. S. 2004. PTEN regulatory functions in tumor suppression and cell biology. *Medical Science Monitor,* 10**,** RA235–RA241.

CLUTTON, S. 1997. The importance of oxidative stress in apoptosis. *British Medical Bulletin,* 53**,** 662-668.

COLUCCI-GUYON, E., RIBOTTA, M., MAURICE, T., BABINET, C. & PRIVAT, A. 1999. Cerebellar defect and impaired motor coordination in mice lacking vimentin. *GLIA,* 25**,** 33-43.

CONDEELIS, J. & SEGALL, J. E. 2003. Intravital imaging of cell movement in tumours. *Nature Reveiws Cancer,* 3**,** 921-930.

CONKLIN, K. A. 2004. Chemotherapy-associated oxidative stress: impact on chemotherapeutic effectiveness. *Integrative Cancer Therapies* 3**,** 294-300.

CONTE, E., FRUCIANO, M., FAGONE, E., GILI, E., CARACI, F., LEMMOLO, M., CRIMI, N. & VANCHERI, C. 2011. Inhibition of PI3K prevents the proliferation and differentiation of human lung fibroblasts into myofibroblasts: the role of class I P110 isoforms. *PLOS one,* 6**,** e24663-e24670.

CORPET, F. 1988. Multiple sequence alignment with hierarchical clustering. *Nucleic Acids Research,* 16**,** 10881-10890.

CROCE, C. M. 2008. Oncogenes and cancer. *The New England Journal of Medicine,* 358**,** 502-511.

CROSSMAN, A. & NEARY, D. 2005. Introduction and overveiw. *Neuroanatomy.* Third ed. Philadelphia, USA: Churchill Livingstone Elsevier.

DALE, P. D., SHERRATTT, J. A. & MAINI, P. K. 1997. Role of fibroblasts migration in collagen fiber formation during fetal and adult dermal wound healing. *Bulletin of Mathematical Biology,* 59**,** 1077-1100.

DALLA-FAVERA, R., GALLO, R., GIALLONGO, C. & CROCE, C. 1982. Chromosomal localization ofthe human homolog (c-sis) ofthe simian sarcoma virus oncogene. *Science,* 218**,** 686-688.

DAVIES, G. C., RYAN, P. E., RAHMAN, L., ZAJAC-KAYE, M. & LIPKOWITZ, S. 2006. EGFRvIII undergoes activation-dependent downregulation mediated by the Cbl proteins. *Oncogene,* 5**,** 6497-6509.

DAVIS, W., RONAL, Z. & TEW, K. D. 2001. Cellular thiols and reactive oxygen species in drug-induced apoptosis. *The Journal of Pharmacology and Experimental Therapeutics,* 296**,** 1-6.

DEAN, M., FOJO, T. & BATES, S. 2005. Tumour stem cells and drug resistance. *Nature Reveiws Cancer,* 5**,** 275–284.

DENKER, S. P. & BARBER, D. L. 2002. Cell migration requires both ion translocation and cytoskeletal anchoring by the Na-H exchanger NHE1. *The Journal of Cell Biology,* 159**,** 1087-1096.

DI LULLO, G. A., SWEENEY, S. M., KORKKO, J., ALA-KOKKO, L. & SAN ANTONIO, J. D. 2002. Mapping the ligand-binding sites and disease-associated mutations on the most abundant protein in the human, type I collagen. *The Journal of Biological Chemistry,* 277**,** 4223-4331.

DOWNWARD, J., YARDEN, Y., MAYES, E., SCRACE, G., TOTTY, N., STOCKWELL, P., ULLRICH, A., SCHLESSINGER, J. & WATERFIELD, M. D. 1984. Close similarity of epidermal growth factor receptor and v-erb-B oncogene protein sequences. *Nature,* 307**,** 521-527.

DOWSEY, A., MORRIS, J., GUTSTEIN, H. & YANG, G. Z. 2010. Informatics and statistics for analyzing 2-D gel electrophoresis images. *In:* HUBBARD, S. & JONES, A. (eds.) *Proteome bioinformatics, methods in molecular biology.* Human press.

EICHHORN, P. J., GILI, M., SCALTRITI, M., SERRA, V., GUZMAN, M., NIJKAMP, W., BEIJERSBERGEN, R. L., VALERO, V., SEOANE, J., BERNARDS, R. & BASELGA, J. 2008. Phosphatidylinositol 3-kinase hyperactivation results in lapatinib resistance that is reversed by the mTOR/phosphatidylinositol 3-kinase inhibitor NVP-BEZ235. *Cancer Research,* 68**,** 9221-9230.

EINSTEIN, D. B., WESSELS, B., BANGERT, B., FU, P., NELSON, A. D., COHEN, M., SAGAR, S., LEWIN, J., SLOAN, A., ZHENG, Y., WILLIAMS, J., COLUSSI, V., VINKLER, R. & MACIUNAS, R. 2012. Phase II trial of radiosurgery to magnetic resonance spectroscopy-defined high-risk tumor volumes in patients with glioblastoma multiforme. *International Journal of Radiation Oncology Biology Physics,* 84**,** 668-674.

ENOCH, S. & LEAPER, D. 2008. Basic science of wound healing. *Surgery,* 26**,** 31-37.

ERMAKOVA, S. P., KANG, B., CHOI, B., CHOI, H. S., SCHUSTER, T. F., MA, W. Y., BODE, A. M. & DONG, Z. 2006. (-) - Epigallocatechin gallate overcomes resistance to etoposide- induced cell death by targeting the molecular chaperone glucose-regulated protein 78. *Cancer Research,* 66**,** 9260-9269.

FAN, W., ZHOU, K., ZHAO, Y., WU, W., CHEN, H., JIN, L., CHEN, G., SHI, J., WEI, Q., ZHANG, T., DU, G., MAO, Y., LU, D. & ZHOU, L. 2011. Possible association between genetic variants in the H2AFX promoter region and risk of adult glioma in a Chinese Han population. *Journal of Neuro-oncology,* 105**,** 211-218.

FARNKEN, N. A., RODERMOND, H. M., STAP, J., HAVEMAN, J. & BREE, C. V. 2006. Clonogenic assay of cells *in vitro*. *Nature Protocols,* 1**,** 2315-2319.

FAVALORO, B., ALLOCATI, N., GRAZIANO, V., DI ILIO, C. & DE LAURENZI, V. 2012. Role of Apoptosis in disease. *Aging,* 4**,** 330-349.

FEDI, P., TRONICK, S. & AARONSON, S. A. 1997. Growth factors *In:* HOLLAND, J. F., BAST, R. C., MORTON, D. L., FREI, E., KUFE, D. W. &

WEICHSELBAUM, R. R. (eds.) *Cancer medicine.* Baltimore, MD: Williams and Wilkins.

FELS, C., SCHÄFER, C., HÜPPE, B., BAHN, H., HEIDECKE, V., KRAMM, C. M., LAUTENSCHLÄGER, C. & RAINOV, N. G. 2000. Bcl-2 expression in higher-grade human glioma: a clinical and experimental study. *Journal of Neuro-oncology,* 48**,** 207-216.

FOLKES, A. J., AHMADI, K., ALDERTON, W. K., ALIX, S., BAKER, S. J., BOX, G., CHUCKOWREE, I. S., CLARKE, P. A., DEPLEDGE, P., ECCLES, S. A., FRIEDMAN, L. S., HAYES, A., HANCOX, T. C., KUGENDRADAS, A., LENSUN, L., MOORE, P., OLIVERO, A. G., PANG, J., PATEL, S., PERGL-WILSON, G., RAYNAUD, F., ROBSON, A., SAGHIR, N., SALPHATI, L., SOHAL, S., ULTSCH, M. H., VALENTI, M., WALLWEBER, H. J., WAN, N., WIESMANN, C., WORKMAN, P., ZHYVOLOUP, A., ZVELEBIL, M. J. & SHUTTLEWORTH, S. J. 2008. The identification of 2-(1H-indazol-4-yl)-6-(4-methanesulfonyl-piperazin-1-ylmethyl)-4-morpholin-4-yl-thieno[3,2-d]pyrimidine (GDC-0941) as a potent, selective, orally bioavailable inhibitor of class I PI3 kinase for the treatment of cancer *Journal of Medicinal Chemistry (ACS Publications),* 51**,** 5522-5532.

FRIEDL, P. & WOLF, K. 2003. Tumour-cell invasion and migration: diversity and escape mechanisms. *Nature Reviews Cancer,* 3**,** 362-374.

FRIEDMAN, H., PETROS, W., FRIEDMAN, A., SCHAAF, L., KERBY, T., LAWYER, J., PARRY, M., HOUGHTON, P., LOVELL, S., RASHEED, K., CLOUGHSEY, T., STEWART, E., COLVIN, O., PROVENZALE, J., MCLENDON, R., BIGNER, D., COKGOR, I., HAGLUND, M., RICH, J., ASHLEY, D., MALCZYN, J., ELFRING, G. & MILLER, L. 1999. Irinotecan therapy in adults with recurrent or progressive malignant glioma. *Journal of Clinical Oncology,* 17**,** 1516-1525.

GAUTIER, L., COPE, L., BOLSTAD, B. M. & IRIZARRY, R. A. 2004. affy - analysis of Affymetrix GeneChip data at the probe level. *Bioinformatics,* 20**,** 307-315.

GENENTECH 2011. A phase II, double-blind, placebo-Controlled, randomized study evaluating the safety and efficacy of carboplatin/paclitaxel and carboplatin/paclitaxel/bevacizumab with and without GDC-0941 in patients with previously untreated advanced or recurrent non-small cell lung cancer.

GHARBI, S. I., ZVELEBIL, M. J., SHUTTLEWORTH, S. J., HANCOX, T., SAGHIR, N., TIMMS, J. F. & WATERFIELD, M. D. 2007. Exploring the specificity of the PI3K family inhibitor LY294002. *Biochemical Journal,* 404**,** 15-21.

GIANCOTTI, F. G. & RUOSLAHTI, E. 1999. Integrin signaling. *Science,* 285**,** 1028-1032.

GILLE, L. & NOHL, H. 1997. Analyses of the molecular mechanism of adriamycin-induced cardiotoxicity. *Free Radical Biology and Medicine,* 23**,** 775-782.

GOLDSTEIN, L. & SCHNEIDER, M. 2010. *Stem cells for dummies,* Indianapolis, Indiana, Wiley publishing, Inc. .

GONZALEZ-ANGULO, A., FERRER-LOZANO, J., STEMKE-HALE, K., SAHIN, A., LIU, S., BARRERA, J., BURGUES, O., LLUCH, A., CHEN, H., HORTOBAGYI, G., MILLS, G. B. & MERIC-BERNSTAM, F. 2011. PI3K pathway mutations and PTEN levels in primary and metastatic breast cancer. *Molecular Cancer Therapeutics,* 10**,** 1093-1101.

GONZALEZ-SUAREZ, I., REDWOOD, A. B. & GONZALO, S. 2009. Loss of A-type lamins and genomic instability. *Cell Cycle,* 8**,** 3860-3865.

GOODELL, M., BROSE, K., PARADIS, G., CONNER, A. & MULLIGAN, R. 1996. Isolation and functional properties of murine hematopoietic stem cells that are replicating in vivo. *The Journal of Experimental Medicine,* 183**,** 1797-1806.

GOTTESMAN, M. 2002a. Mechanisms of cancer drug resistance *Annual Reveiw of Medicine,* 53**,** 615-627.

GOTTESMAN, M. M. 2002b. Multidrug resistance I: P-glycoprotein. *Encyclopedia of Cancer,* 3.

GREEN, D. R. & REED, J. C. 1998. Mitochondria and apoptosis. *Science,* 281**,** 1309-1312.

GRESHOCK, J., NATHANSON, K., MARTIN, A. M., ZHANG, L., COUKOS, G., WEBER, B. L. & ZAKS, T. Z. 2007. Cancer cell lines as genetic models of their parent histology: analyses based on array comparative genomic hybridization. *Cancer Research,* 67**,** 3594-3600.

GUÉRIN, E., RAFFELSBERGER, W., PENCREACH, E., MAIER, A., NEUVILLE, A., SCHNEIDER, A., BACHELLIER, P., ROHR, S., PETITPREZ, A., POCH, O., MORAS, D., OUDET, P., LARSEN, A., GAUB, M. P. & GUENOT, D. 2012. In vivo topoisomerase I inhibition attenuates the expression of hypoxia-inducible factor 1α target genes and decreases tumor angiogenesis. *Molecular Medicine,* 18**,** 83-94.

GUNNERSEN, J. M., SPIRKOSKA, V., SMITH, P. E., DANKS, R. A. & TAN, S. S. 2000. Growth and migration markers of rat C6 glioma cells identified by serial analysis of gene expression. *GLIA,* 32**,** 146-154.

GUO, C. Y., XU, X. F., WU, J. Y. & LIU, S. F. 2008. PCR-SSCP-DNA sequencing method in detecting PTEN gene mutation and its significance in human gastric cancer. *World Journal of Gastroenterology,* 14**,** 3804-3811.

GUO, P., HU, B., GU, W., XU, L., WANG, D. F., HUANG, H. J., CAVENEE, W. K. & CHENG, S. Y. 2003. Platelet-derived growth factor-B enhances glioma angiogenesis by stimulating vascular endothelial growth factor expression in tumor endothelial and by promoting pericyte recruitment. *American Journal of Pathology,* 162**,** 1083-1093.

GYMNOPOULOS, M., ELSLIGER, M. A. & VOGT, P. K. 2007. Rare cancer-specific mutations in PIK3CA show gain of function. *Proceedings of the National Academy of Sciences U.S.A,* 104**,** 5569–5574.

HANAHAN, D. & WEINBERG, R. 2000. The hallmarks of cancer. *Cell,* 100**,** 57-70.

HARDELL, L., CARLBERG, M. & HANSSON MILD, K. 2012. Use of mobile phones and cordless phones is associated with increased risk for glioma and acoustic neuroma. *Pathophysiology,* 12**,** Epub ahead of print.

HARTMANN, C., HENTSCHEL, B., WICK, W., CAPPER, D., FELSBERG, J., SIMON, M., WESTPHAL, M., SCHACKERT, G., MEYERMANN, R., PIETSCH, T., REIFENBERGER, G., WELLER, M., LOEFFLER, M. & VON DEIMLING, A. 2010. Patients with IDH1 wild type anaplastic astrocytomas exhibit worse prognosis than IDH1-mutated glioblastomas, and IDH1 mutation status accounts for the unfavorable prognostic effect of higher age: implications for classification of gliomas. *Acta Neuropathologica,* 120**,** 707-718.

HARVEY, J. J. 1964. An unidentified virus which causes the rapid production of tumors in mice. *Nature,* 204**,** 1104-1105.

HASTINGS, P. J., LUPSKI, J. R., ROSENBERG, S. M. & IRA, G. 2009. Mechanisms of change in gene copy number. *Nature Reviews Genetics,* 10**,** 551–564.

HEGI, M. E., DISERENS, A. C., GORLIA, T., HAMOU, M. F., DETRIBOLET, N., WELLER, M., KROS, J. M., HAINFELLNER, J. A., MASON, W., MARIANI, L., BROMBERG, J. E., HAU, P., MIRIMANOFF, R. O., CAIRNCROSS, J. G., JANZER, R. C. & STUPP, R. 2005. MGMT gene silencing and benefit from temozolomide in glioblastoma. *The New England Journal of Medicine,* 352**,** 997–1003.

HEIDEMAN, R. L., PACKER, R. J., ALBRIGHT, L. A., FREEMAN, C. R. & RORKE, L. B. 1997. Tumors of the central nervous system. *In:* PIZZO, P. A. & POPLACK, D. G. (eds.) *Principles and practice of pediatric oncolgy.* Philadelphia: Lippincott- Raven.

HEIMBERGER, A., HLATKY, R., SUKI, D., YANG, D., WEINBERG, J., GILBERT, M., SAWAYA, R. & ALDAPE, K. 2005a. Prognostic effect of epidermal growth factor receptor and EGFRvIII in glioblastoma multiforme patients. *Clinical Cancer Research,* 11**,** 1462-1466.

HEIMBERGER, A. B., SUKI, D., YANG, D. X., SHI, W. & ALDAPE, K. 2005b. The natural history of EGFR and EGFRvIII in glioblastoma patients. *Journal of Translational Medicine,* 3**,** 38-43.

HELDIN, C., WASTESON, A. & WESTERMARK, B. 1980. Growth of normal human glial cells in a defined medium containing platelet-derived growth factor. *Proceedings of the National Academy of Sciences U.S.A,* 77**,** 6611-6615.

HERMANSON, M., FUNA, K., KOOPMANN, J., MAINTZ, D., WAHA, A., WESTERMARK, B., HELDIN, C. H., WIESTLER, O. D., LOUIS, D. N., VON DEIMLING, A. & NISTÉR, M. 1996. Association of loss of heterozygosity on chromosome 17p with high platelet-derived growth factor alpha receptor expression in human malignant gliomas. *Cancer Research,* 56**,** 164-171.

HERTEL, K. & MANIATIS, T. 1999. Serine–arginine (SR)-rich splicing factors have an exon-independent function in pre-mRNA splicing. *Proceedings of the National Academy of Science U.S.A,* 96**,** 2651–2655.

HIGGINS, C. F. 2007. Multiple molecular mechanisms for multidrug resistance transporters. *Nature,* 446**,** 749-757.

HIGGINS, D. F., KIMURA, K., BERNHARDT, W. M., SHRIMANKER, N., AKAI, Y., HOHENSTEIN, B., SAITO, Y., JOHNSON, R. S., KRETZLER, M., COHEN, C. D., ECKARDT, K. U., IWANO, M. & HAASE, V. H. 2007. Hypoxia promotes fibrogenesis in vivo via HIF-1 stimulation of epithelial-to-mesenchymal transition. *The Journal of Clinical Investigation,* 117**,** 3810-3820.

HOCKENBERY, D., NUNEZ, G., MILLIMAN, C., SCHREIBER, R. D. & KORSMEYER, S. 1990. Bcl-2 is an inner mitochondrial membrane protein that blocks programmed cell death. *Nature,* 348**,** 334-336.

HODGSON, J. G., YEH, R.-F., RAY, A., WANG, N. J., SMIRNOV, I., YU, M., HARIONO, S., SILBER, J., FEILER, H. S., GRAY, J. W., SPELLMAN, P. T., VANDENBERG, S. R., BERGER, M. S. & JAMES, D. 2009. Comparative analyses of gene copy number and mRNA expression in

glioblastoma multiforme tumors and xenografts. *Neuro-oncology,* 11**,** 477-487.

HONG, T. M., YANG, P. C., PECK, K., CHEN, J., YANG, S. C., CHEN, Y. C. & WU, C. W. 2000. Profiling the downstream genes of tumor suppressor PTEN in lung cancer cells by complementary DNA microarray. *American Journal of Respiratory Cell and Molecular Biology,* 23**,** 355-363.

HOOD, J. D. & CHERESH, D. A. 2002. Role of integrins in cell invasion and migration. *Nature Reviews Cancer,* 2**,** 91-100.

HORWITZ, R. & WEBB, D. 2003. Cell migration. *Current Biology,* 13**,** R756-R759.

HU, X., PANDOLFI, P., LIY, Y., KOUTCHERZ, J. A., ROSENBLUM, M. & HOLLAND, E. 2005. mTOR Promotes Survival and Astrocytic Characteristics Induced by Pten/Akt Signaling in Glioblastoma. *Neoplasia,* 7**,** 356–368.

HUIJBERS, I., IRAVANI, M., POPOV, S., ROBERTSON, D., AL-SARRAJ, S., JONES, C. & ISACKE, C. 2010. A role for fibrillar collagen deposition and the collagen internalization receptor endo180 in glioma invasion. *PLOS one,* 5**,** e9808-e9820.

HURT, E. & FARRAR, W. 2010. *Cancer stem cells,* Cambridge, UK, Cambridge University Press.

HURWITZ, H., FEHRENBACHER, L., CARTWRIGHT, T., HAINSWORTH, J., HEIM, W., BERLIN, J., GRIFFING, S., NOVOTNY, W., HOLMGREN, E. & KABBINAVAR, F. 2003. Bevacizumab (a monoclonal antibody to vascular endothelial growth factor) prolongs survival in first-line colorectal cancer (CRC): results of a phase III trial of bevacizumab in combination with bolus IFL (irinotecan, 5-fluorouracil, leucovorin) as first-line therapy in subjects with metastatic CRC. *Proceedings of the Annual Meeting of the American Society of Clinical Oncology.* Chicago, IL.

HUSAIN, I., MOHLER, J., SEIGLER, H. & BESTERMAN, J. 1994. Elevation of topoisomerase I messenger RNA, protein, and catalytic activity in human tumors: demonstration of tumor-type specificity and implications for cancer chemotherapy. *Cancer Research,* 54**,** 539-546.

HUSSEIN, D., PUNJARUK, W., STORER, L., SHAW, L., OTTOMAN, R., PEET, A., MILLER, S., BANDOPADHYAY, G., HEATH, R., KUMARI, R., BOWMAN, K. J., BRAKER, P., RAHMAN, R., JONES, G., WATSON, S., LOWE, J., KERR, I., GRUNDY, R. & COYLE, B. 2011. Pediatric brain tumor cancer stem cells: cell cycle dynamics, DNA repair, and etoposide extrusion. *Neuro-oncology,* 13**,** 70-83.

ILHAN-MUTLU, A., WÖHRER, A., BERGHOFF, A. S., WIDHALM, G., MAROSI, C., WAGNER, L. & PREUSSER, M. 2013. Comparison of microRNA expression levels between initial and recurrent glioblastoma specimens. *Journal of Neuro-oncology***,** Epub ahead of print.

IVASKA, J., PALLARI, H. M., NEVO, J. & J.E., E. 2007. Novel functions of vimentin in cell adhesion, migration, and signaling. *Experimental Cell Research,* 313**,** 2050-2062.

JACOBSON, M. D. 1996. Reactive oxygen species and programmed cell death. *Trends in Biochemical Sciences,* 21**,** 83-86.

JAKOBSEN, J. N., HASSELBALCH, B., STOCKHAUSEN, M. T., LASSEN, U. & POULSEN, H. S. 2011. Irinotecan and bevacizumab in recurrent

glioblastoma multiforme. *Expert Opinion in Pharmacotherapy,* 12**,** 825-833.

JONES, P. M. & GEORGE, A. M. 2004. The ABC transporter structure and mechanism: perspectives on recent research. *Cellular and Molecular Life Sciences,* 61**,** 682-699.

JUNG, C. S., FOERCH, C., SCHÄNZER, A., HECK, A., PLATE, K. H., SEIFERT, V., STEINMETZ, H., RAABE, A. & SITZER, M. 2007. Serum GFAP is a diagnostic marker for glioblastoma multiforme. *Brain,* 130**,** 3336-3341.

JUNTTILA, T., AKITA, R., PARSONS, K., FIELDS, C., LEWIS PHILLIPS, G., FRIEDMAN, L., SAMPATH, D. & SLIWKOWSKI, M. 2009. Ligand-independent HER2/HER3/PI3K complex is disrupted by trastuzumab and is effectively inhibited by the PI3K inhibitor GDC-0941. *Cancer Cell,* 15**,** 429-440.

KALINSKY, K., JACKS, L. M., HEGUY, A., PATIL, S., DROBNJAK, M., BHANOT, U., HEDVAT, C., TRAINA, T., SOLIT, D., GERALD, W. & MOYNAHAN, M. 2009. PIK3CA mutation associates with improved outcome in breast cancer. *Clinical Cancer Research,* 15**,** 5049-5059.

KALLERGI, G., AGELAKI, S., MARKOMANOLAKI, H., GEORGOULIAS, V. & STOURNARAS, C. 2007. Activation of FAK/PI3K/Rac1 signaling controls actin reorganization and inhibits cell motility in human cancer cells. *Cellular Physiology and Biochemistry,* 20**,** 977-986.

KALLURI, R. & WEINBERG, R. A. 2009. The basics of epithelial-mesenchymal transition. *The Journal of Clinical Investigation,* 119**,** 1420-1428.

KANE, D. J., SARAFIAN, T. A., ANTON, R., HAHN, H., GRALLA, E. B., VALENTINE, J. S., ORD, T. & BREDESEN, D. E. 1993. Bcl-2 inhibition of neural death: decreased generation of reactive oxygen species. *Science,* 262**,** 1274-1277.

KASAHARA, Y., IWAI, K., YACHIE, A., OHTA, K., KONNO, A., SEKI, H., MIYAWAKI, T. & TANIGUCHI, N. 1997. Involvement of reactive oxygen intermediates in spontaneous and CD95(Fas/APO-1) – mediated apoptosis of neutrophils. *Blood,* 89**,** 1748-1753.

KAWANABE, Y., HASHIMOTO, N. & MASAKI, T. 2003. Effects of nonselective cation channels and PI3K on endothelin-1- induced PYK2 tyrosine phosphorylation in C6 glioma cells. *American Journal of Physiology-Cell Physiology,* 285**,** C539-C545.

KELLY, K. A., KIRKWOOD, J. M. & KAPP, D. S. 1984. Glioblastoma multiforme: pathology, natural history and treatment. *Cancer Treatment Reviews,* 11**,** 1-26.

KERR, I. D. 2002. Structure and association of ATP-binding cassette transporter nucleotide-binding domains. *Biochimica et Biophysica Acta,* 1561**,** 47-64.

KIRSTEN, W. H. & MAYER, L. A. 1967. Morphologic responses to a murine erythroblastosis virus. *The Journal of the National Cancer Institute,* 39**,** 311-335.

KLEIHUES, P., BURGER, P. C., ALDAPE, K. D., BRAT, D. J., BIERNAT, W., BIGNER, D. D., NAKAZATO, Y., PLATE, K. H., GIANGASPERO, F., VON DEIMLING, A., OHGAKI, H. & VCAVENEE, W. K. 2007a. Glioblastoma. *In:* LOUIS, D. N., OHGAKI, H., WIESTLER, O. D. & CAVENEE, W. K. (eds.) *WHO classification of tumours of the central nervous system.* Lyon: International Agency for Research on Cancer.

KLEIHUES, P., BURGER, P. C., ROSENBLUM, M., PAULUS, W. & SCHEITHAUER, B. 2007b. Anaplastic astrocytoma. *In:* LOUIS, D. N., OHGAKI, H., WIESTLER, O. D. & CAVENEE, W. K. (eds.) *WHO classification of tumours of the central nervous system.* Lyon: IARC.

KORSHUNOV, A., SYCHEVA, R., TIMIRGAZ, V. & GOLANOV, A. 1999. Prognostic value of immunoexpression of the chemoresistance-related proteins in ependymomas: an analysis of 76 cases. *Journal of Neuro-oncology,* 45**,** 219-27.

KORSMEYER, S. J., YIN, X. M., OLTVAI, Z., VEIS-NOVACK, D. & LINETTE, G. 1995. Reactive oxygen species and the regulation of cell death by the Bcl-2 gene family. *Biochimica et Biophysica Acta,* 1271**,** 63-66.

KUN, L. E. 1997. General principles of radiation therapy. *In:* PIZZO, P. A. & POPLACK, D. G. (eds.) *Principles and practice of pediatric oncology.* Third ed. Philadephia: Lippincott-Raven.

KWEI, K. A., BAKER, J. B. & PELHAM, R. J. 2012. Modulators of sensitivity and resistance to inhibition of PI3K identified in a pharmacogenomic screen of the NCI-60 human tumor cell line collection. *PLOS one,* 7**,** e46518.

LAEMMLI, U. K. 1970. Cleavage of structural proteins during the assembly of the head of bacteriophage T4. *Nature,* 227**,** 680-685.

LAMALICE, L., LE BOEUF, F. & HUOT, J. 2007. Endothelial cell migration during angiogenesis. *Circulation Research,* 100**,** 782-794.

LANG, F. F., SHONO, T. & GILBERT, M. R. 2002. Ad-p53 sensitizes wild-type p53 gliomas to the topoisomerase I inhibitor SN-38. *Neuro-oncology,* 4**,** 323-324.

LAPIDOT, T., SIRARD, C., VORMOOR, J., MURDOCH, B., HOANG, T., CACERES-CORTES, J., MINDEN, M., PATERSON, B., CALIGIURI, M. A. & DICK, J. E. 1994. A cell initiating human acute myeloid leukaemia after transplantation into SCID mice. *Nature,* 367**,** 645–648.

LASSMAN, A. B. 2004. Molecular biology of gliomas. *Current Neurology and Neuroscience Reports,* 4**,** 228-233.

LEE, J.-J., KIM, B. C., PARK, M.-J., LEE, Y.-S., KIM, Y.-N., LEE, B. L. & LEE, J.-S. 2011a. PTEN status switches cell fate between premature senescence and apoptosis in glioma exposed to ionizing radiation. *Cell Death and Differentiation,* 18**,** 666-677.

LEE, K. W., LEE, D. J., LEE, J. Y., KANG, D. H., KWON, J. & KANG, S. W. 2011b. Peroxiredoxin II restrains DNA damage-induced death in cancer cells by positively regulating JNK-dependent DNA repair. *The Journal of Biological Chemistry,* 286**,** 8394-8404.

LEE, S., NAM, S., HONG, Y., KANG, C. & LEE, Y. H. 2011c. O^6-methylguanine DNA methyltransferase gene promoter methylation status in glioblastoma and its correlation with other prognostic markers. *Molecular and Cellular Toxicology,* 7**,** 425-430.

LEVY, G. 2011. A phase II, double-blind, placebo controlled, randomized study of GDC-0941 or GDC-0980 with fulvestrant versus fulvestrant in advanced or metastatic breast cancer in patients resistant to aromatase inhibitor therapy. Genetech.

LI, A., WALLING, J. & KOTLIAROV, Y. 2008. Genomic changes and gene expression profiles reveal that established glioma cell lines are poorly representative of primary human gliomas. *Molecular Cancer Research,* 6**,** 21-30.

LI, C., ZHOU, C., WANG, S., FENG, Y., LIN, W., LIN, S., WANG, Y., HUANG, H., LIU, P., MU, Y. G. & SHEN, X. 2011. Sensitization of glioma cells to tamoxifen-induced apoptosis by Pl3-kinase inhibitor through the GSK-3b/b- catenin signaling pathway. *PLOS one,* 6**,** e27053.

LI, S. & LI, D. 2009. DNA microarray technology and data analysis in cancer research. *World Scientific***,** 1-10.

LI, S. Y., RONG, M., GRIEU, F. & IACOPETTA, B. 2006. PIK3CA mutations in breast cancer are associated with poor outcome. *Breast Cancer Research and Treatment,* 96**,** 91-95.

LIANG, C. C., PARK, A. Y. & GUAN, J. L. 2007. *In vitro* scratch assay: a convenient and inexpensive method for analysis of cell migration *in vitro*. *Nature Protocols,* 2**,** 329-333.

LIANG, Y., DIEHN, M., WATSON, N., BOLLEN, A., ALDAPE, K., NICHOLAS, M., LAMBORN, K., BERGER, M., BOTSTEIN, D., BROWN, P. & ISRAEL, M. 2005. Gene expression profiling reveals molecularly and clinically distinct subtypes of glioblastoma multiforme. *Proceedings of the National Academy of Sciences U.S.A,* 102**,** 5814-5819.

LIU, K., ZHANG, J., REN, J. J., WANG, X. J., YANG, H. L. & LIN, P. 2009a. Interference of human Na/K-ATPaseB1 subunit on proliferation and migration of gastric adenocarcinoma cell line SGC-7901. *Chinese Journal of Cancer,* 28**,** 189-194.

LIU, P., CHENG, H., ROBERTS, T. M. & ZHAO, J. J. 2009b. Targeting the phosphoinositide 3-kinase (PI3K) pathway in cancer. *Nature Reviews Drug Discovery,* 8**,** 627-644.

LIU, P., XU, B., LI, J. & LU, H. 2008. LY294002 inhibits leukemia cell invasion and migration through early growth response gene 1 induction independent of phosphatidylinositol 3-kinase-Akt pathway. *Biochemical and Biophysical Research Communications,* 377**,** 187-190.

LIU, Q., NGUYEN, D., DONG, Q., SHITAKU, P., CHUNG, K., LIU, O., TSO, J., LIU, J., KONKANKIT, V., CLOUGHESY, T., MISCHEL, P., LANE, T., LIAU, L., NELSON, S. & TSO, C. L. 2009c. Molecular properties of CD133+ glioblastoma stem cells derived from treatment-refractory recurrent brain tumors. *Journal of Neuro-oncology,* 94**,** 1-19.

LIU, Y., CARSON-WALTER, E. B., COOPER, A., WINANS, B. N., JOHNSON, M. D. & WALTER, K. A. 2010. Vascular gene expression patterns are conserved in primary and metastatic brain tumors. *Journal of Neuro-oncology,* 99**,** 13-24.

LOKE, J. D. & HORWTTZ, S. B. 1976. Effect of VP-16-213 on the intracellular degradation of DNA in HeLa cells. *Biochemistry,* 15**,** 5443-5448.

LONGSTAFF, A. 2009. The nervous system. *In:* NAISH, J., REVEST, P. & COURT, D. S. (eds.) *Medical sciences.* Saunders Elsevier.

LOWE, S. W. & LIN, A. H. 2000. Apoptosis in cancer. *Carcinogenesis,* 21**,** 485-495.

LU, C. & SHERVINGTON, A. 2008. Chemoresistance in gliomas. *Molecular and Cellular Biochemistry,* 312**,** 71-80.

LU, X. & LEGERSKI, R. J. 2007. The Prp19/Pso4 core complex undergoes ubiquitylation and structural alterations in response to DNA damage. *Biochemical and Biophysical Research Communications,* 354**,** 968–974.

MALMQUIST, N. A., ANZINGER, J. J., HIRZEL, D. & BUXTON, I. 2001. Ellagic acid inhibits nucloside diphosphate kinase-B activity. *Proceedings of the Western Pharmacology Society's* 44**,** 57-59.

MALUMBRES, M. & BARBACID, M. 2003. RAS oncogenes: the first 30 years. *Nature Reviews Cancer,* 3**,** 459-465.

MAO-DE, L. & JING, X. 2007. Ribosomal proteins and colorectal cancer. *Current Genomics,* 8**,** 43-49.

MARGARETO, J., LEIS, O., LARRARTE, E., POMPOSO, I. C., GARIBI, J. M. & LAFUENTE, J. V. 2009. DNA copy number variation and gene expression analyses reveal the implication of specific oncogenes and genes in GBM. *Cancer Investigation,* 27**,** 541-548.

MARKERT, J., FULLER, C., GILLESPIE, Y., BUBIEN, J., MCLEAN, L. A., HONG, R., LEE, K. W., GULLANS, S., MAPSTONE, T. & BENOS, D. 2001. Differential gene expression profiling in human brain tumors. *Physiological Genomics,* 5**,** 21-33.

MARNETT, L. J., RIGGINS, J. N. & WEST, J. D. 2003. Endogenous generation of reactive oxidants and electrophiles and their reactions with DNA and proteins. *The Journal of Clinical Investigation,* 111**,** 583-593.

MARONE, R., CMILJANOVIC, V., GIESE, B. & WYMANN, M. 2008. Targeting phosphoinositide 3-kinase—Moving towards therapy. *Biochimica et Biophysica Acta,* 1784**,** 159-185.

MASON, W. P., DEL MAESTRO, R., EISENSTAT, D., FORSYTH, P., FULTON, D., LAPERRIÈRE, N., MACDONALD, D., PERRY, J. & THIESSEN, B. 2007. Canadian recommendations for the treatment of glioblastoma multiforme. *Current Oncology,* 14**,** 110-117.

MAXWELL, M., NABER, S., WOLFE, U., GALANOPOULOS, H., HEDLEY-WHYTE, T., BLACK, P. & ANTONIADES, H. 1990. Coexpression of platelet-derived growth factor (PDGF) and PDGF-receptor genes by primary human astrocytomas may contribute to their development and maintenance. *The Journal of Clinical Investigation,* 86**,** 131-140.

MELEAN, G., SESTINI, R., AMMANNATI, F. & PAPI, L. 2004. Genetic insights into familial tumors of the nervous system. *American Journal of Medical Genetics Part C, Seminars in Medical Genetics,* 129**,** 74–84.

MIMORI, K., MORI, M., INOUE, H., UEO, H., MAFUNE, K., AKIYOSHI, T. & SUGIMACHI, K. 1996. Elongation factor lγ mRNA expression in oesophageal carcinoma. *Gut,* 38**,** 66-70.

MINEO, J., BORDRON, A., BARONCINI, M., RAMIREZ, C., MAURAGE, C., BLOND, S. & DAM-HIEU, P. 2007. Prognosis factors of survival time in patients with glioblastoma multiforme: a multivariate analysis of 340 patients. *Acta Neurochirurgica,* 149**,** 245-253.

MODAN, B., MART, H., BAIDATZ, D., STEINITZ, R. & LEVIN, S. 1974. Radiation- induced head and neck tumours. *The Lancet,* 303**,** 277-279.

MOHRI, M., NITTA, H. & YAMASHITA, J. 2000. Expression of multidrug resistance-associated protein (MRP) in human gliomas. *Journal of Neuro-oncology,* 49**,** 105-115.

MONTANO, N., CENCI, T., MARTINI, M., D'ALESSANDRIS, Q., PELACCHI, F., RICCI-VITIANI, L., MAIRA, G., DE MARIA, R., LAROCCA, L. M. & PALLINI, R. 2011. Expression of EGFRvIII in Glioblastoma: Prognostic Significance Revisited. *Neoplasia,* 13**,** 1113-1121.

MOORE, N. & LYLE, S. 2010. Quiescent, slow-cycling stem cell populations in cancer: A review of the evidence and discussion of significance. *Journal of Oncology,* 2011**,** 1-11.

NAIR, P., MUTHUKKUMAR, S., SELLS, S., HAN, S., SUKHATME, V. P. & RANGNEKAR, V. M. 1997. Early growth response-1-dependent

apoptosis is mediated by p53. *The Journal of Biological Chemistry,* 272**,** 20131–20138.

O'FARRELL, P. H. 1975. High resolution two-dimensional electrophoresis of proteins. *The Journal of Biological Chemistry,* 250**,** 4007-4021.

ODREMAN, F., VINDIGNI, M., GONZALES, M. L., NICCOLINI, B., CANDIANO, G., ZANOTTI, B., SKRAP, M., PIZZOLITTO, S., STANTA, G. & VINDIGNI, A. 2005. Proteomic studies on low- and high-grade human brain astrocytomas. *Journal of Proteome Research (ACS Publications),* 4**,** 698-708.

OFFICE FOR NATIONAL STATISTICS 2010. Cancer Statistics registrations: Registrations of cancer diagnosed in 2008, England. London: National Statistics.

OGAWA, Y., TSUDA, H., HAI, E., TSUJI, N., YAMAGATA, S., TOKUNAGA, S., NAKAZAWA, K., TAMAMORI, Y., OGAWA, M., SHIMIZU, S., INOUE, T. & NISHIGUCHI, Y. 2006. Clinical role of ABCF2 expression in breast cancer. *Anticancer Research,* 26**,** 1809-1814.

OH, S. Y., SOHN, Y. W., PARK, J. W., PARK, H. J., JEON, H. M., KIM, T. K., LEE, J. S., JUNG, J. E., JIN, X., CHUNG, Y., CHOI, Y. K., YOU, S., LEE, J. B. & KIM, H. 2007. Selective cell death of oncogenic Akt-transduced brain cancer cells by etoposide through reactive oxygen species–mediated damage. *Molecular Cancer Therapeutics,* 6**,** 2178-2187.

OHGAKI, H., DESSEN, P., JOURDE, B., HORSTMANN, S., NISHIKAWA, T., DI PATRE, P., BURKHARD, C., SCHÜLER, D., PROBST-HENSCH, N., MAIORKA, P. C., BAEZA, N., PISANI, P., YONEKAWA, Y., YASARGIL, M. G., LÜTOLF, U. & KLEIHUES, P. 2004. Genetic pathways to glioblastoma: A population-based study. *Cancer Research,* 64**,** 6892-6899.

OHGAKI, H. & KLEIHUES, P. 2005. Population-based studies on incidence, survival rates, and genetic alterations in astrocytic and oligodendroglial gliomas. *Journal of Neuropathology and Experimental Neurology,* 64**,** 479-489.

OMARA-OPYENE, A., QIU, J., SHAH, G. & ICZKOWSKI, K. 2004. Prostate cancer invasion is influenced more by expression of a CD44 isoform including variant 9 than by Muc18. *Laboratory Investigation-Nature,* 84**,** 894-907.

PAPACOCEA, T., PAPACOCEA, R., BĂDĂRĂU, A., ION, A. D., BURAGA, I. G., L. & PAPACOCEA, A. 2011. Oxidative stress and antioxidants in brain tumors. *Therapeutics, Pharmacology and Clinical Toxicology,* XV**,** 234-239.

PAREKH, C., JUBRAN, R., ERDREICH-EPSTEIN, A., PANIGRAHY, A., BLUML, S., FINLAY, J. & DHALL, G. 2011. Treatment of children with recurrent high grade gliomas with a bevacizumab containing regimen. *Journal of Neuro-oncology,* 103**,** 673-680.

PASZAT, L., LAPERRIERE, N., GROOME, P., SCHULZE, K., MACKILLOP, W. & HOLOWATY, E. 2001. A population-based study of glioblastoma multiforme. *International Journal of Radiation Oncology Biology Physics,* 51**,** 100-107.

PAUGH, B. S., QU, C., JONES, C., LIU, Z., ADAMOWICZ-BRICE, M., ZHANG, J., BAX, D. A., COYLE, B., BARROW, J., HARGRAVE, D., LOWE, J., GAJJAR, A., ZHAO, W. J., BRONISCER, A., ELLISON, D. W., GRUNDY, R. G. & BAKER, S. 2010. Integrated molecular genetic profiling of

pediatric high-grade gliomas reveals key differences with the adult disease. *Journal of Clinical Oncology,* 28**,** 3061-3068.

PAULUS, W., SAGE, E. H., LISZKA, U., IRUELA-ARISPE, M. L. & JELLINGER, K. 1991. Increased levels of type VIII collagen in human brain tumours compared to normal brain tissue and non-neoplastic cerebral disorders. *British Journal of Cancer,* 63**,** 367-371.

PENG, S. B., PEEK, V., ZHAI, Y., PAUL, D. C., LOU, Q., XIA, X., EESSALU, T., KOHN, W. & TANG, S. 2005. Akt activation, but not extracellular signal–regulated kinase activation, is required for SDF-1α/CXCR4–mediated migration of epitheloid carcinoma cells. *Molecular Cancer Research,* 3**,** 227-236.

PFAFFL, M. W. 2001. A new mathematical model for relative quantification in real -time RT-PCR. *Nucleic Acids Research,* 29**,** e54-e60.

POLLACK, I. F. 1994. Current concept: brain tumours in children. *The New England Journal of Medicine,* 331**,** 1500-1507.

POLLACK, I. F., HAMILTON, R. L., SOBOL, R. W., BURNHAM, J., YATES, A. J., HOLMES, E. J., ZHOU, T. & FINLAY, J. L. 2006. O6-methylguanine-DNA methyltransferase expression strongly correlates with outcome in childhood malignant gliomas: results from the CCG-945 Cohort. *Journal of Clinical Oncology,* 24**,** 3431–3437.

POMMIER, Y. 2006. Topoisomerase I inhibitors: camptothecins and beyond. *Nature Reviews Cancer,* 6**,** 789-802.

POTAPOVA, O., FAKHRAI, H., BAIRD, S. & MERCOLA, D. 1996. Platelet-derived growth factor-B /v-sis confers a tumorigenic and metastatic phenotype to human T98G glioblastoma cells. *Cancer Research,* 56**,** 280-286.

PROVENZANO, P., ELICEIRI, K. W., CAMPBELL, J. M., INMAN, D. R., WHITE, J. G. & KEELY, P. J. 2006. Collagen reorganization at the tumor-stromal interface facilitates local invasion. *BMC Medicine,* 4**,** 38-54.

PUCHADES, M., NILSSON, C., EMMETT, M., ALDAPE, K., JI, Y., LANG, F., LIU, T. J. & CONRAD, C. 2007. Proteomic investigation of glioblastoma cell lines treated with wild-type p53 and cytotoxic chemotherapy demonstrates an association between Galectin-1 and p53 expression. *Journal of Proteome Research (ACS Publications),* 6**,** 869-875.

PUNJARUK, W. 2010. *Contribution of drug resistant cancer stem cells to paediatric brain tumours.* PhD, University of Nottingham.

QI, Y. Y., LIU, K., ZHANG, J., LI, K., REN, J. J. & LIN, P. 2009. [Synergic effect of Na(+)-K(+) ATPaseB1 and adriamycin on inhibition of cell proliferation and reversal of drug resistance in breast cancer MCF-7 cells]. *Ai Zheng,* 28**,** 861-7.

RADISKY, D. C. 2005. Epithelial-mesenchymal transition. *Journal of Cell Science,* 118**,** 4325-4326.

RADISKY, D. C., LEVY, D. D., LITTLEPAGE, L. E., LIU, H., NELSON, C. M., FATA, J., LEAKE, D., GODDEN, E., ALBERTSON, D., NIETO, A., WERB, Z. & BISSELL, M. 2005. Rac1b and reactive oxygen species mediate MMP-3-induced EMT and genomic instability. *Nature,* 436**,** 123-127.

RAGNAUTH, C. D., WARREN, D. T., LIU, Y. W., MCNAIR, R., TAJSIC, T., FIGG, N., SHROFF, R., SKEPPER, J. & SHANAHAN, C. M. 2010. Prelamin A acts to accelerate smooth muscle cell senescence and is a novel biomarker of human vascular aging. *Circulation,* 121**,** 2200-2210.

RAJARAMAN, P., HUTCHINSON, A., ROTHMAN, N., BLACK, P., FINE, H., LOEFFLER, J., SELKER, R., SHAPIRO, W., LINET, M. & INSKIP, P. 2008. Oxidative response gene polymorphisms and risk of adult brain tumors. *Neuro-oncology,* 10**,** 709-715.

RANGARAJ, A., HARDING, K. & LEAPER, D. 2011. Role of collagen in wound management. *Wounds UK,* 7**,** 54-63.

RASHEED, B., STENZEL, T., MCLENDON, R., PARSONS, R., FRIEDMAN, A., FRIEDMAN, H., BIGNER, D. D. & BIGNER, S. 1997. PTEN gene mutations are seen in high -grade but not in low-grade gliomas. *Cancer Research,* 57**,** 4187-4190.

RAYNAUD, F. I., ECCLES, S. A., PATEL, S., ALIX, S., BOX, G., CHUCKOWREE, I., FOLKES, A. J., GOWAN, S., DE HAVEN BRANDON, A., DI STEFANO, F., HAYES, A., HENLEY, A. T., LENSUN, L., PERGL-WILSON, G., ROBSON, A., SAGHIR, N., ZHYVOLOUP, A., MCDONALD, E., SHELDRAKE, P., SHUTTLEWORTH, S., VALENTI, M., WAN, N. C., CLARKE, P. A. & WORKMAN, P. 2009. Biological properties of potent inhibitors of class I phosphatidylinositide 3-kinases: from PI-103 through PI-540, PI-620 to the oral agent GDC-0941. *Molecular Cancer Therapeutics,* 8**,** 1725–1738.

REARDON, D. A., DESJARDINS, A., VREDENBURGH, J. J., GURURANGAN, S., SAMPSON, J. H., SATHORNSUMETEE, S., MCLENDON, R. E., HERNDON, J. E., MARCELLO, J. E., NORFLEET, J., FRIEDMAN, A. H., BIGNER, D. D. & FRIEDMAN, H. S. 2009. Metronomic chemotherapy with daily, oral etoposide plus bevacizumab for recurrent malignant glioma: a phase II study. *British Journal of Cancer,* 101**,** 1986-1994.

REDDY, S. P., BRITTO, R., VINNAKOTA, K., APARNA, H., SREEPATHI, H. K., THOTA, B., KUMARI, A., SHILPA, B. M., VRINDA, M., UMESH, S., SAMUEL, C., SHETTY, M. & AL., E. 2008. Novel glioblastoma markers with diagnostic and prognostic value identified through transcriptome analysis. *Clinical Cancer Research,* 14**,** 2978-2987.

REED, J. C. 1999. Dysregulation of apoptosis in cancer. *Journal of clinical oncology,* 17**,** 2942-2953.

REVEST, P. 2009. Biochemistry and cell biology. *In:* NAISH, J., REVEST, P. & COURT, D. S. (eds.) *Medical sciences.* Saunders Elsevier.

REYA, T., MORRISON, S. J., CLARKE, M. F. & WEISSMAN, I. L. 2001. Stem cells, cancer, and cancer stem cells. *Nature,* 414**,** 105-111.

REYNOLDS, B. & WEISS, S. 1992. Generation of neurons and astrocytes from isolated cells of the adult mammalian central nervous system. *Science,* 255**,** 1707-1710.

RHEE, C. H., HESS, K., JABBUR, J., RUIZ, M., YANG, Y., CHEN, S., CHENCHIK, A., FULLER, G. N. & ZHANG, W. 1999. cDNA expression array reveals heterogeneous gene expression profiles in three glioblastoma cell lines *Oncogene,* 18**,** 2711-2717.

ROJAS, E., MUSSALI, P., TOVAR, E. & VALVERDE, M. 2009. DNA-AP sites generation by etoposide in whole blood cells. *BMC cancer,* 3**,** 398-406.

ROLLISON, D. E., HELZLSOUER, K. J., ALBERG, A. J., HOFFMAN, S., HOU, J., DANIEL, R., SHAH, K. V. & MAJOR, E. O. 2003. Serum antibodies to JC virus, BK virus, simian virus 40, and the risk of incident adult astrocytic brain tumors. *Cancer Epidemiology, Biomarkers and Prevention,* 12**,** 460-463.

RON, E., MODAN, B., BOICE, J. D. J., ALFANDARY, E., STOVALL, M., CHETRIT, A. & KATZ, L. 1988. Tumors of the brain and nervous system after radiotherapy in childhood. *The New England Journal of Medicine,* 319**,** 1033-1039.

SAAL, L. H., HOLM, K., MAURER, M., MEMEO, L., SU, T., WANG, X., YU, J. S., MALMSTRÖM, P. O., MANSUKHANI, M., ENOKSSON, J., HIBSHOOSH, H., BORG, A. & PARSONS, R. 2005. PIK3CA mutations correlate with hormone receptors, node metastasis, and ERBB2, and are mutually exclusive with PTEN loss in human breast carcinoma. *Cancer Research,* 65**,** 2554-2559.

SALPHATI, L., PANG, J., PLISE, E. G., CHOU, B., HALLADAY, J. S., OLIVERO, A. G., RUDEWICZ, P. J., TIAN, Q., WONG, S. & ZHANG, X. 2011. Preclinical pharmacokinetics of the novel PI3K inhibitor GDC-0941 and prediction of its pharmacokinetics and efficacy in human. *Xenobiotica,* 41**,** 1088-1099.

SCAFFIDI, P. & MISTELI, T. 2008. Lamin A-dependent misregulation of adult stem cells associated with accelerated ageing. *Nature Cell Biology,* 10**,** 452-459.

SCHEITHAUER, B., HAWKINS, C., TIHAN, T., VANDENBERG, S. & BURGER, P. C. 2007. Astrocytic tumours. *In:* LOUIS, D. N., OHGAKI, H., WIESTLER, O. D. & CAVENEE, W. K. (eds.) *WHO Classification of Tumours of the Central Nervous System.* Lyon: IARC.

SCHLEHOFER, B., HETTINGER, I., RYAN, P., BLETTNER, M., PRESTON-MARTIN, S., LITTLE, J., ARSLAN, A., AHLBOM, A., GILES, G. G., HOWE, G. R., MÉNÉGOZ, F., RODVALL, Y., CHOI, W. N. & WAHRENDORF, J. 2005. Occupational risk factors for low grade and high grade glioma: results from an international case control study of adult brain tumours. *International Journal of Cancer,* 113**,** 116-125.

SCHUMACKER, P. T. 2006. Reactive oxygen species in cancer cells: live by the sword, die by the sword. *Cancer Cell,* 10**,** 175-176.

SHERIDAN, C., KISHIMOTO, H., FUCHS, R., MEHROTRA, S., BHAT-NAKSHATRI, P., TURNER, C., GOULET, R., BADVE, S. & NAKSHATRI, H. 2006. $CD44^+/CD24^-$ breast cancer cells exhibit enhanced invasive properties: an early step necessary for metastasis. *Breast Cancer Research,* 8**,** R59-R72.

SHIMIZU, K., GOLDFARB, M., PERUCHO, M. & WIGLER, M. 1983. Isolation and preliminary characterization of the transforming gene of a human neuroblastoma cell line. *Proceedings of the National Academy of Sciences U.S.A,* 80**,** 383-387.

SHINGU, T., YAMADA, K., HARA, N., MORITAKE, K., OSAGO, H., TERASHIMA, M., UEMURA, T., YAMASAKI, T. & TSUCHIYA, M. 2003. Synergistic augmentation of antimicrotubule agent-induced cytotoxicity by a phosphoinositide 3-kinase inhibitor in human malignant glioma cells. *Cancer Research,* 63**,** 4044-4047.

SIMPSON, J. R., HORTON, J., SCOTT, C., CURRAN, W. J., RUBIN, P., FISCHBACH, J., ISAACSON, S., ROTMAN, M., ASBELL, S. O. & NELSON, J. S. 1993. Influence of location and extent of surgical resection on survival of patients with glioblastoma multiforme: results of three consecutive Radiation Therapy Oncology Group (RTOG)clinical trials. *International Journal of Radiation Oncology Biology Physics,* 26**,** 239-244.

SINGH, S. K., HAWKINS, C., CLARKE, I. D., SQUIRE, J. A., BAYANI, J., HIDE, T., HENKELMAN, R. M., CUSIMANO, M. D. & DIRKS, P. B. 2004. Identification of human brain tumour initiating cells. *Nature,* 432**,** 396-401.

SONG, M. S., SALMENA, L. & PANDOLFI, P. P. 2012. The functions and regulation of the PTEN tumour suppressor. *Nature Reviews Molecualr Cell Biology,* 13**,** 283-296.

SOUTHAM, C. & BRUNSCHWIG, A. 1961. Quantitative studies of autotransplantation of human cancer. *Cancer,* 14**,** 971–978.

SPIEGL-KREINECKER, S., BUCHROITHNER, J., ELBLING, L., STEINER, E., WURM, G., BODENTEICH, A., FISCHER, J., MICKSCHE, M. & BERGER, W. 2002. Expression and functional activity of the ABC-transporter proteins P-glycoprotein and multidrug-resistance protein 1 in human brain tumor cells and astrocytes. *Journal of Neuro-oncology,* 57**,** 27-36.

STAHLHUT ESPINOSA, C. & SLACK, F. 2006. The role of microRNAs in cancer. *Yale Journal of Biology and Medicine,* 79**,** 131-140.

STILLER, C. 2007. Childhood Cancer in Britain: Incidence, survival, mortality. *Oxford University Press*.

STUMMER, W., MEINEL, T., EWELT, C., MARTUS, P., JAKOBS, O., FELSBERG, J. & REIFENBERGER, G. 2012. Prospective cohort study of radiotherapy with concomitant and adjuvant temozolomide chemotherapy for glioblastoma patients with no or minimal residual enhancing tumor load after surgery. *Journal of Neuro-oncology,* 108**,** 89-97.

STUPP, R., HEGI, M. E., MASON, W. P., VAN DEN BENT, M. J., TAPHOORN, M. J., JANZER, R. C., LUDWIN, S. K., ALLGEIER, A., FISHER, B., BELANGER, K., HAU, P., BRANDES, A. A., GIJTENBEEK, J., MAROSI, C., VECHT, C. J., MOKHTARI, K., WESSELING, P., VILLA, S., EISENHAUER, E., GORLIA, T., WELLER, M., LACOMBE, D., CAIRNCROSS, J. G., MIRIMANOFF, R. O., EUROPEAN ORGANISATION FOR RESEARCH AND TREATMENT OF CANCER BRAIN TUMOUR AND RADIATION ONCOLOGY GROUPS & GROUP, N. C. I. O. C. C. T. 2009. Effects of radiotherapy with concomitant and adjuvant temozolomide versus radiotherapy alone on survival in glioblastoma in a randomised phase III study: 5-year analysis of the EORTC-NCIC trial. *The LANCET Oncology,* 10**,** 459-466.

STUPP, R., MASON, W., BENT, M., WELLER, M., FISHER, B., TAPHOORN, M., BELANGER, K., BRANDES, A., MAROSI, C., BOGDAHN, U., CURSCHMANN, J., JANZER, R., LUDWIN, S., GORLIA, T., ALLGEIER, A., LACOMBE, D., CAIRNCROSS, G., EISSENHAUER, E. & MIRIMANOFF, R. 2005. Radiotherapy plus concomitant and adjuvant temozolomide for glioblastoma. *The New England Journal of Medicine,* 352**,** 987-996.

STURM, D., WITT, H., HOVESTADT, V., KHUONG-QUANG, D., JONES, D. & AL., E. 2012. Hotspot mutations in H3F3A and IDH1 define distinct epigenetic and biological subgroups of glioblastoma. *Cancer Cell,* 22**,** 425-437.

TAKAHASHI, S. 2012. Molecular functions of metallothionein and its role in hematological malignancies. *Journal of Hematology and Oncolgy,* 5**,** 41-48.

TEW, K. D. 1994. Glutatione-associated enzymes in anticancer drug resistance. *Cancer Reasearch,* 54**,** 4313-4320.

TEWS, D. S., NISSEN, A., KÜLGEN, C. & GAUMANN, A. K. 2000. Drug resistance-associated factors in primary and secondary glioblastomas and their precursor tumors. *Journal of Neuro-oncology,* 50**,** 227-237.

THE CANCER GENOME ATLAS RESEARCH NETWORK 2008. Comprehensive genomic characterization defines human glioblastoma genes and core pathways. *Nature,* 455**,** 1061-1068.

THORARINSDOTTIR, H. K., SANTI, M., MCCARTER, R., RUSHING, E. J., CORNELISON, C. R., JALES, A. & MACDONALD, T. J. 2008. Protein expression of platelet-derived growth factor receptor correlates with malignant histology and PTEN with survival in childhood gliomas. *Clinical Cancer Research,* 14**,** 3386–3394.

TIAN, Q., CUI1, H., LI, Y. & LU, H. 2012. LY294002 induces differentiation and inhibits invasion of glioblastoma cells by targeting GSK-3β and MMP. *EXCLI Journal,* 11**,** 68-77.

TOYOKUNI, S., OKAMOTO, K., YODOIB, J. & HIAI, H. 1995. Persistent oxidative stree in cancer. *FEBS Letters,* 358**,** 1-3.

UCHIDA, N., BUCK, D., HE, D., REITSMA, M., MASEK, M., PHAN, T., TSUKAMOTO, A., GAGE, F. & WEISSMAN, I. 2000. Direct isolation of human central nervous system stem cells. *Proceedings of the National Academy of Sciences U.S.A,* 97**,** 14720-14725.

VAN MAANEN, J. M. S., RETEL, J., DE VRIES, J. & PINEDO, H. M. 1988. Mechanism of Action of Antitumor Drug Etoposide: A Review. *Journal of the National Cancer Institute,* 80**,** 1526-1533.

VAN RIJN, J., HEIMANS, J., VAN DEN BERG, J., VAN DER VALK, P. & SLOTMAN, B. J. 2000. Survival of human glioma cells treated with various combination of temozolomide and X-rays. *International Journal of Radiation Oncology Biology Physics,* 47**,** 779-784.

VANDESOMPELE, J., DE PRETER, K., PATTYN, F., POPPE, B., VAN ROY, N., DE PAEPE, A. & SPELEMAN, F. 2002. Accurate normalization of real-time quantitative RT-PCR data by geometric averaging of multiple internal control genes. *Genome Biology,* 3**,** 0034.I-0034.II.

VANHAESEBROECK, B., STEPHENS, L. & HAWKINS, P. 2012. PI3K signalling: the path to discovery and understanding. *Nature Reviews Molecular Cell Biology,* 13**,** 195-203.

VOGEL, T. W., ZHUANG, Z., LI, J., OKAMOTO, H., FURUTA, M., LEE, Y. S., ZENG, W., OLDFIELD, E. H., VORTMEYER, A. O. & WEIL, R. J. 2005. Proteins and protein pattern differences between glioma cell lines and glioblastoma multiforme. *Clinical Cancer Research,* 11**,** 3624-3632.

VON DEIMLING, A., BURGER, P. C., NAKAZATO, Y., OHGAKI, H. & KLEIHUES, P. 2007. Diffuse astrocytoma. *In:* LOUIS, D. N., OHGAKI, H., WIESTLER, O. D. & CAVENEE, W. K. (eds.) *WHO classification of tumours of the central nervous system.* Lyon: IARC.

WALKER, J. E., SARASTE, M., RUNSWICK, M. J. & GAY, N. J. 1982. Distantly related sequences in the a- and b-subunits of ATP synthase, myosin, kinases and other ATP-requiring enzymes and a common nucleotide binding fold. *The EMBO Journal,* 1**,** 945-951.

WALLACE-BRODEUR, R. R. & LOWE, S. W. 1999. Clinical implications of p53 mutations. *Cellular and Molecular Life Sciences,* 55**,** 64-75.

WALLIN, J. J., GUAN, J., PRIOR, W. W., LEE, L. B., BERRY, L., BELMONT, L. D., KOEPPEN, H., BELVIN, M., FRIEDMAN, L. S. & SAMPATH, D. 2012. GDC-0941, a novel class I selective PI3K inhibitor, enhances the

efficacy of docetaxel in human breast cancer models by increasing cell death in vitro and in vivo *Clinical Cancer Research,* 18**,** 3901-3911.

WANG, H. & JOSEPH, J. A. 1999. Quantifying cellular oxidative stree by dichlorofluorescein assay using microplate reader. *Free Radical Biology and Medicine,* 27**,** 612-616.

WANG, X., CHEN, J. X., LIU, Y. H., YOU, C. & MAO, Q. 2012. Mutant TP53 enhances the resistance of glioblastoma cells to temozolomide by up-regulating O(6)-methylguanine DNA-methyltransferase. *Neurological Sciences***,** Epub ahead of print.

WARD, B. A. & GUTMANN, D. H. 2005. Neurofibromatosis 1: from lab bench to clinic. *Pediatric Neurology,* 32**,** 221-228.

WHITEHOUSE, C. M., DREYER, R. N., YAMASHITA, M. & FENN, J. B. 1985. Electrospray interface for liquid chromatographs and mass spectrometers. *Analytical Chemistry,* 57**,** 675-679.

WICK, W., WICK, A., SCHULZ, J. B., DICHGANS, J., RODEMANN, H. P. & WELLER, M. 2002. Prevention of irradiation-induced glioma cell invasion by temozolomide involves caspase 3 activity and cleavage of focal adhesion kinase. *Cancer Research,* 62**,** 1915-1919.

WIENCKE, J. K., ZHENG, S., JELLUMA, N., TIHAN, T., VANDENBERG, S., TAMGÜNEY, T., BAUMBER, R., PARSONS, R., LAMBORN, K. R., BERGER, M. S., WRENSCH, M. R., HAAS-KOGAN, D. A. & STOKOE, D. 2007. Methylation of the PTEN promoter defines low-grade gliomas and secondary glioblastoma. *Neuro-oncology,* 9**,** 271-279.

WONG, G. H. & GOEDDEL, D. V. 1988. Induction of manganous superoxide dismutase by tumor necrosis factor: Possible protective mechanism. *Science,* 242**,** 941-944.

WYLLIE, A. H. 1997. Apoptosis: an overview. *British Medical Bulletin,* 53**,** 451-465.

XU, Y. & VILLALONA-CALERO, M. 2002. Irinotecan: mechanisms of tumor resistance and novel strategies for modulating its activity. *Annals of oncology,* 13**,** 1841-1851.

YAMADA, M., FUJII, K., KOYAMA, K., HIROHASHI, S. & KONDO, T. 2009. The proteomic profile of pancreatic cancer cell lines corresponding to carcinogenesis and metastasis. *Journal of Proteomics and Bioinformatics,* 2**,** 001-018.

YANCY, H. F., MASON, J. A., PETERS, S., THOMPSON, C. E., LITTLETON, G. K., JETT, M. & DAY, A. A. 2007. Metastatic progression and gene expression between breast cancer cell lines from African American and Caucasian women. *Journal of Carcinogenesis,* 6**,** 8-19.

YANG, J., REN, Y., WANG, L., LI, B., CHEN, Y., ZHAO, W., XU, W., LI, T. & DAI, F. 2010. PTEN mutation spectrum in breast cancers and breast hyperplasia. *Journal of Cancer Research and Clinical Oncology,* 136**,** 1303-1311.

YANG, J. & WEINBERG, R. A. 2008. Epithelial-mesenchymal transition: at the crossroads of development and tumor metastasis. *Developmental Cell,* 14**,** 818-829.

ZHANG, K., WANG, X., ZHOU, B. & ZHANG, L. 2013. The prognostic value of MGMT promoter methylation in Glioblastoma multiforme: a meta-analysis. *Familial Cancer***,** Epub ahead of print.

ZHOU, S., SCHUETZ, J., BUNTING, K., COLAPIETRO, A., SAMPATH, J., MORRIS, J., LAGUTINA, I., GROSVELD, G., OSAWA, M., NAKAUCHI, H.

& SORRENTINO, B. 2001. The ABC transporter Bcrp1/ ABCG2 is expressed in a wide variety of stem cells and is a molecular determinant of the side-population phenotype. *Nature Medicine,* 7**,** 1028-1034.

ZHU, Y., HOELL, P., AHLEMEYER, B., SURE, U., BERTALANFFY, H. & KRIEGLSTEIN, J. 2007. Implication of PTEN in production of reactive oxygen species and neuronal death in in vitro models of stroke and Parkinson's disease. *Neurochemistry International,* 50**,** 507-516.

APPENDICES

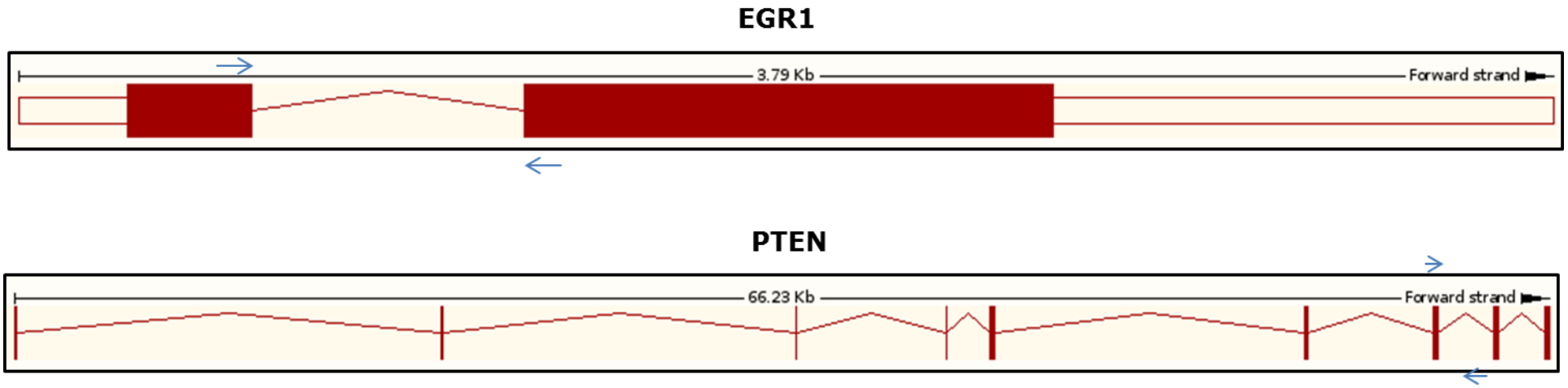

Appendix 1 (Designing the qPCR primers for candidate genes which are correlated with the oxidative stress damage). These figures represent the full length transcript, in which, the bold red boxes represent the exons and the red line between them represents the introns. All transcripts information was obtained from Ensembl website. The blue arrows represent the exons used to design the primers for qRT-PCR on primer blast.

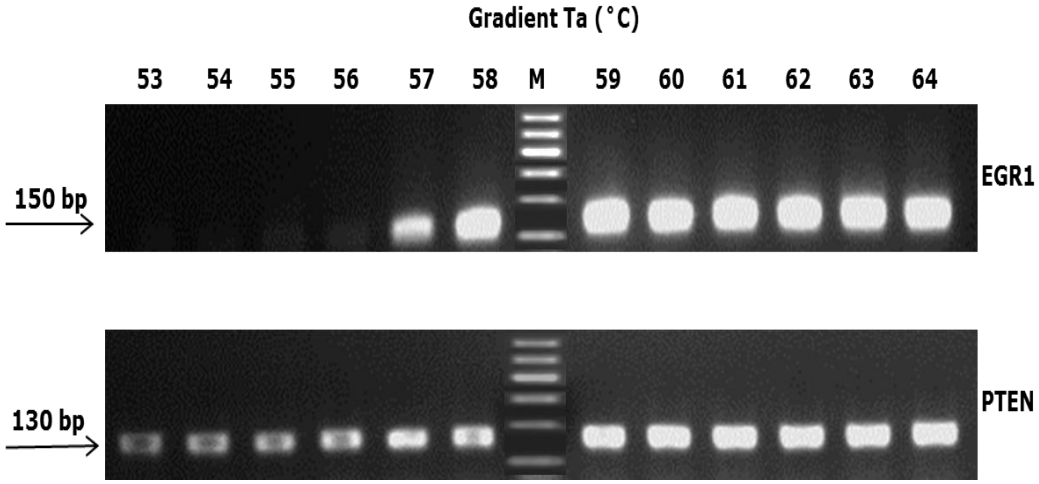

Appendix 2 (The optimisation PCR reaction for the annealing temperatures for EGR1 and PTEN primers). PCR reactions were performed following the protocol in section (2.8.3). Gel representation for the PCR products from gradient annealing temperatures for EGR1 primer which result in a 150 bp PCR product and PTEN primer with 130 bp PCR product. Under the protocol we designed, we had strong PCR products bands within the appropriate range for qRT-PCR reactions. Both primers were designed specifically for the qRT-PCR and they didn't produce any non-specific product or primer dimers. The DNA ladder (M) is a 100 bp Ladder (QIAGEN).

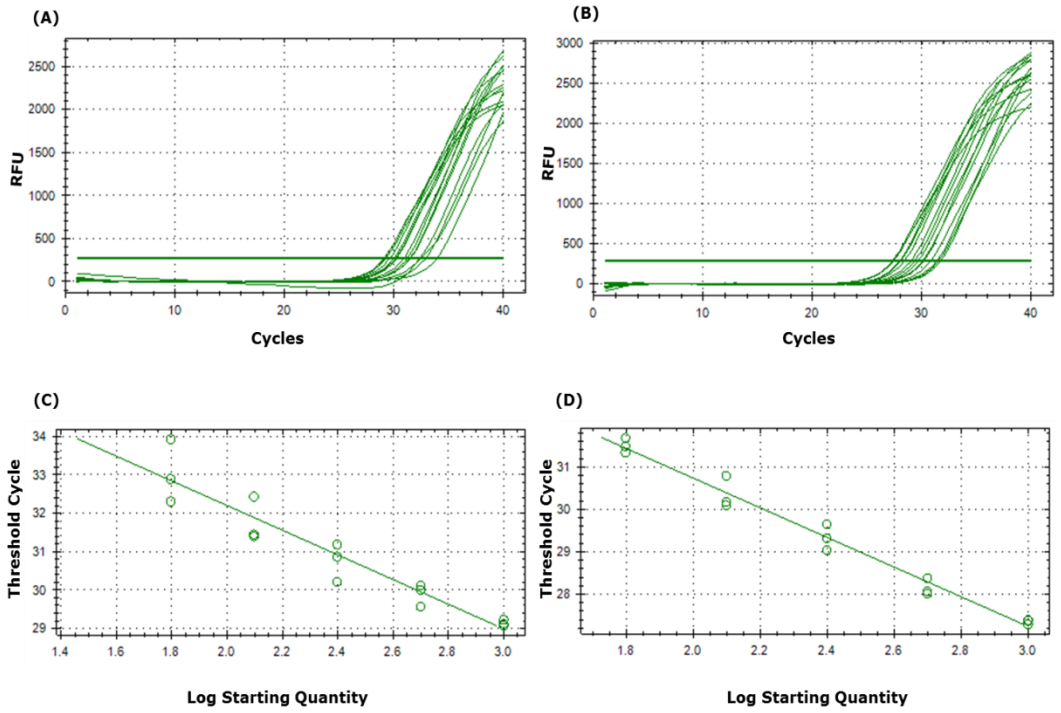

Appendix 3. Optimisation of the primer efficiencies for PTEN and EGR1 primers. Optimisation of primer pairs were performed following protocol in section 2.8.4 on C6 cell line. (A) & (B) represent the amplification curves for PTEN and EGR1, respectively. (C) and (D) represent the standard curves for PTEN and EGR1, respectively. This curve was plotted by using the CT values obtained from the amplification curve vs. serial dilution of C6 cDNA to determine the slope. For PTEN (C) the slope is -3.491 and for EGR1 (D) the slope is -3.213 indicating that primers resulted in efficient quantitative doubling of product per cycle.

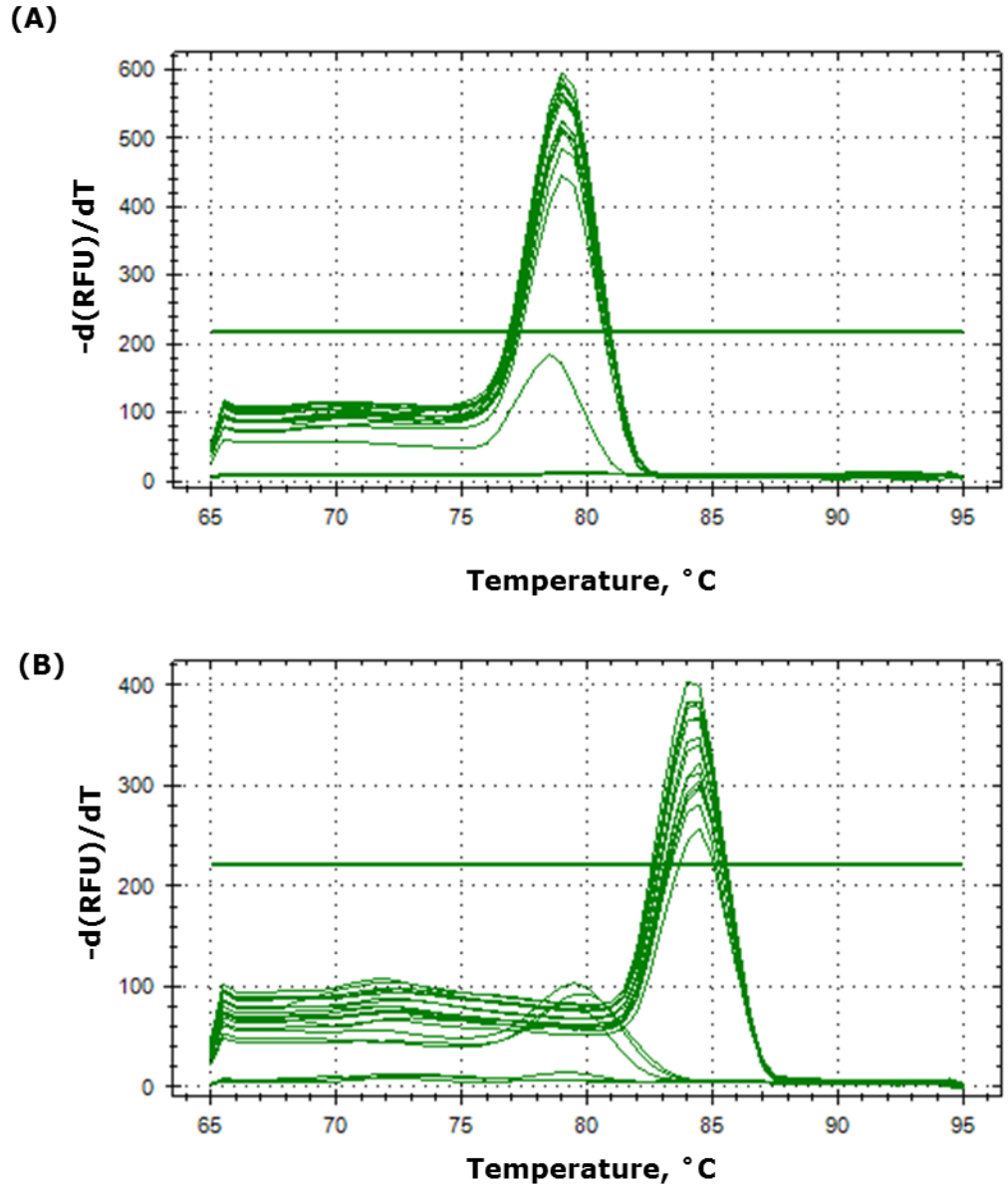

Appendix 4. Melting curves for PTEN and EGR1. This curve is produced as a result of a reduction in the fluorescent signal of SYBR Green I as the temperature is gradually increased. The ideal melting temperature curve is indicated by a symmetrical curve of products peaks with short temperature range. (A) & (B) represent the melting curves produced from the optimisation of primer efficiency for PTEN and EGR1 primers, respectively. In both cases, a major symmetrical melting is seen at Tm>80°C indicating a single specific amplicon.